Faculty of Science
Department of Applied Mathematics and Computer Science
Academic year 2012–2013

Computational Analysis of Bifurcations of Periodic Orbits

Virginie De Witte

Supervisors: Prof. Dr. Willy Govaerts
Prof. Dr. Yuri A. Kuznetsov

Dissertation submitted in fulfilment of the requirements for the degree of
Doctor of Science: Mathematics

Contents

Dankwoord

Een doctoraat schrijf je niet alleen. Na meer dan 5 jaar wordt het dan ook dringend tijd om iedereen te bedanken die op een directe of indirecte manier heeft bijgedragen tot dit werk.

Naar goede gewoonte wil ik eerst mijn promotor Willy Govaerts vermelden. Willy, bedankt voor de vele discussiemomenten en om mij wegwijs te maken in het onderzoekswereldje. Je hebt vaak de vinger op de wonde gelegd en even vaak kwam je af met een oplossing voor een probleem. Bedankt om me veel vrijheid te geven en om op me te vertrouwen.

Yuri, bedankt voor het aanbrengen van de boeiende onderwerpen. Dit doctoraat was nooit tot stand gekomen zonder jouw suggesties, die dit werk telkens weer verbeterden.

Fabio, I really enjoyed our cooperation. The many skype sessions, your hospitality when visiting you in the Netherlands, all this meant a lot to me. You are certainly one of the best coworkers ever.

Het laatste project in dit doctoraat was in samenwerking met Hil aan wie ik ook veel dank verschuldigd ben. Wanneer ik even vast zat, slaagde je er telkens in om te verduidelijken waar het probleem school en wat de volgende stap was. Bedankt om steeds tijd voor me vrij te maken.

Een groot deel van je tijd breng je door op je werk. Een goede werksfeer is dan ook uiterst belangrijk. En die was alleszins dik in orde hier op de S9. Niet alleen tijdens de werkuren maar ook daarbuiten zorgden de collega's voor de broodnodige ontspanning.

Kim, velen denken dat je 'ne stillen' bent. Geen idee waarom, want hier op de bureau was je een echte spraakwaterval. Bedankt voor al je tips, ondermeer over hoe we het efficiëntst Animal kingdom konden doorkruisen of voor sites met de goedkoopste vluchten naar New York. Charlotte, als onderzoeksgroepgenootje konden we samen op conferentie en die waren telkens heel geslaagd. Bedankt om samen met me weg te smelten tijdens Blue Horizons en voor je dvd's van een heel

verslavende serie. Dank je alle twee voor de leuke babbels, de lekkere tussendoortjes en zo veel meer. Ik had alleszins geen betere bureaugenootjes kunnen treffen.

Ergens als nieuweling toekomen schrikt toch wel wat af. Gelukkig had ik direct mijn maatje gevonden. Stéphanie, de uren die ik bij jou in de bureau heb gestaan, kan ik zeker niet op twee handen tellen. Dank je om naar mijn geklaag te luisteren als het onderzoek niet vlotte en om een even enthousiaste babbelkont te zijn als ik. Dat ik me hier onmiddellijk op mijn gemak voelde, is voor een groot deel aan jou te danken.

Ook de deur van de bureau van Tom en Jeroen heb ik plat gelopen. Tom, als 'ancien' heb je me vaak geholpen met van alles en nog wat. Die rol lijk je (samen met Sofie) nog steeds op jou te nemen. Bedankt Tom en Jeroen voor het gezever en het aanhoren van mijn frustraties. Bedankt Tom en Sofie voor de leuke kerstfeestjes en het bijbehorende cadeautjesgeknutsel.

Bedankt ook aan de gekke-kousen-bureau van Davy en Bart. Davy, bedankt om mijn metgezel te zijn op de PhDays en ICCAM conferenties en voor de gezondheid-mailtjes. Bart, bedankt om onze bureau te laten mee genieten van je bakkunsten. Jullie vele binnenvalmomenten worden ten zeerste geapprecieerd.

Aan de nieuwelingen, dank je om mijn fysieke conditie weer op peil te brengen. Cathérine, merci om mijn vaste zumba-compagnon te zijn en voor de vele gezellige babbels. De badmintongenootjes mag ik ook niet vergeten. Machteld, bedankt dat je me altijd liet winnen. Ik kijk nog steeds vol ongeduld uit naar ons etentje en ik beloof plechtig dat ik je niet meer zal vragen om me op te pikken bij garage Willems. Karel, bedankt voor de uitputtingsslagen in het enkel. Het was leuk dubbelen met jou, al werd het vaak onnodig spannend omdat er misschien iets te veel werd afgelachen. Jan, bedankt om me steeds op mijn gemak te doen voelen. Op uitstapjes met jou erbij is het fun verzekerd. Ik hoop dat er nog veel mogen volgen.

Als laatsten in het rijtje collega's zou ik Glad en Ann willen bedanken. Glad, merci om als latex-expert mijn hulplijn te zijn. Ann, bedankt voor het briefje naar de sint en de leuke koffiepauzemomenten.

De laatste jaren zijn niet altijd gemakkelijk geweest en mijn zonnetje was soms ver te zoeken. Daarom een hele grote dankjewel aan degenen die me gesteund hebben wanneer ik het hard nodig had. In het bijzonder wil ik Annelies bedanken. Toen ik je vroeg om die bewuste dag mee te helpen zei je zonder aarzelen ja. Het doet echt deugd te weten dat jij altijd klaar staat. Je bent een schat.

Julie, ook jij bedankt dat ik altijd op jou kan rekenen. Ik kijk al uit naar ons volgende filmavondje, Huize Colette uitstapje, ... Annelies en Valérie, merci om mijn

ski-enthousiasme aan te wakkeren. Liesbeth en Simon, bedankt voor de geslaagde etentjes en om een luisterend oor te zijn. Barbara en Davy, ook jullie heel erg bedankt om me altijd zo goed op te vangen. Jutho en Karolien, merci om zo leuke samenhuizers te zijn geweest. Lien en Kristof, bedankt voor de uitjes en om mijn frustraties van de ellenlange file en het totaal incompetente personeel te aanhoren op het brussels summer festival. Jullie festivalberichtje maakte alles onmiddellijk weer goed.

Mijn ouders en zusje wil ik natuurlijk ook ontzettend bedanken. Bedankt om altijd voor me klaar te staan en in de bres te springen. Bedankt mama om me zo te verwennen in de blok. De gebrachte toastjes waren echt wel een opkikker tijdens het studeren. Bedankt papa voor het gepingpong tot het pikdonker was en de vleermuis tijdens het voorbij vliegen opschrok van het balletje. 'De kleinste' mist je. Val, bedankt om altijd zo enthousiast te zijn en je portefeuille vol te steken met lakjes voor als ik weer eens te wild was geweest. Sorry alle drie voor elke keer dat ik er niet was. Hiep, jij bedankt om zo goed voor mijn zusje te zorgen.

Een mens kan soms verstrooid zijn. En dan is het wel handig dat iemand er je op wijst dat je voor Amerika een internationaal reispas nodig hebt, een esta formulier moet invullen en je met dollars moet betalen. Bedankt Jeroen om mijn reddende engel (of duivel?) te zijn, om zo begripvol te zijn tijdens de stressy periodes en om er te zijn als ik je nodig heb. Je knuffels maken mijn dag steeds goed.

Ik ben aan het einde gekomen van dit dankwoord. Bedankt om verder te bladeren, er volgen nog een aantal leuke prentjes.

1 Introduction

This chapter is an introduction to the fascinating world of dynamical systems.

The analysis of dynamical systems concerns the study of time-varying phenomena. A dynamical system consists of an evolution rule, which specifies the future and past states of a system, given only the current state. The modern theory of dynamical systems goes back to the end of the 19^{th} century with Poincaré's groundbreaking work on celestial mechanics, where fundamental questions concerning the stability and evolution of the solar system were addressed. His work has laid the basis for the local and global analysis of dynamical systems.

A simple example of a dynamical system is provided by a pendulum. A planar pendulum consists of a rod, suspended at a fixed point, which oscillates in the vertical plane. Its state at any time is specified by the position and the speed of the pendulum. The pendulum is subject to gravity, and the evolution rule is determined by Newton's law $F = ma$, where F denotes the gravitational force, m the mass and a the acceleration.

There is a wide area of applications, which ranges from fields as physics, biology, chemistry, economics, engineering, sociology, demography, etc. In fact, this broad

scope of applications is one of the main reasons for the popularity of dynamical systems over the last decades. To describe these real-world applications, a mathematical model has to be built on which we can apply algorithms and computational methods to determine the state of the observations.

A dynamical system can either refer to continuous-time or discrete-time phenomena. The evolution rule in the first case corresponds with a set of ordinary differential equations (**ODEs**), in the second case with a map. Most concepts and results present in a continuous-time dynamical system have an analogon in the discrete case. This thesis focuses on ODEs, but we will also apply the existing theory for maps.

The ordered family of points obtained by applying the evolution rule is called a **trajectory** (or **orbit**). If a trajectory that starts in a point, remains in that point, the point is called an equilibrium. An example is given by the motionless pendulum. The equilibrium is called **stable** if all nearby trajectories converge to the equilibrium.

One of the main concepts in the theory of dynamical systems is that of bifurcations. As a parameter is varied, the dynamical system may encounter points where the qualitative behaviour changes. At such a point the dynamical system is said to have gone through a bifurcation. The simplest example of a bifurcation is the loss of stability of an equilibrium.

There are two types of bifurcations, namely local and global bifurcations. A **local bifurcation** is a bifurcation that can be detected by looking at any small neighbourhood of the equilibrium or periodic orbit. For example, a Hopf bifurcation, where the equilibrium changes stability and a periodic orbit is born, is a local bifurcation. However, there are also bifurcations that can not be detected by looking at any small vicinity of an equilibrium or periodic orbit. These are **global bifurcations**. A heteroclinic orbit, which converges to a first equilibrium forwards in time and to a second equilibrium backwards in time, is an example of a global bifurcation.

At the detection of a bifurcation, the main goal is to find a division of the parameter space around the bifurcation point into different strata such that for all parameter values belonging to a certain stratum, the same dynamical behaviour is performed. A diagram representing such a division is called a bifurcation diagram. To each stratum corresponds a phase portrait, which shows all possible orbits in the state space.

The analysis of a (nonlinear) dynamical system can be a daunting task. Even a simple system can demonstrate complex behaviour that can not be represented in analytical formulae. Numerical methods are then needed. One way to study a

dynamical system is by numerical simulation. Through time-integration one may detect the presence of (stable) equilibria or periodic orbits, and in this way obtain a rough sketch of how the bifurcation diagram looks like. A second option is by making use of **continuation**, which is a predictor-corrector method. The idea is to compute a curve that satisfies a suitable system of equations, which define the dynamical object under consideration. For example, once a (stable) equilibrium is detected, one can apply continuation techniques starting from this equilibrium point and compute a curve of equilibria when varying a parameter.

One of the continuation software packages that can be used for the study of continuous-time dynamical systems and their bifurcations is MatCont [31–33]. Research groups from Belgium and The Netherlands, as well as individual scientists from other countries, cooperated in the development of MatCont. It is written in Matlab and therefore platform-independent. The graphical user interface is quite easy to handle and allows for an interactive study of the bifurcations. The software is based on numerical continuation where first a tangent prediction is made, which is then corrected by Moore-Penrose continuation.

When continuing a curve of equilibria, one may detect a bifurcation, i.e. a Limit Point or a Hopf bifurcation. These bifurcations are codimension 1 bifurcations, which generically occur at the variation of 1 system parameter. Next, a Limit Point or Hopf curve can be computed through continuation, on which in turn bifurcations can be detected. These are codimension 2 bifurcations in which the variation of 2 system parameters is involved. In fact, such a bifurcation is determined by imposing two independent conditions. The transversal or tangential intersection of codimension 1 bifurcation curves happens at codimension 2 bifurcation points. Therefore, codimension 2 points play the role of **organizing centers**. Codimension 1 bifurcation curves can root at a codimension 2 point, e.g. in the case of a Bogdanov-Takens point, a homoclinic bifurcation curve originates.

Generically, in a system that contains m parameters, up to codimension m bifurcations can occur. In practice, the analysis of codimension 2 points can already be very complex and in some cases, the complete bifurcation picture is still unknown. Therefore, one in general restricts to the study of bifurcations up to codimension 2.

A periodic orbit can be found in several ways, e.g. by time-integration, or at a Hopf bifurcation. The first method can only be applied in the case of a stable orbit and the initialization of a periodic orbit from a Hopf bifurcation sometimes fails. This clarifies that it is important to have alternatives for the initialization of higher order codimension bifurcations.

Next to equilibria and periodic orbits, homoclinic orbits play an important role

in applications. A homoclinic orbit can be seen as a periodic orbit whose period tends to infinity. In the case of homoclinic orbits, the continuation of periodic orbits with an ever-increasing period can lead to the detection of a homoclinic orbit. An alternative method is given by the homotopy method, on which we will focus in Chapter 3. This method allows one to initiate a homoclinic orbit starting from an equilibrium. The method consists of a systematic procedure in which each step aims for a better approximation of the searched homoclinic orbit. At the end of the homotopy process, (hopefully) a well enough approximation is achieved, which can be used as start-up for the Newton correction method and converges to the exact homoclinic orbit. Also in the case of heteroclinic orbits, a homotopy method can provide one with an approximating starting orbit for the continuation of heteroclinic orbits. In Chapter 3 we describe the homotopy methods for both types of orbits and their implementation in a software package, in our case MatCont. We also made the continuation of heteroclinic orbits available in MatCont. We present several examples that demonstrate the effectiveness of this systematic procedure.

To determine the bifurcation scenario around a bifurcation point, one can scan the neighbourhood of the bifurcation point to search for the presence of local and global bifurcations. But it would be much easier if at detection of the bifurcation, one would immediately know what bifurcation curves are involved and in what stratum they are situated. This issue is addressed by looking at the normal form coefficients.

When encountering a bifurcation, first a reduction of the dynamical system to a center manifold is made. Two-dimensional **manifolds** are also called surfaces. Examples include the plane, the sphere, the torus, etc. The center manifold is usually lower dimensional. The defining equations in the center manifold are then put in a simplified form, i.e. a normal form. The type of bifurcation that occurs in the dynamical system can be deduced from a study of this normal form. Indeed, the coefficients appearing in the normal form, i.e. the normal form coefficients, distinguish between the different scenarios that can happen at the bifurcation point. For example, a negative normal form coefficient at a Hopf bifurcation corresponds with the birth of a stable periodic orbit, a positive one with an unstable periodic orbit. Through the introduction of parameters, to each possible case one can associate an **unfolding** of the normal form, which shows the division of the parameter space into its strata and the corresponding phase portraits. The number of unfolding parameters present in the normal form is equal to the codimension of the bifurcation.

In Chapter 4, Chapter 5 and Chapter 6 we focus on local codimension 2 bifur-

cations of periodic orbits, of which there are 11 cases. The dimension of the center manifold varies from 2 to 5 and the bifurcations are classified according to this dimension, which is determined by the eigenvalues of a matrix specific to the periodic orbit. A map can be associated to every periodic orbit, namely the Poincaré map. The periodic orbit then corresponds with a fixed point of this Poincaré map. An advantage of this association is that results earlier developed for maps can to some extent be used in the study of bifurcations of periodic orbits.

In Chapter 4 we derive the normal forms for all 11 codimension 2 bifurcations of periodic orbits and state what normal form coefficients determine what bifurcation scenario happens near the bifurcation point. We present their unfoldings and clarify the interpretation of the orbits appearing in the phase portraits. Remark that we present the unfolding for the truncated normal form. The question then raises whether the higher order terms present in the original normal form influence the dynamics derived from a study of the truncated normal form. In some cases, the higher order perturbations do not affect the bifurcation portrait corresponding with the truncated normal form. Unfortunately, this is not always the case. The appearance of global bifurcations may obstruct the topological equivalence between the bifurcation diagrams corresponding with the truncated and original normal forms. A perturbation by higher order terms makes the dynamics in the vicinity of global bifurcations much more complex and sometimes the exact sequence of events is unknown.

We then need expressions for the normal form coefficients. We determine them by the use of the homological equation. In Chapter 5 we elucidate the method and derive the formulae for all coefficients of interest. Note that long expressions are involved. Though the approach is the same in all cases, each case has its own specifics.

The logical next step is then to concentrate on the implementation of the normal form coefficients. In Chapter 6 we discuss how the formulae can efficiently be incorporated in MatCont. Concerning the interpretation of the normal form coefficients of the codimension 2 bifurcations of periodic orbits where the dimension of the center manifold equals 4 (i.e. the Limit Point-Neimark-Sacker and Period-Doubling-Neimark-Sacker bifurcation) or 5 (i.e. the Double Neimark-Sacker bifurcation), a distinction is made between 'simple' and 'difficult' cases. In the 'difficult' case the dynamics is more complex and an extra torus is involved. Higher order terms in the normal form determine the stability of this extra torus. Since this extra torus is not always present and for complexity reasons, in general, we omit their computation. However, the expressions are implemented in MatCont such that the interested user

can obtain all details.

To confirm the correctness of our method, we present a series of examples that contain all codimension 2 bifurcations of periodic orbits. On the one hand, at the bifurcation point we compute the normal form coefficients that allow us to make a prediction about the dynamics around the detected point by the use of the unfoldings discussed in Chapter 4. On the other hand, we scan the vicinity of the detected point for possible bifurcation curves. In all the examples, the two approaches lead to the same dynamical picture, and therefore it corroborates us of the correctness of the computation of the normal form coefficients.

The contents of this thesis have been published in or submitted for publication, see [24], [25], [21], [26], [28] and [27]. Next to the content of this thesis, I also made contributions to [50], [22], [83] and [23].

2 Preliminaries

In this introductory chapter we review some concepts in the theory of dynamical systems that will be needed for a good comprehension of the rest of this thesis. Most of the material in this chapter is based on [67].

2.1 Basics

Consider the following continuous-time dynamical system

$$\dot{x}(t) \equiv \frac{dx}{dt} = f(x(t), \alpha), \tag{2.1}$$

where $x \in \mathbb{R}^n$ is a state vector, $\alpha \in \mathbb{R}^p$ is a parameter vector and $f : \mathbb{R}^n \times \mathbb{R}^p \to \mathbb{R}^n$ is sufficiently smooth.

Definition 2.1. *The map $\varphi^t : X \to X$ defined in the state space X that transforms an initial state $x_0 \in X$ into the state $x_t \in X$ at time t, namely $x_t = \varphi^t x_0$, is called the **evolution operator** of the dynamical system.*

The family $\{\varphi^t\}_{t\in T}$ of evolution operators is called a **flow**.

Definition 2.2. *A **dynamical system** is a triple $\{T, X, \varphi^t\}$, where T is a time set, X is a state space, and $\varphi^t : X \to X$ is a family of evolution operators parametrized by $t \in T$ and satisfying:*

- $\varphi^0 = id$,
- $\varphi^{t+s} = \varphi^t \circ \varphi^s$.

General theory guarantees that for smooth right-hand sides f a solution (x_0, α_0) to (2.1) exists that is unique for any (x_0, α_0) for small $|t|$. Moreover, the degree of smoothness of the solution x is the same as the one for f.

Definition 2.3. *A dynamical system $\{T, \mathbb{R}^n, \varphi^t\}$ is called **topologically equivalent** to a dynamical system $\{T, \mathbb{R}^n, \psi^t\}$ if there is a homeomorphism $h : \mathbb{R}^n \to \mathbb{R}^n$ mapping orbits of the first system onto orbits of the second system, preserving the direction of time.*

A **phase portrait** is the representation of a collection of trajectories corresponding to multiple initial conditions of the dynamical system. The phase portrait gives us information about, e.g., the stable and unstable objects present in the system. Figure 2.1 (a) shows an example of a phase portrait.

Definition 2.4. *The appearance of a topologically inequivalent phase portrait under variation of parameters is called a **bifurcation**.*

A **bifurcation diagram** shows the topological inequivalent strata in parameter space, together with their corresponding phase portraits. Figure 2.1 (b) shows an example of a bifurcation diagram.

Definition 2.5. *The **codimension** of a bifurcation in (2.1) is the difference between the dimension of the parameter space and the dimension of the corresponding bifurcation set.*

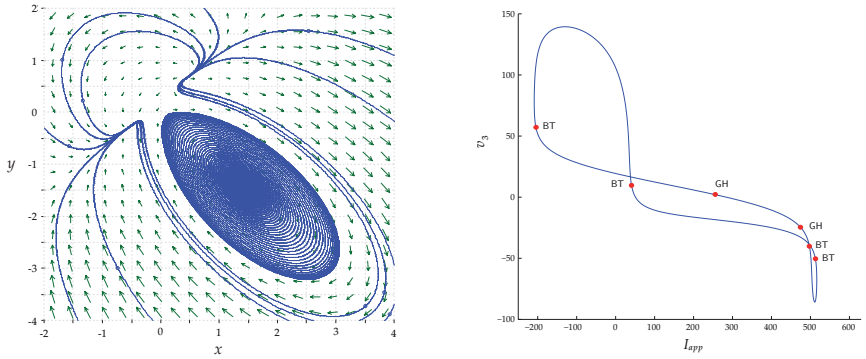

(a) (b)

Figure 2.1: (a) Phase portrait (x, y are state variables). (b) Partial bifurcation diagram (I_{app}, v_3 are parameters).

So, the codimension of a bifurcation is the number of conditions that define the bifurcation, or thus the number of parameters that have to be varied for the detection of the bifurcation.

Definition 2.6. *An **invariant set** of a dynamical system $\{T, X, \varphi^t\}$ is a subset $S \subset X$ such that $x_0 \in S$ implies that $\varphi^t x_0 \in S$ for all $t \in T$.*

Examples of invariant sets are given by equilibria, periodic orbits or tori, where an equilibrium is defined as follows.

Definition 2.7. *A point $x_0 \in X$ is called an **equilibrium** if $\varphi^t x_0 = x_0$ for all $t \in T$.*

A periodic orbit is defined as follows.

Definition 2.8. *A **cycle** or **periodic orbit** Γ is an orbit such that for each point $x_0 \in \Gamma$ holds that $\varphi^{t+T_0} x_0 = \varphi^t x_0$ with some $T_0 > 0$, for all $t \in \mathbb{R}$. The minimal T_0 with this property is called the **period** of the cycle Γ. A cycle of a*

continuous-time dynamical system, in a neighbourhood of which there are no other cycles, is called a ***limit cycle****.*

Another important concept in dynamical systems, which will be extensively discussed in this thesis, is the one of normal forms. To report the definition, we need to extend the concept of topologically equivalent systems to parameter-dependent systems.

Definition 2.9. *Let*

$$\dot{x} = f(x,\alpha), x \in \mathbb{R}^n, \alpha \in \mathbb{R}^p \tag{2.2}$$

and

$$\dot{y} = g(y,\beta), y \in \mathbb{R}^n, \beta \in \mathbb{R}^p \tag{2.3}$$

be two dynamical systems. (2.2) is called locally ***topologically equivalent*** *to (2.3) near the equilibrium x_0 for certain parameter values α_0, if there exists a map $(x,\alpha) \mapsto (h_\alpha(x), p(\alpha))$, defined in a neighbourhood of $(x,\alpha) = (x_0,\alpha_0)$ in the direct product $\mathbb{R}^n \times \mathbb{R}^p$ and such that*

(i) $p : \mathbb{R}^p \to \mathbb{R}^p$ is a homeomorphism defined in a neighbourhood of $\alpha = \alpha_0$, $\beta = p(\alpha)$;

(ii) $h_\alpha : \mathbb{R}^n \to \mathbb{R}^n$ is a parameter-dependent homeomorphism defined in a neighborhood U_α of $x = x_0, y = h_\alpha(x)$, and mapping orbits of (2.2) in U_α onto orbits of (2.3) in $h_\alpha(U_\alpha)$, preserving the direction of time.

A **generic system** (2.1) is a system that satisfies a finite number of genericity conditions, i.e.

$$N_i[f] \neq 0, i = 1,2,\ldots,s,$$

where each N_i is some (algebraic) function of certain partial derivatives of $f(x,\alpha)$ with respect to x and α evaluated at the equilibrium. Genericity conditions where partial derivatives with respect to x are considered, are **nondegeneracy conditions** and the conditions for which partial derivatives with respect to the parameters are involved, are called **transversality conditions**.

Definition 2.10. *System $\dot{\xi} = g(\xi,\beta;\sigma), \xi \in \mathbb{R}^n, \beta \in \mathbb{R}^k, \sigma \in \mathbb{R}^l$ is called a topological* ***normal form*** *for a bifurcation if any generic system (2.1) in which*

the equilibrium $x = 0$ satisfies the same bifurcation conditions at $\alpha = 0$, is locally topologically equivalent near the origin to $\dot{\xi} = g(\xi, \beta; \sigma)$ for some values of the coefficients σ_i.

A normal form is not uniquely determined. This however does not affect the conclusions that are drawn from these normal forms.

Definition 2.11. *The operator V^* is called the **adjoint operator** of the operator V if*

$$\langle V^* f, g \rangle = \langle f, Vg \rangle,$$

for all functions f and g.

Note that $\langle u, v \rangle = u^{\mathrm{H}} v = \bar{u}^{\mathrm{T}} v$ is the standard scalar product in an appropriate complex (or real) finite-dimensional vectorspace.

2.2 Equilibria and their bifurcations

Let x_0 be an equilibrium of the system (2.1). Let A denote the **Jacobian matrix** $\frac{\partial f}{\partial x}$ evaluated at x_0. The values of the eigenvalues of the Jacobian matrix are essential in the study of the dynamical system. Denote the second up to fifth order derivatives as $B(x,y), C(x,y,z), D(x,y,z,u), E(x,y,z,u,v)$ where

$$\begin{aligned}
B_i(x,y) &= \sum_{j,k=1}^{n} \left.\frac{\partial^2 f_i(\xi)}{\partial \xi_j \partial \xi_k}\right|_{\xi=x_0} x_j y_k, \\
C_i(x,y,z) &= \sum_{j,k,l=1}^{n} \left.\frac{\partial^3 f_i(\xi)}{\partial \xi_j \partial \xi_k \partial \xi_l}\right|_{\xi=x_0} x_j y_k z_l, \\
D_i(x,y,z,u) &= \sum_{j,k,l,m=1}^{n} \left.\frac{\partial^4 f_i(\xi)}{\partial \xi_j \partial \xi_k \partial \xi_l \partial \xi_m}\right|_{\xi=x_0} x_j y_k z_l u_m, \\
E_i(x,y,z,u,v) &= \sum_{j,k,l,m,o=1}^{n} \left.\frac{\partial^5 f_i(\xi)}{\partial \xi_j \partial \xi_k \partial \xi_l \partial \xi_m \partial \xi_o}\right|_{\xi=x_0} x_j y_k z_l u_m v_o,
\end{aligned}$$

for $i = 1, 2, \ldots, n$.

Definition 2.12. *An equilibrium is called* ***hyperbolic*** *if the Jacobian has no eigenvalues on the imaginary axis.*

An equilibrium is locally **asymptotically stable** if for all eigenvalues λ of the Jacobian matrix holds that $\Re(\lambda) < 0$. If for at least one eigenvalue holds that $\Re(\lambda) > 0$, the equilibrium is **unstable**. Here, $\Re(\lambda)$ stands for the real part of λ.

There are five kinds of hyperbolic equilibria in the plane. At a stable node, there are two negative real eigenvalues, see Figure 2.2 (a). At a stable focus, there is a complex conjugate pair of eigenvalues with negative real part, see Figure 2.2 (b). Also the unstable analogues of these equilibria exist. At a saddle, there is a positive and a negative real eigenvalue, see Figure 2.2 (c).

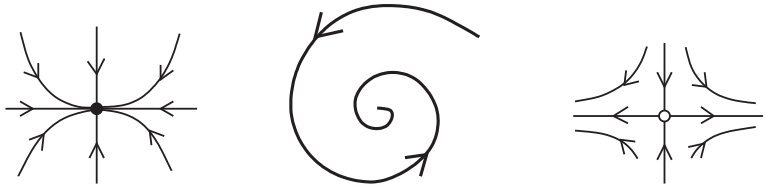

(a) Node (b) Focus (c) Saddle

Figure 2.2: Several types of equilibria.

Two invariant sets are associated to a hyperbolic equilibrium x_0, i.e. the stable and unstable sets of x_0 given by

$$W^S(x_0) = \{x | \varphi^t x \to x_0, t \to +\infty\},$$
$$W^U(x_0) = \{x | \varphi^t x \to x_0, t \to -\infty\},$$

respectively.

2.2.1 Codimension 1 bifurcations of equilibria

Limit Point bifurcation

Definition 2.13. *The bifurcation associated with the appearance of an eigenvalue $\lambda_1 = 0$ is called a **Limit Point bifurcation** (LP, or **Fold** or **Saddle-Node bifurcation**).*

This bifurcation corresponds with a collision and disappearance of two equilibria when crossing the bifurcation parameter value, see Figure 2.3. At parameter value α_0 a **saddle-node equilibrium** appears. The normal form at the LP bifurcation is given by the one-dimensional system

$$\dot{u} = au^2 + \ldots, u \in \mathbb{R}.$$

If $a = 0$, then the bifurcation is **degenerate** (i.e. the bifurcation is not the typical, generic case).

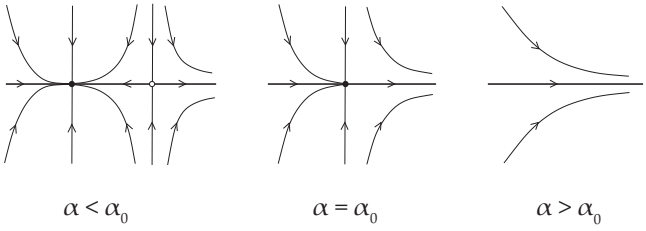

Figure 2.3: A Fold bifurcation of equilibria.

Hopf bifurcation

Definition 2.14. *The bifurcation corresponding to the presence of eigenvalues $\lambda_{1,2} = \pm i\omega_0, \omega_0 > 0$, is called a **Hopf bifurcation** (H, or Andronov-Hopf bifurcation).*

At the Hopf bifurcation a periodic orbit is born and there is an exchange of stability of the equilibrium. The normal form at the Hopf bifurcation is given by the two-dimensional system

$$\dot{z} = i\omega_0 z + c_1 z|z|^2 + \ldots, z \in \mathbb{C}$$

where $l_1 = \Re(c_1)$ is called the **first Lyapunov coefficient** at the Hopf bifurcation. The periodic orbit is stable if the first Lyapunov coefficient is negative, in which case the bifurcation is **supercritical** or soft, see Figure 2.4. Otherwise, the periodic orbit is unstable, which corresponds with a **subcritical** or sharp bifurcation. If $l_1 = 0$, then the bifurcation is degenerate.

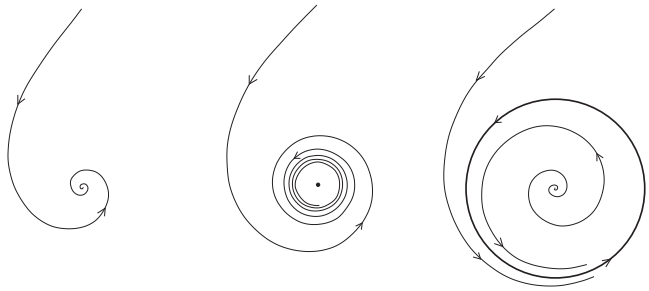

Figure 2.4: Supercritical Hopf bifurcation of equilibria.

2.2.2 Codimension 2 bifurcations of equilibria

Codimension 2 bifurcation points are points where curves corresponding to codim 1 bifurcations intersect transversally or tangentially. In generic systems (2.1) only five codim 2 bifurcations of equilibria are possible [3, 56, 67]. We list them in Table 2.1. Note that the coefficients a and l_1 appear in the critical normal forms of the LP and H bifurcation, respectively. The eigenvalues mentioned in the table are assumed to be the only ones for which holds that $\Re(\lambda) = 0$.

2.3 Fixed points

Consider the following discrete-time dynamical system

$$x \mapsto f(x, \alpha), \quad x \in \mathbb{R}^n, \alpha \in \mathbb{R}^p, \tag{2.4}$$

where the map f is smooth with respect to x and α. A **fixed point** of the system (2.4) is a point x_0 that is mapped to itself, i.e. $f(x_0, \alpha_0) = x_0$. The second

Label	Name	Properties
CP	Cusp	$\lambda_1 = 0, a = 0$
GH	Bautin	$\lambda_{1,2} = \pm i\omega_0, l_1 = 0$
BT	Bogdanov-Takens	$\lambda_{1,2} = 0$
ZH	Zero-Hopf	$\lambda_1 = 0, \lambda_{2,3} = \pm i\omega_0, \omega_0 > 0$
HH	Double Hopf (Hopf-Hopf)	$\lambda_{1,2} = \pm i\omega_1, \lambda_{3,4} = \pm i\omega_2, \omega_{1,2} > 0$

Table 2.1: Codim 2 bifurcations of equilibria.

iterate of the map f is given by $f^2 = f \circ f$. The eigenvalues of the Jacobian matrix evaluated at a fixed point are called **multipliers**. A fixed point is said to be hyperbolic if it has no multipliers on the unit circle. There are three ways in which the hyperbolicity can be lost. Either a simple positive multiplier approaches the unit circle where then $\mu_1 = 1$, or a simple negative multiplier approaches the unit circle, where $\mu_1 = -1$, or a pair of simple complex multipliers reaches the unit circle where $\mu_{1,2} = e^{\pm i\theta_0}, 0 < \theta_0 < \pi$.

We now state a powerful result in dynamical systems, namely the Hartman-Grobman theorem. This result gives us the ability to locally reduce the dynamical system to its linear part near fixed points. We first explain the concept of locally topologically conjugacy.

Definition 2.15. *Two maps $f, g : \mathbb{R}^n \mapsto \mathbb{R}^n$ satisfying $f = h^{-1} \circ g \circ h$ for some homeomorphism $h : \mathbb{R}^n \mapsto \mathbb{R}^n$ are called locally topologically **conjugate**.*

Theorem 2.16 (**Hartman-Grobman theorem**). *Let x_0 be a hyperbolic fixed point of the map f. Then, there exists a neighborhood U of x_0 and a homeomorphism $h : U \to \mathbb{R}^n$ such that $h(x_0) = 0$, and such that in a neighbourhood U of x_0, the map f is locally topologically conjugate by h to the map of its linearization A.*

From each continuous-time dynamical system $\{\mathbb{R}^n, X, \varphi^t\}$ we can derive a discrete-time dynamical system. This can be done by fixing some $T_0 > 0$ and considering a system generated by iteration of the map $f = \varphi^{T_0}$. This map is called a T_0-**shift map** along orbits of $\{\mathbb{R}^n, X, \varphi^t\}$. The T_0-shift of a continuous-time dynamical

system $\dot{x} = f(x(t))$ can be obtained by **Picard iterations**. The successive iterations are defined by

$$\begin{cases} x_0(t) = x_0, \\ x_{n+1}(t) = x_0 + \int_0^t f(x_n(s))ds, \quad n \geq 0 \end{cases}$$

such that the T_0-shift map is given by $x_0 \mapsto x(T_0)$, with $x(T_0) = \lim_{n\to+\infty} x_n(T_0)$.

2.4 Limit cycles and their bifurcations

The defining system that we typically use for a limit cycle is given by

$$\begin{cases} \dot{x}(t) - Tf(x(t), \alpha) = 0, \\ x(0) - x(1) = 0, \\ \int_0^1 \dot{\tilde{x}}(t)^{\mathrm{T}} x(t)dt = 0, \end{cases} \tag{2.5}$$

where $t \in [0,1]$. Indeed, when studying periodic solutions to (2.1) it is convenient to introduce the period T as an explicit unknown by rescaling time to the interval $[0, 1]$. The second equation represents the periodicity condition. The third equation is the **phase condition**, which is an integral condition that makes the periodic solution unique. This is necessary since the phase of the limit cycle has to be fixed. Indeed, each point on the limit cycle can be represented as initial point of the periodic orbit. The solution with minimal 2-norm distance to $\tilde{x}$ is chosen, with $\tilde{x}(t)$ an initial guess for the solution, typically obtained from a previous step in a continuation method (see Section 2.8.1). This approach is by now standard in numerical bifurcation software, see [31, 37, 41, 53, 69].

To every periodic orbit, a map can be coupled. This is very useful since the results concerning maps can then be applied to differential equations.

Definition 2.17. *Let Σ be a $(n-1)$-dimensional hypersurface transverse to the vector field at the periodic orbit Γ. Let x_0 be the intersection of Σ and the periodic orbit. The map P that associates points $x \in \Sigma$ sufficiently close to x_0 with their first return points $P(x)$ to Σ is called a **Poincaré map** associated with the cycle Γ.*

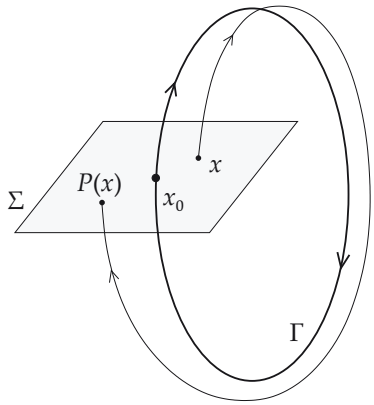

Figure 2.5: The Poincaré map associated with a limit cycle Γ.

As can be seen in Figure 2.5, the intersection x_0 of the hypersurface Σ with the periodic orbit Γ is a fixed point of the Poincaré map P. Note that the dimension of the cross-section Σ is one lower than the dimension of the state space of the ODE.

Concerning the next definition, recall that A represents the Jacobian matrix $\frac{\partial f}{\partial x}$.

Definition 2.18. *The fundamental matrix solution of (2.1) is the time-dependent matrix $M(t)$ that satisfies*

$$\dot{M} = A\,M,$$

*with the initial condition $M(0) = I_n$, the unit $n \times n$-matrix. The matrix $M(T)$ is called a **monodromy matrix** of the cycle Γ.*

The following theorem makes it possible to determine the multipliers of a periodic orbit without computation of the Poincaré map.

Theorem 2.19. *The monodromy matrix $M(T)$ has eigenvalues*

$$1, \mu_1, \mu_2, \ldots, \mu_{n-1},$$

where μ_i are the multipliers of the Poincaré map associated with the cycle Γ.

The eigenvalues of the monodromy matrix are called the **Floquet multipliers** of the limit cycle. The previous theorem shows that there is always a 'trivial' multiplier 1, which is denoted as μ_0. The multipliers with $|\mu| = 1$ are called the **critical multipliers**. If the trivial multiplier is simple and there are no other multipliers for which $|\mu| = 1$ holds, then the limit cycle is called **hyperbolic**. The limit cycle is locally **asymptotically stable** if for all multipliers μ except the trivial one it holds that $|\mu| < 1$. The limit cycle is **unstable** if for at least one multiplier it holds that $|\mu| > 1$.

We will now list the codim 1 and 2 bifurcations of limit cycles. Note that these bifurcations are exactly the codim 1 and codim 2 bifurcations of the fixed points of the Poincaré map.

2.4.1 Codimension 1 bifurcations of limit cycles

Limit Point of Cycles bifurcation

Definition 2.20. *The bifurcation associated with the appearance of $\mu_1 = 1$ is called a **Limit Point of Cycles bifurcation** (LPC, or Fold of Cycles bifurcation).*

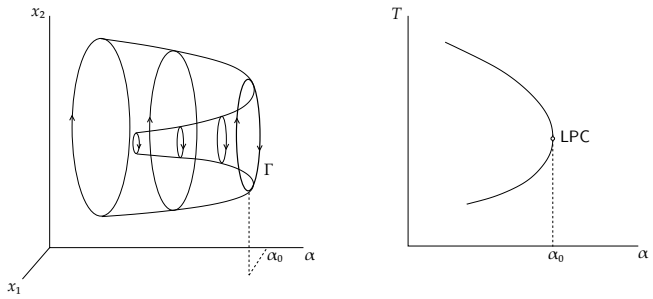

Figure 2.6: Limit Point of Cycles bifurcation.

As can be seen in Figure 2.6, an LPC point forms a turning point for periodic orbits. The normal form at the LPC bifurcation is given by the T-periodic two-dimensional

system

$$\begin{cases} \dot{\tau} = 1 - \xi + a\xi^2 + \dots, \\ \dot{\xi} = b\xi^2 + \dots. \end{cases} \tag{2.6}$$

Here, τ plays the role of the phase coordinate along the orbit and $\xi \in \mathbb{R}$ is a coordinate along a direction transversal to the periodic orbit. If $b = 0$, then the bifurcation is degenerate.

Period-Doubling bifurcation

Definition 2.21. *The bifurcation associated with the appearance of $\mu_1 = -1$ is called a **Period-Doubling bifurcation** (PD, or **Flip bifurcation**).*

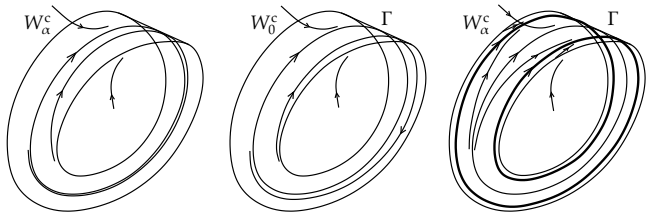

Figure 2.7: Period-Doubling bifurcation.

At a PD bifurcation a limit cycle emerges from the original limit cycle with a period that is approximately twice the original period (see Figure 2.7). The normal form at the PD bifurcation is given by the $2T$-periodic two-dimensional system

$$\begin{cases} \dot{\tau} = 1 + a\xi^2 + \dots, \\ \dot{\xi} = c\xi^3 + \dots. \end{cases} \tag{2.7}$$

The coordinates τ and $\xi \in \mathbb{R}$ have the same meaning as in the LPC case. In Figure 2.8, we have illustrated these coordinates for a PD bifurcation. If $c < 0$, the period doubled orbit is stable, if $c > 0$, the period doubled orbit is unstable. If $c = 0$, then the bifurcation is degenerate.

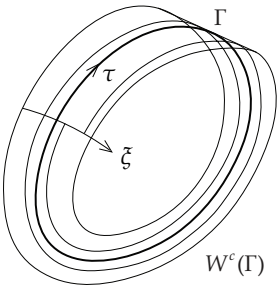

Figure 2.8: Illustration of τ- and ξ-coordinate for a PD bifurcation.

Neimark-Sacker bifurcation

Definition 2.22. *The bifurcation corresponding to the presence of* $\mu_{1,2} = e^{\pm i\theta_0}, 0 < \theta_0 < \pi$, *is called a* ***Neimark-Sacker bifurcation*** *(NS, or* ***torus bifurcation****).*

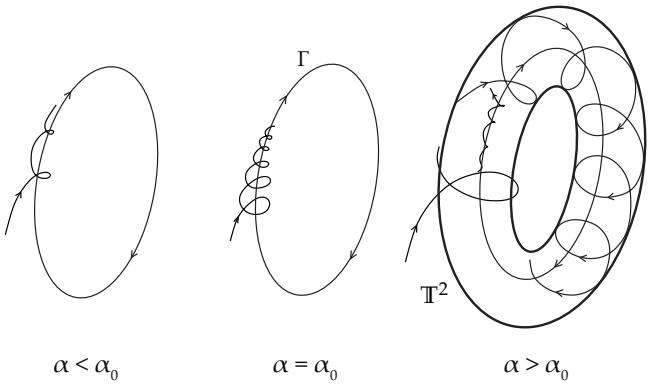

Figure 2.9: Neimark-Sacker bifurcation.

When crossing the critical parameter value, an invariant two-dimensional torus is born that leads to a change of stability of the periodic orbit (see Figure 2.9). The

normal form at the NS bifurcation is given by the T-periodic three-dimensional system

$$\begin{cases} \dot{\tau} = 1 + a|\xi|^2 + \dots, \\ \dot{\xi} = \frac{i\theta}{T}\xi + d\xi|\xi|^2 + \dots, \end{cases} \tag{2.8}$$

where $\xi \in \mathbb{C}$. If $\Re(d) < 0$, the born torus is stable, if $\Re(d) > 0$, the born torus is unstable. If $\Re(d) = 0$, then the bifurcation is degenerate.

2.4.2 Codimension 2 bifurcations of limit cycles

It is well known [3,67] that in generic two-parameter systems (2.1) only eleven codim 2 local bifurcations of limit cycles occur. We list them in Table 2.2. Note that the coefficients b, c and d appear in the critical normal forms of the LPC, PD and NS bifurcations, respectively. The multipliers mentioned in the table are assumed to be the only ones for which holds that $|\mu| = 1$.

Label	Name	Properties
CPC	Cusp Point of Cycles	$\mu_{0,1} = 1, b = 0$
GPD	Generalized Period-Doubling	$\mu_0 = 1, \mu_1 = -1, c = 0$
CH	Chenciner	$\mu_0 = 1, \mu_{1,2} = e^{\pm i\theta_0}, \Re(d) = 0$
R1	Strong Resonance 1:1	$\mu_{0,1,2} = 1$
R2	Strong Resonance 1:2	$\mu_0 = 1, \mu_{1,2} = -1$
R3	Strong Resonance 1:3	$\mu_0 = 1, \mu_{1,2} = e^{\pm i\frac{2\pi}{3}}$
R4	Strong Resonance 1:4	$\mu_0 = 1, \mu_{1,2} = e^{\pm i\frac{\pi}{2}}$
LPPD	Fold-Flip	$\mu_{0,1} = 1, \mu_2 = -1$
LPNS	Limit Point-Neimark-Sacker	$\mu_{0,1} = 1, \mu_{2,3} = e^{\pm i\theta_0}$
PDNS	Period-Doubling-Neimark-Sacker	$\mu_0 = 1, \mu_1 = -1, \mu_{2,3} = e^{\pm i\theta}$
NSNS	Double Neimark-Sacker	$\mu_0 = 1, \mu_{1,2} = e^{\pm i\theta_0}, \mu_{3,4} = e^{\pm i\theta_1}$

Table 2.2: Codim 2 bifurcations of limit cyles.

2.5 Homoclinic and heteroclinic orbits

Definition 2.23. *An orbit Γ starting at a point $x \in \mathbb{R}^n$ is called a **homoclinic orbit** to the equilibrium point x_0 of system (2.1) if $\varphi^t x \to x_0$ as $t \to \pm\infty$.*

Depending on the type of equilibrium there are two kinds of homoclinic orbits with codimension 1. For a **Homoclinic-to-Hyperbolic-Saddle orbit** (HHS orbit), the equilibrium is a saddle, for a **Homoclinic-to-Saddle-Node orbit** (HSN orbit), the equilibrium is a saddle-node.

Definition 2.24. *An orbit Γ starting at a point $x \in \mathbb{R}^n$ is called a **heteroclinic orbit** to the equilibrium points x_1 and x_2 of system (2.1) if $\varphi^t x \to x_1$ as $t \to -\infty$ and $\varphi^t x \to x_2$ as $t \to +\infty$.*

Heteroclinic orbits can have codimension 0, i.e. they are persistent under parameter variations, or a higher codimension. Pictures of a Homoclinic-to-Hyperbolic-Saddle and a heteroclinic orbit are given in Figure 2.10 (a), (b) respectively.

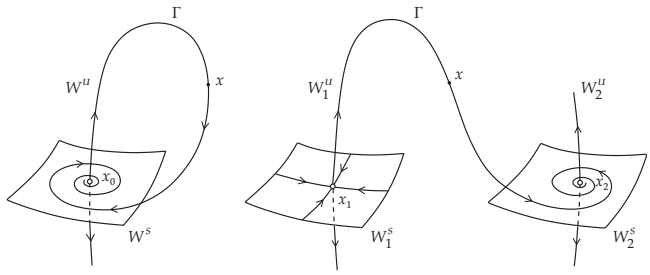

Figure 2.10: (a) Homoclinic orbit in $\mathbb{R}^3$. (b) Heteroclinic orbit in $\mathbb{R}^3$.

Consider a homoclinic orbit for a fixed parameter value α_0 at equilibrium x_0. There are two invariant sets related to this orbit, namely the stable and unstable

sets given by

$$W^S(x_0) = \{x \in \mathbb{R}^n | \varphi^t_{\alpha_0}(x) \to x_0 \text{ if } t \to +\infty\},$$
$$W^U(x_0) = \{x \in \mathbb{R}^n | \varphi^t_{\alpha_0}(x) \to x_0 \text{ if } t \to -\infty\},$$

respectively. These manifolds are tangent to the **stable (generalized) eigenspace** T^S, corresponding to the union of all eigenvalues μ of A with $\Re(\mu) < 0$, and the **unstable (generalized) eigenspace** T^U, corresponding to the union of all eigenvalues λ of A with $\Re(\lambda) > 0$, respectively. Denote with n_S the number of eigenvalues μ for which holds that $\Re(\mu) < 0$ and with n_U the number of eigenvalues λ for which holds that $\Re(\lambda) > 0$. Stable eigenvalues with maximal $\Re(\mu)$ are called the **leading stable eigenvalues**, while unstable eigenvalues with minimal $\Re(\lambda)$ are called the **leading unstable eigenvalues**.

2.6 Center manifolds

Hyperbolic equilibria are robust, i.e. small perturbations do not change qualitatively the phase portrait near the equilibrium. This is a consequence of the Hartman-Grobman theorem (continuous version of the theorem in Section 2.3). Therefore, when dealing with hyperbolic equilibria, it is sufficient to study the linearization of the system.

However, when dealing with nonhyperbolic equilibria, things get more complicated. This is the point where center manifolds are introduced. Next to the stable subspace, which corresponds to all eigenvalues with $\Re(\mu) < 0$ and the unstable subspace, which corresponds to all eigenvalues with $\Re(\lambda) > 0$, denote with T^c the **linear (generalized) eigenspace** of A corresponding to the union of the n_c eigenvalues on the imaginary axis. These eigenvalues are called the **critical eigenvalues**.

Theorem 2.25 (Center manifold theorem). *There is a locally defined smooth n_c-dimensional invariant manifold W^c of (2.1) that is tangent to T^c at $x = 0$. Moreover, there is a neighbourhood U of $x_0 = 0$ such that if $\varphi^t x \in U$ for all $t \geq 0$ $(t \leq 0)$, then $\varphi^t x \to W^c$ for $t \to +\infty$ $(t \to -\infty)$.*
There also exists a stable (unstable) invariant manifold W^S (W^U) that is tangent to the stable (unstable) eigenspace.

The manifold W^c is called the **center manifold**. To understand the bifurcation scenario around the equilibrium point, it is sufficient to investigate what happens in

the center manifold since this manifold is exponentially attractive or repelling. In this way, the study of a high-dimensional dynamical system can be reduced to the study of a low-dimensional center manifold.

2.7 Normal form theorems

In this section we concentrate on nonhyperbolic periodic orbits. Let $M(T) \in \mathbb{R}^{n\times n}$ be the monodromy matrix. From Theorem 2.19 it follows that 1 is always a multiplier of the periodic orbit. Let M_0 be the critical Jordan structure, i.e. the block diagonal matrix consisting of the critical Jordan blocks, starting with the block of the trivial multiplier 1. Let $\mu_k = e^{i\theta_k}(0 \leq \theta_k < \pi)$ be a critical multiplier with multiplicity m_k. The matrix $L_k \in \mathbb{R}^{m_k\times m_k}$ is defined as

$$L_k = \begin{pmatrix} \sigma_k & 1 & \dots & 0 \\ 0 & \sigma_k & \dots & 0 \\ \vdots & \ddots & \ddots & 1 \\ 0 & \dots & 0 & \sigma_k \end{pmatrix},$$

where σ_k is the Floquet exponent of multiplier μ_k, with $\sigma_k = i\theta_k/T$ in the case of multiplier 1 or a complex multiplier μ_k, and $\sigma_k = 0$ for $\mu_k = -1$. The matrix L_0 is the block diagonal matrix formed from the blocks L_k for which $|\mu_k| = 1$, starting with the block that corresponds with multiplier 1. The matrix $\tilde{L}_0$ is the matrix L_0 without the first row and the first column.

Proposition 2.26. *[59] To each Jordan block of size m_k of the monodromy matrix $M(T)$ corresponding to a critical multiplier $\mu_k \neq -1$, there exist m_k independent T-periodic C^l vector functions $w_j^{(\mu_k)}(\tau)$ such that*

$$\left(-\frac{d}{d\tau} + A(\tau) - \sigma_k\right) w_j^{(\mu_k)}(\tau) = \begin{cases} 0, & j = 0, \\ w_{j-1}^{(\mu_k)}(\tau), & j = 1,\dots,m_k - 1. \end{cases}$$

We consider the case $\mu_k = -1$ separately.

Proposition 2.27. *[59] For a Jordan block of size m_k of the monodromy matrix $M(T)$ belonging to multiplier -1, there exist m_k C^l vector functions $w_j^{(-1)}(\tau)$ such that*

- $w_j^{(-1)}(\tau + T) = -w_j^{(-1)}(\tau)$,
- $\left(-\frac{d}{d\tau} + A(\tau)\right) w_j^{(-1)}(\tau) = \begin{cases} 0, & j = 0, \\ w_{j-1}^{(-1)}(\tau), & j = 1, \ldots, m_k - 1. \end{cases}$

Define a Floquet operator $Q^{(\mu_k)}(\tau)$ to the subspace spanned by the vector functions $\{w_0^{(\mu_k)}, \ldots, w_{m_k-1}^{(\mu_k)}\}$ from Proposition 2.26 or Proposition 2.27 as

$$Q^{(\mu_k)}(\tau)\xi = \sum_{j=0}^{m_k-1} \xi_j w_j^{(\mu_k)}(\tau), \quad \forall \xi = (\xi_0, \ldots, \xi_{m_k-1}).$$

Denote with $E_0(\tau)$ the subspace spanned by the n_c vector functions $w_j^{(\mu_k)}(\tau), \forall j$, μ_k, built in Proposition 2.26 and Proposition 2.27. We can write

$$E_0(\tau) = \tilde{E}_0(\tau) \oplus \{\mathbb{R}\dot{u}_0(\tau)\},$$

where $\dot{u}_0(\tau)$ is the eigenfunction corresponding to the trivial multiplier 1. Denote with $Q_0(\tau)$ the Floquet operator to the $(n_c - 1)$-dimensional subspace spanned by $\tilde{E}_0(\tau)$. If all vector functions $w_j^{(\mu_k)}(\tau)$ correspond with multiplier 1 or a complex multiplier, the Floquet operator $Q_0(\tau)$ is T-periodic. However, if multiplier -1 is involved, we can write

$$Q_0(\tau)\xi = Q_{00}(\tau)\xi_{00} + Q_{01}(\tau)\xi_{01},$$

where $\xi = (\xi_{00}, \xi_{01})$. $Q_{00}(\tau)\xi_{00}$ belongs to the subspace spanned by the vector functions given in Proposition 2.26 and thus corresponding with multiplier 1 or a complex multiplier, and $Q_{01}(\tau)\xi_{01}$ belongs to the subspace spanned by the vector functions given in Proposition 2.27 and thus corresponding with multiplier -1. $Q_{00}(\tau)$ is T-periodic, while $Q_{01}(\tau)$ is $2T$-periodic.

We now give the normal form theorem in the simple case.

Theorem 2.28. *[59] Assume that*

- *the Jordan block of $M(T)$ belonging to the eigenvalue 1 is 1-dimensional,*
- *-1 is not an eigenvalue of $M(T)$.*

Then a center manifold for (2.1) in the neighbourhood of the periodic orbit Γ may be represented as

$$Z = u_0(\tau) + Q_0(\tau)\xi + H(\tau, \xi),$$

where $Q_0(\tau)$ is the T-periodic Floquet operator and H is T-periodic in τ and at least quadratic in ξ. A normal form for the vector field on the center manifold may be found such that (2.1) becomes

$$\begin{cases} \dfrac{d\tau}{dt} = 1 + p(\tau, \xi), \\ \dfrac{d\xi}{d\tau} = \tilde{L}_0\xi + P(\tau, \xi), \end{cases}$$

where p and P are T-periodic in τ, are polynomials at least quadratic in ξ and satisfy for any $\tau \in \mathbb{R}, \xi \in \mathbb{R}^{n_c-1}$

$$\begin{aligned} &\frac{d}{d\tau}p(\tau, \xi) - \frac{d}{d\xi}p(\tau, \xi)\tilde{L}_0^*\xi = 0, \\ &\frac{d}{d\tau}P(\tau, \xi) + \tilde{L}_0^*P(\tau, \xi) - \frac{d}{d\xi}P(\tau, \xi)\tilde{L}_0^*\xi = 0. \end{aligned}$$

We now consider the case that the Jordan block of $M(T)$ belonging to the trivial multiplier is more than one-dimensional. The normal form theorem in this nonsimple case is stated as follows.

Theorem 2.29. *[59] Assume that*

- *the Jordan block of $M(T)$ belonging to the eigenvector $\dot{u}_0$ is more than 1-dimensional,*
- *-1 is not an eigenvalue of $M(T)$.*

Then a center manifold for (2.1) in the neighbourhood of the periodic orbit Γ

may be represented as

$$Z = u_0(\tau) + Q_0(\tau)\xi + H(\tau, \xi),$$

where H is T-periodic in τ and at least quadratic in ξ. A normal form for the vector field on the center manifold may be found such that (2.1) becomes

$$\begin{cases} \dfrac{d\tau}{dt} = 1 + \xi_1 + p(\tau, \xi), \\ \dfrac{d\xi}{d\tau} = \tilde{L}_0\xi + P(\tau, \xi), \end{cases}$$

where p and P are T-periodic in τ, are polynomials at least quadratic in ξ and satisfy for any $\tau \in \mathbb{R}, \xi \in \mathbb{R}^{n_c-1}$

$$\begin{aligned} &\frac{d}{d\tau}p(\tau, \xi) - \frac{d}{d\xi}p(\tau, \xi)\tilde{L}_0^*\xi = 0, \\ &\frac{d}{d\tau}P(\tau, \xi) + \tilde{L}_0^*P(\tau, \xi) - \frac{d}{d\xi}P(\tau, \xi)\tilde{L}_0^*\xi = 0. \end{aligned}$$

Note that ξ_1 is the first coordinate of ξ and corresponds with multiplier 1. The last normal form theorem investigates the case when -1 is a Floquet multiplier. Define a symmetry $\tilde{S}_0$

$$\mathrm{Y} = (\mathrm{Y}_0, \mathrm{Y}_1) \mapsto \tilde{S}_0\mathrm{Y} = (\mathrm{Y}_0, -\mathrm{Y}_1)$$

such that

$$Q_0(\tau + T)\mathrm{Y} = Q_0(\tau)\tilde{S}_0\mathrm{Y}.$$

Theorem 2.30. *[59] Assume that*

- *-1 is an eigenvalue of $M(T)$.*

Then the results of Theorem 2.28 or Theorem 2.29 hold with the following modification: H, p and P are $2T$-periodic in τ such that

$$H(\tau + T, \xi) = H(\tau, \tilde{S}_0\xi)$$

and

$$p(\tau + T, \xi) = p(\tau, \tilde{S}_0\xi), \qquad P(\tau + T, \tilde{S}_0\xi) = \tilde{S}_0P(\tau, \xi),$$

for all $\tau \in \mathbb{R}$ *and* $\xi \in \mathbb{R}^{n_c-1}$.

The eigenfunctions $w_1, \ldots, w_{m_k-1}$ from Proposition 2.26 and Proposition 2.27 are called the **generalized eigenfunctions**. The (generalized) eigenfunctions of the adjoint operator are called the (generalized) **adjoint eigenfunctions**.

2.8 MatCont

MatCont is a numerical bifurcation software package in Matlab for the interactive study of dynamical systems and bifurcations. The package is freely available at *http://sourceforge.net/projects/matcont*. MatCont is a successor package to AUTO [37] and CONTENT [69], which are written in compiled languages (Fortran, C, C++).

2.8.1 MatCont: a continuation software

MatCont is based on **continuation** where a sequence of points that approximate a desired branch are computed starting from an initial guess. The continuation algorithm makes use of a predictor-corrector method.

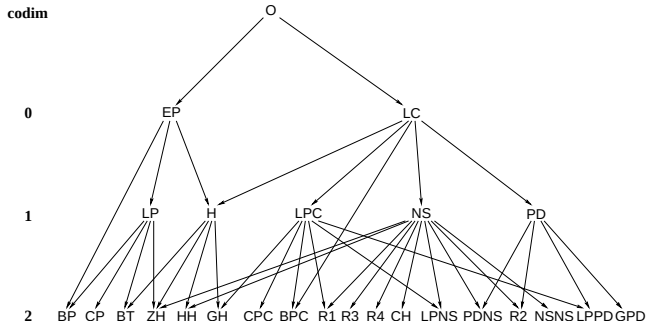

Figure 2.11: Graph of adjacency for equilibrium and limit cycle bifurcations in MatCont.

The relationships between the bifurcations of codim 0, 1 and 2 that are implemented in MatCont are visualized in Figure 2.11. By time-integration, represented

by the orbit O at the top, we can converge to a stable equilibrium (EP) or a stable periodic orbit (LC). From then on, continuation is used through which higher codimension bifurcations can be detected. For example, by continuation of a PD curve (codim 1), four codim 2 bifurcations can be detected, namely GPD, R2, LPPD and PDNS.

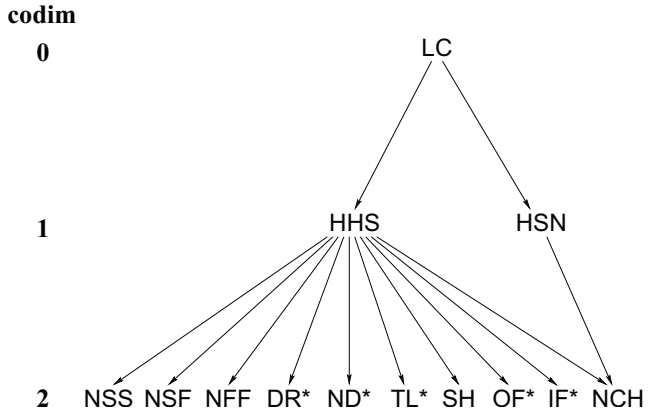

Figure 2.12: Graph of adjacency for homoclinic bifurcations in MatCont. * stands for S or U.

Relationships between homoclinic objects of codimension 1 and 2 computed by MatCont are presented in Figure 2.12. '*' stands for either S or U, depending on whether a stable or an unstable invariant manifold is involved. The labels of the bifurcations are listed in Table 2.3. During HSN continuation, only one bifurcation is tested for, namely the Noncentral Homoclinic-to-Saddle-Node orbit or NCH orbit. This orbit forms the transition between HHS and HSN curves. During HHS continuation, next to the detection of an NCH orbit 9 types of bifurcations are tested for. The characteristics and test functions for these bifurcations can be found in [25].

2.8.2 Discretization by collocation at Gauss points

In MatCont, the continuation of limit cycles makes use of orthogonal collocation. For the numerical study, the continuous limit cycle has to be discretized. Therefore, we first rescale the interval $[0, T]$ to the unit interval $[0, 1]$. We then deal with a standard boundary problem with function $Y(t) \in \mathbb{R}^n, t \in [0, 1]$, as unknown and

Type of object	Label
Neutral saddle	NSS
Neutral saddle-focus	NSF
Neutral Bi-Focus	NFF
Shilnikov-Hopf	SH
Double Real Stable leading eigenvalue	DRS
Double Real Unstable leading eigenvalue	DRU
Neutrally-Divergent saddle-focus (Stable)	NDS
Neutrally-Divergent saddle-focus (Unstable)	NDU
Three Leading eigenvalues (Stable)	TLS
Three Leading eigenvalues (Unstable)	TLU
Orbit-Flip with respect to the Stable manifold	OFS
Orbit-Flip with respect to the Unstable manifold	OFU
Inclination-Flip with respect to the Stable manifold	IFS
Inclination-Flip with respect to the Unstable manifold	IFU
Noncentral Homoclinic-to-Saddle-Node	NCH

Table 2.3: Bifurcations related to homoclinic orbits.

satisfying

$$\begin{cases} \dot{Y} = F(Y), \\ aY(0) + bY(1) = 0, \end{cases} \tag{2.9}$$

where F is a sufficiently smooth function and a, b are constant matrices.

To discretize it by a **collocation** method, the interval $[0,1]$ is subdivided into N intervals with grid points:

$$0 = \tau_0 < \tau_1 < \cdots < \tau_N = 1.$$

The points $\tau_0, \tau_1, \ldots, \tau_N$ form the **coarse mesh** Δ. We define $h = \max_i h_i$ where $h_i = \tau_{i+1} - \tau_i$. $Y(t)$ is approximated by a continuous function $Y^{\Delta}(t)$ that in each interval $[\tau_i, \tau_{i+1}]$ is a degree m polynomial, whose values are represented at equidistant mesh points, namely at

$$\tau_{i,j} = \tau_i + \frac{j}{m} h_i \quad (j = 0, 1, ..., m).$$

We note that $\tau_{i,m} = \tau_{i+1} = \tau_{i+1,0}$ for $0 \leq i \leq N-1$. These grid points form the **fine mesh**. In each interval $[\tau_i, \tau_{i+1}]$ we require the polynomials to satisfy the

differential equation in (2.9) exactly at m collocation points, i.e. Nmn conditions that have to be specified. Denote with x_M the vector of the function values at the fine mesh points, with x_C the vector of the function values at the collocation points and with $\dot{x}_C$ the vector of the derivative values at the collocation points. The best choice for the collocation points are the Gauss points $\zeta_{i,j}$, i.e. the roots of the Legendre polynomial of degree m, relative to the interval $[\tau_i, \tau_{i+1}]$ [20, 30]. Note that the mesh is nonuniform and adaptive. We also require the polynomials to satisfy the boundary conditions in (2.9). Under generic regularity conditions for system (2.9) De Boor and Swartz [20] proved that $Y^{\Delta}(t)$ converges uniformly over $[0,1]$ to $Y(t)$ with order h^{m+1} and with order h^{2m} ('**superconvergence**') at the points of the coarse mesh.

3

Interactive Initialization and Continuation of Homoclinic and Heteroclinic Orbits

In this chapter we discuss a homotopy method that makes it possible to initiate a homoclinic or heteroclinic orbit, starting from an equilibrium point.

3.1 Introduction

Homoclinic and heteroclinic orbits, also called **connecting orbits**, are important in applications for a number of reasons. They underlie phenomena in fluid mechanics [7], model 'excitation' in models of biological cells [86], chaotic vibration of structures [81], chaotic behaviour of electronic circuits [18, 46, 47], light pulses in fiber optics [80], chemical reactions [54], wave solutions in combustion models [9], etc.

The detection of a connecting orbit is a quite delicate work because of the sensitive dependence on initial conditions and on parameter values. MatCont sup-

ports several methods to initialize homoclinic orbits, including one that is based on the approximation of the homoclinic orbit by a limit cycle with large period [32]. However, there are many ODEs (e.g. ODEs describing travelling impulses) where the corresponding limit cycles are of the saddle type (i.e. unstable) and cannot be found by numerical integration. Often such cycles are not born via local Hopf-like bifurcations. We therefore need a method with a good chance of success in finding the connecting orbits, even in difficult problems.

The **homotopy** (i.e. successive continuations) method first described in [39, 40] is a powerful tool that makes use of a systematic procedure to detect a sufficiently accurate starting orbit for the continuation of the connecting orbits. Starting from the same basic ideas, we present new and improved algorithms for the numerical initialization and continuation of homoclinic and heteroclinic orbits.

The first efficient methods for continuation of homoclinic or heteroclinic orbits to equilibria were implemented as HomCont toolbox in the standard software AUTO, see [10, 15, 16, 38]. As in MatCont, these methods are based on the truncated boundary value problems (**BVPs**) with projection boundary conditions and integral phase conditions, which are discretized using piecewise-polynomial approximation with orthogonal collocation. However, there are essential differences between HomCont and our implementation. HomCont employs a technique due to [10] to ensure the smoothness of the bases in the generalized eigenspaces used in the projection boundary conditions. These bases are originally computed in each step by black-box linear algebra routines. As a consequence some blocks of the Jacobian matrix of the discretized projection BVP are approximated by finite differences, even if all partial derivatives of the right-hand side of (2.1) w.r.t. (x, α) are provided by the user. Our construction of the projection boundary conditions is different and is based on the 'Continuation of Invariant Subspaces' algorithm [35], where the Riccati equations play the central role. However, unlike [29], we include the Riccati equations in the defining truncated BVP. This allows us to set up the Jacobian matrix of the discretized defining system avoiding finite differences, if the user-supplied derivatives are available. In this way we simultaneously continue the connecting solution and the (orthogonal complements to) stable and unstable invariant subspaces of the Jacobian, which makes the continuation more robust.

In this chapter, we rigourously describe the homotopy methods for Homoclinic-to-Hyperbolic-Saddle orbits, for Homoclinic-to-Saddle-Node orbits and for heteroclinic orbits and discuss their implementation details in MatCont. We begin by introducing the defining system for HHS orbits in Section 3.2.1. The differences for the defining systems for HSN and heteroclinic orbits are highlighted in Section 3.2.2

and Section 3.2.3. In Section 3.3 we discuss the possible ways of initializing a HHS orbit in MatCont, i.e. either starting from a limit cycle with large period, or making use of the successive continuations method. A detailed decription of the algorithm of the homotopy method and the interactive implementation in MatCont is given in Section 3.3.2. Variants of the homotopy methods for HSN orbits, starting from only a saddle-node equilibrium, and heteroclinic orbits, starting from two equilibria, are discussed in Section 3.4 and in Section 3.5, respectively. The successive homotopy and continuation steps are implemented in a user-friendly way in the graphical user interface in MatCont. We illustrate the effectiveness of the homotopy method by numerous examples in Section 3.6, which should convince the reader of its robustness.

3.2 Extended Defining System for Continuation

In this section we describe the defining equations for the continuation of HHS orbits, HSN orbits and heteroclinic orbits.

3.2.1 Homoclinic-to-Hyperbolic-Saddle orbits

Suppose that the eigenvalues of the Jacobian matrix $f_x(x_0, \alpha_0)$ can be ordered according to

$$\Re(\mu_{n_S}) \leq ... \leq \Re(\mu_1) < 0 < \Re(\lambda_1) \leq ... \leq \Re(\lambda_{n_U}).$$

For the continuation of HHS orbits, two system parameters have to be varied. We will now discuss the defining system for the continuation of these homoclinic orbits.

Defining system

To allow a discretization of the HHS orbits, the infinite time interval is truncated, so that instead of $[-\infty, +\infty]$ we use $[-T, +T]$, where T is the half-return time. The discretization is then the same as for limit cycles, see Section 2.8.2, which means that the equation

$$\dot{x}(t) - 2Tf(x(t), \alpha) = 0, \tag{3.1}$$

must be satisfied in the collocation points.

The second part in the defining system is the equilibrium condition

$$f(x_0, \alpha) = 0. \tag{3.2}$$

Third, there is a so-called **phase condition** for the homoclinic solution, which is not always used but helps to improve the homoclinic continuation

$$\int_0^1 \dot{\widetilde{x}}^*(t)[x(t) - \widetilde{x}(t)]dt = 0. \tag{3.3}$$

As for limit cycles, $\widetilde{x}(t)$ is some initial guess for the solution, typically obtained from the previous continuation step. Note that in the literature also another phase condition is used, see for example [38]. However, in the present implementation we employ condition (3.3).

Fourth, there are the homoclinic-specific constraints to the solution. For these we need access to the stable and unstable eigenspaces of the system linearized about the equilibrium after each step. It is not efficient to recompute these spaces from scratch in each continuation-step. Instead, we use the algorithm for continuing invariant subspaces using only algebraic arguments, a modification of the method from [12, 29, 35]. We now summarize the steps in this algorithm; details and an extensive algebraic justification are given in [64].

Suppose we have the following block Schur factorization for $A(0) = f_x(x_0, \alpha_0)$, the Jacobian matrix at the equilibrium point of a known homoclinic orbit, taken as a base point for the continuation

$$A(0) = Q(0)\ R(0)\ Q^{\mathrm{T}}(0), \quad Q(0) = [Q_1(0)\ Q_2(0)],$$

where $A(0)$, $R(0)$ and $Q(0)$ are $n \times n$-matrices, $Q(0)$ is orthogonal, $Q_1(0)$ has dimensions $n \times k$ and $R(0)$ is block upper triangular

$$R(0) = \begin{bmatrix} R_{11} & R_{12} \\ 0 & R_{22} \end{bmatrix},$$

where R_{11} is an $k \times k$-block (R_{11} and R_{22} are not required to be triangular). Then the columns of $Q_1(0)$ span an invariant subspace $P(0)$ of dimension k (e.g. the stable or unstable subspace) of $A(0)$, and the columns of $Q_2(0)$ span the orthogonal complement $P(0)^{\perp}$.

What we need for the continuation are the subspace-defining columns for a matrix $A(s)$ close to $A(0)$, without having to compute everything explicitly again. We will call these matrices $Q_1(s)$ and $Q_2(s)$ with

$$A(s) = Q(s)\ R(s)\ Q^{\mathrm{T}}(s), \quad Q(s) = [Q_1(s)\ Q_2(s)],$$

where s parameterizes the curve of homoclinic orbits.

As shown in [34], it is always possible to obtain a smooth path of block Schur factorizations and we can accumulate all transformations in such a way that we are always looking for corrections close to the identity. Therefore, we can write (for s sufficiently small)

$$Q(s) = Q(0)\ U(s), \quad U(0) = I_{n\times n}, \tag{3.4}$$

so that we now need to compute the $n \times n$-matrix $U(s)$. By partitioning $U(s)$ in blocks of the same size as we partitioned $R(0)$, we obtain

$$U(s) = [U_1(s)\ U_2(s)] = \begin{bmatrix} U_{11}(s) & U_{12}(s) \\ U_{21}(s) & U_{22}(s) \end{bmatrix},$$

where $U_{11}(s)$ has dimensions $k \times k$, and $U_{22}(s)$ has dimensions $(n-k) \times (n-k)$.

In [64] it is proven that we can always assume that $U_{11}(s)$ and $U_{22}(s)$ are symmetric positive-definite, by redefining $Q(s)$ and $R(s)$ if necessary. Now define for all s the $(n-k) \times k$-matrix $Y(s)$ as

$$Y(s) = U_{21}(s)U_{11}^{-1}(s).$$

It is shown in [12, 64] that $U(s)$ can be written completely in terms of $Y(s)$:

$$U(s) = \tag{3.5}$$
$$\left[\begin{pmatrix} I \\ Y(s) \end{pmatrix} (I + Y(s)^{\mathrm{T}}Y(s))^{-\frac{1}{2}} \quad \begin{pmatrix} -Y(s)^{\mathrm{T}} \\ I \end{pmatrix} (I + Y(s)Y(s)^{\mathrm{T}})^{-\frac{1}{2}}\right].$$

We now define $T_{11}(s), T_{12}(s), T_{21}(s)$ and $T_{22}(s)$ by

$$Q(0)^{\mathrm{T}}\ A(s)\ Q(0) = \begin{bmatrix} T_{11}(s) & T_{12}(s) \\ T_{21}(s) & T_{22}(s) \end{bmatrix}. \tag{3.6}$$

Here $T_{11}(s)$ is of size $k \times k$ and $T_{22}(s)$ is an $(n-k) \times (n-k)$-matrix. Using the invariant subspace relation

$$Q_2^{\mathrm{T}}(s)\ A(s)\ Q_1(s) = 0,$$

and executing substitutions using (3.4), (3.5) and (3.6), we obtain the following algebraic **Riccati equation** for $Y(s)$:

$$T_{22}(s)\ Y(s) - Y(s)\ T_{11}(s) + T_{21}(s) - Y(s)\ T_{12}(s)\ Y(s) = 0. \tag{3.7}$$

So to do a quick and smooth subspace continuation of both stable and unstable subspaces, we only need to keep track of the two small matrices $Y_S(s) \in \mathbb{R}^{(n-n_S)\times n_S}$ (with S for stable) and $Y_U(s) \in \mathbb{R}^{(n-n_U)\times n_U}$ (with U for unstable). We use a similar notation for the stable and unstable variants of $T_{11}(s), T_{12}(s), T_{21}(s)$ and $T_{22}(s)$. From the matrices $Y_S(s)$ and $Y_U(s)$, we can easily compute the span of the stable and unstable subspaces, and their orthogonal complements.

Therefore, a stable and an unstable variant of the Ricatti equation (3.7) are added to the defining system for the continuation to keep track of the matrices $Y_S(s)$ and $Y_U(s)$

$$\begin{aligned} T_{22U}(s)Y_U(s) - Y_U(s)T_{11U}(s) + T_{21U}(s) - Y_U(s)T_{12U}(s)Y_U(s) = 0, \\ T_{22S}(s)Y_S(s) - Y_S(s)T_{11S}(s) + T_{21S}(s) - Y_S(s)T_{12S}(s)Y_S(s) = 0. \end{aligned} \tag{3.8}$$

We can now formulate constraints on the behaviour of the solution close to the equilibrium x_0. The initial vector $x(0) - x_0$ of the orbit is placed in the unstable eigenspace of the system in the equilibrium. We express this by the requirement that it is orthogonal to the orthogonal complement of the unstable eigenspace. Analogously, the end vector $x(1) - x_0$ of the orbit is placed in the stable eigenspace of the system in the equilibrium. This is expressed by the requirement that the vector is orthogonal to the orthogonal complement of the stable eigenspace.

Let $Q_U(0)$ be the orthogonal matrix from the base point related to the unstable invariant subspace. From (3.4) and (3.5) it follows that a basis of that subspace in a point s can be computed by

$$Q^U(s) = Q_U(0) \begin{bmatrix} I \\ Y_U(s) \end{bmatrix},$$

while a basis for the orthogonal complement to that subspace can be computed by

$$Q^{U^\perp}(s) = Q_U(0) \begin{bmatrix} -Y_U(s)^{\mathrm{T}} \\ I \end{bmatrix}.$$

Note that in general the bases $Q^U(s)$ and $Q^{U^\perp}(s)$ are not orthogonal. The matrices for the stable subspace can be computed similarly. The equations to be added to the system are then

$$\begin{aligned} Q^{U^\perp}(s)^{\mathrm{T}}(x(0) - x_0) = 0, \\ Q^{S^\perp}(s)^{\mathrm{T}}(x(1) - x_0) = 0. \end{aligned} \tag{3.9}$$

Note that the initial values of $Y_U(0), Y_S(0)$ are the zero matrices.

Finally, the distances between $x(0)$ and x_0 and between $x(1)$ and x_0 must be taken into account, so that the following equations are added

$$\begin{aligned} \|x(0) - x_0\| - \varepsilon_0 = 0, \\ \|x(1) - x_0\| - \varepsilon_1 = 0. \end{aligned} \tag{3.10}$$

These distances ε_0 and ε_1 should be small enough. The half-return time T, ε_0 and ε_1 are called the **homoclinic parameters**.

After a user-chosen number of steps, the base point is adapted. This means that $Q_U(0)$ and $Q_S(0)$ are recomputed, Y_U and Y_S are reset to zero, and the mesh is adapted.

Implementation in MatCont

The basic defining system for the continuation of a HHS orbit in two free system parameters consists of (3.1), (3.2), (3.8), (3.9) and (3.10) with T free and ε_0 and ε_1 fixed. So the phase condition (3.3) is not used.

Alternatively, the phase condition (3.3) is added automatically if from the triple (T, ε_0, ε_1) two homoclinic parameters are freed, instead of just one. Any combination of one or two parameters of that triple is possible.

The variables in the defining system are stored in one vector. It contains consecutively the values of $x(t)$ in the fine mesh points (including $x(0)$ and $x(1)$), the free homoclinic parameters, two free system parameters, the coordinates of the saddle x_0, and the elements of the matrices Y_S and Y_U.

3.2.2 Homoclinic-to-Saddle-Node orbits

When the equilibrium x_0 is a saddle-node, the eigenvalues of $f_x(x_0, \alpha_0)$ can be ordered as

$$\Re(\mu_{n_S}) \leq ... \leq \Re(\mu_1) < \nu = 0 < \Re(\lambda_1) \leq ... \leq \Re(\lambda_{n_U}).$$

For a Homoclinic-to-Saddle-Node orbit, the extended defining system undergoes some small changes. The vector $x(0) - x_0$ has to be placed in the **center-unstable subspace** (i.e. the subspace spanned by the eigenvectors corresponding to the eigenvalues $\nu, \lambda_1, \ldots, \lambda_{n_U}$), instead of the unstable space. Analogously, $x(1) - x_0$ must be in the **center-stable subspace** (i.e. the subspace spanned by the eigenvectors corresponding to the eigenvalues $\nu, \mu_1, \ldots, \mu_{n_S}$).

The vector-condition is again implemented by requiring that the vector is orthogonal to the orthogonal complement of the corresponding space. So the equations (3.9) themselves do not really change; the changes happen in the computation of the matrices Q. Indeed, the equations (3.9) correspond now with $n-1$ restrictions, i.e. one condition less than in the case of Homoclinic-to-Hyperbolic-Saddle orbits.

The number of equations is restored by adding the constraint that the equilibrium must be a saddle-node, i.e. the equilibrium has the eigenvalue $\nu = 0$. For this we use the **bordering technique**, as described in Section 4.2.1 of [49]. The technique basically requires g to be zero, where g is obtained by solving

$$\begin{pmatrix} f_x(x_0,\alpha) & w_{bor} \\ v_{bor}^{\mathrm{T}} & 0 \end{pmatrix} \begin{pmatrix} v \\ g \end{pmatrix} = \begin{pmatrix} 0 \\ 1 \end{pmatrix}. \tag{3.11}$$

Here w_{bor} and v_{bor} are bordering vectors, chosen in such a way that the matrix in (3.11) is nonsingular. These vectors have to be adapted at the adaptation steps. Taking the previous remarks into account, the defining system for the continuation of HSN orbits is given by $(3.1) - (3.2) - (g = 0) - (3.3) - (3.8) - (3.9) - (3.10)$.

3.2.3 Heteroclinic Orbits

The defining equations for the continuation of heteroclinic orbits are very similar to the ones of HHS orbits. The following small changes have to be executed. The vector $x(1) - x_1$ has to be placed in the stable eigenspace of x_1, the end distance $\|x(1) - x_1\|$ has to be small enough and the Schur decomposition in the stable variant of the Ricatti equation factorizes the matrix $f_x(x_1, \alpha_0)$. Therefore, the defining system is given by

$$\begin{aligned}
&\dot{x}(t) - 2Tf(x(t),\alpha) = 0,\\
&f(x_0,\alpha) = 0,\\
&f(x_1,\alpha) = 0,\\
&\int_0^1 \dot{\tilde{x}}^*(t)[x(t) - \tilde{x}(t)]dt = 0,\\
&T_{22U}(s)Y_U(s) - Y_U(s)T_{11U}(s) + T_{21U}(s) - Y_U(s)T_{12U}(s)Y_U(s) = 0,\\
&T_{22S}(s)\,Y_S(s) - Y_S(s)\,T_{11S}(s) + T_{21S}(s) - Y_S(s)\,T_{12S}(s)\,Y_S(s) = 0,\\
&Q^{U^\perp}(s)^{\mathrm{T}}(x(0) - x_0) = 0,
\end{aligned}$$

$$Q^{S^\perp}(s)^{\mathrm{T}}(x(1)-x_1)=0,$$
$$\|x(0)-x_0\|-\varepsilon_0=0,$$
$$\|x(1)-x_1\|-\varepsilon_1=0.$$

3.3 Starting Strategies for Homoclinic-to-Hyperbolic-Saddle orbits

In this section we examine two ways in which the continuation of HHS orbits in MatCont can be initialized. We briefly review the earlier implemented method where the HHS orbit is started from a limit cycle with a large period [32]. The algorithm and our implementation of the initialization by making use of the homotopy method, starting from a saddle equilibrium will be extensively discussed in Section 3.3.2.

3.3.1 Starting from a limit cycle with large period

When starting from a limit cycle with large period, the user must first declare the cycle to be close to a Homoclinic-to-Hyperbolic-Saddle orbit. Automatically, initial values for the homoclinic parameters are computed. The program looks for the point on the cycle with smallest $\|f(x,\alpha)\|$. This point is taken as a first approximation for the equilibrium x_0.

The mesh points of the limit cycle are kept as mesh points for the homoclinic orbit, except for the mesh interval that contains the current equilibrium approximation. This mesh interval is deleted, as it will grow to infinity in the homoclinic orbit. In memory, the stored cycle then needs to be 'rotated', so that the first point $x(0)$ and the last point $x(1)$ of the homoclinic orbit are effectively stored as first and last point, respectively. Half of the time span of the remaining part of the cycle is kept as initial value for T. Initial values for ε_0 and ε_1 are also computed; these are found by simply computing the distance from $x(0)$ and $x(1)$ to the approximated equilibrium.

Then the user has to select 2 free system parameters, and 1 or 2 of the homoclinic parameters $T,\varepsilon_0,\varepsilon_1$. The defining system (i.e. the number of equations) is automatically adjusted according to the choice of the user.

3.3.2 Starting by homotopy

The method

For the initialization of HHS orbits, there is an efficient method that constructs a Homoclinic-to-Hyperbolic-Saddle orbit starting from only the saddle equilibrium $x_0^{(0)}$.

As described in Section 3.2.1, the defining equations for the continuation of a homoclinic orbit can be written as

$$\begin{aligned}
&\dot{x}(t) - 2Tf(x(t),\alpha) = 0,\\
&f(x_0,\alpha) = 0,\\
&\int_0^1 \dot{\tilde{x}}^*(t)[x(t) - \tilde{x}(t)]dt = 0,\\
&Q^{U^\perp,\mathrm{T}}(x(0) - x_0) = 0,\\
&Q^{S^\perp,\mathrm{T}}(x(1) - x_0) = 0,\\
&T_{22U}Y_U - Y_U T_{11U} + T_{21U} - Y_U T_{12U} Y_U = 0,\\
&T_{22S}Y_S - Y_S T_{11S} + T_{21S} - Y_S T_{12S} Y_S = 0,\\
&\|x(0) - x_0\| - \varepsilon_0 = 0,\\
&\|x(1) - x_0\| - \varepsilon_1 = 0,
\end{aligned} \tag{3.12}$$

where $Q^{U^\perp} \in \mathbb{R}^{n\times n_S}, Q^{S^\perp} \in \mathbb{R}^{n\times n_U}, Y_U \in \mathbb{R}^{n_S\times n_U}$ and $Y_S \in \mathbb{R}^{n_U\times n_S}$.

If the phase condition is added in the continuation, two of the three homoclinic parameters $T, \varepsilon_0, \varepsilon_1$ are freed, otherwise just one homoclinic parameter is freed. Without phase condition the number of constraints is equal to $Nmn + 2n + 2 + 2n_U n_S$. The free scalar variables are given by $x_M, x_0, \alpha_1, T, Y_U, Y_S$, where α_1 is the free system parameter, so that the number of free scalar variables equals $Nmn + 2n + 2 + 2n_U n_S$. If the phase condition is added, the number of constraints is augmented by one and an extra homoclinic parameter has to be freed. For continuation, a second system parameter has to be freed.

Initially the projections $Q^{U^\perp,(0)}$ and $Q^{S^\perp,(0)}$ are constructed using the real Schur factorizations:

$$\begin{aligned}
f_x(x_0^{(0)},\alpha) &= Q_0^{(0)} R_0^{(0)} Q_0^{(0),T}, \quad Q_0^{(0)} = [Q^{U,(0)}\ Q^{U^\perp,(0)}],\\
f_x(x_0^{(0)},\alpha) &= Q_1^{(0)} R_1^{(0)} Q_1^{(0),T}, \quad Q_1^{(0)} = [Q^{S,(0)}\ Q^{S^\perp,(0)}].
\end{aligned} \tag{3.13}$$

These first factorizations are chosen so that the n_U columns $q^{(0)}_{0,1},...,q^{(0)}_{0,n_U}$ of $Q^{U,(0)}$ form an orthonormal basis of the right invariant subspace S^U_0 of $f_x(x^{(0)}_0,\alpha)$, corresponding to the eigenvalues $\lambda^{(0)}_1,...,\lambda^{(0)}_{n_U}$, and the $n_S = n - n_U$ columns $q^{(0)}_{0,n_U+1},...,$ $q^{(0)}_{0,n_U+n_S}$ of $Q^{U^\perp,(0)}$ form an orthonormal basis of the orthogonal complement $S^{U^\perp}_0$. Similarly, the n_S columns $q^{(0)}_{1,1},...,q^{(0)}_{1,n_S}$ of $Q^{S,(0)}$ form an orthonormal basis of the right invariant subspace S^S_0 of $f_x(x^{(0)}_0,\alpha)$, corresponding to the eigenvalues $\mu^{(0)}_1,...,$ $\mu^{(0)}_{n_S}$, and the n_U columns $q^{(0)}_{1,n_S+1},...,q^{(0)}_{1,n_S+n_U}$ of $Q^{S^\perp,(0)}$ form an orthonormal basis of the orthogonal complement $S^{S^\perp}_0$.

Moreover, let $S^U_{0,k}$, $k = 1,...,n_U$, be the right invariant subspace of $f_x(x^{(0)}_0,\alpha)$ corresponding to the eigenvalues $\lambda^{(0)}_1,...,\lambda^{(0)}_k$, whenever either $\lambda^{(0)}_k$ is real or the couple $(\lambda^{(0)}_{k-1},\lambda^{(0)}_k)$ forms a conjugate pair of complex eigenvalues. Then the first k columns $q^{(0)}_{0,1},...,q^{(0)}_{0,k}$ of $Q^{(0)}_0$ form an orthonormal basis of $S^U_{0,k}$ and the remaining $n-k$ columns $q^{(0)}_{0,k+1},...,q^{(0)}_{0,n}$ of $Q^{(0)}_0$ form an orthonormal basis of the orthogonal complement $S^{U^\perp}_{0,k}$. The analog holds for the subspace corresponding to the negative eigenvalues.

The construction process of a homoclinic orbit fitting the equations (3.12), from a saddle equilibrium, is splitted into several steps in the algorithm below. The basic ideas of this homotopy method were formulated in [39,40]. We first give the outline of the algorithm and then write down the explicit equations.

The beginning vector $x(0) - x_0$ of a homoclinic orbit lies in the eigenspace of the leading unstable eigenvalues. We start by choosing an initial point in this space, not far from the saddle equilibrium $x^{(0)}_0$, say $x(0) = x^{(0)}_0 + \varepsilon_0(c_1 q^{(0)}_{0,1} + c_2 q^{(0)}_{0,2})$. Here, c_2 is nonzero only when λ_1 and λ_2 form a complex conjugate pair. Now there are two possibilities. Either, we obtain an initial connecting orbit by time integration, starting from the above mentioned point $x(0)$. Or, we initialize a small connecting orbit segment $[0,T]$ by the constant $x(0)$ and extend this initial orbit segment by continuation with respect to T.

Define $\tau_i = \frac{1}{\varepsilon_1}\langle x(1) - x^{(0)}_0, q^{(0)}_{1,n_S+i}\rangle$, for $i = 1,\ldots,n_U$. Typically, the initial connecting orbit is a crude orbit with initial point $x(0) \in S^U_0$ but the terminal point $x(1) \notin S^S_0$. Hence the τ_i's are, in general, nonzero. However, for a HHS orbit it must hold that $x(1) \in S^S_0$ so $\tau_i = 0$, for $i = 1,\ldots,n_U$. By a sequence of

homotopies we will locate zero intercepts of the τ_i's.

Define now c_i as $c_i = \frac{1}{\varepsilon_0}\langle x(0) - x_0^{(0)}, q_{0,i}^{(0)}\rangle$, for $i = 1, \ldots, n_U$. This is consistent with the use of c_1 and c_2 in the definition of $x(0)$ above. In the first homotopy step we try to locate a zero intercept of one of the τ_i's. To this end, all τ_i's are free and both c_1 and c_2 are free under the restriction that $c_1^2 + c_2^2 = 1$, since $\|x(0) - x_0\| = \varepsilon_0$. In the following homotopy steps, we fix all τ_j's that are zero already, and try to locate a zero of another τ_i, while each time freeing an additional c_i, to replace the fixed equation $\tau_j = 0$ and thus to keep the same number of free variables. So, in the successive steps we let the initial point $x(0)$ vary within a wider subspace of the unstable eigenspace S_0^U of $x_0^{(0)}$ in order to place the end point $x(1)$ in the stable eigenspace S_0^S of $x_0^{(0)}$. More specifically, we keep $x(1)$ free, while $x(0)$ is allowed to vary on the hypersphere in S_0^U of radius ε_0.

In the previous successive homotopies, zero intercepts are detected of all τ_i's except for one. This last τ_i can be made zero, by varying one component of the system parameter α. This requires recalculation of the saddle equilibrium x_0, and of the matrices $Q^{U^\perp}$ and $Q^{S^\perp}$, by use of the matrices Y_U and Y_S. When having detected a zero intercept of the last τ_i, the end vector $x(1) - x_0$ lies within the stable eigenspace S_0^S of x_0. However, the distance ε_1 is not necessarily small. Therefore, one more continuation, with T, ε_1 and one system parameter free, is needed to make ε_1 small enough in order to find a proper starting orbit for the continuation of homoclinic orbits.

In each homotopy step we compute a branch, i.e. a one-dimensional manifold, of solutions. For this there must hold that $n_c - n_v = -1$, where n_c is the number of constraints and n_v is the number of free scalar variables.

The described procedure converges, provided the initialization is sufficiently close to the homoclinic situation, see convergence theorem in [39].

The algorithm

We now describe the algorithm in detail.

ALGORITHM. Locating a homoclinic orbit by homotopy.

Input.
$x_0^{(0)} \in \mathbb{R}^n$, $\alpha \in \mathbb{R}^p$, $f_x(x_0^{(0)}, \alpha)$, and the real Schur factorizations (3.13).

1. **Locating a connecting orbit, α is fixed.**

Step 1. We have already mentioned that either a time integration or a continuation can be used to compute an initial connecting orbit. When we use time integration, the starting point is given by

$$x(0) = x_0^{(0)} + \varepsilon_0(c_1 q_{0,1}^{(0)} + c_2 q_{0,2}^{(0)}),$$

where c_2 is zero, except in the case that the eigenvalues with smallest positive real part consist of a complex conjugate pair. Note that $c_1^2 + c_2^2 = 1$ and $c_3 = \ldots = c_{n_U} = 0$.

If continuation is used, set the algorithm parameters ε_0 and T to small, positive values, so that $x(t)$ is approximately constant on $[0, T]$, or after rescaling on $[0, 1]$. To be specific, set

$$x(t) = x_0^{(0)} + \varepsilon_0(c_1 q_{0,1}^{(0)} + c_2 q_{0,2}^{(0)}), \quad 0 \le t \le 1,$$

with the same remark for c_2 as above. Extend this small starting segment by continuation where the defining equations are given by

$$\begin{aligned}
&\dot{x}_C - 2Tf(x_C, \alpha) = 0,\\
&\varepsilon_0 c_i - \langle x(0) - x_0^{(0)}, q_{0,i}^{(0)} \rangle = 0, \quad i = 1, \ldots, n_U,\\
&\tau_i - \frac{1}{\varepsilon_1}\langle x(1) - x_0^{(0)}, q_{1,n_S+i}^{(0)} \rangle = 0, \quad i = 1, \ldots, n_U,\\
&\langle x(0) - x_0^{(0)}, q_{0,n_U+i}^{(0)} \rangle = 0, \quad i = 1, \ldots, n_S,\\
&\| x(1) - x_0^{(0)} \| - \varepsilon_1 = 0.
\end{aligned} \tag{3.14}$$

This gives us $n_c = Nmn + n + n_U + 1$ constraints and the free scalar variables are $x_M, \tau_1, \ldots \tau_{n_U}, T, \varepsilon_1$ so that $n_v = Nmn + n + n_U + 2$. Therefore, it is possible to compute a branch of solutions to system (3.14) in the direction of increasing T.

Typically ε_1 initially increases and then starts to decrease. In practice one usually executes time-integration or continuation until ε_1 stops decreasing, its value being not necessarily small.

Steps k, $k = 2, \ldots, n_U$ *(for* $n_U > 1$*).* Compute a branch of solutions to the

system

$$\begin{aligned}
&\dot{x}_C - 2Tf(x_C, \alpha) = 0,\\
&\varepsilon_0 c_i - \langle x(0) - x_0^{(0)}, q_{0,i}^{(0)} \rangle = 0, \quad i = 1, ..., n_U,\\
&\tau_i - \frac{1}{\varepsilon_1} \langle x(1) - x_0^{(0)}, q_{1,n_S+i}^{(0)} \rangle = 0, \quad i = 1, ..., n_U,\\
&\langle x(0) - x_0^{(0)}, q_{0,n_U+i}^{(0)} \rangle = 0, \quad i = 1, ..., n_S,\\
&\|x(0) - x_0^{(0)}\| - \varepsilon_0 = 0,\\
&\|x(1) - x_0^{(0)}\| - \varepsilon_1 = 0,
\end{aligned}$$

to locate a zero of, say, τ_{k-1} (while $\tau_1, ..., \tau_{k-2} = 0$ are fixed). Free scalar variables are $x_M, c_1, ..., c_k, \tau_{k-1}, ..., \tau_{n_U}, \varepsilon_1$. Therefore, there are $n_c = Nmn + n + n_U + 2$ constraints and $n_v = Nmn + n + n_U + 3$ free scalar variables, so $n_c - n_v = -1$.

At the end of these successive steps, all the τ's are zero except for one. Remark that zero intercepts of the τ_i's don't have to be located in the order $\tau_1, \tau_2, \ldots$, but any order is possible.

2. **Locating a connecting orbit, α varies.**

Step $n_U + 1$. Compute a branch of solutions to the system

$$\begin{aligned}
&\dot{x}_C - 2Tf(x_C, \alpha) = 0,\\
&f(x_0, \alpha) = 0,\\
&\langle x(0) - x_0, q_{0,n_U+i} \rangle = 0, \quad i = 1, ..., n_S,\\
&\tau_i - \frac{1}{\varepsilon_1} \langle x(1) - x_0, q_{1,n_S+i} \rangle = 0, \quad i = 1, ..., n_U,\\
&T_{22U} Y_U - Y_U T_{11U} + T_{21U} - Y_U T_{12U} Y_U = 0,\\
&T_{22S} Y_S - Y_S T_{11S} + T_{21S} - Y_S T_{12S} Y_S = 0,\\
&\|x(0) - x_0\| - \varepsilon_0 = 0,\\
&\|x(1) - x_0\| - \varepsilon_1 = 0,
\end{aligned}$$

where $Y_U \in \mathbb{R}^{n_S \times n_U}, Y_S \in \mathbb{R}^{n_U \times n_S}$, to locate a zero of τ_{n_U} (while $\tau_1, ..., \tau_{n_U-1} = 0$ are fixed). Free scalar variables are $x_M, x_0, \alpha_1, \tau_{n_U}, \varepsilon_1, Y_U, Y_S$. This gives us $n_c = Nmn + 2n + 2 + 2n_U n_S$ constraints and $n_v = Nmn + 2n + 3 + 2n_U n_S$ free scalar variables, so $n_c - n_v = -1$.

Now, the end vector $x(1) - x_0$ lies within the stable eigenspace of the saddle equilibrium.

3. **Increasing the accuracy of the connecting orbit, α varies**.

   Step $n_U + 2$. Compute a branch of solutions to the system

$$\begin{aligned}
&\dot{x}_C - 2Tf(x_C, \alpha) = 0,\\
&f(x_0, \alpha) = 0,\\
&\langle x(0) - x_0, q_{0,n_U+i}\rangle = 0, \quad i = 1, ..., n_S,\\
&\langle x(1) - x_0, q_{1,n_S+i}\rangle = 0, \quad i = 1, ..., n_U,\\
&T_{22U}Y_U - Y_U T_{11U} + T_{21U} - Y_U T_{12U} Y_U = 0,\\
&T_{22S}Y_S - Y_S T_{11S} + T_{21S} - Y_S T_{12S} Y_S = 0,\\
&\|x(0) - x_0\| - \varepsilon_0 = 0,\\
&\|x(1) - x_0\| - \varepsilon_1 = 0,
\end{aligned}$$

   where $Y_U \in \mathbb{R}^{n_S \times n_U}, Y_S \in \mathbb{R}^{n_U \times n_S}$, in the direction of decreasing ε_1 until this distance is 'small'. Free scalar variables are $x_M, x_0, \alpha_1, T, \varepsilon_1, Y_U, Y_S$. As before, $n_c = Nmn + 2n + 2 + 2n_U\, n_S$ and $n_v = Nmn + 2n + 3 + 2n_U\, n_S$.

By executing the successive steps of the algorithm, a connecting orbit is constructed with the beginning vector lying in the unstable eigenspace of the saddle equilibrium, the end vector lying in the stable eigenspace, and ε_0 and ε_1 small. Now, the continuation of HHS orbits can be started, with (3.12) as defining system.

Implementation in MatCont

In MatCont, the initial connecting orbit in the first step is obtained by time-integration since in our experiments this approach led to more stable results. Further, the c_i's are denoted as UParam1, UParam2, etc. (the notation refers to **unstable connection parameters**) and the τ_i's are denoted as SParam1, SParam2, etc. (the notation refers to **stable connection parameters**). In the 'Type' menu in the MatCont window, the curve type of the initial orbit is ConnectionSaddle and the curve type of the successive continuations is denoted as HomotopySaddle. In the MatCont window these curve types are abbreviated to ConnecHom and HTHom. So the curve of the time-integration appears in the MatCont window as `EP_ConnecHom` and the possible continuations as `ConnecHom_HTHom`, `HTHom_HTHom`, `HTHom_Hom`.

We now consider the starter windows of the successive curves. The left Starter of Figure 3.1 shows the starter window of `EP_ConnecHom`. The coordinates of the saddle equilibrium $x_0^{(0)}$, the system parameters, UParam1 and UParam2 and the distance ε_0 have to be filled in by the user. When the eigenvalue with smallest positive real part is real, only UParam1 is taken into account (whatever value to UParam2 is given). Then two opposite directions are candidates for the position of the starting point $x(0)$. The chosen direction is determined by the sign of UParam1. When the eigenvalues with smallest positive real part consist of a complex conjugate pair, the starting point is determined by $x(0) = x_0^{(0)} + \varepsilon_0(\text{UParam1}\, q_{0,1}^{(0)} + \text{UParam2}\, q_{0,2}^{(0)})$. So the beginning vector can lie in a two-dimensional space that doesn't make it obvious at all in which direction we have to start. Only trial and error helps in this case.

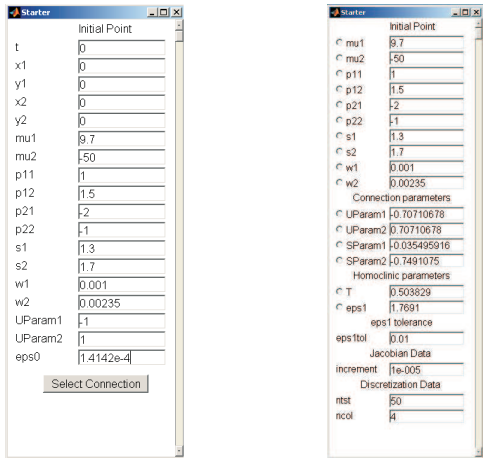

Figure 3.1: Starter windows.

To make it easier for the user when choosing the unstable connection parameters, the condition $\text{UParam1}^2 + \text{UParam2}^2 = 1$ can be ignored in the first step. UParam1 and UParam2 are automatically rescaled by MatCont so that this condition is fulfilled.

When the user obtains a satisfactory connecting orbit after time integration, the button 'Select Connection' has to be pressed. The user can then choose the number of mesh intervals and collocation points. By default, 40 mesh intervals and 4 collocation points are used. The code now searches for the point on the

time-integrated orbit where ε_1 stops decreasing for the last time. If such a point doesn't exist, the last point of the orbit is taken. This point is selected as the end point of the initial connecting orbit.

The starter window for `ConnecHom_HTHom` and `HTHom_HTHom` is illustrated on the right of Figure 3.1. In the successive continuations the user has to indicate the free system parameter, the free connection parameters and the free homoclinic parameters. Error catches are provided, e.g. if a stable connection parameter equal to zero is denoted as free, an error window appears.

In the successive continuations that locate zero intercepts of the SParams, a test function determines whether an SParam has become zero. This test function is the product of the free stable connection parameters. In the continuation to make ε_1 small, the test function is given by $\varepsilon_1 -$eps1tol, where eps1tol is a tolerance, chosen by the user, which determines how small ε_1 is wanted.

Examples of the homotopy method for HHS orbits are given in Section 3.6.1, Section 3.6.2 and Section 3.6.3.

3.4 Starting Homoclinic-to-Saddle-Node orbits by homotopy

We also have implemented the homotopy method for HSN orbits.

3.4.1 The method

In the homotopy method for HSN orbits, we start from a saddle-node equilibrium $x_0^{(0)}$ to construct a Homoclinic-to-Saddle-Node orbit. The defining equations for the continuation of a HSN orbit consist of (3.12), where $Q^{U^\perp} \in \mathbb{R}^{n\times n_S}, Q^{S^\perp} \in \mathbb{R}^{n\times n_U}$ as before but $Y_U \in \mathbb{R}^{(n_S+1)\times n_U}$ and $Y_S \in \mathbb{R}^{(n_U+1)\times n_S}$, supplemented by the equation

$$g = 0, \tag{3.15}$$

where g is computed by solving (3.11).

If the phase condition is added in the continuation, two of the three homoclinic parameters $T, \varepsilon_0, \varepsilon_1$ are freed, otherwise just one homoclinic parameter is freed. Without phase condition, the number of constraints equals $Nmn + 2n + 2 + (n_S + 1)n_U + (n_U + 1)n_S$ and $x_M, x_0, \alpha_1, T, Y_U, Y_S$ are the free scalar variables so $n_v =$

$Nmn + 2n + 2 + (n_S + 1)n_U + (n_U + 1)n_S$. If the phase condition is added, the number of constraints is augmented by one and an extra homoclinic parameter has to be freed. For continuation a second parameter has to be varied so that $n_c - n_v = -1$.

In the system given by the equations (3.12) and equation (3.15) the columns of $Q^{U^\perp}$ span the orthogonal complement of the center-unstable eigenspace of the saddle-node equilibrium while the columns of $Q^{S^\perp}$ span the orthogonal complement of the center-stable eigenspace. As in the homotopy method for HHS orbits, initially these projections are constructed using the real Schur factorizations:

$$\begin{aligned} f_x(x_0^{(0)}, \alpha) &= Q_0^{(0)} R_0^{(0)} Q_0^{(0),\mathrm{T}}, \quad Q_0^{(0)} = [Q^{U,(0)}\ Q^{U^\perp,(0)}], \\ f_x(x_0^{(0)}, \alpha) &= Q_1^{(0)} R_1^{(0)} Q_1^{(0),\mathrm{T}}, \quad Q_1^{(0)} = [Q^{S,(0)}\ Q^{S^\perp,(0)}]. \end{aligned} \tag{3.16}$$

These first factorizations are chosen so that the $n_U + 1$ columns $q_{0,1}^{(0)}, ..., q_{0,n_U+1}^{(0)}$ of $Q^{U,(0)}$ form an orthonormal basis of the right invariant subspace S_0^U of $f_x(x_0^{(0)}, \alpha)$, corresponding to the eigenvalues $\lambda_1^{(0)}, ..., \lambda_{n_U}^{(0)}, \lambda_{n_U+1}^{(0)}$ (with $\lambda_{n_U+1}^{(0)} = \nu^{(0)}$) and the $n_S = n - n_U - 1$ columns $q_{0,n_U+1+i}^{(0)}, i = 1, \ldots, n_S$, of $Q^{U^\perp,(0)}$ form an orthonormal basis of the orthogonal complement $S_0^{U^\perp}$. Similarly, the $n_S + 1$ columns $q_{1,1}^{(0)}, ...,$ $q_{1,n_S+1}^{(0)}$ of $Q^{S,(0)}$ form an orthonormal basis of the right invariant subspace S_0^S of $f_x(x_0^{(0)}, \alpha)$, corresponding to the eigenvalues $\mu_1^{(0)}, ..., \mu_{n_S}^{(0)}, \mu_{n_S+1}^{(0)}$ (with $\mu_{n_S+1}^{(0)} = \nu^{(0)}$), and the n_U columns $q_{1,n_S+1+i}^{(0)}, i = 1, \ldots, n_U$, of $Q^{S^\perp,(0)}$ form an orthonormal basis of the orthogonal complement $S_0^{S^\perp}$.

Moreover, let $S_{0,k}^U$, $k = 1, ..., n_U + 1$, be the right invariant subspace of $f_x(x_0^{(0)}, \alpha)$ corresponding to the eigenvalues $\lambda_1^{(0)}, ..., \lambda_k^{(0)}$, whenever either $\lambda_k^{(0)}$ is real or the couple $(\lambda_{k-1}^{(0)}, \lambda_k^{(0)})$ forms a conjugate pair of complex eigenvalues. Then the first k columns $q_{0,1}^{(0)}, \ldots, q_{0,k}^{(0)}$ of $Q_0^{(0)}$ form an orthonormal basis of $S_{0,k}^U$ and the remaining $n - k$ columns $q_{0,k+1}^{(0)}, ..., q_{0,n}^{(0)}$ of $Q_0^{(0)}$ form an orthonormal basis of the orthogonal complement $S_{0,k}^{U^\perp}$. The analog holds for the subspace corresponding to the negative eigenvalues.

The construction process of a HSN orbit fitting equations (3.12) and equation (3.15) from a saddle-node equilibrium is analogous to the homotopy method for

HHS orbits, although there are some essential differences. We discuss them first, before giving the explicit equations.

The beginning vector of a HSN orbit lies in the eigenspace corresponding to the zero eigenvalue. Therefore, only two opposite directions are candidates for starting direction, which makes it easier to find a proper initial connecting orbit compared to a HHS orbit where the proper direction can have to be searched for in a two-dimensional space.

Now, possibly n_U or n_S is equal to zero. If n_U equals zero, the center-stable space is the whole phase space so only one homotopy step in which ε_1 is made small, needs to be executed.

Since the number of c's is one more than the number of τ's, no system parameter has to be varied in the series of continuations that makes the stable connection parameters zero. Indeed, when n_U is strictly positive, in the first homotopy step two c's are free and all the τ's are free, and in the following steps each time one more c is freed to replace the fixed equation $\tau = 0$. Also the continuation that makes ε_1 small requires no free system parameter.

3.4.2 The algorithm

We now consider the algorithm in more detail.

ALGORITHM. Locating a Homoclinic-to-Saddle-Node orbit by homotopy.

Input.
$x_0^{(0)} \in \mathbb{R}^n$, $f_x(x_0^{(0)}, \alpha)$, and the real Schur factorizations (3.16).

1. **Locating a connecting orbit.**

   Step 1. A HSN orbit starts in the direction of the eigenvector q corresponding to the zero eigenvalue ν. The first step of the homotopy method can be done either by time integration or continuation. If we choose time integration, we start from the point $x(0) = x_0^{(0)} + \varepsilon_0 c_1 q^{(0)}$. The value of c_1 is either 1 or -1 and $c_2, \ldots, c_{n_U+1}$ are put equal to zero. If continuation is used, we set a small orbit segment equal to a constant, namely $x(t) = x_0^{(0)} + \varepsilon_0 c_1 q^{(0)}$ in $[0, T]$ for small values of T and ε_0, and with the same remark for the c's. We

then extend this segment by continuation using the following equations

$$\begin{aligned}
&\dot{x}_C - 2Tf(x_C,\alpha) = 0,\\
&\varepsilon_0 c_i - \langle x(0) - x_0^{(0)}, q_{0,i}^{(0)}\rangle = 0, \quad i = 1,...,n_U+1,\\
&\tau_i - \frac{1}{\varepsilon_1}\langle x(1) - x_0^{(0)}, q_{1,n_S+1+i}^{(0)}\rangle = 0, \quad i = 1,...,n_U,\\
&\langle x(0) - x_0^{(0)}, q_{0,n_U+1+i}^{(0)}\rangle = 0, \quad i = 1,...,n_S,\\
&\|x(1) - x_0^{(0)}\| - \varepsilon_1 = 0.
\end{aligned}$$

This gives us $n_c = Nmn + n + n_U + 1$ constraints and the free scalar variables are $x_M, \tau_1, \ldots \tau_{n_U}, T, \varepsilon_1$, so $n_v = Nmn + n + n_U + 2$.

Again, typically ε_1 first increases and then starts to decrease. We stop the time integration or continuation when ε_1 stops decreasing.

Steps k, $k = 2,...,n_U+1$ $(n_U \geq 1)$. Compute a branch of solutions to the system

$$\begin{aligned}
&\dot{x}_C - 2Tf(x_C,\alpha) = 0,\\
&\varepsilon_0 c_i - \langle x(0) - x_0^{(0)}, q_{0,i}^{(0)}\rangle = 0, \quad i = 1,...,n_U+1,\\
&\tau_i - \frac{1}{\varepsilon_1}\langle x(1) - x_0^{(0)}, q_{1,n_S+1+i}^{(0)}\rangle = 0, \quad i = 1,...,n_U,\\
&\langle x(0) - x_0^{(0)}, q_{0,n_U+1+i}^{(0)}\rangle = 0, \quad i = 1,...,n_S,\\
&\|x(0) - x_0^{(0)}\| - \varepsilon_0 = 0,\\
&\|x(1) - x_0^{(0)}\| - \varepsilon_1 = 0,
\end{aligned}$$

to locate a zero of, say, τ_{k-1} (while $\tau_1, \ldots, \tau_{k-2} = 0$ are fixed). The number of constraints is $n_c = Nmn + n + n_U + 2$ and the free scalar variables are given by $x_M, c_1, \ldots c_k, \tau_{k-1}, \ldots \tau_{n_U}, \varepsilon_1$, so that $n_v = Nmn + n + n_U + 3$, and thus $n_c - n_v = -1$.

The τ's can be made zero in any possible order. At the end of these successive continuations the end vector $x(1) - x_0^{(0)}$ lies within the center-stable eigenspace of $x_0^{(0)}$.

2. **Increasing the accuracy of the connecting orbit.**

Step $n_U + 2$. Compute a branch of solutions to the system

$$\begin{aligned}
&\dot{x}_C - 2Tf(x_C, \alpha) = 0,\\
&\langle x(0) - x_0^{(0)}, q^{(0)}_{0,n_U+1+i}\rangle = 0, \quad i = 1, ..., n_S,\\
&\langle x(1) - x_0^{(0)}, q^{(0)}_{1,n_S+1+i}\rangle = 0, \quad i = 1, ..., n_U,\\
&\|x(0) - x_0^{(0)}\| - \varepsilon_0 = 0,\\
&\|x(1) - x_0^{(0)}\| - \varepsilon_1 = 0,
\end{aligned}$$

in the direction of decreasing ε_1 until this distance is 'small'. The number of constraints is $n_c = Nmn + n + 1$ and the free scalar variables are x_M, T, ε_1, so that $n_v = Nmn + n + 2$.

The successive homotopies give a connecting orbit where the starting vector lies within the center-unstable eigenspace of the equilibrium, where the end vector lies within the center-stable eigenspace and where the distances ε_0 and ε_1 are small, so the continuation of HSN orbits can be started.

3.4.3 Implementation in MatCont

Analogous notation as for HHS orbits is used. In the 'Type' menu in the MatCont window the types ConnectionSaddleNode and HomotopySaddleNode are used. In the MatCont window, the curve of the time-integration is `LP_ConnecHSN` and `ConnecHSN_HTHSN`, `HTHSN_HTHSN` and `HTHSN_HSN` form the successive continuations. The starter windows are similar to the Starters used in the homotopy method for HHS orbits, except that in the Starter of `LP_ConnecHSN` only UParam1 has to be filled in by the user, since the starting vector lies in the direction of the eigenvector corresponding to the zero eigenvalue.

We give an example of the method in Section 3.6.4.

3.5 Starting heteroclinic orbits by homotopy

We also have implemented the homotopy method for heteroclinic orbits.

3.5.1 The method

An analogous homotopy method for heteroclinic orbits is also implemented. Let

$$\Re(\mu_{n_S}) \leq ... \leq \Re(\mu_1) < 0 < \Re(\lambda_1) \leq ... \leq \Re(\lambda_{n_U}),$$

where $\lambda_1, ..., \lambda_{n_U}$ are the eigenvalues of $f_x(x_0, \alpha)$ with nonnegative real part and μ_1, ..., μ_{n_S} are the eigenvalues of $f_x(x_1, \alpha)$ with nonpositive real part (with $x(t) \to x_0$ as $t \to -\infty$ and $x(t) \to x_1$ as $t \to +\infty$). The defining system for the continuation of heteroclinic orbits is given by

$$\begin{aligned}
&\dot{x}_C - 2Tf(x_C, \alpha) = 0,\\
&f(x_0, \alpha) = 0,\\
&f(x_1, \alpha) = 0,\\
&\int_0^1 \dot{\tilde{x}}^*(t)[x(t) - \tilde{x}(t)]dt = 0,\\
&Q^{U^\perp,\mathrm{T}}(x(0) - x_0) = 0,\\
&Q^{S^\perp,\mathrm{T}}(x(1) - x_1) = 0,\\
&T_{22U}Y_U - Y_U T_{11U} + T_{21U} - Y_U T_{12U} Y_U = 0,\\
&T_{22S}Y_S - Y_S T_{11S} + T_{21S} - Y_S T_{12S} Y_S = 0,\\
&\|x(0) - x_0\| - \varepsilon_0 = 0,\\
&\|x(1) - x_1\| - \varepsilon_1 = 0,
\end{aligned} \tag{3.17}$$

with $Q^{U^\perp} \in \mathbb{R}^{n\times(n-n_U)}, Q^{S^\perp} \in \mathbb{R}^{n\times(n-n_S)}, Y_U \in \mathbb{R}^{(n-n_U)\times n_U}, Y_S \in \mathbb{R}^{(n-n_S)\times n_S}$.

If the phase condition is added in the continuation, two of the three heteroclinic parameters $T, \varepsilon_0, \varepsilon_1$ are freed, otherwise just one heteroclinic parameter is freed. We remark that without phase condition in system (3.17) the number of constraints equals $Nmn + 4n - n_U - n_S + 2 + (n - n_U)n_U + (n - n_S)n_S$ and the free scalar variables are given by $x_M, x_0, x_1, \alpha_1, \ldots, \alpha_{n_\alpha - 1}, T, Y_U, Y_S$, so that $n_v = Nmn + 3n + n_\alpha + (n - n_U)n_U + (n - n_S)n_S$. If the phase condition is added, the number of constraints is augmented by one and an extra heteroclinic parameter has to be freed. For continuation another parameter has to be freed. Since for continuation $n_c - n_v$ has to be equal to -1, we can conclude that the number of free system parameters has to be equal to $n_\alpha = n - (n_U + n_S) + 2$.

The method is very similar to the homotopy method for HHS orbits. Remark that since we deal with two different equilibria, in the first step ε_1 is not necessarily

initially increasing. But again, generally, we stop time integration or continuation when ε_1 stops decreasing.

3.5.2 The algorithm

ALGORITHM. Locating a heteroclinic orbit by homotopy.

Input.
$x_0^{(0)} \in \mathbb{R}^n$, $x_1^{(0)} \in \mathbb{R}^n$, $\alpha = (\alpha_1, \ldots, \alpha_{n_\alpha - 1}) \in \mathbb{R}^{n_\alpha - 1}$, $f_x(x_0^{(0)}, \alpha)$, $f_x(x_1^{(0)}, \alpha)$, and the real Schur factorizations of these matrices.

1. **Locating a connecting orbit, α is fixed.**

   Step 1. The first step can be done either by time integration or by continuation. If we choose time integration, we start from $x(0) = x_0^{(0)} + \varepsilon_0(c_1 q_{0,1}^{(0)} + c_2 q_{0,2}^{(0)})$, with the same remark about c_1 and c_2 as for HHS orbits. If continuation is used, we set $x(t) = x_0^{(0)} + \varepsilon_0(c_1 q_{0,1}^{(0)} + c_2 q_{0,2}^{(0)})$ in $[0, T]$ for a small value of T and ε_0, and extend this segment by continuation using the following equations

$$
\begin{aligned}
&\dot{x}_C - 2Tf(x_C, \alpha) = 0, \\
&\varepsilon_0 c_i - \langle x(0) - x_0^{(0)}, q_{0,i}^{(0)} \rangle = 0, \quad i = 1, ..., n_U, \\
&\tau_i - \frac{1}{\varepsilon_1} \langle x(1) - x_1^{(0)}, q_{1,n_S+i}^{(0)} \rangle = 0, \quad i = 1, ..., n - n_S, \\
&\langle x(0) - x_0^{(0)}, q_{0,n_U+i}^{(0)} \rangle = 0, \quad i = 1, ..., n - n_U, \\
&\| x(1) - x_1^{(0)} \| - \varepsilon_1 = 0.
\end{aligned}
$$

   This gives us $n_c = Nmn + 2n - n_S + 1$ constraints and the free scalar variables are $x_M, \tau_1, \ldots \tau_{n-n_S}, T, \varepsilon_1$, so that $n_v = Nmn + 2n - n_S + 2$.

   We stop the time integration or continuation when ε_1 stops decreasing.

   Steps k, $k = 2, ..., n_U$ *(for* $n_U > 1$*).* Compute a branch of solutions to the

system

$$\begin{aligned}
&\dot{x}_C - 2Tf(x_C,\alpha) = 0,\\
&\varepsilon_0 c_i - \langle x(0) - x_0^{(0)}, q_{0,i}^{(0)}\rangle = 0, \quad i = 1,...,n_U,\\
&\tau_i - \frac{1}{\varepsilon_1}\langle x(1) - x_1^{(0)}, q_{1,n_S+i}^{(0)}\rangle = 0, \quad i = 1,...,n-n_S,\\
&\langle x(0) - x_0^{(0)}, q_{0,n_U+i}^{(0)}\rangle = 0, \quad i = 1,...,n-n_U,\\
&\|x(0) - x_0^{(0)}\| - \varepsilon_0 = 0,\\
&\|x(1) - x_1^{(0)}\| - \varepsilon_1 = 0,
\end{aligned}$$

to locate a zero of, say, τ_{k-1} (while $\tau_1,\ldots,\tau_{k-2} = 0$, fixed). The number of constraints is $n_c = Nmn + 2n - n_S + 2$ and the free scalar variables are given by $x_M, c_1,\ldots c_k, \tau_{k-1},\ldots \tau_{n-n_S}, \varepsilon_1$, so that $n_v = Nmn + 2n - n_S + 3$, and thus $n_c - n_v = -1$.

At the end of these successive continuations $\tau_1 = \ldots = \tau_{n_U-1} = 0$. Remark that the τ's can be made zero in any possible order.

2. **Locating a connecting orbit, α varies**.

   Steps k, $k = n_U + 1,...,n - n_S + 1$ *(for* $n - n_S \geq n_U$*).* Compute a branch of solutions to the system

$$\begin{aligned}
&\dot{x}_C - 2Tf(x_C,\alpha) = 0,\\
&f(x_0,\alpha) = 0,\\
&f(x_1,\alpha) = 0,\\
&\langle x(0) - x_0, q_{0,n_U+i}\rangle = 0, \quad i = 1,...,n-n_U,\\
&\tau_i - \frac{1}{\varepsilon_1}\langle x(1) - x_1, q_{1,n_S+i}\rangle = 0, \quad i = 1,...,n-n_S,\\
&T_{22U}Y_U - Y_U T_{11U} + T_{21U} - Y_U T_{12U} Y_U = 0,\\
&T_{22S}Y_S - Y_S T_{11S} + T_{21S} - Y_S T_{12S} Y_S = 0,\\
&\|x(0) - x_0\| - \varepsilon_0 = 0,\\
&\|x(1) - x_1\| - \varepsilon_1 = 0,
\end{aligned}$$

   where $Y_U \in \mathbb{R}^{(n-n_U)\times n_U}, Y_S \in \mathbb{R}^{(n-n_S)\times n_S}$, to locate a zero of τ_{k-1} (while $\tau_1,...,\tau_{k-2} = 0$, fixed). The number of constraints is $n_c = Nmn + 4n - n_U -$

$n_S + 2 + (n - n_U)n_U + (n - n_S)n_S$ and the free scalar variables are x_M, x_0, $x_1, \alpha_1, \ldots \alpha_{k-n_U}, \tau_{k-1}, \ldots \tau_{n-n_S}, \varepsilon_1, Y_U, Y_S$, so that $n_v = Nmn + 4n - n_U - n_S + 3 + (n - n_U)n_U + (n - n_S)n_S$.

At the end of these homotopies all the τ's are zero. Again, any order in which zero intercepts of the τ's are detected is possible.

3. **Increasing the accuracy of the connecting orbit, α varies**.

   Step $n - n_S + 2$. Compute a branch of solutions to the system

$$
\begin{aligned}
&\dot{x}_C - 2Tf(x_C, \alpha) = 0,\\
&f(x_0, \alpha) = 0,\\
&f(x_1, \alpha) = 0,\\
&\langle x(0) - x_0, q_{0,n_U+i} \rangle = 0, \quad i = 1, ..., n - n_U,\\
&\langle x(1) - x_1, q_{1,n_S+i} \rangle = 0, \quad i = 1, ..., n - n_S,\\
&T_{22U}Y_U - Y_U T_{11U} + T_{21U} - Y_U T_{12U} Y_U = 0,\\
&T_{22S}Y_S - Y_S T_{11S} + T_{21S} - Y_S T_{12S} Y_S = 0,\\
&\|x(0) - x_0\| - \varepsilon_0 = 0,\\
&\|x(1) - x_1\| - \varepsilon_1 = 0,
\end{aligned}
$$

   where $Y_U \in \mathbb{R}^{(n-n_U)\times n_U}, Y_S \in \mathbb{R}^{(n-n_S)\times n_S}$, in the direction of decreasing ε_1 until this end distance is 'small'. The number of constraints is $n_c = Nmn + 4n - n_U - n_S + 2 + (n - n_U)n_U + (n - n_S)n_S$ and the free scalar variables are $x_M, x_0, x_1, \alpha_1, \ldots \alpha_{n_\alpha - 1}, T, \varepsilon_1, Y_U, Y_S$, so that $n_v = Nmn + 3n + n_\alpha + 1 + (n - n_U)n_U + (n - n_S)n_S = Nmn + 4n - n_U - n_S + 3 + (n - n_U)n_U + (n - n_S)n_S$.

After these homotopies, a proper starting orbit for the continuation of heteroclinic orbits is obtained.

3.5.3 Implementation in MatCont

Analogous notation as for HHS and HSN orbits is used. The curve of the time-integration is `EP_ConnecHet` and the possible continuations are denoted as `Connec-Het_HTHet, HTHet_HTHet, HTHet_Het`. The full notation in the 'Type' menu is given by ConnectionHet and HomotopyHet. The starter windows are similar to the

starters used in the homotopy method for HHS orbits, except that in the starter of `EP_ConnecHet` $x_0^{(0)}$ and $x_1^{(0)}$ has to be filled in by the user.

We give an example of the method in Section 3.6.5.

3.6 Examples

In this section we examine examples in which the homotopy method is applied. In Section 3.6.1 we consider a homoclinic bifurcation curve, obtained by the successive continuations method, that spirals towards the so-called T-point in the Lorenz system. In Section 3.6.2 and Section 3.6.3 we focus on the difficult case where the leading unstable eigenvalues of the HHS orbit consist of a complex conjugate pair and thus the starting direction has to be searched in a two-dimensional space. Section 3.6.4 and Section 3.6.5 illustrate the robustness of the homotopy method for HSN orbits and heteroclinic orbits, respectively.

3.6.1 HHS orbits in the Lorenz system

One of the best-known dynamical systems that contains homoclinic orbits is the three-dimensional system [77], given by

$$\begin{cases} \dot{x} = \sigma(y - x), \\ \dot{y} = rx - y - xz, \\ \dot{z} = -bz + xy, \end{cases} \tag{3.18}$$

with the standard values $\sigma = 10$, $b = 8/3$, and where r is the primary bifurcation parameter. For these parameter values, a supercritical pitchfork bifurcation from the trivial equilibrium occurs at $r = 1$, giving rise to two symmetric nontrivial equilibria. At $r \approx 13.926$ there are two symmetry-related orbits that are homoclinic to the origin, and from which two primary families of saddle cycles arise (together with a nontrivial hyperbolic invariant set containing many other periodic and nonperiodic orbits). One of these homoclinic orbits is located entirely in the half-space $x > 0$ and has one maximum of the x-component of its solution. We will refer to this orbit as the $(1,0)$-loop and say that it makes one turn around the corresponding nontrivial equilibrium. It is well known that, at other parameter values, the Lorenz system has homoclinic orbits with one positive maximum and n negative minima of the x-component of the corresponding solution. Such homoclinic orbits make one

turn around the nontrivial equilibrium with $x > 0$ and n turns around the nontrivial equilibrium with $x < 0$. We will call these orbits the $(1, n)$-loops, following [82].

Our aim here is to illustrate how one can compute bifurcation values of the parameter r at which $(1, n)$-loops exist and how to continue the corresponding bifurcation curves in the (σ, r)-plane. Note that the number of turns n can change along a homoclinic bifurcation curve. In particular, we will compute (a segment of) a homoclinic bifurcation curve that spirals towards the so-called T-point $(\sigma_\infty, r_\infty) \approx (10.16, 30.87)$, where the Lorenz system has a codimension 2 heteroclinic orbit connecting the trivial and nontrivial equilibria. Along this curve, n goes to infinity when we approach the T-point. This codim 2 global bifurcation has been analyzed in detail in [13, 14] and was later rediscovered in [48].

To begin with, fix $r = 15.5$. Then, the origin is a saddle equilibrium of (3.18) with eigenvalues

$$\lambda_1^{(0)} = 7.7382, \quad \mu_1^{(0)} = -2.6667, \quad \mu_2^{(0)} = -18.7382,$$

and the normalized unstable eigenvector corresponding to $\lambda_1^{(0)} > 0$ equals

$$q_{0,1}^{(0)} = \begin{pmatrix} -0.4911 \\ -0.8711 \\ 0 \end{pmatrix}.$$

Since we want to compute homoclinic orbits departing from the origin in the half-space $x > 0$, we take UParam1 $= -1$. We then integrate the orbit starting at distance $\varepsilon_0 = 0.01$ from the origin over time interval $T = 1.3$ by computing in MatCont the `EP_ConnecHom` curve. The integration procedure produces the orbit segment shown in Figure 3.2 (a), which is far from being homoclinic but is sufficient to start the homotopy method.

By selecting the connection in the Starter window, we are automatically prepared to compute the `ConnecHom_HTHom` curve. The last point obtaind by time integration is selected as the end point of the new curve. In this continuation, where we use 20 mesh intervals, the system parameter r, as well as SParam1 and ε_1 are active. The initial values of these last two parameters are Sparam1 $= -0.0668$ and $\varepsilon_1 = 18.5152$, respectively. While the value of SParam1 indicates that the end-point of the integrated orbit is rather close to the plane tangent to the two-dimensional stable invariant manifold of the origin, its distance ε_1 to the equilibrium is quite large. The `ConnecHom_HTHom` continuation produces a family of orbit segments attaining SParam1 $= 0$ at $r = 16.1793$ (see Figure 3.2 (b)), where $\varepsilon_1 = 17.4523$.

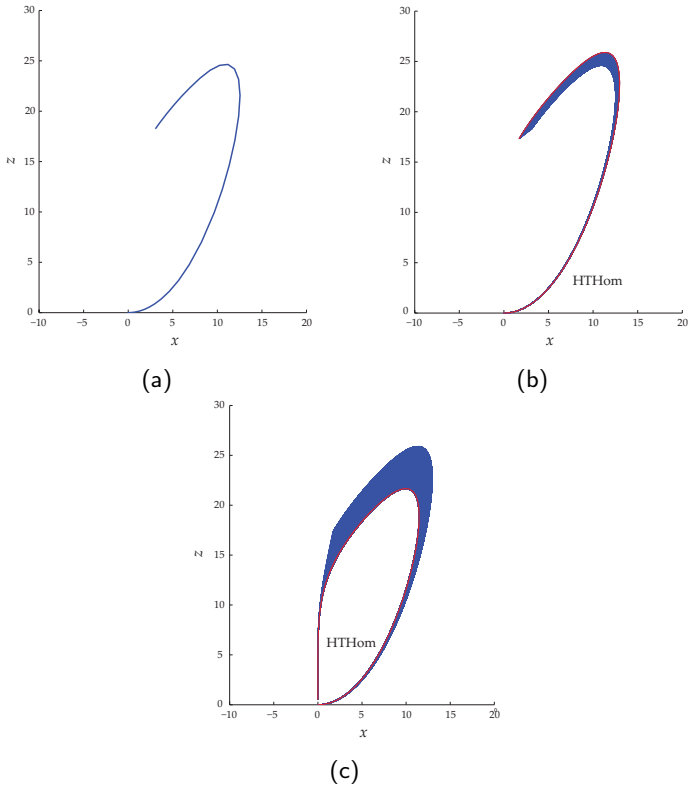

Figure 3.2: Initializing the $(1,0)$-homoclinic orbit by homotopy.

Selecting the last point as the initial point for the next continuation, we can compute the `HTHom_HTHom` curve with r, T and ε_1 as active parameters (note that now T is set to 0.65, that is one-half of its initial value). Our goal at this stage is to reach $\varepsilon_1 = 0.5$ by increasing the interval T. This indeed happens at $T = 1.3476$ with $r = 13.9266$, which is a good approximation for the $(1,0)$-homoclinic parameter value, see Figure 3.2 (c).

After selecting the last point and the curve type `HTHom_Hom`, we are ready to continue the found homoclinic orbit in the two system parameters σ and r, keeping T and ε_1 active. It produces the $(1,0)$-homoclinic curve on Figure 3.3.

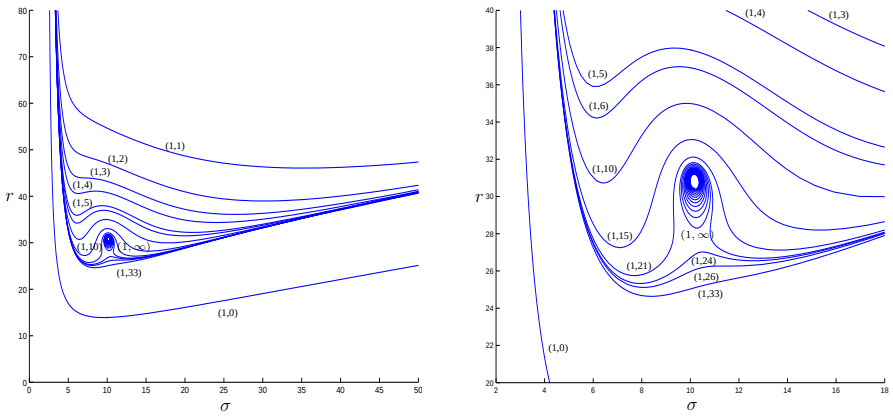

Figure 3.3: Partial two-parameter bifurcation diagram of the Lorenz system and its magnification near the T-point.

Similar steps, but starting with $r = 55$, produce Figure 3.4. We take a mesh consisting of $N = 40$ intervals and use the standard value $m = 4$. Selecting the last orbit as the initial orbit for the continuation of the `ConnecHom_HTHom`-curve with r, SParam1 and ε_1 active, gives us Figure 3.4 (b) where SParam1 $= 0$ at $r = 56.9941$ and $\varepsilon_1 = 49.8634$. From this last point, the continuation of the `HTHom_HTHom`-curve is executed with r, T and ε_1 free, until $\varepsilon_1 = 0.5$. This is obtained at the $(1,1)$-homoclinic parameter value $r = 54.6460$ and the improved connection is shown in Figure 3.4 (c). Figure 3.5 and Figure 3.3 (left) show the family of the $(1,1)$-homoclinic orbits along the corresponding `HTHom_Hom`-curve.

Figure 3.3 includes results of similar computations for the $(1,n)$-homoclinic curves with various n, obtained with the homotopy method. The $(1,\infty)$-curve spirals towards the T-point mentioned above; along this curve, the homoclinic orbit approaches the heteroclinic cycle connecting the origin to the nontrivial equilibrium and from this equilibrium back to the origin. Most of the curves in Figure 3.3 were first reported in [82]; we present several more of them with the main purpose to illustrate the power of MatCont that allows to produce such figures in a matter of minutes. The continuation took 22.2 seconds to compute 100 $(1,0)$-homoclinic orbits. The runs were executed in Matlab version 7.5.0, on an Intel 2.99 GHz

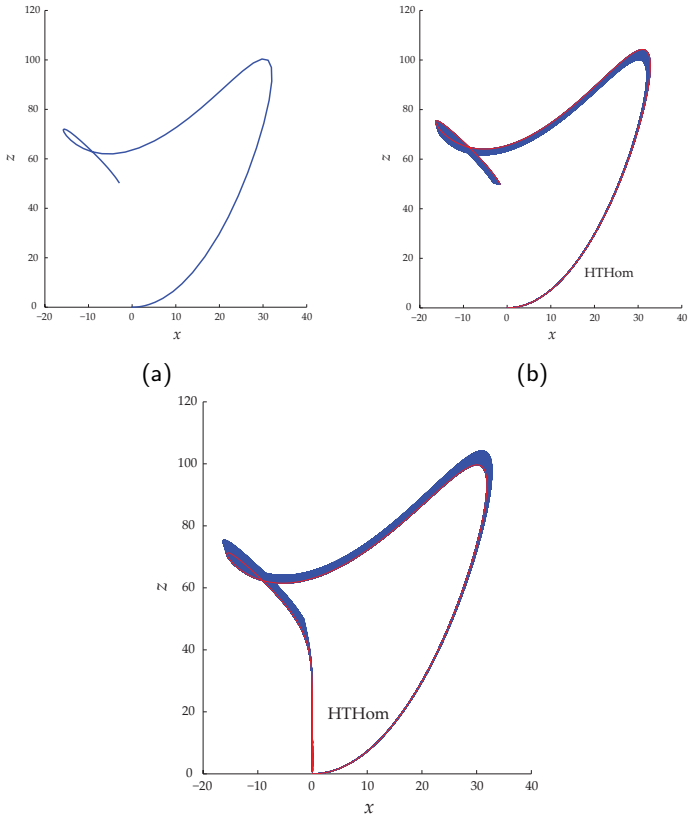

Figure 3.4: Initializing the $(1,1)$-homoclinic orbit by homotopy.

machine with 1.99 Gigabyte RAM. We also stress that the figure shows only a small portion of the (σ, r)-bifurcation diagram of the Lorenz system, even if one is concerned only with homoclinic bifurcations. For example, there are sequences of T-points corresponding to different heteroclinic contours, with their own homoclinic spirals.

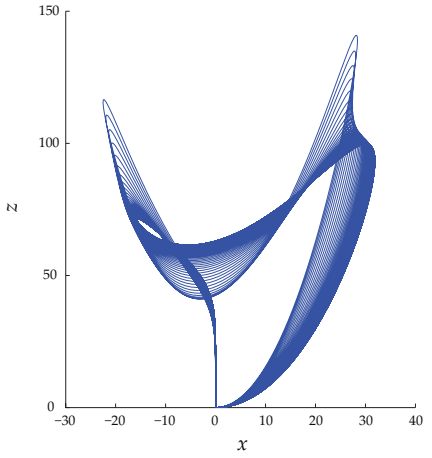

Figure 3.5: A family of $(1,1)$-homoclinic orbits.

3.6.2 HHS orbits in Hopf-Hopf normal form with broken symmetry

We consider the normal form of the Hopf-Hopf codimension 2 bifurcation in polar coordinates, given by

$$\begin{cases} \dot{r_1} = r_1(\mu_1 + p_{11}r_1^2 + p_{12}r_2^2 + s_1 r_2^4), \\ \dot{r_2} = r_2(\mu_2 + p_{21}r_1^2 + p_{22}r_2^2 + s_2 r_1^4), \\ \dot{\varphi_1} = \omega_1, \\ \dot{\varphi_2} = \omega_2. \end{cases}$$

We rewrite this system in the cartesian (x_1, y_1, x_2, y_2)-coordinates and add order 6 terms to break the symmetry so that we obtain the following equations

$$\begin{cases} \dot{x_1} = x_1(\mu_1 + p_{11}(x_1^2+y_1^2) + p_{12}(x_2^2+y_2^2) + s_1(x_2^2+y_2^2)^2) - y_1\omega_1 + \mathbf{3y_1^6} \\ \dot{y_1} = y_1(\mu_1 + p_{11}(x_1^2+y_1^2) + p_{12}(x_2^2+y_2^2) + s_1(x_2^2+y_2^2)^2) + x_1\omega_1 - \mathbf{2x_2^6} \\ \dot{x_2} = x_2(\mu_2 + p_{21}(x_1^2+y_1^2) + p_{22}(x_2^2+y_2^2) + s_2(x_1^2+y_1^2)^2) - y_2\omega_2 - \mathbf{7y_1^6} \\ \dot{y_2} = y_2(\mu_2 + p_{21}(x_1^2+y_1^2) + p_{22}(x_2^2+y_2^2) + s_2(x_1^2+y_1^2)^2) + x_2\omega_2 + \mathbf{x_1^6}. \end{cases}$$

The initial parameter values are given by $\mu_1 = 9.7, \mu_2 = -50, p_{11} = 1, p_{12} = 1.5$, $p_{21} = -2, p_{22} = -1, s_1 = 1.3, s_2 = 1.7, \omega_1 = 0.001, \omega_2 = 0.00235$. The origin is

an equilibrium of this system and the eigenvalues are given by $\lambda_1^{(0)} = 9.7 + 0.001i$, $\lambda_2^{(0)} = 9.7 - 0.001i, \mu_1^{(0)} = -50 + 0.00235i, \mu_2^{(0)} = -50 - 0.00235i$; so we have a two-dimensional unstable manifold and a two-dimensional stable manifold where in both cases the eigenvalues consist of a complex conjugate pair. Therefore, the equilibrium is called a bifocus. This gives us an interesting example to apply the homotopy method on.

Since the eigenvalues with smallest positive real part constitute a complex conjugate pair, both UParam1 and UParam2 play a role in the initialization, we set them equal to -1 and 1, respectively. The unstable parameters are now automatically rescaled such that $\text{UParam1}^2 + \text{UParam2}^2 = 1$ holds, so $\text{UParam1} = -0.7071$ and $\text{UParam2} = 0.7071$. We set the value of ε_0 equal to $1.4142 \cdot 10^{-4}$. Therefore, we start time integration from the point

$$x(0) = (0,0,0,0)^{\mathrm{T}} + 1.4142 \cdot 10^{-4}(-0.7071 q_{0,1}^{(0)} + 0.7071 q_{0,2}^{(0)}),$$

where $q_{0,1}^{(0)} = (1,0,0,0)^{\mathrm{T}}$ and $q_{0,2}^{(0)} = (0,1,0,0)^{\mathrm{T}}$ span the two-dimensional eigenspace corresponding to the eigenvalues $9.7 \pm 0.001i$.

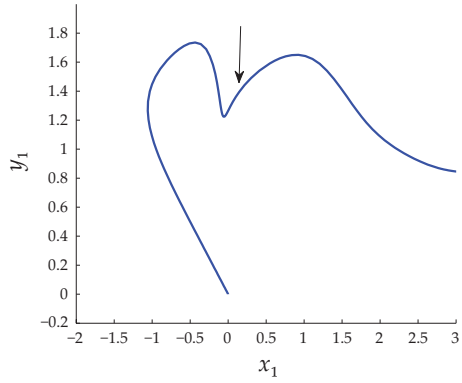

Figure 3.6: Starting orbit after time integration.

When we execute time-integration over an interval of length 1.1, we obtain Figure 3.6. First, ε_1 increases, then this distance decreases, and then starts to increase again. MatCont searches for the point where ε_1 stops decreasing, indicated by the arrow, and takes it as endpoint of the initial connecting orbit. None of the

stable connection parameters equals zero, but they are quite small, namely -0.03550 and -0.7491. We now start the successive homotopies where we use a discretization of 50 mesh intervals and 4 collocation points.

Executing a continuation with both unstable and both stable connection parameters and ε_1 free, SParam1 becomes zero and SParam2 attains the value of -0.7472. To make this last stable connection parameter zero, a system parameter has to be varied, we choose μ_2. This gives $\varepsilon_1 = 1.2490$, so a continuation, with T, ε_1 and μ_2 free, is needed to decrease the value of ε_1. We put eps1tol equal to 10^{-4}, which is reached when $T = 0.8299$ and $\mu_2 = -14.3953$. A family of homoclinic orbits originating at this end orbit is presented in Figure 3.7, where T and ε_1 are the free homoclinic parameters and μ_1 and μ_2 the free system parameters. The continuation of 100 HHS orbits took 118.6 seconds. The runs were executed in Matlab version 7.5.0, on an Intel 2.99 GHz machine with 1.99 Gigabyte RAM.

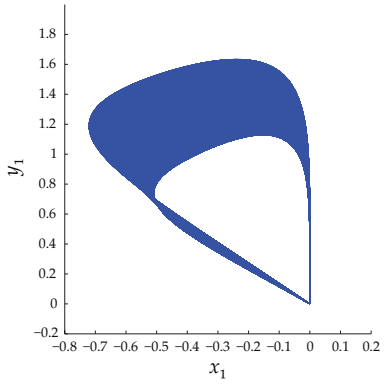

Figure 3.7: A family of bifocus homoclinic orbits.

3.6.3 HHS orbits in a model with bifocus homoclinic orbits

We consider the following system introduced in [75]

$$\begin{cases} \dot{x} = y - w, \\ \dot{y} = z - \nu w, \\ \dot{z} = -x^2 + \alpha x - \gamma y - z - \nu^2 w, \\ \dot{w} = \varepsilon \left(\dfrac{\alpha\nu x + (\alpha - \gamma\nu) y + \nu^2 z}{\nu^4 + \gamma\nu^2 + 2\alpha\nu} \right) + \nu w, \end{cases}$$

where ν is the positive real root of $s^3 + s^2 + \gamma s - \alpha = 0$. The initial parameter values are $\alpha = 4, \gamma = 2$ and $\varepsilon = 1$. The origin $x_0^{(0)} = (0,0,0,0)^{\mathrm{T}}$ is an equilibrium of the system and the eigenvalues are given by $(\lambda_1^{(0)}, \lambda_2^{(0)}, \mu_1^{(0)}, \mu_2^{(0)}) = (1.0000 + 0.7977i, 1.0000 - 0.7977i, -1.0000 + 1.7321i, -1.0000 - 1.7321i)$. So we have a two-dimensional stable manifold and a two-dimensional unstable manifold where the eigenvalues consist of a complex conjugate pair.

The following point is taken as starting point: $x(0) = x_0^{(0)} + 1.4142 \cdot 10^{-4} (0.7071 q_{0,1}^{(0)} - 0.7071 q_{0,2}^{(0)})$, with $q_{0,1}^{(0)}$ the real part and $q_{0,2}^{(0)}$ the imaginary part of the eigenvector corresponding to $\lambda_1^{(0)}$. By time integration we obtain the left plot in Figure 3.8 where the arrow indicates the point where ε_1 stops decreasing.

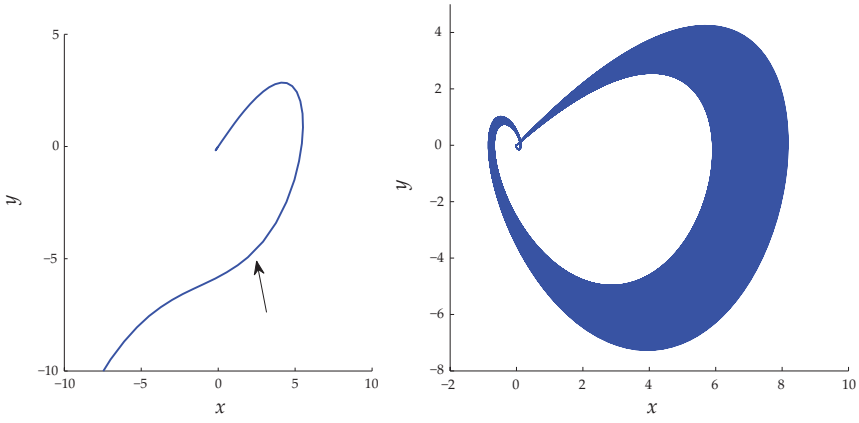

Figure 3.8: Starting orbit after time integration and continuation of HHS orbits.

The τ's are nonzero, namely $\tau_1 = -0.06920$ and $\tau_2 = 0.4978$. We execute a first homotopy with c_1, c_2, τ_1, τ_2 and ε_1 free, such that τ_1 equals zero and $\tau_2 = 0.4076$. A second continuation with τ_2, the system parameter ε and ε_1 free, makes the second stable connection parameter zero, however ε_1 equals 13.2364. Therefore, a continuation that makes ε_1 smaller (with $5 \cdot 10^{-4}$ as goal value), with ε, T and ε_1 free is executed. The end values of the system parameter ε and homoclinic parameter T are given by 0.3218 and 10.9177, respectively. Now, the continuation of HHS orbits can be started, with α and ε as free system parameters and ε_0 and ε_1 as free homoclinic parameters, see the right plot of Figure 3.8.

3.6.4 HSN orbits in a cell cycle model

As an example of the homotopy method for Homoclinic-to-Saddle-Node orbits, we study the following cell cycle model

$$\begin{cases} \dot{X} = k_1 - (k_2' + k_2'' Y) X, \\ \dot{Y} = \dfrac{(k_3' + k_3'' A)(1 - Y)}{J_3 + 1 - Y} - \dfrac{k_4 m X Y}{J_4 + Y}, \\ \dot{A} = k_5' + k_5'' \dfrac{(mX)^n}{J_5^n + (mX)^n} - k_6 A, \end{cases}$$

introduced in [93]. A continuum of HSN orbits was computed in [50] where the continuation was started up from a limit cycle of a large period. During this continuation a Noncentral Homoclinic-to-Saddle-Node orbit was detected. We will recompute these orbits making use of the homotopy method. We consider the Limit Point $x_0^{(0)} = (0.0461, 0.8269, 0.0504)^{\mathrm{T}}$ with the initial parameter values given by $k_1 = 0.04, k_2' = 0.04, k_2'' = 1, k_3' = 1, k_3'' = 10, k_4 = 35, J_3 = 0.04, J_4 = 0.04, k_5' = 0.005, k_5'' = 0.2, k_6 = 0.1, J_5 = 0.3, n = 4, m = 0.7933$. The eigenvalues of the Jacobian evaluated in $x_0^{(0)}$ equal $\nu^{(0)} = 8.9930 \cdot 10^{-7}, \mu_1^{(0)} = -9.3355 \cdot 10^{-2}$, $\mu_2^{(0)} = -2.2666$, so $n_U = 0$.

Figure 3.9 shows the time integrated orbit, started from $x_0^{(0)}$ with UParam1 $= 1$ and $\varepsilon_0 = 0.01$ over an interval of length 200. This is clearly a proper starting orbit. For discretization during the successive homotopies we use 50 mesh intervals and 4 collocation points. Since there are no strictly positive eigenvalues, no τ's have to be made zero, so we can immediately execute the continuation that makes ε_1 small. Although, the value of ε_1 is already very small, namely 0.0036, a homotopy is done

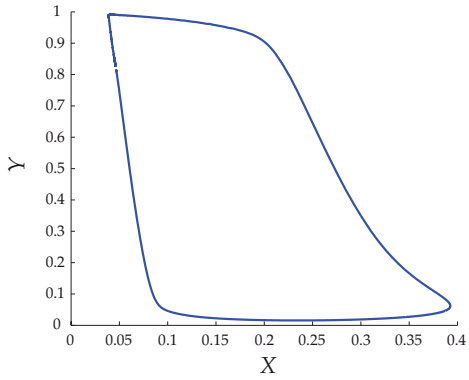

Figure 3.9: Starting orbit after time integration.

until $\varepsilon_1 = 10^{-4}$ is attained. The half-return time T is then equal to 1445.6988. The `HTHSN_HSN` continuation can now be started, with ε_0 and ε_1 as free homoclinic parameters, and k_4 and m as free system parameters. The continuation works well and the NCH orbit is detected. The continuation of 100 HSN orbits took 79.3 seconds, with the same computer specifications as before.

The HSN orbits that converge to the NCH orbit are the lower orbits in Figure 3.10. Note that the NCH orbit can also be detected on a branch of HHS orbits that approach from the opposite direction in Figure 3.10. After a neutral saddle bifurcation, these HHS orbits disappear when encountering the NCH orbit for $k_4 = 21.2940$ and $m = 1.3310$.

3.6.5 Heteroclinic orbits in a model of the Josephson Junction

We study the following three-dimensional Josephson Junction problem, introduced in [40]

$$\begin{cases} \dot{x} = y, \\ \dot{y} = z, \\ \dot{z} = ((1-c^2)z + \alpha c\, y - \sin(x) + \gamma)/(\beta c). \end{cases}$$

This system contains the two equilibria $x_0^{(0)} = (\arcsin(\gamma), 0, 0)^{\mathrm{T}}$ and $x_1^{(0)} = (\pi - \arcsin(\gamma), 0, 0)^{\mathrm{T}}$. Consider the parameter values $\alpha = 0.18, \beta = 0.1, \gamma = 0.1, c = 0.6$, such that $x_0^{(0)} = (0.1002, 0, 0)^{\mathrm{T}}$ and $x_1^{(0)} = (3.0414, 0, 0)^{\mathrm{T}}$. The eigenvalues in

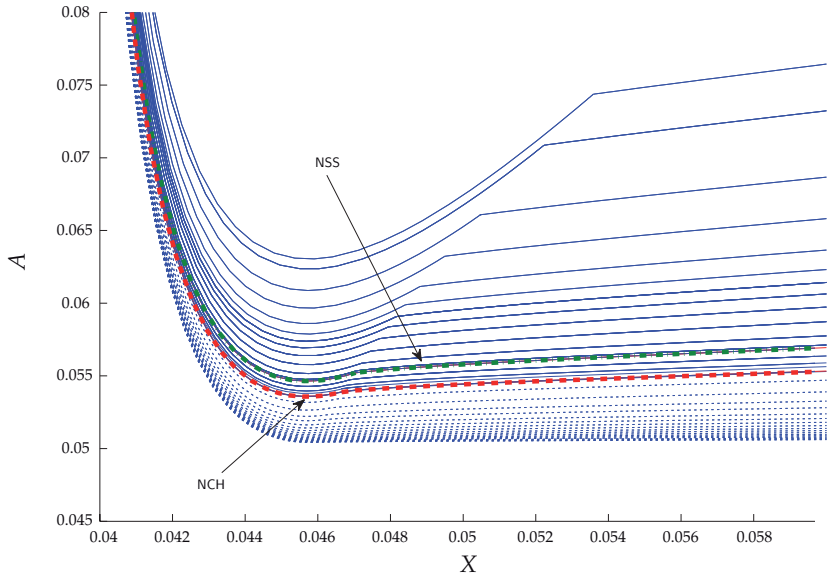

Figure 3.10: Continuum of HHS orbits (upper orbits) and HSN orbits (lower orbits) that converge to the NCH orbit.

$x_0^{(0)}$ and $x_1^{(0)}$ are given by

$$\begin{pmatrix} 10.6899 \\ 1.2339 \\ -1.2572 \end{pmatrix} \quad \text{and} \quad \begin{pmatrix} 10.9686 \\ -0.1510 + 1.2203i \\ -0.1510 - 1.2203i \end{pmatrix},$$

respectively. Therefore, there is a two-dimensional unstable manifold in $x_0^{(0)}$ with a real leading eigenvalue, so only one unstable connection parameter, namely Uparam1, has to be taken into account in the first step, and a two-dimensional stable manifold in $x_1^{(0)}$. Due to the eigenvalues in $x_0^{(0)}$ and $x_1^{(0)}$, there are two unstable connection parameters and one stable connection parameter. The starting point is given by $x(0) = x_0^{(0)} + \varepsilon_0 \text{UParam1} q_{0,1}^{(0)}$ with $q_{0,1}^{(0)} = (-0.4545, -0.5608, -0.6920)^{\mathrm{T}}$, the eigenvector corresponding to $\lambda_1^{(0)} = 1.2339$. We initialize UParam1 $= -1$ and $\varepsilon_0 = 10^{-4}$ and integrate over an interval of length 3. MatCont takes that part of

the time-integrated orbit up to the point where ε_1 stops decreasing, which in this case is only a very small segment, for which SParam1 $= -0.8175$.

In the successive homotopies we use a discretization of 50 mesh intervals and 4 collocation points. A continuation with all the connection parameters and ε_1 free places the end-vector $x(1) - x_1^{(0)}$ in the stable eigenspace of $x_1^{(0)}$, the end value of ε_1 equals 5.1783. Note that $n_\alpha = n - (n_U + n_S) + 2 = 3 - (2+2) + 2 = 1$, so no free system parameters are needed in the continuation to make ε_1 small.

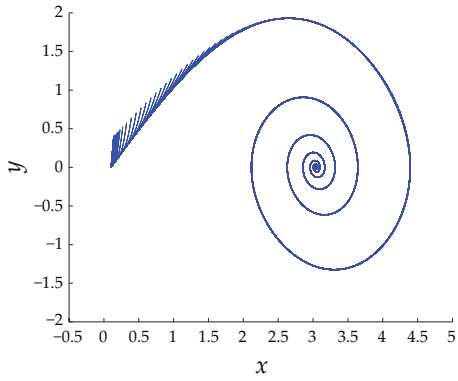

Figure 3.11: Continuation that makes ε_1 small.

A plot of this continuation is given in Figure 3.11. The initial orbit is only the small vertical line on the left, however, through the homotopy we succeed in finding a proper starting orbit for the computation of a branch of heteroclinic orbits. This gives us an indication of the robustness of the method. The stable eigenspace of $x_1^{(0)}$ is two-dimensional because of the complex conjugate pair of eigenvalues with negative real part. This explains the spiral convergence to $x_1^{(0)}$ as can be seen in the figure. The end values of the heteroclinic parameters are $T = 30.4026$ and $\varepsilon_1 = 10^{-4}$. Finally, we can start the continuation of heteroclinic orbits, taking c as the free system parameter and T as the free heteroclinic parameter. The result is shown in Figure 3.12. The continuation of 100 heteroclinic orbits took 49.7 seconds.

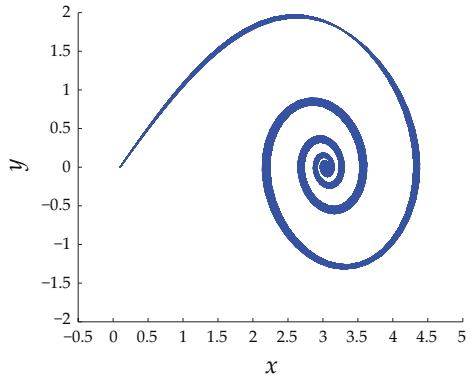

Figure 3.12: A family of heteroclinic orbits.

3.7 Conclusion

In this chapter we have introduced a defining BVP for the continuation of connecting orbits, in which the Riccati equations used to set up the projection boundary conditions are explicitly included. We have presented a homotopy method for the initialization of connecting orbits. The power of the successive continuations approach was affirmed by the success of the method in a large variety of chosen examples. Moreover, the possibility of reaching a solution from a far away starting point contributes to the strength of the method. Therefore, the homotopy method is a valuable alternative for the detection of a connecting orbit, which often gives results where other methods fail.

We have remarked that the first step in the homotopy method can be done either by a time integration or a continuation. In HomCont the first step is done by continuation. We have tested both strategies, and in our examples the time-integration seemed to be the most effective. That is why in MatCont the homotopy always starts from a solution obtained via time integration.

In [22] we have given an overview of the test functions for all codimension 2 homoclinic bifurcations and paid special attention to the orbit- and inclination-flip cases, for which we have generalized the test functions such that they can also be applied when the leading eigenvalues are complex.

4

Normal forms for Codim 2 Bifurcations of Limit Cycles

In this chapter we derive normal forms for the codimension 2 bifurcations of limit cycles and discuss the possible bifurcation scenarios that can happen in a neighbourhood of these bifurcation points.

4.1 Introduction

High-dimensional systems occur frequently in the study of dynamical systems. The higher the dimension, the more complex and time-consuming the computations are. First reducing the dimensionality of the system then seems a very tempting idea. The center manifold theory tackles this problem. When encountering a bifurcation, the center manifold theorem guarantees the existence of a stable, an unstable and a low-dimensional center invariant manifold near the bifurcation point. The study of the dynamics in the whole system can then be restricted to the study of the dynamics in the center manifold. The dynamics in the center manifold is determined by the

normal forms, which exhibit the relevant bifurcation. Although the center manifold is not unique, and the normal form is not unique either, the drawn bifurcation conclusions are not affected by the choices made.

The Hartman-Grobman theorem states that in the case of hyperbolicity the linearization of the system determines the bifurcation scenario. However, in the case of nonhyperbolicity nonlinear terms enter the field. The nonlinear terms are **resonant terms** in the normal forms when they can not be removed by coordinate changes. Luckily, not all nonlinear terms are equally important. At a bifurcation point, several situations may occur. The value of the normal form coefficients allows us to select the right scenario and to determine the essential features happening around the bifurcation point. Normal form coefficients then provide initial guesses for where to search for new phenomena.

In Section 4.2 we present the normal forms for the codim 2 bifurcations of limit cycles, i.e. the bifurcations listed in Table 2.2. We hereby make a distinction between the normal forms corresponding with a two- or three-dimensional center manifold, i.e. $n_c = 2$ or 3, and the normal forms where $n_c = 4$ or 5. We also briefly discuss the possible bifurcations in their unfoldings. In Section 4.3 we give a derivation of the normal forms presented in Section 4.2, based on the theory of Iooss. In Section 4.4 we investigate in detail the possible bifurcation scenarios around the bifurcation points. Quantities in terms of the normal form coefficients make a distinction between the several possible situations at the corresponding bifurcation point. To check the genericity of the system, nondegeneracy conditions are formulated. Finally, in Section 4.A we derive quadratic approximations of the Hopf and heteroclinic bifurcation curves that are needed in the interpretation of the PDNS and NSNS bifurcations.

4.2 Critical normal forms

Isolated periodic orbits (limit cycles) of smooth differential equations

$$\dot{x} = f(x, \alpha), \quad x \in \mathbb{R}^n, \ \alpha \in \mathbb{R}^p, \tag{4.1}$$

play an important role in applications. Write (4.1) at the critical parameter values as

$$\dot{u} = F(u), \tag{4.2}$$

and suppose that there is a limit cycle Γ corresponding to a periodic solution $u_0(t)$, where $T > 0$ is its (minimal) period. Develop $F(u_0(t) + v(t))$ into the Taylor series

$$\begin{aligned} &F(u_0(t)+v(t)) \\ &\quad = F(u_0(t)) + A(t)v(t) + \frac{1}{2}B(t;v(t),v(t)) + \frac{1}{3!}C(t;v(t),v(t),v(t)) \\ &\quad + \frac{1}{4!}D(t;v(t),v(t),v(t),v(t)) + \frac{1}{5!}E(t;v(t),v(t),v(t),v(t),v(t)) + O(|v|^6), \end{aligned} \tag{4.3}$$

where $A(t)v = F_u(u_0(t))v$, $B(t;v_1,v_2) = F_{uu}(u_0(t))[v_1,v_2]$, $C(t;v_1,v_2,v_3) = F_{uuu}(u_0(t))[v_1,v_2,v_3]$, etc. The multilinear forms A, B, C, D, and E are periodic in t with period T. Assume that the limit cycle is nonhyperbolic, i.e. the number of critical multipliers $n_c > 1$. Then, there exists an invariant n_c-dimensional critical center manifold $W^c(\Gamma) \subset \mathbb{R}^n$ near Γ.

To describe the normal forms of a generic system (4.2) on the critical center manifold for the codim 2 bifurcations of limit cycles, we parameterize $W^c(\Gamma)$ near Γ by (τ,ξ), where $\tau \in [0,kT]$ for $k \in \{1,2,3,4\}$ is a cyclic coordinate, and ξ is a real or complex transverse coordinate, depending on the bifurcation. It follows from [59] that it is possible to select the τ- and ξ-coordinates so that the restriction of (4.2) to the corresponding critical center manifold $W^c(\Gamma)$ will have a periodic normal form. Each normal form can be written as

$$\begin{cases} \dfrac{d\tau}{dt} = 1 + p(\xi) + r(\tau,\xi), \\ \dfrac{d\xi}{dt} = P(\xi) + R(\tau,\xi), \end{cases} \tag{4.4}$$

where p and P are polynomials in ξ of some degree N and without constant terms, while r and R are smooth $O(|\xi|^{N+1})$-functions that are kT-periodic in τ.

Below, we list the critical normal forms and briefly describe bifurcations possible in their generic unfoldings (see [3–5,67], as well as [21], for more details). Note that the α's present in the normal forms have no relation with the parameters α, present in (4.1). From Section 5.2 however, it will follow that in two cases, namely the Cusp Point of Cycles bifurcation and the Fold-Flip bifurcation, further simplification of the normal forms is possible. We stress that the normal forms below are valid for generic systems. In particular, it is assumed that a multiple critical eigenvalue of the monodromy matrix M (when present) is nonsemisimple and that the corresponding Jordan chain has maximal length.

4.2.1 Bifurcations with a 2D center manifold

Cusp Point of Cycles bifurcation

The cycle exhibits a Cusp Point of Cycles bifurcation if the eigenvalue $\mu_{0,1} = 1$ is double nonsemisimple (i.e. the corresponding Jordan block of the monodromy matrix $M(T)$ is two-dimensional), while there are no other critical multipliers and the coefficient b in (2.6) vanishes. The two-dimensional periodic normal form at the CPC bifurcation is

$$\begin{cases} \dfrac{d\tau}{dt} = 1 - \xi + \alpha_1\xi^2 + \alpha_2\xi^3 + \dots, \\ \dfrac{d\xi}{dt} = c\xi^3 + \dots, \end{cases} \tag{4.5}$$

where $\tau \in [0, T]$, ξ is a real coordinate on $W^c(\Gamma)$ that is transverse to Γ, α_1, α_2, $c \in \mathbb{R}$ and the dots denote the $O(|\xi|^4)$-terms, which are T-periodic in τ. If $c \neq 0$, the limit cycle Γ is a triple root. In generic two-parameter systems (4.1), three hyperbolic limit cycles exist in a cuspidal wedge approaching the codim 2 point that is delimited by two bifurcation curves, where two cycles collide and disappear via a Limit Point of Cycles bifurcation.

Generalized Period-Doubling bifurcation

The cycle exhibits a Generalized Period-Doubling bifurcation if the trivial eigenvalue $\mu_0 = 1$ of the monodromy matrix $M(T)$ is simple and there is only one other critical simple eigenvalue $\mu_1 = -1$ and the coefficient c in (2.7) vanishes. The two-dimensional periodic normal form at the GPD bifurcation is

$$\begin{cases} \dfrac{d\tau}{dt} = 1 + \alpha_1\xi^2 + \alpha_2\xi^4 + \dots, \\ \dfrac{d\xi}{dt} = e\xi^5 + \dots, \end{cases} \tag{4.6}$$

where $\tau \in [0, 2T]$, ξ is a real coordinate on $W^c(\Gamma)$ that is transverse to Γ, α_1, α_2, $e \in \mathbb{R}$ and the dots denote the $O(|\xi|^6)$-terms, which are $2T$-periodic in τ. If $e \neq 0$, at most two period doubled limit cycles can bifurcate from the critical limit cycle Γ. In generic two-parameter systems (4.1), the GPD point in the Period-Doubling bifurcation curve separates its sub- and supercritical branch and is the origin of a unique Limit Point of Cycles bifurcation curve, where two period doubled cycles collide and disappear.

4.2.2 Bifurcations with a 3D center manifold

In all following cases, 'chaotic motions' in the full system on the center manifold are possible (see [3–5, 67] and references therein).

Chenciner bifurcation

The cycle exhibits a Chenciner bifurcation if the trivial critical eigenvalue $\mu_0 = 1$ of $M(T)$ is simple and there are only two more critical simple multipliers $\mu_{1,2} = e^{\pm i\theta}$ with $\theta \neq \frac{2\pi}{j}$, for $j = 1, 2, 3, 4, 5, 6$, and the coefficient $\Re(d)$ in (2.8) vanishes. The three-dimensional periodic normal form at the CH bifurcation can be written as

$$\begin{cases} \dfrac{d\tau}{dt} = 1 + \alpha_1|\xi|^2 + \alpha_2|\xi|^4 + \dots, \\ \dfrac{d\xi}{dt} = i\omega\xi + ic\xi|\xi|^2 + e\xi|\xi|^4 + \dots, \end{cases} \tag{4.7}$$

where $\tau \in [0, T]$, $\omega = \theta/T$, ξ is a complex coordinate on $W^c(\Gamma)$ transverse to Γ, $\alpha_1, \alpha_2, c \in \mathbb{R}$, $e \in \mathbb{C}$ and the dots denote the $O(|\xi|^6)$-terms, which are T-periodic in τ. In generic two-parameter systems (4.1), at the CH point the Neimark-Sacker bifurcation changes its criticality (i.e. the bifurcating invariant torus changes its stability). A complicated bifurcation set responsible for 'collision' and destruction of two tori of opposite stability is rooted at this codim 2 point.

Strong Resonance 1:1 bifurcation

The cycle exhibits a Strong Resonance 1:1 bifurcation if the trivial critical eigenvalue $\mu_{0,1,2} = 1$ of $M(T)$ is triple and the corresponding Jordan block is three-dimensional, while there are no other critical multipliers. The three-dimensional periodic normal form at the R1 bifurcation is

$$\begin{cases} \dfrac{d\tau}{dt} = 1 - \xi_1 + \alpha\xi_1^2 + \dots, \\ \dfrac{d\xi_1}{dt} = \xi_2 - \xi_1\xi_2 + \dots, \\ \dfrac{d\xi_2}{dt} = a\xi_1^2 + b\xi_1\xi_2 + \dots, \end{cases} \tag{4.8}$$

where $\tau \in [0, T]$, (ξ_1, ξ_2) are real coordinates on $W^c(\Gamma)$ transverse to Γ, $\alpha, a, b \in \mathbb{R}$ and the dots denote the $O(|\xi|^3)$-terms, which are T-periodic in τ. In generic two-parameter systems (4.1), the R1 point is located on a Limit Point of Cycles curve.

At this point, a torus bifurcation curve is rooted together with global homoclinic bifurcation curves, along which the stable and the unstable invariant manifolds of a saddle cycle are tangent. The intersection of the invariant manifolds generates a Poincaré homoclinic structure with the associated periodic and 'chaotic motions'.

Strong Resonance 1:2 bifurcation

The cycle exhibits a Strong Resonance 1:2 bifurcation if the trivial critical multiplier $\mu_0 = 1$ is simple and the only other critical multiplier $\mu_{1,2} = -1$ is double nonsemisimple. The three-dimensional periodic normal form at the R2 bifurcation is

$$\begin{cases} \dfrac{d\tau}{dt} = 1 + \alpha\xi_1^2 + \dots, \\ \dfrac{d\xi_1}{dt} = \xi_2 + \alpha\xi_1^2\xi_2 + \dots, \\ \dfrac{d\xi_2}{dt} = a\xi_1^3 + b\xi_1^2\xi_2 + \dots, \end{cases} \tag{4.9}$$

where $\tau \in [0, 2T]$, (ξ_1, ξ_2) are real coordinates on $W^c(\Gamma)$ transverse to Γ, α, a, $b \in \mathbb{R}$ and the dots denote the $O(|\xi|^4)$-terms, which are $2T$-periodic in τ. In generic two-parameter systems (4.1), the R2 point is the endpoint of a torus bifurcation curve. The Period-Doubling bifurcation curve passes through this point, and (depending on the normal form coefficients) a torus bifurcation curve of the period doubled limit cycle can originate there. As in the R1 case, global bifurcation curves related to homoclinic tangencies can be present.

Strong Resonance 1:3 bifurcation

The cycle exhibits a Strong Resonance 1:3 bifurcation if the trivial critical multiplier $\mu_0 = 1$ is simple and there are only two more critical simple multipliers $\mu_{1,2} = e^{\pm i\frac{2\pi}{3}}$. The three-dimensional periodic normal form at the R3 bifurcation can be written as

$$\begin{cases} \dfrac{d\tau}{dt} = 1 + \alpha_1|\xi|^2 + \alpha_2\xi^3 + \bar{\alpha}_2\bar{\xi}^3 + \dots, \\ \dfrac{d\xi}{dt} = b\bar{\xi}^2 + c\xi|\xi|^2 + \dots, \end{cases} \tag{4.10}$$

where $\tau \in [0, 3T]$, ξ is a complex coordinate on $W^c(\Gamma)$ transverse to Γ, $\alpha_1 \in \mathbb{R}$, $\alpha_2, b, c \in \mathbb{C}$ and the dots denote the $O(|\xi|^4)$-terms, which are $3T$-periodic in τ. In generic two-parameter systems (4.1), near the R3 point a homoclinic

Poincaré structure of the $3T$-periodic limit cycle destroys the torus that is born at the Neimark-Sacker bifurcation curve passing through this point. Curves of homoclinic tangencies are rooted there.

Strong Resonance 1:4 bifurcation

The cycle exhibits a Strong Resonance 1:4 bifurcation if the trivial critical multiplier $\mu_0 = 1$ is simple and there are only two more critical simple multipliers $\mu_{1,2} = e^{\pm i\frac{\pi}{2}}$. The three-dimensional periodic normal form at the R4 bifurcation can be written as

$$\begin{cases} \dfrac{d\tau}{dt} = 1 + \alpha_1|\xi|^2 + \alpha_2\xi^4 + \bar{\alpha}_2\bar{\xi}^4 + \ldots, \\ \dfrac{d\xi}{dt} = c\xi|\xi|^2 + d\bar{\xi}^3 + \ldots, \end{cases} \tag{4.11}$$

where $\tau \in [0, 4T]$, ξ is a complex coordinate on $W^c(\Gamma)$ transverse to Γ, $\alpha_1 \in \mathbb{R}$, $\alpha_2, c, d \in \mathbb{C}$ and the dots denote the $O(|\xi|^5)$-terms, which are $4T$-periodic in τ. In generic two-parameter systems (4.1), at the R4 point there can be eight different situations, depending upon the values of c and d. In the simplest case a homoclinic structure associated to a $4T$-periodic cycle destroys an invariant torus that is born at the Neimark-Sacker bifurcation curve that passes through this point.

Fold-Flip bifurcation

The cycle exhibits a Fold-Flip bifurcation if the trivial critical multiplier $\mu_{0,1} = 1$ is double nonsemisimple and there is only one more critical multiplier $\mu_2 = -1$. The three-dimensional periodic normal form at the LPPD bifurcation is

$$\begin{cases} \dfrac{d\tau}{dt} = 1 - \xi_1 + \alpha_{20}\xi_1^2 + \alpha_{02}\xi_2^2 + \alpha_{30}\xi_1^3 + \alpha_{12}\xi_1\xi_2^2 + \ldots, \\ \dfrac{d\xi_1}{dt} = a_{20}\xi_1^2 + a_{02}\xi_2^2 + a_{30}\xi_1^3 + a_{12}\xi_1\xi_2^2 + \ldots, \\ \dfrac{d\xi_2}{dt} = b_{11}\xi_1\xi_2 + b_{21}\xi_1^2\xi_2 + b_{03}\xi_2^3 + \ldots, \end{cases} \tag{4.12}$$

where $\tau \in [0, 2T]$, (ξ_1, ξ_2) are real coordinates on $W^c(\Gamma)$ transverse to Γ, all the coefficients are real and the dots denote the $O(|\xi|^4)$-terms, which are $2T$-periodic in τ. In generic two-parameter systems (4.1), the Period-Doubling and Limit Point of Cycles bifurcation curves are tangent at the LPPD point, where (depending on the normal form coefficients) a Neimark-Sacker bifurcation curve of the $2T$-periodic

cycle can be rooted. Global bifurcations of heteroclinic structures and invariant tori are also possible.

4.2.3 Bifurcations with a 4D center manifold

Note that in the normal forms of the previous 8 cases, with a 2- or 3-dimensional center manifold, the derivative of the ξ-variable with respect to the time t appeared. In the cases where the dimension of the center manifold equals 4 or 5, the derivative of the ξ-variable is taken with respect to the phase coordinate τ. We will discuss the two approaches in Section 4.3 and the following chapter.

Limit Point-Neimark-Sacker bifurcation

The Limit Point-Neimark-Sacker bifurcation occurs when the trivial critical multiplier $\mu_{0,1} = 1$ corresponds to a two-dimensional Jordan block and there are only two more critical simple multipliers $\mu_{2,3} = e^{\pm i\theta}$ with $\theta \neq \frac{2\pi}{j}$, for $j = 1,2,3,4$. The four-dimensional Iooss normal form at the LPNS bifurcation can be written as

$$\begin{cases} \dfrac{d\tau}{dt} = 1 - \xi_1 + \alpha_{200}\xi_1^2 + \alpha_{011}\left|\xi_2\right|^2 + \alpha_{300}\xi_1^3 + \alpha_{111}\xi_1\left|\xi_2\right|^2 + \dots, \\ \dfrac{d\xi_1}{d\tau} = a_{200}\xi_1^2 + a_{011}\left|\xi_2\right|^2 + a_{300}\xi_1^3 + a_{111}\xi_1\left|\xi_2\right|^2 + \dots, \\ \dfrac{d\xi_2}{d\tau} = i\omega\xi_2 + b_{110}\xi_1\xi_2 + b_{210}\xi_1^2\xi_2 + b_{021}\xi_2\left|\xi_2\right|^2 + \dots, \end{cases} \tag{4.13}$$

where $\tau \in [0,T]$, $\omega = \theta/T$, ξ_1 is a real and ξ_2 a complex coordinate on $W^c(\Gamma)$ that are transverse to Γ, $\alpha_{ijk}, a_{ijk} \in \mathbb{R}, b_{ijk} \in \mathbb{C}$, and the dots denote the $O(|\xi|^4)$-terms, which are T-periodic in τ. In generic two-parameter systems (4.1), the Neimark-Sacker and Limit Point of Cycles bifurcation curves are tangent at the LPNS point, where (depending on the normal form coefficients) a 3-torus can be born. The equations (4.13) implicitly describe motions on the 4-dimensional invariant manifold $W^c(\Gamma)$ with one cyclic coordinate τ.

Period-Doubling-Neimark-Sacker bifurcation

The Period-Doubling-Neimark-Sacker bifurcation occurs when the trivial critical multiplier $\mu_0 = 1$ is simple and there are only three more critical simple multipliers,

namely $\mu_1 = -1$ and $\mu_{2,3} = e^{\pm i\theta}$ with $\theta \neq \frac{2\pi}{j}$, for $j = 1,2,3,4$. The four-dimensional looss normal form at the PDNS bifurcation can be written as

$$\begin{cases} \frac{d\tau}{dt} = 1 + \alpha_{200}\xi_1^2 + \alpha_{011}|\xi_2|^2 + \alpha_{400}\xi_1^4 + \alpha_{022}|\xi_2|^4 + \alpha_{211}\xi_1^2|\xi_2|^2 + \dots, \\ \frac{d\xi_1}{d\tau} = a_{300}\xi_1^3 + a_{111}\xi_1|\xi_2|^2 + a_{500}\xi_1^5 + a_{122}\xi_1|\xi_2|^4 + a_{311}\xi_1^3|\xi_2|^2 + \dots, \\ \frac{d\xi_2}{d\tau} = i\omega\xi_2 + b_{210}\xi_1^2\xi_2 + b_{021}\xi_2|\xi_2|^2 + b_{410}\xi_1^4\xi_2 + b_{221}\xi_1^2\xi_2|\xi_2|^2 \\ \qquad + b_{032}\xi_2|\xi_2|^4 + \dots, \end{cases} \tag{4.14}$$

where $\tau \in [0, 2T]$, $\omega = \theta/T$, ξ_1 is a real and ξ_2 a complex coordinate on $W^c(\Gamma)$ that are transverse to Γ, $\alpha_{ijk}, a_{ijk} \in \mathbb{R}, b_{ijk} \in \mathbb{C}$, and the dots denote the $O(|\xi|^6)$-terms, which are $2T$-periodic in τ. In generic two-parameter systems (4.1), depending on the normal form coefficients a distinction is made between the 'simple' and 'difficult' cases. In the 'difficult' case, a 3-torus can be present.

4.2.4 Bifurcations with a 5D center manifold

Double Neimark-Sacker bifurcation

The Double Neimark-Sacker bifurcation occurs when the trivial critical multiplier $\mu_0 = 1$ is simple and there are only four more critical simple multipliers $\mu_{1,2} = e^{\pm i\theta_1}$ and $\mu_{3,4} = e^{\pm i\theta_2}$ with $\theta_{1,2} \neq \frac{2\pi}{j}$, for $j = 1,2,3,4,5,6$ and $l\theta_1 \neq j\theta_2$ for $l, j \in \mathbb{Z}$ with $l + j \leq 4$ (see [51]). The five-dimensional periodic normal form at the NSNS bifurcation can be written as

$$\begin{cases} \frac{d\tau}{dt} = 1 + \alpha_{1100}|\xi_1|^2 + \alpha_{0011}|\xi_2|^2 \\ \qquad + \alpha_{2200}|\xi_1|^4 + \alpha_{0022}|\xi_2|^4 + \alpha_{1111}|\xi_1|^2|\xi_2|^2 + \dots, \\ \frac{d\xi_1}{d\tau} = i\omega_1\xi_1 + a_{2100}\xi_1|\xi_1|^2 + a_{1011}\xi_1|\xi_2|^2 \\ \qquad + a_{3200}\xi_1|\xi_1|^4 + a_{1022}\xi_1|\xi_2|^4 + a_{2111}\xi_1|\xi_1|^2|\xi_2|^2 + \dots, \\ \frac{d\xi_2}{d\tau} = i\omega_2\xi_2 + b_{0021}\xi_2|\xi_2|^2 + b_{1110}\xi_2|\xi_1|^2 \\ \qquad + b_{0032}\xi_2|\xi_2|^4 + b_{2210}\xi_2|\xi_1|^4 + b_{1121}\xi_2|\xi_1|^2|\xi_2|^2 + \dots, \end{cases} \tag{4.15}$$

where $\tau \in [0, T]$, $\omega_{1,2} = \theta_{1,2}/T$, ξ_1 and ξ_2 are complex coordinates on $W^c(\Gamma)$ that are transverse to Γ, $\alpha_{ijkl} \in \mathbb{R}$, $a_{ijkl}, b_{ijkl} \in \mathbb{C}$, and the dots denote the $O(|\xi|^6)$-terms, which are T-periodic in τ. In generic two-parameter systems (4.1), depending on the normal form coefficients a distinction is made between 'simple' and 'difficult' cases. In the 'difficult' case a 4-torus can be present. The equations (4.15) implicitly describe motions on a 5-dimensional manifold with one cyclic coordinate τ.

4.3 Derivation of the normal forms

In this section we give the derivation of the normal forms for all codim 2 bifurcations of limit cycles, i.e. the normal forms (4.5)-(4.15). This derivation is based on the theory of Iooss, described in Section 2.7.

4.3.1 Bifurcations with 2 critical eigenvalues

Cusp Point of Cycles bifurcation

At the CPC bifurcation the monodromy matrix has the critical Jordan structure

$$M_0 = \begin{pmatrix} 1 & 1 \\ 0 & 1 \end{pmatrix},$$

i.e. the multiplier $\mu = 1$ is double nonsemisimple. Following the notation used in Section 2.7, $\sigma = 0$ and thus

$$L_0 = \begin{pmatrix} 0 & 1 \\ 0 & 0 \end{pmatrix}, \quad \tilde{L}_0 = 0.$$

We are in a situation in which Theorem 2.29 can be applied. In particular, a periodic normal form of (4.2) on the center manifold of the cycle can be written as

$$\frac{d\tau}{dt} = 1 + \xi + p(\tau, \xi), \quad \frac{d\xi}{d\tau} = \tilde{L}_0\xi + P(\tau, \xi),$$

where τ plays the role of phase coordinate along the orbit and ξ is a coordinate along a direction transversal to the periodic orbit. Here, p and P are at least quadratic polynomials in ξ with T-periodic in τ coefficients, and are such that

$$\frac{d}{d\tau}p(\tau, \xi) - \frac{d}{d\xi}p(\tau, \xi)\tilde{L}_0^*\xi = 0, \quad \frac{d}{d\tau}P(\tau, \xi) + \tilde{L}_0^*P(\tau, \xi) - \frac{d}{d\xi}P(\tau, \xi)\tilde{L}_0^*\xi = 0,$$

for all τ and $\xi \in \mathbb{R}$. Putting $\tilde{L}_0 = 0$ we obtain

$$\frac{d}{d\tau}p(\tau,\xi) = 0, \quad \frac{d}{d\tau}P(\tau,\xi) = 0,$$

i.e. the two polynomials p and P are independent of τ. So by explicitly writing the lowest order terms of the two polynomials, the normal form becomes

$$\begin{cases} \dfrac{d\tau}{dt} = 1 + \xi + p(\xi) = 1 + \xi + \alpha_1\xi^2 + \alpha_2'\xi^3 + \dots, \\ \dfrac{d\xi}{d\tau} = P(\xi) = b\xi^2 + c\xi^3 + \dots, \end{cases}$$

where the dots denote $O(|\xi|^4)$-terms. At a CPC point holds that $b = 0$. By making the substitution $\xi \mapsto -\xi$, we obtain the normal form (4.5) with $\alpha_2 = -\alpha_2'$.

Generalized Period-Doubling bifurcation

At the GPD bifurcation, we obtain

$$M_0 = \begin{pmatrix} 1 & 0 \\ 0 & -1 \end{pmatrix}, \quad L_0 = \begin{pmatrix} 0 & 0 \\ 0 & 0 \end{pmatrix}, \quad \tilde{L}_0 = 0.$$

We are in a case in which we can apply Theorem 2.30. It gives the following $2T$-periodic normal form on the center manifold (using the formula of Theorem 2.28)

$$\frac{d\tau}{dt} = 1 + p(\tau,\xi), \quad \frac{d\xi}{d\tau} = \tilde{L}_0\xi + P(\tau,\xi),$$

with polynomials p and P at least quadratic in ξ, having $2T$-periodic in τ coefficients, and such that

$$\frac{d}{d\tau}p(\tau,\xi) - \frac{d}{d\xi}p(\tau,\xi)\tilde{L}_0^*\xi = 0, \quad \frac{d}{d\tau}P(\tau,\xi) + \tilde{L}_0^*P(\tau,\xi) - \frac{d}{d\xi}P(\tau,\xi)\tilde{L}_0^*\xi = 0,$$
$$p(\tau+T,\xi) = p(\tau,-\xi), \qquad P(\tau+T,-\xi) = -P(\tau,\xi).$$

Putting $\tilde{L}_0 = 0$ in the first two formulas brings us back to the situation of the previous case

$$\frac{d}{d\tau}p(\tau,\xi) = 0, \quad \frac{d}{d\tau}P(\tau,\xi) = 0,$$

i.e. the two polynomials are independent of τ. This makes it possible to rewrite the last two formulas as

$$p(\xi) = p(-\xi), \quad P(-\xi) = -P(\xi),$$

so polynomial p is even ($p = \phi(\xi^2)$) and polynomial P is odd ($P = \xi\psi(\xi^2)$). Therefore, we can write our normal form as

$$\begin{cases} \dfrac{d\tau}{dt} = 1 + \phi(\xi^2) = 1 + \alpha_1\xi^2 + \alpha_2\xi^4 + \dots, \\ \dfrac{d\xi}{d\tau} = \xi\psi(\xi^2) = c\xi^3 + e\xi^5 + \dots, \end{cases}$$

where the dots denote $O(|\xi|^6)$-terms. By taking the GPD-condition $c = 0$ into account, we obtain the normal form (4.6).

4.3.2 Bifurcations with 3 critical eigenvalues

Chenciner bifurcation

In the CH case the Jordan block associated to the trivial multiplier is one-dimensional. We have

$$M_0 = \begin{pmatrix} 1 & 0 & 0 \\ 0 & e^{i\omega T} & 0 \\ 0 & 0 & e^{-i\omega T} \end{pmatrix}, \quad L_0 = \begin{pmatrix} 0 & 0 & 0 \\ 0 & i\omega & 0 \\ 0 & 0 & -i\omega \end{pmatrix}, \quad \tilde{L}_0 = \begin{pmatrix} i\omega & 0 \\ 0 & -i\omega \end{pmatrix}.$$

This puts us in a situation in which we can apply Theorem 2.28. If we assume that $\frac{\omega T}{2\pi} \notin \mathbb{Q}$, then it follows immediately from Example III.9 from [60] that a periodic normal form on the center manifold is given by

$$\begin{cases} \dfrac{d\tau}{dt} = 1 + \phi(|\xi|^2), \\ \dfrac{d\xi}{d\tau} = i\omega\xi + \xi\psi(|\xi|^2), \end{cases}$$

where the polynomials ϕ and ψ are at least linear in their argument; ϕ is real, while ψ takes values in $\mathbb{C}$. If we explicitly write terms up to and including the fifth order, namely

$$\begin{cases} \dfrac{d\tau}{dt} = 1 + \alpha_1|\xi|^2 + \alpha_2|\xi|^4 + \dots, \\ \dfrac{d\xi}{d\tau} = i\omega\xi + c'\xi|\xi|^2 + e'\xi|\xi|^4 + \dots, \end{cases}$$

where the dots denote $O(|\xi|^6)$-terms, we obtain the normal form (4.7) with $ic = i\omega\alpha_1 + c'$ (since the Lyapunov coefficient of the Neimark-Sacker bifurcation is purely imaginary) and $e = i\omega\alpha_2 + \alpha_1 c' + e'$.

Strong Resonance 1:1 bifurcation

At the R1 bifurcation we have

$$M_0 = \begin{pmatrix} 1 & 1 & 0 \\ 0 & 1 & 1 \\ 0 & 0 & 1 \end{pmatrix}, \quad L_0 = \begin{pmatrix} 0 & 1 & 0 \\ 0 & 0 & 1 \\ 0 & 0 & 0 \end{pmatrix}, \quad \tilde{L}_0 = \begin{pmatrix} 0 & 1 \\ 0 & 0 \end{pmatrix}.$$

We are in a case in which we can apply Theorem 2.29. The truncated T-periodic normal form on the center manifold has the form

$$\frac{d\tau}{dt} = 1 + \xi_1 + p(\tau, \xi), \quad \frac{d\xi}{d\tau} = \tilde{L}_0\xi + P(\tau, \xi),$$

where $\xi = (\xi_1, \xi_2)$. Here p and P are at least quadratic polynomials in (ξ_1, ξ_2) with T-periodic in τ coefficients, and are such that

$$\frac{d}{d\tau}p(\tau,\xi) - \frac{d}{d\xi}p(\tau,\xi)\tilde{L}_0^*\xi = 0, \quad \frac{d}{d\tau}P(\tau,\xi) + \tilde{L}_0^*P(\tau,\xi) - \frac{d}{d\xi}P(\tau,\xi)\tilde{L}_0^*\xi = 0.$$

If we write the Fourier expansions for p and P, namely

$$p(\tau,\xi) = \sum_{l=-\infty}^{\infty} p_l(\xi)e^{i\frac{2\pi l\tau}{T}}, \quad P(\tau,\xi) = \sum_{l=-\infty}^{\infty} P_l(\xi)e^{i\frac{2\pi l\tau}{T}},$$

we obtain, for any $l \in \mathbb{Z}$, the following differential equations

$$\frac{d}{d\xi}p_l(\xi)\tilde{L}_0^*\xi - i\frac{2\pi l}{T}p_l(\xi) = 0,$$
$$\frac{d}{d\xi}P_l(\xi)\tilde{L}_0^*\xi - i\frac{2\pi l}{T}P_l(\xi) - \tilde{L}_0^*P_l(\xi) = 0.$$

Putting our $\tilde{L}_0$ into the equations and writing $P_l(\xi_1,\xi_2) = (P_l^{(1)}(\xi_1,\xi_2), P_l^{(2)}(\xi_1, \xi_2))$, we can rewrite them as a set of differential equations in variable ξ_2

$$\begin{aligned}
&\frac{d}{d\xi_2}p_l(\xi_1,\xi_2) = i\frac{2\pi l}{T\xi_1}p_l(\xi_1,\xi_2),\\
&\frac{d}{d\xi_2}P_l^{(1)}(\xi_1,\xi_2) = i\frac{2\pi l}{T\xi_1}P_l^{(1)}(\xi_1,\xi_2),\\
&\frac{d}{d\xi_2}P_l^{(2)}(\xi_1,\xi_2) = \frac{1}{\xi_1}\left(i\frac{2\pi l}{T}P_l^{(2)}(\xi_1,\xi_2) + P_l^{(1)}(\xi_1,\xi_2)\right).
\end{aligned}$$

Since $p_l(\xi_1,\xi_2), P_l^{(1)}(\xi_1,\xi_2)$ and $P_l^{(2)}(\xi_1,\xi_2)$ are polynomials, if $l \neq 0$ the only solution is the trivial one. Therefore, l equals zero and thus the polynomials are τ-independent. We obtain

$$\frac{d}{d\xi_2}p_0(\xi_1,\xi_2) = \frac{d}{d\xi_2}P_0^{(1)}(\xi_1,\xi_2) = 0, \qquad \frac{d}{d\xi_2}P_0^{(2)}(\xi_1,\xi_2) = \frac{1}{\xi_1}P_0^{(1)}(\xi_1,\xi_2).$$

The first two equations show that p_0 and $P_0^{(1)}$ are independent from ξ_2, thus

$$p_0(\xi_1) = \phi_0(\xi_1), \qquad P_0^{(1)}(\xi_1) = \xi_1\chi(\xi_1).$$

Integrating the last differential equation gives

$$P_0^{(2)}(\xi_1,\xi_2) = \xi_2\chi(\xi_1) + \psi(\xi_1).$$

Now we can further simplify our normal form. In fact, we can make a change of variables such that polynomial $P_0^{(1)}$ vanishes (see page 19–20 in [60]). We then have

$$\tilde{P}_0^{(1)}(\xi_1) = 0, \qquad \tilde{P}_0^{(2)}(\xi_1,\xi_2) = \xi_2\phi_1(\xi_1) + \phi_2(\xi_1),$$

where ϕ_1 and ϕ_2 are polynomials satisfying $\phi_1(0) = \phi_2(0) = \left.\frac{d\phi_2}{d\xi_1}\right|_{\xi_1=0} = 0$.

Assembling all the information gives us the following normal form

$$\begin{cases}
\dfrac{d\tau}{dt} = 1 + \xi_1 + \phi_0(\xi_1) = 1 + \xi_1 + \alpha\xi_1^2 + \ldots,\\
\dfrac{d\xi_1}{d\tau} = \xi_2,\\
\dfrac{d\xi_2}{d\tau} = \xi_2\phi_1(\xi_1) + \phi_2(\xi_1) = a'\xi_1^2 + b'\xi_1\xi_2 + \ldots,
\end{cases}$$

where the dots denote $O(|\xi|^3)$-terms. Note that the polynomials ϕ_0 and ϕ_2 are at least quadratic in ξ_1, while ϕ_1 is at least linear in its argument. To obtain the normal form (4.8), make the substitutions $\xi_1 \mapsto -\xi_1$ and $\xi_2 \mapsto -\xi_2$ and impose that $a = -a'$ and $b = -b'$.

Strong Resonance 1:2 bifurcation

At the R2 bifurcation it holds that

$$M_0 = \begin{pmatrix} 1 & 0 & 0 \\ 0 & -1 & 1 \\ 0 & 0 & -1 \end{pmatrix}, \quad L_0 = \begin{pmatrix} 0 & 0 & 0 \\ 0 & 0 & 1 \\ 0 & 0 & 0 \end{pmatrix}, \quad \tilde{L}_0 = \begin{pmatrix} 0 & 1 \\ 0 & 0 \end{pmatrix}.$$

We are in a case in which we can apply Theorem 2.30. So we have the following $2T$-periodic normal form on the center manifold

$$\frac{d\tau}{dt} = 1 + p(\tau, \xi), \quad \frac{d\xi}{d\tau} = \tilde{L}_0\xi + P(\tau, \xi),$$

where $\xi = (\xi_1, \xi_2)$. The polynomials p and P are at least quadratic in ξ with $2T$-periodic in τ coefficients, and are such that

$$\begin{aligned} &\frac{d}{d\tau}p(\tau,\xi) - \frac{d}{d\xi}p(\tau,\xi)\tilde{L}_0^*\xi = 0, \\ &\frac{d}{d\tau}P(\tau,\xi) + \tilde{L}_0^*P(\tau,\xi) - \frac{d}{d\xi}P(\tau,\xi)\tilde{L}_0^*\xi = 0, \\ &p(\tau+T,\xi) = p(\tau,-\xi), \quad P(\tau+T,-\xi) = -P(\tau,\xi). \end{aligned} \tag{4.16}$$

Similar to the R1 case (since the $\tilde{L}_0$ matrix is the same), we obtain that all polynomials are independent from τ, l has to be equal to zero and the polynomials p and $P^{(1)}$ are independent from ξ_2.

Because of the independence from τ, we can rewrite (4.16) as

$$p(\xi) = p(-\xi), \quad P(-\xi) = -P(\xi),$$

obtaining that the polynomial p is even ($p(\xi_1) = \phi_0(\xi_1^2)$) and the polynomials $P^{(1)}$ and $P^{(2)}$ are odd ($P^{(1)}(\xi_1) = \xi_1\tilde{\phi}_1(\xi_1^2)$ and $P^{(2)}(\xi_1,\xi_2) = \xi_2\tilde{\phi}_1(\xi_1^2) + \xi_1\tilde{\phi}_2(\xi_1^2)$). Now we can simplify our normal form by changing variables (as discussed in the R1 case) such that

$$\tilde{P}^{(1)}(\xi_1) = 0, \qquad \tilde{P}^{(2)}(\xi_1,\xi_2) = \xi_2\phi_1(\xi_1^2) + \xi_1\phi_2(\xi_1^2).$$

Putting all information in the normal form equations gives the system

$$\begin{cases} \dfrac{d\tau}{dt} = 1 + \phi_0(\xi_1^2) = 1 + \alpha\xi_1^2 + \dots, \\ \dfrac{d\xi_1}{d\tau} = \xi_2, \\ \dfrac{d\xi_2}{d\tau} = \xi_2\phi_1(\xi_1^2) + \xi_1\phi_2(\xi_1^2) = a\xi_1^3 + b\xi_1^2\xi_2 + \dots, \end{cases}$$

where the dots denote $O(|\xi|^4)$-terms. From this follows the normal form (4.9).

Strong Resonance 1:3 bifurcation

An R3 point is a simple case, since the Jordan block associated with the trivial multiplier is one-dimensional and -1 is not a multiplier of the critical limit cycle. So we have

$$M_0 = \begin{pmatrix} 1 & 0 & 0 \\ 0 & e^{i\frac{2\pi}{3}} & 0 \\ 0 & 0 & e^{-i\frac{2\pi}{3}} \end{pmatrix}, \quad L_0 = \begin{pmatrix} 0 & 0 & 0 \\ 0 & i\frac{2\pi}{3T} & 0 \\ 0 & 0 & -i\frac{2\pi}{3T} \end{pmatrix}, \quad \tilde{L}_0 = \begin{pmatrix} i\frac{2\pi}{3T} & 0 \\ 0 & -i\frac{2\pi}{3T} \end{pmatrix}.$$

We can apply Theorem 2.28, which gives the following T-periodic normal form on the center manifold

$$\frac{d\tau}{dt} = 1 + p(\tau, z), \quad \frac{dz}{d\tau} = \tilde{L}_0 z + P(\tau, z),$$

where $z = (z_1, \bar{z}_1)$. The polynomials p and P are at least quadratic in z with T-periodic in τ coefficients, and are such that

$$\frac{d}{d\tau}p(\tau,z) - \frac{d}{dz}p(\tau,z)\tilde{L}_0^* z = 0, \quad \frac{d}{d\tau}P(\tau,z) + \tilde{L}_0^* P(\tau,z) - \frac{d}{dz}P(\tau,z)\tilde{L}_0^* z = 0.$$

We apply the results derived in Example III.9 from [60] with $\omega T/2\pi = 1/3$ to obtain

$$\begin{cases} \dfrac{d\tau}{dt} = 1 + \psi_0(|z_1|^2, \bar{z}_1^3 e^{i2\pi\tau/T}, z_1^3 e^{-i2\pi\tau/T}), \\ \dfrac{dz_1}{d\tau} = i\dfrac{2\pi}{3T}z_1 + z_1\psi_1(|z_1|^2, z_1^3 e^{-i2\pi\tau/T}) + \bar{z}_1^2 e^{i2\pi\tau/T}\psi_2(|z_1|^2, \bar{z}_1^3 e^{i2\pi\tau/T}). \end{cases}$$

Defining a new variable $\xi = e^{-i\frac{2\pi\tau}{3T}} z_1$, this system can be rewritten as

$$\begin{cases} \dfrac{d\tau}{dt} = 1 + \phi_0(|\xi|^2, \bar{\xi}^3, \xi^3), \\ \dfrac{d\xi}{d\tau} = \xi\phi_1(|\xi|^2, \xi^3) + \bar{\xi}^2\phi_2(|\xi|^2, \bar{\xi}^3), \end{cases}$$

with the polynomials ϕ_0 and ϕ_1 at least linear in their arguments, while ϕ_2 may contain constant terms. Notice that this system is autonomous and equivariant under the rotations of angle $2\pi/3$. Writing the leading terms of the polynomials gives

$$\begin{cases} \dfrac{d\tau}{dt} = 1 + \alpha_1|\xi|^2 + \alpha_2\xi^3 + \bar{\alpha}_2\bar{\xi}^3 + \dots, \\ \dfrac{d\xi}{d\tau} = b\bar{\xi}^2 + c\xi|\xi|^2 + \dots, \end{cases}$$

where the dots denote $O(|\xi|^4)$-terms, so that (4.10) follows.

Strong Resonance 1:4 bifurcation

As in the R3 case the Jordan block associated with the trivial multiplier is one-dimensional. The matrices are

$$M_0 = \begin{pmatrix} 1 & 0 & 0 \\ 0 & e^{i\frac{\pi}{2}} & 0 \\ 0 & 0 & e^{-i\frac{\pi}{2}} \end{pmatrix}, \quad L_0 = \begin{pmatrix} 0 & 0 & 0 \\ 0 & i\frac{\pi}{2T} & 0 \\ 0 & 0 & -i\frac{\pi}{2T} \end{pmatrix}, \quad \tilde{L}_0 = \begin{pmatrix} i\frac{\pi}{2T} & 0 \\ 0 & -i\frac{\pi}{2T} \end{pmatrix}.$$

We can apply Theorem 2.28 and obtain a T-periodic normal form on the center manifold

$$\frac{d\tau}{dt} = 1 + p(\tau, z), \quad \frac{dz}{d\tau} = \tilde{L}_0 z + P(\tau, z),$$

where $z = (z_1, \bar{z}_1)$. The polynomials p and P are at least quadratic in z, having T-periodic in τ coefficients, and are such that

$$\frac{d}{d\tau}p(\tau, z) - \frac{d}{dz}p(\tau, z)\tilde{L}_0^* z = 0, \quad \frac{d}{d\tau}P(\tau, z) + \tilde{L}_0^* P(\tau, z) - \frac{d}{dz}P(\tau, z)\tilde{L}_0^* z = 0.$$

Again, we make use of Example III.9 from [60] with $\omega T/2\pi = 1/4$ and obtain

$$\begin{cases} \dfrac{d\tau}{dt} = 1 + \psi_0(|z_1|^2, \bar{z}_1^4 e^{i2\pi\tau/T}, z_1^4 e^{-i2\pi\tau/T}), \\ \dfrac{dz_1}{d\tau} = i\dfrac{\pi}{2T}z_1 + z_1\psi_1(|z_1|^2, z_1^4 e^{-i2\pi\tau/T}) + \bar{z}_1^3 e^{i2\pi\tau/T}\psi_2(|z_1|^2, \bar{z}_1^4 e^{i2\pi\tau/T}). \end{cases}$$

Defining a new variable $\xi = e^{-i\frac{\pi\tau}{2T}} z_1$, the system can be rewritten as

$$\begin{cases} \dfrac{d\tau}{dt} = 1 + \phi_0(|\xi|^2, \bar{\xi}^4, \xi^4), \\ \dfrac{d\xi}{d\tau} = \xi\phi_1(|\xi|^2, \xi^4) + \bar{\xi}^3\phi_2(|\xi|^2, \bar{\xi}^4), \end{cases}$$

with the polynomials ϕ_0 and ϕ_1 at least linear in their arguments, while ϕ_2 may contain constant terms. Notice that this system is autonomous and equivariant under the rotations of angle $\pi/2$. Writing the leading terms of the polynomials gives

$$\begin{cases} \dfrac{d\tau}{dt} = 1 + \alpha_1|\xi|^2 + \alpha_2\xi^4 + \bar{\alpha}_2\bar{\xi}^4 + \dots, \\ \dfrac{d\xi}{d\tau} = c\xi|\xi|^2 + d\bar{\xi}^3 + \dots, \end{cases}$$

where the dots denote $O(|\xi|^5)$-terms, implying the normal form (4.11).

Fold-Flip bifurcation

At the LPPD bifurcation it holds that

$$M_0 = \begin{pmatrix} 1 & 1 & 0 \\ 0 & 1 & 0 \\ 0 & 0 & -1 \end{pmatrix}, \quad L_0 = \begin{pmatrix} 0 & 1 & 0 \\ 0 & 0 & 0 \\ 0 & 0 & 0 \end{pmatrix}, \quad \tilde{L}_0 = \begin{pmatrix} 0 & 0 \\ 0 & 0 \end{pmatrix}.$$

Theorem 2.30 gives the following truncated $2T$-periodic normal form on the center manifold

$$\frac{d\tau}{dt} = 1 + \xi_1 + p(\tau, \xi), \quad \frac{d\xi}{d\tau} = \tilde{L}_0\xi + P(\tau, \xi),$$

where $\xi = (\xi_1, \xi_2)$. The polynomials p and P are at least quadratic in ξ, having $2T$-periodic in τ coefficients, and are such that

$$\frac{d}{d\tau}p(\tau, \xi) - \frac{d}{d\xi}p(\tau, \xi)\tilde{L}_0^*\xi = 0, \tag{4.17}$$

$$\frac{d}{d\tau}P(\tau, \xi) + \tilde{L}_0^*P(\tau, \xi) - \frac{d}{d\xi}P(\tau, \xi)\tilde{L}_0^*\xi = 0, \tag{4.18}$$

$$p(\tau + T, \xi_1, \xi_2) = p(\tau, \xi_1, -\xi_2), \tag{4.19}$$

$$P^{(1)}(\tau + T, \xi_1, -\xi_2) = P^{(1)}(\tau, \xi_1, \xi_2), \tag{4.20}$$

$$P^{(2)}(\tau + T, \xi_1, -\xi_2) = -P^{(2)}(\tau, \xi_1, \xi_2). \tag{4.21}$$

By putting $\tilde{L}_0$ into (4.17) and (4.18), we obtain

$$\frac{d}{d\tau}p(\tau,\xi_1,\xi_2) = \frac{d}{d\tau}P^{(1)}(\tau,\xi_1,\xi_2) = \frac{d}{d\tau}P^{(2)}(\tau,\xi_1,\xi_2) = 0,$$

so the polynomials are independent from τ. From (4.19), (4.20) and (4.21), it then follows that

$$\begin{aligned}
p(\xi_1,\xi_2) &= p(\xi_1,-\xi_2),\\
P^{(1)}(\xi_1,-\xi_2) &= P^{(1)}(\xi_1,\xi_2),\\
P^{(2)}(\xi_1,-\xi_2) &= -P^{(2)}(\xi_1,\xi_2),
\end{aligned}$$

so the polynomials are of the following form

$$\begin{aligned}
p(\xi_1,\xi_2) &= \chi_1(\xi_1) + \chi_2(\xi_2^2)(1+\chi_3(\xi_1)),\\
P^{(1)}(\xi_1,\xi_2) &= \psi_1(\xi_1) + \psi_2(\xi_2^2)(1+\psi_3(\xi_1)),\\
P^{(2)}(\xi_1,\xi_2) &= \xi_2\varphi_1(\xi_1) + \xi_2\varphi_2(\xi_2^2)(1+\varphi_3(\xi_1)),
\end{aligned}$$

with χ_1 and ψ_1 at least quadratic in their argument and all the other polynomials at least linear in their argument.

Assembling all the information gives the following system

$$\begin{cases}
\dfrac{d\tau}{dt} &= 1+\xi_1+\chi_1(\xi_1)+\chi_2(\xi_2^2)(1+\chi_3(\xi_1))\\
&= 1+\xi_1+\alpha_{20}\xi_1^2+\alpha_{02}\xi_2^2+\alpha'_{30}\xi_1^3+\alpha'_{12}\xi_1\xi_2^2+\ldots,\\
\dfrac{d\xi_1}{d\tau} &= \psi_1(\xi_1)+\psi_2(\xi_2^2)(1+\psi_2(\xi_1))\\
&= a'_{20}\xi_1^2+a'_{02}\xi_2^2+a'_{30}\xi_1^3+a'_{12}\xi_1\xi_2^2+\ldots,\\
\dfrac{d\xi_2}{d\tau} &= \xi_2\varphi_1(\xi_1)+\xi_2\varphi_2(\xi_2^2)(1+\varphi_3(\xi_1))\\
&= b'_{11}\xi_1\xi_2+b'_{21}\xi_1^2\xi_2+b_{03}\xi_2^3+\ldots,
\end{cases}$$

where the dots denote $O(|\xi|^4)$-terms. By making the substitution $\xi_1 \mapsto -\xi_1$, we obtain the normal form (4.12) with $\alpha_{30} = -\alpha'_{30}, \alpha_{12} = -\alpha'_{12}$, $a_{30} = a'_{30}+a'_{20}$, $a_{12} = a'_{12}+a'_{02}, a_{20} = -a'_{20}, a_{02} = -a'_{02}, b_{11} = -b'_{11}, b_{21} = b'_{21}+b'_{11}$.

4.3.3 Bifurcations with 4 critical eigenvalues

In the previous 8 cases we determined the normal forms based on the theorems of Iooss, in which the derivative of the ξ-variable with respect to the phase coordinate τ appears. We then reparametrized the obtained system so that in the final normal forms the derivative of the ξ-variable with respect to the time t appears. In the next three cases however, we omit this time reparameterization. In fact, this last step is not necessary for the theory developed in the rest of this thesis.

Limit Point-Neimark-Sacker bifurcation

At the LPNS bifurcation we have

$$M_0 = \begin{pmatrix} 1 & 1 & 0 & 0 \\ 0 & 1 & 0 & 0 \\ 0 & 0 & e^{i\omega T} & 0 \\ 0 & 0 & 0 & e^{-i\omega T} \end{pmatrix},$$

$$L_0 = \begin{pmatrix} 0 & 1 & 0 & 0 \\ 0 & 0 & 0 & 0 \\ 0 & 0 & i\omega & 0 \\ 0 & 0 & 0 & -i\omega \end{pmatrix}, \quad \tilde{L}_0 = \begin{pmatrix} 0 & 0 & 0 \\ 0 & i\omega & 0 \\ 0 & 0 & -i\omega \end{pmatrix}.$$

We are in a situation in which we can apply Theorem 2.29. So we can define a T-periodic normal form on the center manifold

$$\frac{d\tau}{dt} = 1 + \xi_1 + p(\tau, \xi), \quad \frac{d\xi}{d\tau} = \tilde{L}_0\xi + P(\tau, \xi),$$

where $\xi = (\xi_1, \xi_2, \bar{\xi}_2)^{\mathrm{T}}$ with $\xi_1 \in \mathbb{R}, \xi_2 \in \mathbb{C}$. The polynomials p, P are real, respectively complex, T-periodic in τ and at least quadratic in $(\xi_1, \xi_2, \bar{\xi}_2)$ such that

$$\frac{d}{d\tau}p(\tau,\xi) - \frac{d}{d\xi}p(\tau,\xi)\tilde{L}_0^*\xi = 0, \quad \frac{d}{d\tau}P(\tau,\xi) + \tilde{L}_0^*P(\tau,\xi) - \frac{d}{d\xi}P(\tau,\xi)\tilde{L}_0^*\xi = 0.$$

If we write the polynomials in a Fourier expansion, namely

$$p(\tau,\xi) = \sum_{l=-\infty}^{\infty} p_l(\xi)e^{i\frac{2\pi l\tau}{T}}, \quad P(\tau,\xi) = \sum_{l=-\infty}^{\infty} P_l(\xi)e^{i\frac{2\pi l\tau}{T}},$$

we obtain for any $l \in \mathbb{Z}$ the following differential equations

$$\frac{d}{d\xi} p_l(\xi)\tilde{L}_0^*\xi - i\frac{2\pi l}{T} p_l(\xi) = 0,$$
$$\frac{d}{d\xi} P_l(\xi)\tilde{L}_0^*\xi - i\frac{2\pi l}{T} P_l(\xi) - \tilde{L}_0^* P_l(\xi) = 0.$$

Putting $\tilde{L}_0$ into the equations with

$$P_l(\xi_1,\xi_2,\bar{\xi}_2) = (P_l^{(1)}(\xi_1,\xi_2,\bar{\xi}_2), P_l^{(2)}(\xi_1,\xi_2,\bar{\xi}_2), \bar{P}_l^{(2)}(\xi_1,\xi_2,\bar{\xi}_2))^{\mathrm{T}}$$

we can rewrite them as a set of differential equations in variable ξ_2

$$i\omega\xi_2\frac{d}{d\xi_2} p_l(\xi) + i\frac{2\pi l}{T} p_l(\xi) = i\omega\bar{\xi}_2\frac{d}{d\bar{\xi}_2} p_l(\xi),$$
$$i\omega\xi_2\frac{d}{d\xi_2} P_l^{(1)}(\xi) + i\frac{2\pi l}{T} P_l^{(1)}(\xi) = i\omega\bar{\xi}_2\frac{d}{d\bar{\xi}_2} P_l^{(1)}(\xi),$$
$$i\omega\xi_2\frac{d}{d\xi_2} P_l^{(2)}(\xi) + i\frac{2\pi l}{T} P_l^{(2)}(\xi) = i\omega\bar{\xi}_2\frac{d}{d\bar{\xi}_2} P_l^{(2)}(\xi) + i\omega P_l^{(2)}(\xi),$$
$$i\omega\xi_2\frac{d}{d\xi_2} \bar{P}_l^{(2)}(\xi) + i\frac{2\pi l}{T} \bar{P}_l^{(2)}(\xi) = i\omega\bar{\xi}_2\frac{d}{d\bar{\xi}_2} \bar{P}_l^{(2)}(\xi) - i\omega\bar{P}_l^{(2)}(\xi).$$

Since $p_l(\xi_1,\xi_2,\bar{\xi}_2), P_l^{(1)}(\xi_1,\xi_2,\bar{\xi}_2)$ and $P_l^{(2)}(\xi_1,\xi_2,\bar{\xi}_2)$ are polynomials, it follows from the equations that they are zero if $l \neq 0$. Therefore, the polynomials are τ-independent. We then obtain

$$\xi_2\frac{d}{d\xi_2} p_0(\xi_1,\xi_2,\bar{\xi}_2) = \bar{\xi}_2\frac{d}{d\bar{\xi}_2} p_0(\xi_1,\xi_2,\bar{\xi}_2),$$
$$\xi_2\frac{d}{d\xi_2} P_0^{(1)}(\xi_1,\xi_2,\bar{\xi}_2) = \bar{\xi}_2\frac{d}{d\bar{\xi}_2} P_0^{(1)}(\xi_1,\xi_2,\bar{\xi}_2),$$
$$\xi_2\frac{d}{d\xi_2} P_0^{(2)}(\xi_1,\xi_2,\bar{\xi}_2) = \bar{\xi}_2\frac{d}{d\bar{\xi}_2} P_0^{(2)}(\xi_1,\xi_2,\bar{\xi}_2) + P_0^{(2)}(\xi_1,\xi_2,\bar{\xi}_2),$$

and the complex conjugate of the last equation. From the first equation it follows that

$$p_0(\xi_1,\xi_2,\bar{\xi}_2) = \psi_1(\xi_1) + \psi_2(|\xi_2|^2) + \psi_3(\xi_1)\psi_4(|\xi_2|^2),$$

where ψ_2, ψ_3 and ψ_4 are at least linear in their argument and ψ_1 at least quadratic. Similarly, we obtain

$$P_0^{(1)}(\xi_1, \xi_2, \bar{\xi}_2) = \phi_1(\xi_1) + \phi_2(|\xi_2|^2) + \phi_3(\xi_1)\phi_4(|\xi_2|^2),$$

with the same conditions for ϕ as the ones for ψ. At last, from the third equation we can derive that

$$P_0^{(2)}(\xi_1, \xi_2, \bar{\xi}_2) = \xi_2\chi_1(\xi_1) + \xi_2\chi_2(|\xi_2|^2) + \xi_2\chi_3(\xi_1)\chi_4(|\xi_2|^2),$$

where χ_1, χ_2, χ_3 and χ_4 are at least linear in their argument.

Assembling all the information gives us the following normal form

$$\begin{cases} \dfrac{d\tau}{dt} = 1 + \xi_1 + \alpha_{200}\xi_1^2 + \alpha_{011}|\xi_2|^2 + \alpha'_{300}\xi_1^3 + \alpha'_{111}\xi_1|\xi_2|^2 + \dots, \\ \dfrac{d\xi_1}{d\tau} = a'_{200}\xi_1^2 + a'_{011}|\xi_2|^2 + a_{300}\xi_1^3 + a_{111}\xi_1|\xi_2|^2 + \dots, \\ \dfrac{d\xi_2}{d\tau} = i\omega\xi_2 + b'_{110}\xi_1\xi_2 + b_{210}\xi_1^2\xi_2 + b_{021}\xi_2|\xi_2|^2 + \dots. \end{cases}$$

By applying the substitution $\xi_1 \mapsto -\xi_1$, we find the Iooss normal form (4.13), i.e.

$$\begin{cases} \dfrac{d\tau}{dt} = 1 - \xi_1 + \alpha_{200}\xi_1^2 + \alpha_{011}|\xi_2|^2 + \alpha_{300}\xi_1^3 + \alpha_{111}\xi_1|\xi_2|^2 + \dots, \\ \dfrac{d\xi_1}{d\tau} = a_{200}\xi_1^2 + a_{011}|\xi_2|^2 + a_{300}\xi_1^3 + a_{111}\xi_1|\xi_2|^2 + \dots, \\ \dfrac{d\xi_2}{d\tau} = i\omega\xi_2 + b_{110}\xi_1\xi_2 + b_{210}\xi_1^2\xi_2 + b_{021}\xi_2|\xi_2|^2 + \dots, \end{cases}$$

with $\alpha_{300} = -\alpha'_{300}, \alpha_{111} = -\alpha'_{111}, a_{200} = -a'_{200}, a_{011} = -a'_{011}, b_{110} = -b'_{110}$ and the dots denote $O(|\xi|^4)$ terms. Note that the time evolution is given by

$$\begin{cases} \dfrac{d\tau}{dt} = 1 - \xi_1 + \alpha_{200}\xi_1^2 + \alpha_{011}|\xi_2|^2 + \alpha_{300}\xi_1^3 + \alpha_{111}\xi_1|\xi_2|^2 + \dots, \\ \dfrac{d\xi_1}{dt} = a_{200}\xi_1^2 + a_{011}|\xi_2|^2 + a^*_{300}\xi_1^3 + a^*_{111}\xi_1|\xi_2|^2 + \dots, \\ \dfrac{d\xi_2}{dt} = i\omega\xi_2 + b^*_{110}\xi_1\xi_2 + b^*_{210}\xi_1^2\xi_2 + b^*_{021}\xi_2|\xi_2|^2 + \dots, \end{cases}$$

with $a^*_{300} = -a_{200} + a_{300}, a^*_{111} = -a_{011} + a_{111}, b^*_{110} = -i\omega + b_{110}, b^*_{210} = i\omega\alpha_{200} - b_{110} + b_{210}, b^*_{021} = i\omega\alpha_{011} + b_{021}$. We could use this system as our starting

normal form, as in the previous cases. However, since the time reparametrized ODE has exactly the same form as (4.13), we can as well use (4.13). Therefore, (as mentioned before) in this and the next two cases, we will use the looss normal form as the starting normal form and thus we will not make use of the time reparametrized version of this normal form.

Period-Doubling-Neimark-Sacker bifurcation

At the PDNS bifurcation it holds that

$$M_0 = \begin{pmatrix} 1 & 0 & 0 & 0 \\ 0 & -1 & 0 & 0 \\ 0 & 0 & e^{i\omega T} & 0 \\ 0 & 0 & 0 & e^{-i\omega T} \end{pmatrix},$$

$$L_0 = \begin{pmatrix} 0 & 0 & 0 & 0 \\ 0 & 0 & 0 & 0 \\ 0 & 0 & i\omega & 0 \\ 0 & 0 & 0 & -i\omega \end{pmatrix}, \tilde{L}_0 = \begin{pmatrix} 0 & 0 & 0 \\ 0 & i\omega & 0 \\ 0 & 0 & -i\omega \end{pmatrix}.$$

We are in a case in which we can apply Theorem 2.30. So we can define a $2T$-periodic normal form on the center manifold

$$\frac{d\tau}{dt} = 1 + p(\tau, \xi), \quad \frac{d\xi}{d\tau} = \tilde{L}_0\xi + P(\tau, \xi),$$

where $\xi = (\xi_1, \xi_2, \bar{\xi}_2)$. The polynomials p and P are $2T$-periodic in τ and at least quadratic in their argument such that

$$\begin{aligned}
&\frac{d}{d\tau}p(\tau,\xi) - \frac{d}{d\xi}p(\tau,\xi)\tilde{L}_0^*\xi = 0,\\
&\frac{d}{d\tau}P(\tau,\xi) + \tilde{L}_0^*P(\tau,\xi) - \frac{d}{d\xi}P(\tau,\xi)\tilde{L}_0^*\xi = 0,\\
&p(\tau+T,\xi_1,\xi_2,\bar{\xi}_2) = p(\tau,-\xi_1,\xi_2,\bar{\xi}_2),\\
&P^{(1)}(\tau+T,-\xi_1,\xi_2,\bar{\xi}_2) = -P^{(1)}(\tau,\xi_1,\xi_2,\bar{\xi}_2),\\
&P^{(2)}(\tau+T,-\xi_1,\xi_2,\bar{\xi}_2) = P^{(2)}(\tau,\xi_1,\xi_2,\bar{\xi}_2),
\end{aligned}$$

and the complex conjugate of the last equation.

As in the LPNS case (since the $\tilde{L}_0$ matrix is the same) we obtain that all polynomials are independent from τ, so that we can rewrite the last three equations as

$$\begin{aligned}
&p(\xi_1,\xi_2,\bar{\xi}_2) = p(-\xi_1,\xi_2,\bar{\xi}_2),\\
&P^{(1)}(-\xi_1,\xi_2,\bar{\xi}_2) = -P^{(1)}(\xi_1,\xi_2,\bar{\xi}_2),\\
&P^{(2)}(-\xi_1,\xi_2,\bar{\xi}_2) = P^{(2)}(\xi_1,\xi_2,\bar{\xi}_2),
\end{aligned}$$

thus p and $P^{(2)}$ are even in ξ_1 and $P^{(1)}$ is odd in ξ_1. Similar to the results of the LPNS case, we obtain

$$\begin{aligned}
p_0(\xi_1,\xi_2,\bar{\xi}_2) &= \psi_1(\xi_1^2) + \psi_2(|\xi_2|^2) + \psi_3(\xi_1^2)\psi_4(|\xi_2|^2),\\
P_0^{(1)}(\xi_1,\xi_2,\bar{\xi}_2) &= \xi_1\phi_1(\xi_1^2) + \xi_1\phi_2(|\xi_2|^2) + \xi_1\phi_3(\xi_1^2)\phi_4(|\xi_2|^2),\\
P_0^{(2)}(\xi_1,\xi_2,\bar{\xi}_2) &= \xi_2\chi_1(\xi_1^2) + \xi_2\chi_2(|\xi_2|^2) + \xi_2\chi_3(\xi_1^2)\chi_4(|\xi_2|^2),
\end{aligned}$$

with all functions at least linear in their argument.

Assembling all the information gives us the Iooss normal form (4.14), i.e.

$$\begin{cases}
\dfrac{d\tau}{dt} = 1 + \alpha_{200}\xi_1^2 + \alpha_{011}|\xi_2|^2 + \alpha_{400}\xi_1^4 + \alpha_{022}|\xi_2|^4 + \alpha_{211}\xi_1^2|\xi_2|^2 + \dots,\\
\dfrac{d\xi_1}{d\tau} = a_{300}\xi_1^3 + a_{111}\xi_1|\xi_2|^2 + a_{500}\xi_1^5 + a_{122}\xi_1|\xi_2|^4 + a_{311}\xi_1^3|\xi_2|^2 + \dots,\\
\dfrac{d\xi_2}{d\tau} = i\omega\xi_2 + b_{210}\xi_1^2\xi_2 + b_{021}\xi_2|\xi_2|^2 + b_{410}\xi_1^4\xi_2 + b_{221}\xi_1^2\xi_2|\xi_2|^2\\
\qquad + b_{032}\xi_2|\xi_2|^4 + \dots,
\end{cases}$$

where the dots denote $O(|\xi|^6)$ terms. Note that the time evolution is given by

$$\begin{cases}
\dfrac{d\tau}{dt} = 1 + \alpha_{200}\xi_1^2 + \alpha_{011}|\xi_2|^2 + \alpha_{400}\xi_1^4 + \alpha_{022}|\xi_2|^4 + \alpha_{211}\xi_1^2|\xi_2|^2 + \dots,\\
\dfrac{d\xi_1}{dt} = a_{300}\xi_1^3 + a_{111}\xi_1|\xi_2|^2 + a'_{500}\xi_1^5 + a'_{311}\xi_1^3|\xi_2|^2 + a'_{122}\xi_1|\xi_2|^4 + \dots,\\
\dfrac{d\xi_2}{dt} = i\omega\xi_2 + b'_{210}\xi_1^2\xi_2 + b'_{021}\xi_2|\xi_2|^2 + b'_{410}\xi_1^4\xi_2 + b'_{221}\xi_1^2\xi_2|\xi_2|^2\\
\qquad + b'_{032}\xi_2|\xi_2|^4 + \dots,
\end{cases}$$

with $a'_{500} = a_{300}\alpha_{200} + a_{500}, a'_{311} = a_{300}\alpha_{011} + a_{111}\alpha_{200} + a_{311}$, $a'_{122} = a_{111}\alpha_{011} + a_{122}$, $b'_{210} = i\omega\alpha_{200} + b_{210}, b'_{021} = i\omega\alpha_{011} + b_{021}, b'_{410} = i\omega\alpha_{400} + b_{210}\alpha_{200} + b_{410}$,

$b'_{221} = i\omega\alpha_{211} + b_{210}\alpha_{011} + b_{021}\alpha_{200} + b_{221}, b'_{032} = i\omega\alpha_{022} + b_{021}\alpha_{011} + b_{032}.$

4.3.4 Bifurcations with 5 critical eigenvalues

Double Neimark-Sacker bifurcation

At the NSNS bifurcation we have the matrices

$$M_0 = \begin{pmatrix} 1 & 0 & 0 & 0 & 0 \\ 0 & e^{i\omega_1 T} & 0 & 0 & 0 \\ 0 & 0 & e^{-i\omega_1 T} & 0 & 0 \\ 0 & 0 & 0 & e^{i\omega_2 T} & 0 \\ 0 & 0 & 0 & 0 & e^{-i\omega_2 T} \end{pmatrix},$$

$$L_0 = \begin{pmatrix} 0 & 0 & 0 & 0 & 0 \\ 0 & i\omega_1 & 0 & 0 & 0 \\ 0 & 0 & -i\omega_1 & 0 & 0 \\ 0 & 0 & 0 & i\omega_2 & 0 \\ 0 & 0 & 0 & 0 & -i\omega_2 \end{pmatrix}, \tilde{L}_0 = \begin{pmatrix} i\omega_1 & 0 & 0 & 0 \\ 0 & -i\omega_1 & 0 & 0 \\ 0 & 0 & i\omega_2 & 0 \\ 0 & 0 & 0 & -i\omega_2 \end{pmatrix}.$$

We are in a case in which we can apply Theorem 2.28. So we can define a T-periodic normal form on the center manifold

$$\frac{d\tau}{dt} = 1 + p(\tau, \xi), \quad \frac{d\xi}{d\tau} = \tilde{L}_0\xi + P(\tau, \xi),$$

where $\xi = (\xi_1, \bar{\xi}_1, \xi_2, \bar{\xi}_2)$. The polynomials p and P are T-periodic in τ and at least quadratic in $(\xi_1, \bar{\xi}_1, \xi_2, \bar{\xi}_2)$ such that

$$\frac{d}{d\tau}p(\tau, \xi) - \frac{d}{d\xi}p(\tau, \xi)\tilde{L}_0^*\xi = 0, \quad \frac{d}{d\tau}P(\tau, \xi) + \tilde{L}_0^*P(\tau, \xi) - \frac{d}{d\xi}P(\tau, \xi)\tilde{L}_0^*\xi = 0.$$

Writing down the polynomials in a Fourier expansion results in the following equations

$$\begin{aligned} &i\omega_1\xi_1\frac{d}{d\xi_1}p_l(\xi) + i\omega_2\xi_2\frac{d}{d\xi_2}p_l(\xi) + i\frac{2\pi l}{T}p_l(\xi) \\ &= i\omega_1\bar{\xi}_1\frac{d}{d\bar{\xi}_1}p_l(\xi) + i\omega_2\bar{\xi}_2\frac{d}{d\bar{\xi}_2}p_l(\xi), \end{aligned}$$

$$
\begin{aligned}
&i\omega_1\xi_1\frac{d}{d\xi_1}P_l^{(1)}(\xi)+i\omega_2\xi_2\frac{d}{d\xi_2}P_l^{(1)}(\xi)+i\frac{2\pi l}{T}P_l^{(1)}(\xi)\\
&\quad=i\omega_1\bar{\xi}_1\frac{d}{d\bar{\xi}_1}P_l^{(1)}(\xi)+i\omega_2\bar{\xi}_2\frac{d}{d\bar{\xi}_2}P_l^{(1)}(\xi)+i\omega_1P_l^{(1)}(\xi),\\
&i\omega_1\xi_1\frac{d}{d\xi_1}\bar{P}_l^{(1)}(\xi)+i\omega_2\xi_2\frac{d}{d\xi_2}\bar{P}_l^{(1)}(\xi)+i\omega_1\bar{P}_l^{(1)}(\xi)\\
&\quad=i\omega_1\bar{\xi}_1\frac{d}{d\bar{\xi}_1}\bar{P}_l^{(1)}(\xi)+i\omega_2\bar{\xi}_2\frac{d}{d\bar{\xi}_2}\bar{P}_l^{(1)}(\xi)-i\frac{2\pi l}{T}\bar{P}_l^{(1)}(\xi),\\
&i\omega_1\xi_1\frac{d}{d\xi_1}P_l^{(2)}(\xi)+i\omega_2\xi_2\frac{d}{d\xi_2}P_l^{(2)}(\xi)+i\frac{2\pi l}{T}P_l^{(2)}(\xi)\\
&\quad=i\omega_1\bar{\xi}_1\frac{d}{d\bar{\xi}_1}P_l^{(2)}(\xi)+i\omega_2\bar{\xi}_2\frac{d}{d\bar{\xi}_2}P_l^{(2)}(\xi)+i\omega_2P_l^{(2)}(\xi),\\
&i\omega_1\xi_1\frac{d}{d\xi_1}\bar{P}_l^{(2)}(\xi)+i\omega_2\xi_2\frac{d}{d\xi_2}\bar{P}_l^{(2)}(\xi)+i\omega_1\bar{P}_l^{(2)}(\xi)\\
&\quad=i\omega_1\bar{\xi}_1\frac{d}{d\bar{\xi}_1}\bar{P}_l^{(2)}(\xi)+i\omega_2\bar{\xi}_2\frac{d}{d\bar{\xi}_2}\bar{P}_l^{(2)}(\xi)-i\frac{2\pi l}{T}\bar{P}_l^{(2)}(\xi).
\end{aligned}
$$

Since $p_l(\xi_1,\bar{\xi}_1,\xi_2,\bar{\xi}_2)$, $P_l^{(1)}(\xi_1,\bar{\xi}_1,\xi_2,\bar{\xi}_2)$ and $P_l^{(2)}(\xi_1,\bar{\xi}_1,\xi_2,\bar{\xi}_2)$ are polynomials, it follows from the equations that they are zero if $l\neq 0$. So p and P are τ-independent and $p_0(\xi_1,\bar{\xi}_1,\xi_2,\bar{\xi}_2)$, $P_0^{(1)}(\xi_1,\bar{\xi}_1,\xi_2,\bar{\xi}_2)$ and $P_0^{(2)}(\xi_1,\bar{\xi}_1,\xi_2,\bar{\xi}_2)$ satisfy

$$
\begin{aligned}
&\xi_1\frac{d}{d\xi_1}p_0(\xi_1,\bar{\xi}_1,\xi_2,\bar{\xi}_2)=\bar{\xi}_1\frac{d}{d\bar{\xi}_1}p_0(\xi_1,\bar{\xi}_1,\xi_2,\bar{\xi}_2),\\
&\xi_2\frac{d}{d\xi_2}p_0(\xi_1,\bar{\xi}_1,\xi_2,\bar{\xi}_2)=\bar{\xi}_2\frac{d}{d\bar{\xi}_2}p_0(\xi_1,\bar{\xi}_1,\xi_2,\bar{\xi}_2),\\
&\xi_1\frac{d}{d\xi_1}P_0^{(1)}(\xi_1,\bar{\xi}_1,\xi_2,\bar{\xi}_2)=\bar{\xi}_1\frac{d}{d\bar{\xi}_1}P_0^{(1)}(\xi_1,\bar{\xi}_1,\xi_2,\bar{\xi}_2)+P_0^{(1)}(\xi_1,\bar{\xi}_1,\xi_2,\bar{\xi}_2),\\
&\xi_2\frac{d}{d\xi_2}P_0^{(1)}(\xi_1,\bar{\xi}_1,\xi_2,\bar{\xi}_2)=\bar{\xi}_2\frac{d}{d\bar{\xi}_2}P_0^{(1)}(\xi_1,\bar{\xi}_1,\xi_2,\bar{\xi}_2),\\
&\xi_1\frac{d}{d\xi_1}P_0^{(2)}(\xi_1,\bar{\xi}_1,\xi_2,\bar{\xi}_2)=\bar{\xi}_1\frac{d}{d\bar{\xi}_1}P_0^{(2)}(\xi_1,\bar{\xi}_1,\xi_2,\bar{\xi}_2),\\
&\xi_2\frac{d}{d\xi_2}P_0^{(2)}(\xi_1,\bar{\xi}_1,\xi_2,\bar{\xi}_2)=\bar{\xi}_2\frac{d}{d\bar{\xi}_2}P_0^{(2)}(\xi_1,\bar{\xi}_1,\xi_2,\bar{\xi}_2)+P_0^{(2)}(\xi_1,\bar{\xi}_1,\xi_2,\bar{\xi}_2).
\end{aligned}
$$

From the first two equations follows that

$$p_0(\xi_1,\bar{\xi}_1,\xi_2,\bar{\xi}_2)=\psi_1(|\xi_1|^2)+\psi_2(|\xi_2|^2)+\psi_3(|\xi_1|^2)\psi_4(|\xi_2|^2).$$

From the third and fourth equation, we obtain

$$P_0^{(1)}(\xi_1,\bar{\xi}_1,\xi_2,\bar{\xi}_2) = \xi_1\phi_1(|\xi_1|^2) + \xi_1\phi_2(|\xi_2|^2) + \xi_1\phi_3(|\xi_1|^2)\phi_4(|\xi_2|^2),$$

and analogously

$$P_0^{(2)}(\xi_1,\bar{\xi}_1,\xi_2,\bar{\xi}_2) = \xi_2\chi_1(|\xi_2|^2) + \xi_2\chi_2(|\xi_1|^2) + \xi_2\chi_3(|\xi_1|^2)\chi_4(|\xi_2|^2),$$

where all functions are at least linear in their argument.

Assembling all the information gives us the looss normal form (4.15), i.e.

$$\begin{cases} \dfrac{d\tau}{dt} = 1 + \alpha_{1100}|\xi_1|^2 + \alpha_{0011}|\xi_2|^2 + \alpha_{2200}|\xi_1|^4 + \alpha_{0022}|\xi_2|^4 \\ \qquad + \alpha_{1111}|\xi_1|^2|\xi_2|^2 + \dots, \\ \dfrac{d\xi_1}{d\tau} = i\omega_1\xi_1 + a_{2100}\xi_1|\xi_1|^2 + a_{1011}\xi_1|\xi_2|^2 + a_{3200}\xi_1|\xi_1|^4 + a_{1022}\xi_1|\xi_2|^4 \\ \qquad + a_{2111}\xi_1|\xi_1|^2|\xi_2|^2 + \dots, \\ \dfrac{d\xi_2}{d\tau} = i\omega_2\xi_2 + b_{0021}\xi_2|\xi_2|^2 + b_{1110}\xi_2|\xi_1|^2 + b_{0032}\xi_2|\xi_2|^4 + b_{2210}\xi_2|\xi_1|^4 \\ \qquad + b_{1121}\xi_2|\xi_1|^2|\xi_2|^2 + \dots, \end{cases}$$

where the dots denote $O(|\xi|^6)$ terms. Note that the time evolution is of the form

$$\begin{cases} \dfrac{d\tau}{dt} = 1 + \alpha_{1100}|\xi_1|^2 + \alpha_{0011}|\xi_2|^2 + \alpha_{2200}|\xi_1|^4 + \alpha_{0022}|\xi_2|^4 \\ \qquad + \alpha_{1111}|\xi_1|^2|\xi_2|^2 + \dots, \\ \dfrac{d\xi_1}{d\tau} = i\omega_1\xi_1 + a'_{2100}\xi_1|\xi_1|^2 + a'_{1011}\xi_1|\xi_2|^2 + a'_{3200}\xi_1|\xi_1|^4 + a'_{1022}\xi_1|\xi_2|^4 \\ \qquad + a'_{2111}\xi_1|\xi_1|^2|\xi_2|^2 + \dots, \\ \dfrac{d\xi_2}{d\tau} = i\omega_2\xi_2 + b'_{0021}\xi_2|\xi_2|^2 + b'_{1110}\xi_2|\xi_1|^2 + b'_{0032}\xi_2|\xi_2|^4 + b'_{2210}\xi_2|\xi_1|^4 \\ \qquad + b'_{1121}\xi_2|\xi_1|^2|\xi_2|^2 + \dots, \end{cases}$$

where the coefficients with primes are functions of the original coefficients.

4.4 Generic unfoldings of the critical normal forms

In this section we describe how the coefficients of the critical normal forms can be used to predict bifurcations of the phase portraits near the critical limit cycles for nearby parameter values. Certain quantities that are functions of these critical coefficients, are introduced and used to distinguish between various bifurcation scenarios.

We first concentrate on the first 8 cases in which we represent the normal form as (4.4). After a time reparametrization, (4.4) can be rewritten as

$$\begin{cases} \dfrac{d\tau}{dt} = 1, \\ \dfrac{d\xi}{dt} = \tilde{P}(\xi) + \tilde{R}(\tau, \xi), \end{cases}$$

where $\tilde{P}$ and $\tilde{R}$ have the same properties as P and R. The equation for ξ will then become the nonautonomous system

$$\frac{d\xi}{dt} = \tilde{P}(\xi) + \hat{R}(t, \xi)$$

with the right-hand side kT-periodic in t. The kT-shift along orbits of the resulting autonomous truncated system,

$$\dot{\xi} = \tilde{P}(\xi), \tag{4.22}$$

will approximate the k-th iterate of the Poincaré map associated with the limit cycle and restricted to the center manifold, in appropriate coordinates. Notice that the right-hand side of (4.22) has the same terms as the corresponding equation in the Iooss normal form in [59].

This construction can be extended to parameter-dependent systems. In appropriate coordinates, a canonical unfolding of (4.22) will approximate the restricted Poincaré map of the generic two-parameter system (4.1) [59]. The new unfolding parameters will be denoted as (β_1, β_2).

Note that we study the truncated normal form. Higher order terms, however, can alter the bifurcation portrait obtained from this truncated normal form. For a detailed description of the effect of the higher order terms, we refer to [67]. In the CPC and GPD cases, the general and truncated normal forms are topologically equivalent.

4.4.1 Bifurcations with 2 critical eigenvalues

Cusp Point of Cycles bifurcation

In this case, (4.22) takes the form

$$\dot{\xi} = c\xi^3, \quad \xi \in \mathbb{R},$$

and the T-shift along its orbits approximates the restricted Poincaré map associated with the critical limit cycle. Indeed, the T-shift can be obtained by making one Picard iteration (as discussed in Section 2.3), i.e.

$$\xi_0(t) = \eta, \qquad \xi_1(t) = \eta + \int_0^t c\eta^3 ds$$

and thus

$$\eta \mapsto \eta + cT\eta^3. \tag{4.23}$$

Further iterations do not change this expansion. The canonical two-parameter unfolding of (4.23) is (up to a rescaling given by (9.10) in [67])

$$\eta \mapsto \eta + \beta_1 + \beta_2\eta + cT\eta^3,$$

provided $c \neq 0$. Fixed points of this equation correspond to fixed points of the Poincaré maps, i.e. cycles in (4.1). When two fixed points collide at a Limit Point bifurcation, a Limit Point of Cycles bifurcation occurs in (4.1). The bifurcation diagram of this equation is shown in Figure 4.1. On the curves T_1 and T_2, which meet tangentially at the Cusp Point of Cyles, two limit cycles collide and disappear. When detecting a CPC point, the output given by MatCont is the normal form coefficient c.

Generalized Period-Doubling bifurcation

In this case, (4.22) reduces to

$$\dot{\xi} = e\xi^5, \quad \xi \in \mathbb{R},$$

and the $2T$-shift along its orbits approximates the second iterate of the restricted Poincaré map associated with the critical limit cycle. Indeed, by doing one Picard iteration up to $2T$ we obtain

$$\eta \mapsto \eta + 2Te\eta^5. \tag{4.24}$$

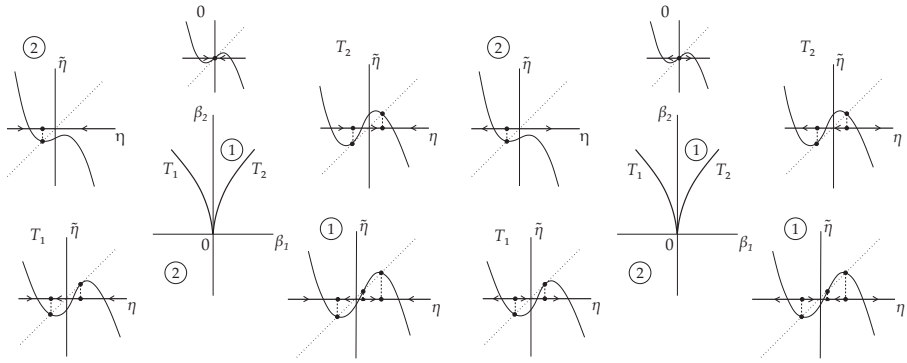

(a) $c < 0$ (b) $c > 0$

Figure 4.1: Bifurcation diagram of the Cusp bifurcation of the fixed point normal form.

The canonical two-parameter unfolding of (4.24) when $e \neq 0$ is (given on page 416 of [67])

$$\eta \mapsto (1 + 2\beta_1)\eta - 2\beta_2\eta^3 + e2T\eta^5.$$

The fixed point $\eta = 0$ of this equation corresponds to the fixed point of the Poincaré map, while symmetric nonzero fixed points of this equation correspond to its period doubled cycles. Thus, a pitchfork bifurcation in this equation will describe a Period-Doubling bifurcation of a limit cycle in (4.1). The coefficient of the fifth order term of the $2T$-shift has opposite sign than the one for maps derived in [67]. Therefore, the behaviour of the system at the bifurcation is the same but with opposite sign of the normal form coefficient. If $e < 0$ we obtain the bifurcation diagram reported in Figure 4.2 (b), in which the Limit Point curve of the period doubled limit cycles $T^{(2)}$ is tangent to the subcritical Period-Doubling branch labeled as $F_-^{(1)}$. If $e > 0$ we are in the opposite situation, depicted in Figure 4.2 (a). The output given by MatCont is the normal form coefficient e.

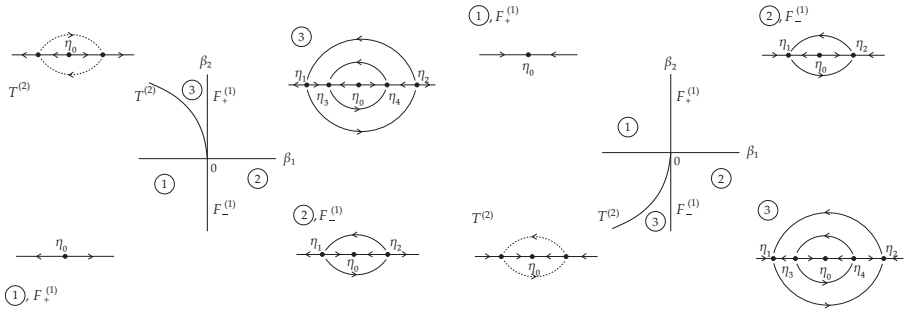

(a) $e > 0$ (b) $e < 0$

Figure 4.2: Bifurcation diagram of the degenerate Period-Doubling point bifurcation of the fixed point normal form.

4.4.2 Bifurcations with 3 critical eigenvalues

Chenciner bifurcation

In this case, (4.22) becomes

$$\dot{\xi} = i\omega\xi + i(c - \alpha_1\omega)\xi|\xi|^2 + (e - i(\alpha_1 c - \alpha_1^2\omega + \alpha_2\omega))\xi|\xi|^4, \tag{4.25}$$

and the T-shift along its orbits approximates the restricted Poincaré map associated with the critical limit cycle. Indeed, this can be shown by making use of Picard iterations. However, before we can do this, we need to make a change of variables in order to obtain a quasi-identity flow. By introducing the new complex variable $z = e^{-i\omega t}\xi$, (4.25) can be rewritten as

$$\dot{z} = i(c - \alpha_1\omega)z\,|z|^2 + \left(e - i(\alpha_1 c - \alpha_1^2\omega + \alpha_2\omega)\right) z\,|z|^4 .$$

Doing two Picard iterations up to time T, we obtain

$$\begin{aligned} z \mapsto & z + iT(c - \alpha_1\omega)z\,|z|^2 \\ & + T\left(e - \frac{c^2 T}{2} + \alpha_1 cT\omega - \frac{1}{2}\alpha_1^2 T\omega^2 + i\left(\alpha_1^2\omega - \alpha_1 c - \alpha_2\omega\right)\right) z\,|z|^4 . \end{aligned} \tag{4.26}$$

The canonical two-parameter unfolding of (4.26) is locally topologically equivalent to the normal form for the degenerate Hopf (Bautin) bifurcation ((9.22) in [67])

$$\begin{aligned} z \mapsto & (1+\beta_1)z + (\beta_2 + iT(c-\alpha_1\omega))z|z|^2 \\ & + T\left(e - \frac{c^2T}{2} + \alpha_1 cT\omega - \frac{1}{2}\alpha_1^2 T\omega^2 + i\left(\alpha_1^2\omega - \alpha_1 c - \alpha_2\omega\right)\right)z|z|^4, \end{aligned}$$

provided $\Re(e) \neq 0$. The trivial fixed point $z = 0$ corresponds to the bifurcating cycle in (4.1), while limit cycles in the $(\Re(z), \Im(z))$-plane correspond to closed invariant curves of the approximate Poincaré map, i.e. approximate invariant tori in (4.1). Note that actual invariant sets of (4.1) can be close to tori but have a much more complicated structure. The Hopf bifurcation will correspond to the Neimark-Sacker bifurcation, while the LPC curve at which two limit cycles collide and disappear will be substituted by a complicated bifurcation set where an 'annihilation' of two closed invariant curves occurs. This set is however close to the LPC curve, therefore we will refer to it as the 'Limit Point of Tori curve'.

The sign of the second Lyapunov coefficient L_2 (as defined on page 420 of [67]) determines the bifurcation scenario. However, from (4.7) we can derive that $\Re(e) < 0$ corresponds with a stable critical limit cycle and $\Re(e) > 0$ with an unstable critical limit cycle. Therefore, the case $\Re(e) < 0$ corresponds with the case $L_2 < 0$ and $\Re(e) > 0$ corresponds with $L_2 > 0$. So $\Re(e)$ and the second Lyapunov coefficient L_2 as defined in [67] have the same sign and vanish at the same time. Since both coefficients have the same effect and L_2 requires more computations, we compute $\Re(e)$ to determine the bifurcation scenario, and we will call $\Re(e)$ the **second Lyapunov coefficient**. When $\Re(e) < 0$, the outer invariant curve is stable and the Limit Point of Tori curve T_c is tangent to the subcritical Neimark-Sacker branch N_+, as shown in Figure 4.3 (a). When $\Re(e) > 0$, the outer invariant curve is unstable and the Limit Point of Tori curve T_c is tangent to the supercritical Neimark-Sacker branch N_-. The output given by MatCont is $\Re(e)$.

Strong Resonance 1:1 bifurcation

In this case, (4.22) has the form

$$\begin{cases} \dot{\xi}_1 = \xi_2, \\ \dot{\xi}_2 = a\xi_1^2 + b\xi_1\xi_2, \end{cases} \tag{4.27}$$

where it is assumed that $ab \neq 0$. The T-shift along orbits of this system approximates the restricted Poincaré map associated with the critical limit cycle. The

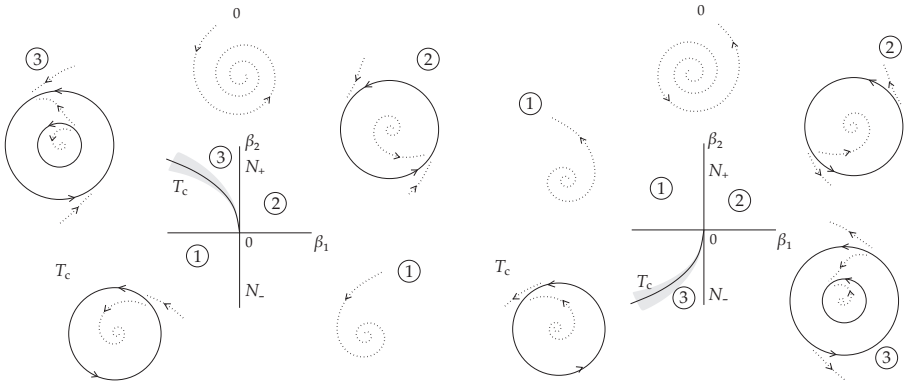

(a) $\Re(e) < 0$ (b) $\Re(e) > 0$

Figure 4.3: Bifurcation diagram of the generalized Neimark-Sacker bifurcation of the fixed point normal form.

canonical two-parameter unfolding of (4.27) is given by the Bogdanov-Takens normal form (up to a rescaling given by (9.53) in [67])

$$\begin{cases} \dot{\xi}_1 = \xi_2, \\ \dot{\xi}_2 = \beta_1 + \beta_2\xi_1 + a\xi_1^2 + b\xi_1\xi_2, \end{cases}$$

with bifurcation diagrams depending on the sign of the product ab. Equilibria of this system correspond to fixed points of the Poincaré map, i.e. to cycles of (4.1), while its limit cycles approximate closed invariant curves of the map, i.e. invariant tori of (4.1). The Hopf bifurcation will thus correspond to the Neimark-Sacker bifurcation. In particular, as shown in Figure 4.4, if the two coefficients have a different sign, the Neimark-Sacker curve H is supercritical, while in the other case it is subcritical. The saddle homoclinic bifurcation in the Bogdanov-Takens normal form will correspond to a complicated sequence of bifurcations through which the torus destructs near a homoclinic tangle. The output given by MatCont is the product of the coefficients a and b.

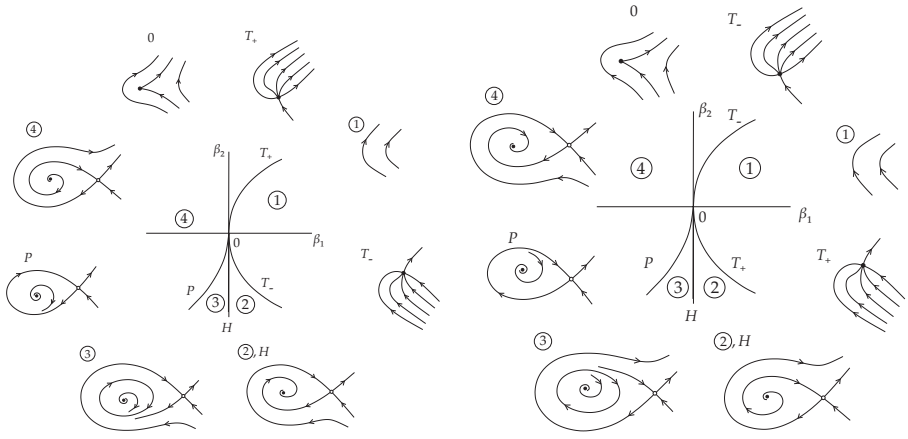

(a) $a > 0$, $ab < 0$ (b) $a > 0$, $ab > 0$

Figure 4.4: Bifurcation diagram of the Strong Resonance 1:1 bifurcation of the fixed point normal form. The other two cases in which $a < 0$ can be obtained by a reflection around the origin of the state portraits and a left-right flip of the bifurcation diagrams.

Strong Resonance 1:2 bifurcation

If we reparametrize time, (4.22) takes the form

$$\begin{cases} \dot{\xi}_1 = \xi_2, \\ \dot{\xi}_2 = a\xi_1^3 + b\xi_1^2\xi_2. \end{cases} \tag{4.28}$$

The $2T$-shift along its orbits approximates the second iterate of the restricted Poincaré map associated with the critical limit cycle. The canonical two-parameter unfolding of (4.28) when $ab \neq 0$ is ((9.74) in [67])

$$\begin{cases} \dot{\xi}_1 = \xi_2, \\ \dot{\xi}_2 = \beta_1\xi_1 + \beta_2\xi_2 + a\xi_1^3 + b\xi_1^2\xi_2. \end{cases}$$

There are four different bifurcation diagrams, determined by the signs of the coefficients. The ones with negative b are reported in Figure 4.5. The other two cases can be obtained by reversing the arrows of the phase portraits and making an

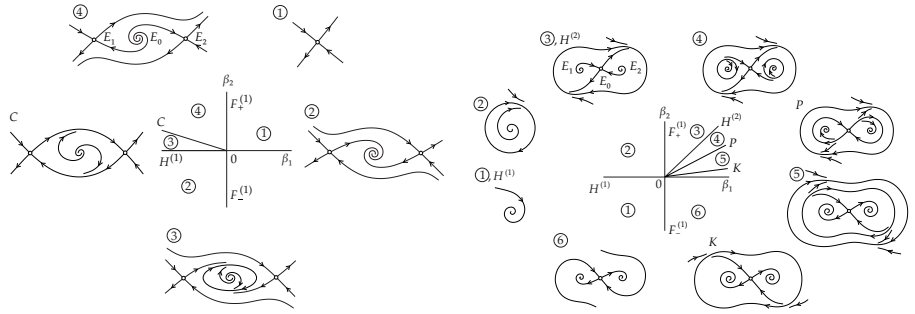

(a) $b < 0$, $a > 0$ (b) $b < 0$, $a < 0$

Figure 4.5: Bifurcation diagram of the Strong Resonance 1:2 bifurcation of the fixed point normal form. The other two possible cases in which $b > 0$ can be obtained by reversing time and making an up-down flip both of the state portraits and of the bifurcation diagrams.

up-down flip both of the state portraits and of the bifurcation diagrams. The trivial equilibrium $\xi = 0$ corresponds to the fixed point of the restricted Poincaré map, i.e. the bifurcating cycle of (4.1), while the nontrivial equilibria are the fixed points of the second iterate of the Poincaré map and correspond to one period doubled cycle in (4.1). Thus, a pitchfork implies the Period-Doubling bifurcation F, and a Hopf bifurcation corresponds to a Neimark-Sacker bifurcation that generates an invariant torus. More complicated invariant sets and bifurcations are also possible. The primary Neimark-Sacker curve $H^{(1)}$ is supercritical (with negative normal form coefficient) if the critical coefficient b is negative, subcritical otherwise. Moreover, if $a < 0$, a secondary Neimark-Sacker curve $H^{(2)}$ is rooted at the R2 point with opposite criticality of the primary one. The output given by MatCont is (a, b).

Strong Resonance 1:3 bifurcation

In this case, (4.22) takes the form

$$\dot{\xi} = b\bar{\xi}^2 + c\xi|\xi|^2, \quad \xi \in \mathbb{C}. \tag{4.29}$$

The $3T$-shift along its orbits approximates the third iterate of the restricted Poincaré map associated with the critical limit cycle. The canonical two-parameter unfolding

of (4.29) when $b \neq 0$ and $\Re(c) \neq 0$ is ((9.88) in [67])

$$\dot{\xi} = (\beta_1 + i\beta_2)\xi + b\bar{\xi}^2 + c\xi|\xi|^2.$$

Its trivial equilibrium corresponds to the bifurcating limit cycle, while three nontrivial equilibria correspond to fixed points of the third iterate of the Poincaré map, i.e. the cycle in (4.1) with triple period. Moreover, a limit cycle in the $(\Re(\xi), \Im(\xi))$-plane approximates a closed invariant curve of the Poincaré map, i.e. an invariant torus in (4.1). So a Hopf bifurcation corresponds to a Neimark-Sacker bifurcation. As can be seen in Figure 4.6, if $\Re(c) < 0$, the Neimark-Sacker bifurcation N is supercritical (with negative normal form coefficient), while in the other case it is subcritical. The output given by MatCont is $(b, \Re(c))$.

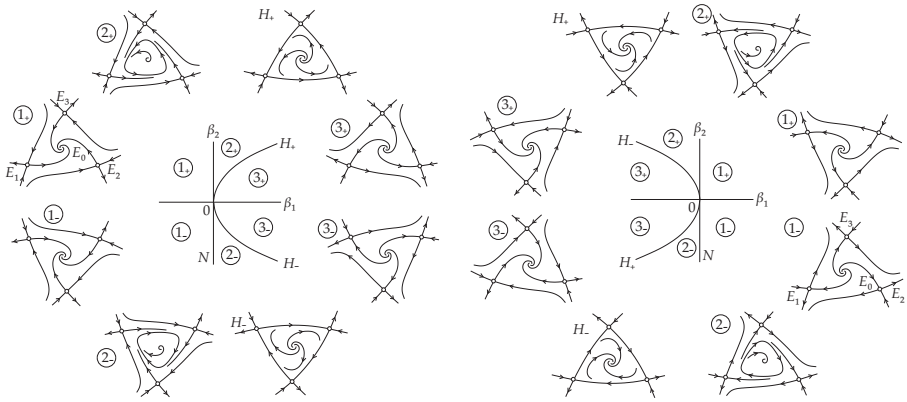

(a) $\Re(c) < 0$ (b) $\Re(c) > 0$

Figure 4.6: Bifurcation diagram of the Strong Resonance 1:3 bifurcation of the fixed point normal form.

Strong Resonance 1:4 bifurcation

Here, (4.22) has the form

$$\dot{\xi} = c\xi|\xi|^2 + d\bar{\xi}^3, \quad \xi \in \mathbb{C}. \tag{4.30}$$

The $4T$-shift along its orbits approximates the fourth iterate of the restricted Poincaré map associated with the critical limit cycle. The canonical two-parameter unfolding

of (4.30) when the complex product $cd \neq 0$ is ((9.98) in [67])

$$\dot{\xi} = (\beta_1 + i\beta_2)\xi + c\xi|\xi|^2 + d\bar{\xi}^3$$

and its equilibria, cycles, and their bifurcations have the standard interpretations in terms of the original system (4.1). In particular, nonzero equilibria correspond to the fixed points of the fourth iterate of the Poincaré map, i.e. one cycle with an approximate period of $4T$ in (4.1). The bifurcation diagram of the unfolding depends on the complex number

$$A = \frac{c}{|d|}$$

(see [65, 67] and references therein). Many topologically different bifurcation diagrams can be found near the R4 point. The analysis, if one excludes higher codimension situations, can be reduced to 22 different cases. First of all, by analyzing the unfolding, one can divide the A-plane into two big regions: in the semiplane $\Re(A) < 0$ the primary Neimark-Sacker bifurcation is supercritical, in the semiplane $\Re(A) > 0$ it is subcritical. What happens in the semiplane $\Re(A) > 0$ can therefore be obtained from the semiplane $\Re(A) < 0$ by inverting the direction of the vector fields and doing the transformation $\beta \to -\beta$. We can further reduce the analysis to the third quadrant of the A-plane, since the 12 possible cases are topologically equivalent paired through the transformation $\xi \mapsto \bar{\xi}$. The different regions are shown in Figure 4.7, in which some curves are computed numerically.

Figure 4.8 and Figure 4.9 show the possible bifurcation diagrams with the sketches of the phase portraits for the Poincaré maps in the case $\Re(A) < 0$. We use the following notation:

- N: Neimark-Sacker bifurcation. In regions VII and VIII there is also a Neimark-Sacker bifurcation of the period 4 limit cycle.
- T: Fold bifurcation of the period 4 limit cycles. There are three possibilities. Superscript `in`, `on` or `out` means that the bifurcation happens inside, on or outside a 'big' invariant curve.
- H: Homoclinic connection of the period 4 saddle limit cycle. Superscript S means that the born invariant curve is smaller than the limit cycle (a square looking homoclinic connection), C that it is bigger (a clover looking homoclinic connection), and L means that the born invariant curve is around the period 4 limit cycle; subscript + (-) means that the saddle quantity is positive (negative), and thus the born invariant curve is repelling (attracting).

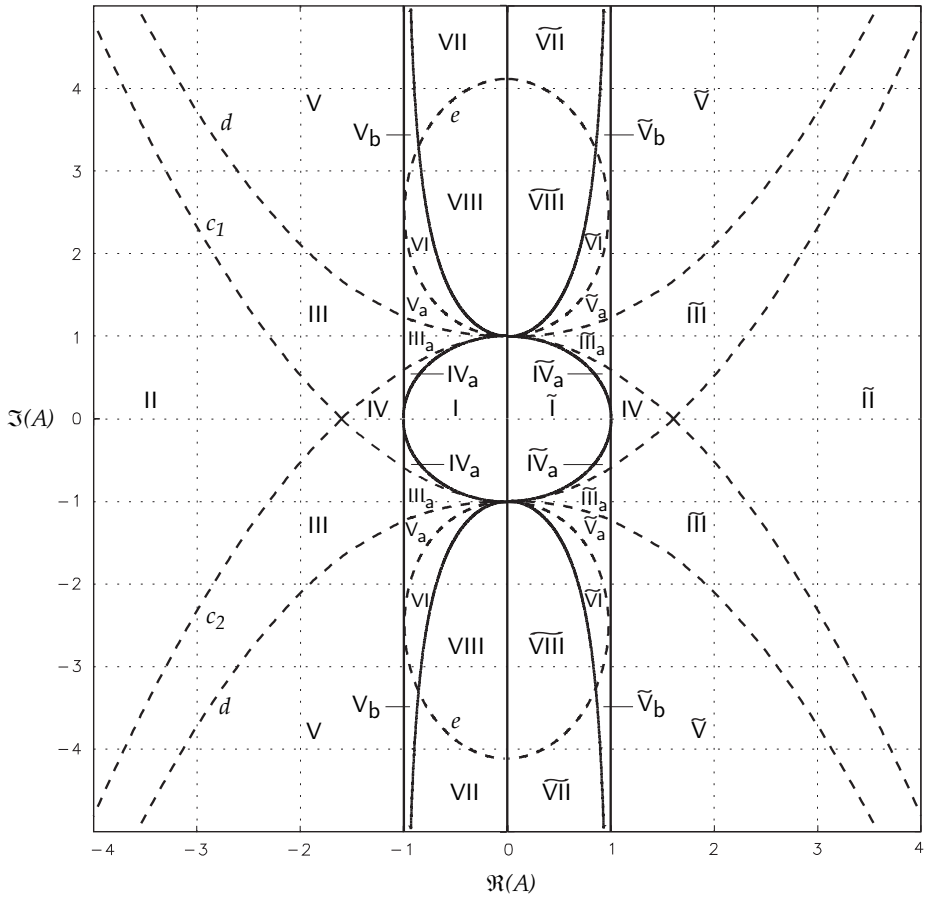

Figure 4.7: Partitioning of the A-plane into topologically different regions.

F: Fold bifurcation of the tori.

The output given by MatCont is (A, d).

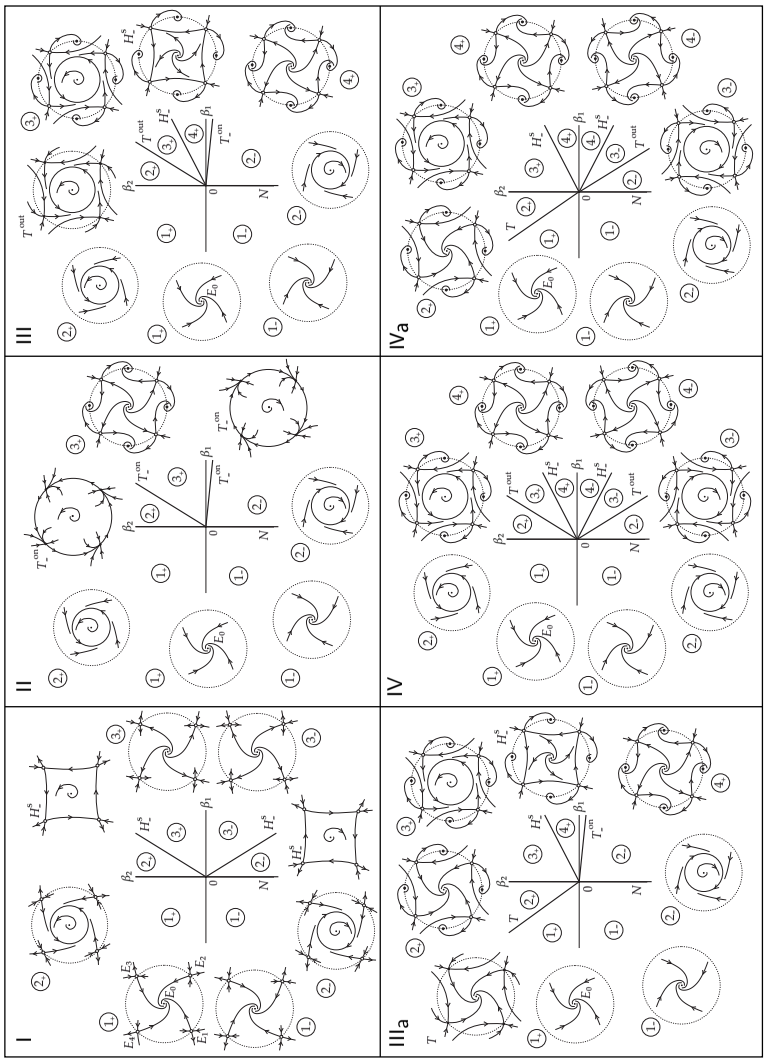

Figure 4.8: Bifurcation diagrams locally to the Strong Resonance 1:4 bifurcation in regions I to IVa of the semiplane $\Re(A) < 0$ of Figure 4.7. The cases in which $\Re(A) > 0$ can be obtained by the transformation $t \to -t$, $\beta \to -\beta$.

Figure 4.9: Bifurcation diagrams locally to the Strong Resonance 1:4 bifurcation in regions V to VIII of the semiplane $\Re(A) < 0$ of Figure 4.7. The cases in which $\Re(A) > 0$ can be obtained by the transformation $t \to -t$, $\beta \to -\beta$.

Fold-Flip bifurcation

In this case, (4.22) has the form

$$\begin{cases} \dot{\xi}_1 = a_{20}\xi_1^2 + a_{02}\xi_2^2 + (a_{30} + a_{20})\xi_1^3 + (a_{12} + a_{02})\xi_1\xi_2^2, \\ \dot{\xi}_2 = b_{11}\xi_1\xi_2 + (b_{21} + b_{11})\xi_1^2\xi_2 + b_{03}\xi_2^3. \end{cases} \tag{4.31}$$

The $2T$-shift along its orbits approximates the second iterate of the restricted Poincaré map associated with the critical limit cycle. Indeed, the $2T$-shift of (4.31) is the same, up to cubic terms, as the 1-shift of

$$\begin{cases} \dot{\xi}_1 = 2Ta_{20}\xi_1^2 + 2Ta_{02}\xi_2^2 + 2T(a_{30} + a_{20})\xi_1^3 + 2T(a_{12} + a_{02})\xi_1\xi_2^2, \\ \dot{\xi}_2 = 2Tb_{11}\xi_1\xi_2 + 2T(b_{21} + b_{11})\xi_1^2\xi_2 + 2Tb_{03}\xi_2^3. \end{cases} \tag{4.32}$$

System (4.32) is topologically equivalent with

$$\begin{cases} \dot{\zeta}_1 = a_1\zeta_1^2 + b_1\zeta_2^2 + (c_1 - a_1^2)\zeta_1^3 + (d_1 - a_1b_1 + b_1)\zeta_1\zeta_2^2, \\ \dot{\zeta}_2 = -\zeta_1\zeta_2 + \frac{1}{2}(a_1 - 1)\zeta_1^2\zeta_2 + \frac{1}{2}b_1\zeta_2^3, \end{cases} \tag{4.33}$$

since this second system can be obtained (neglecting higher order terms) from (4.32) using the transformation

$$\begin{cases} \zeta_1 = -2b_{11}T\xi_1 - 2T\left(b_{11} + b_{21} + a_{20}b_{11}T + b_{11}^2T\right)\xi_1^2 - 2T(b_{03} + a_{02}b_{11}T)\xi_2^2, \\ \zeta_2 = 2b_{11}T\xi_2. \end{cases}$$

This transformation should be invertible, so one nondegeneracy condition is involved, namely

$$b_{11} \neq 0.$$

If this condition is satisfied, the system can be put in the form (4.33), where the constants are defined as

$$a_1 = -\frac{a_{20}}{b_{11}}, \qquad b_1 = -\frac{a_{02}}{b_{11}}, \qquad c_1 = \frac{a_{20} + a_{30} + 2a_{20}^2T}{2b_{11}^2T},$$

$$d_1 = \frac{-2a_{20}b_{03} + 3a_{02}b_{11} + a_{12}b_{11} + 2b_{03}b_{11} + 2a_{02}b_{21} + 2a_{02}a_{20}b_{11}T + 6a_{02}b_{11}^2T}{2b_{11}^3T}.$$

If $b_{11} \neq 0$, the canonical two-parameter unfolding is provided by ((9.120) in [67])

$$\begin{cases} \dot{\zeta}_1 = \beta_1 + (-a_1\beta_1 + \beta_2)\zeta_1 + a_1\zeta_1^2 + b_1\zeta_2^2 + (c_1 - a_1^2)\zeta_1^3 + (d_1 - a_1b_1 + b_1)\zeta_1\zeta_2^2, \\ \dot{\zeta}_2 = \frac{1}{2}\beta_1\zeta_2 - \zeta_1\zeta_2 + \frac{1}{2}(a_1 - 1)\zeta_1^2\zeta_2 + \frac{1}{2}b_1\zeta_2^3. \end{cases}$$

Its equilibria and cycles have standard interpretations in terms of the original system (4.1). In particular, equilibria with $\zeta_2 \neq 0$ correspond to a period doubled cycle, while a Hopf bifurcation represents a Neimark-Sacker bifurcation of this cycle in (4.1). Bifurcations of limit cycles approximate torus bifurcations. The critical coefficients allow to determine what bifurcation scenario takes place. In particular (see [67, 73] for more details), three additional nondegeneracy conditions are involved:

- if $a_{20} \neq 0$ there are two limit cycles that collide and disappear (on F);
- if $a_{02} \neq 0$ a period doubled limit cycle is born (on P);
- if $a_{02}b_{11} < 0$ a nondegenerate torus bifurcation NS occurs for the period doubled cycle, with a Lyapunov coefficient that might differ by a positive factor from

  $$C_{NS} = -2a_{20}b_{21}a_{02} + 6b_{03}a_{20}^2 + (-2a_{02}b_{21} - 6a_{20}a_{02} + 2a_{20}b_{03} - 3a_{02}a_{30} - a_{12}a_{20})b_{11} + b_{11}^2(a_{12} - a_{02}),$$

  provided $C_{NS} \neq 0$.

In Figure 4.10 four possible scenarios are reported depending on the sign of the normal form coefficients. The output given by MatCont is $(b_{11}, a_{20}, a_{02}, C_{NS})$.

4.4.3 Bifurcations with 4 critical eigenvalues

We now concentrate on the last 3 cases in which the original Iooss representation is used as starting normal form. These normal forms are closely related to the normal forms for the Zero-Hopf and Hopf-Hopf bifurcations of equilibria. We can consider an unfolding of the corresponding bifurcation and study its canonical local bifurcation diagram for nearby parameter values. One can transform the restricted system into a parameter-dependent normal form in which the ξ-equations have a

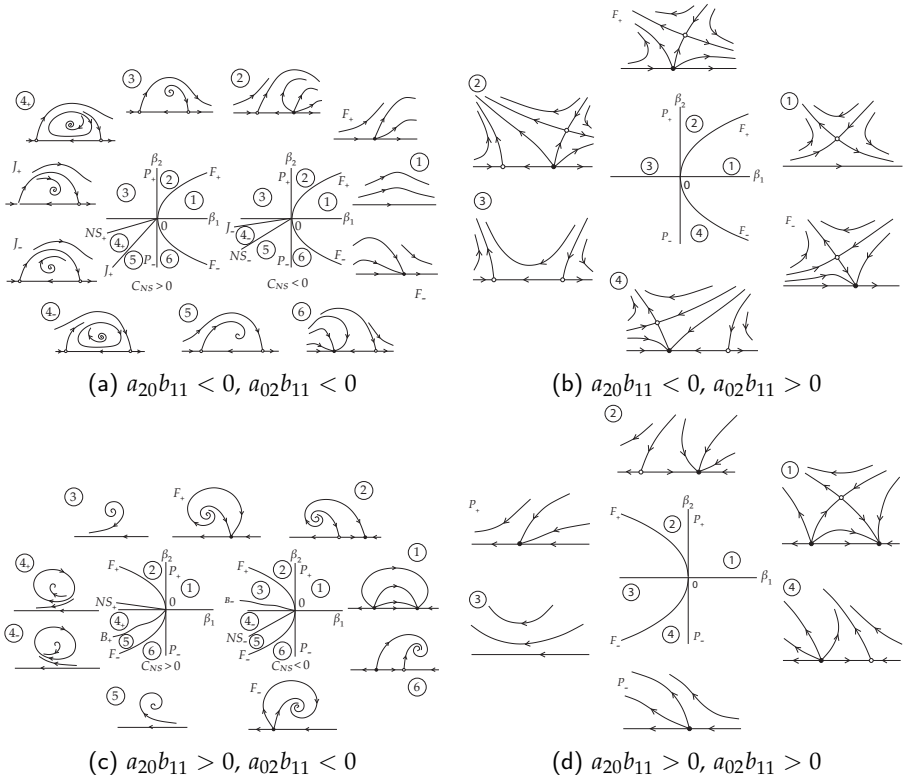

(a) $a_{20}b_{11} < 0$, $a_{02}b_{11} < 0$ (b) $a_{20}b_{11} < 0$, $a_{02}b_{11} > 0$

(c) $a_{20}b_{11} > 0$, $a_{02}b_{11} < 0$ (d) $a_{20}b_{11} > 0$, $a_{02}b_{11} > 0$

Figure 4.10: Bifurcation diagrams of a Fold-Flip bifurcation of the fixed point normal form.

τ-independent principle part and higher order terms that are kT-periodic in τ with $k = 1$ for LPNS and NSNS and $k = 2$ for PDNS. Below we describe bifurcations of these principle parts, i.e. the truncated parameter-dependent autonomous normal forms. Since the dynamics is determined by the ξ-equations, we first focus on their bifurcations by discussing the correspondence and the interpretation of the bifurcation diagrams of the generic unfoldings of the LPNS, PDNS and NSNS bifurcations. We then interpret the appearing bifurcation diagrams for the original system (4.1).

Limit Point-Neimark-Sacker bifurcation

Generically, a two-parameter unfolding of (4.1) near this bifurcation restricted to the center manifold is smoothly orbitally equivalent (with possible time reversal) to a system in which the equations for the transverse coordinates have the form (see Lemma 8.10 and expression (8.77) on page 336 in [67])

$$\begin{cases} \dfrac{d\xi}{d\tau} = \beta_1 + \xi^2 + s\,|\zeta|^2 + O(|(\xi,\zeta,\bar{\zeta})|^4), \\ \dfrac{d\zeta}{d\tau} = (\beta_2 + i\omega_1)\zeta + (\theta + i\vartheta)\xi\zeta + \xi^2\zeta + O(|(\xi,\zeta,\bar{\zeta})|^4), \end{cases} \tag{4.34}$$

where the O-terms are T-periodic in τ. This system is similar to the normal form for the Zero-Hopf bifurcation of equilibria (cf. Theorem 8.6 on page 338 in [67]). In Figure 4.11 the four possible bifurcation diagrams of the amplitude system for (4.34) without the higher order terms, i.e.

$$\begin{cases} \dfrac{d\xi}{d\tau} = \beta_1 + \xi^2 + s\rho^2, \\ \dfrac{d\rho}{d\tau} = \rho(\beta_2 + \theta\xi + \xi^2), \end{cases} \tag{4.35}$$

are reported depending on the sign of the normal form coefficients s and θ [67].

Let us now discuss the interpretation of the phase portraits in the (ξ,ρ)-plane of the truncated amplitude system in the context of the bifurcating limit cycle. The fixed points or limit cycles have additional dimensions from the phases of the periodic orbit itself plus the phases ignored in the reduction to the amplitude system. We note that in the amplitude system the vertical direction always corresponds to a Neimark-Sacker bifurcation, but that the horizontal component of the phase space has a different meaning. For LPNS, equilibria on the horizontal axis correspond to limit cycles. Equilibria off the horizontal axis correspond to invariant 2-dimensional tori $\mathbb{T}^2$ and the periodic orbit that exists if $s\theta < 0$ corresponds to an invariant 3-dimensional torus $\mathbb{T}^3$.

The critical values of s and θ can be expressed in terms of the coefficients of (4.13) as

$$s = \text{sign}\ (a_{200}a_{011}), \quad \theta = \frac{\Re(b_{110})}{a_{200}}.$$

These values determine the bifurcation scenario. For $s\theta < 0$, a 3-torus appears in the unfolding via a Neimark-Sacker bifurcation T. The stability of this torus is

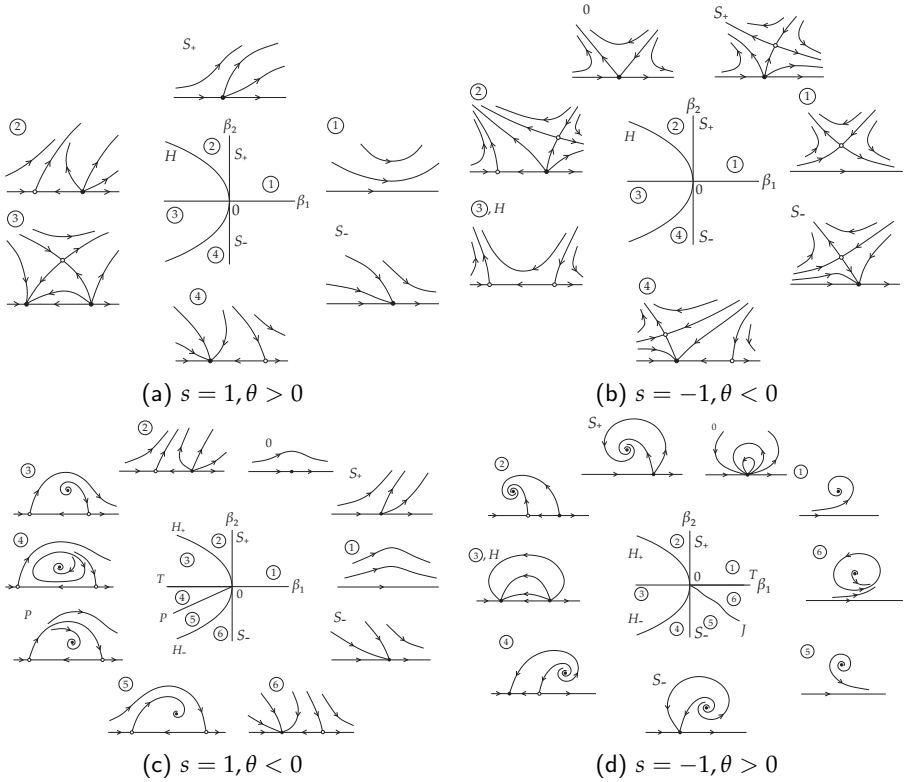

Figure 4.11: Bifurcation diagrams of the truncated amplitude system (4.35) for the LPNS bifurcation.

determined by the third order terms in (4.13). Indeed, the sign of the corresponding first Lyapunov coefficient for the Hopf bifurcation in (4.35) is opposite to that of θ but the 'time' in (4.34) is rescaled with factor

$$E = \Re\left(b_{210} + b_{110}\left(\frac{\Re(b_{021})}{a_{011}} - \frac{3a_{300}}{2a_{200}} + \frac{a_{111}}{2a_{011}}\right) - \frac{b_{021}a_{200}}{a_{011}}\right),$$

(see page 337 in [67]). If $E \cdot l_1 < 0$, a stable 3-torus appears, if $E \cdot l_1 > 0$, the 3-torus is unstable. The output given by MatCont is (s, θ, E).

Note that Figure 4.11 presents bifurcations of the truncated system (4.34) that only approximates the full normalized unfolding. In particular, the orbit structure on the invariant tori can differ from that for the approximating system due to phase locking. Moreover, the destruction of $\mathbb{T}^3$ via a heteroclinic bifurcation P in case (c) of Figure 4.11 becomes a complicated sequence of global bifurcations involving stable and unstable invariant sets of cycles and tori. All these bifurcations, however, occur in the exponentially small parameter wedge near the heteroclinic bifurcation curve P. For detailed discussions of the effects of the truncation, also in the PDNS and NSNS cases, we refer to [71, 95] and references therein.

Period-Doubling-Neimark-Sacker bifurcation

Generically, a two-parameter unfolding of (4.1) near this bifurcation restricted to the center manifold is smoothly orbitally equivalent to a system in which the equations for the transverse coordinates have the form (see Lemma 8.14 on page 354 of [67])

$$\begin{cases} \dfrac{dv_1}{d\tau} = \beta_1 v_1 + P_{11} v_1^3 + P_{12} v_1 |v_2|^2 + S_1 v_1 |v_2|^4 + O(|(v_1, v_2, \bar{v}_2)|^6), \\ \dfrac{dv_2}{d\tau} = (\beta_2 + i\omega_2) v_2 + P_{21} v_1^2 v_2 + P_{22} v_2 |v_2|^2 + S_2 v_1^4 v_2 + i R_2 v_2 |v_2|^4 \\ \qquad\qquad + O(|(v_1, v_2, \bar{v}_2)|^6), \end{cases} \tag{4.36}$$

where the O-terms are $2T$-periodic in τ. This system is similar to the normal form for the Hopf-Hopf bifurcations of equilibria (cf. Theorem 8.8 on page 357 in [67]).

The amplitude system for (4.36) without the higher order terms is

$$\begin{cases} \dfrac{dr_1}{d\tau} = r_1(\beta_1 + p_{11} r_1^2 + p_{12} r_2^2 + s_1 r_2^4), \\ \dfrac{dr_2}{d\tau} = r_1(\beta_2 + p_{21} r_1^2 + p_{22} r_2^2 + s_2 r_1^4), \end{cases} \tag{4.37}$$

where

$$p_{11} = P_{11},\ p_{12} = P_{12},\ p_{21} = \Re(P_{21}),\ p_{22} = \Re(P_{22}),\ s_1 = S_1,\ s_2 = \Re(S_2).$$

The values of p_{jk} and s_j, for $j, k = 1, 2$, and the quantities

$$\theta = \frac{p_{12}}{p_{22}}, \delta = \frac{p_{21}}{p_{11}}, \Theta = \frac{s_1}{p_{22}^2}, \Delta = \frac{s_2}{p_{11}^2}$$

indicate in which bifurcation scenario we are (see Section 8.6.2 in [67]).

In the 'simple' case where $p_{11}p_{22} > 0$, there are five topologically different bifurcation diagrams of the truncated amplitude system (4.37), corresponding to the following cases:

I. $\theta > 0, \delta > 0, \theta\delta > 1$

II. $\theta > 0, \delta > 0, \theta\delta < 1$

III. $\theta > 0, \delta < 0$

IV. $\theta < 0, \delta < 0, \theta\delta < 1$

V. $\theta < 0, \delta < 0, \theta\delta > 1.$

If $\delta > \theta$, reverse the role of θ and δ. Each case corresponds with a region in the (θ, δ)-plane, see Figure 4.12 (a). The parametric portraits belonging to the different regions can be seen in Figure 4.13 (a), with corresponding phase portraits in the (r_1, r_2)-plane in Figure 4.13 (b). The phase portraits are only shown for the case $p_{11} < 0$ and $p_{22} < 0$. The case $p_{11} > 0$ and $p_{22} > 0$ can be reduced to the considered one by reversing time.

In the 'difficult' case where $p_{11}p_{22} < 0$, however, there are six essentially different bifurcation diagrams:

I. $\theta > 1, \delta > 1$

II. $\theta > 1, \delta < 1, \theta\delta > 1$

III. $\theta > 0, \delta > 0, \theta\delta < 1$

IV. $\theta > 0, \delta < 0$

V. $\theta < 0, \delta < 0, \theta\delta < 1$

VI. $\theta < 0, \delta < 0, \theta\delta > 1.$

The regions in the (θ, δ)-plane are shown in Figure 4.12 (b). The related parametric portraits and phase portraits of (4.37) are given in Figure 4.14. Only the case $p_{11} > 0$ and $p_{22} < 0$ is presented, to which the opposite one can be easily reduced.

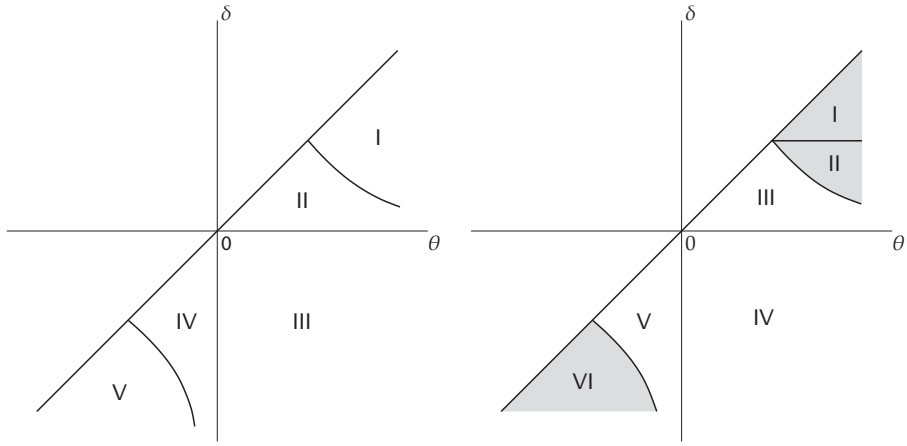

Figure 4.12: (a) The five subregions in the (θ, δ)-plane in the 'simple' case. (b) The six subregions in the (θ, δ)-plane in the 'difficult' case.

We note that Section 8.6.2 in [67] for the 'difficult' case contains a few errors in the figures and in the asymptotic expression for the heteroclinic bifurcation curve[1]. Therefore, for completeness, we provide the correct asymptotics in Section 4.A.

The critical values of P_{jk} and S_j can be expressed in terms of the coefficients of (4.14) as

$$P_{11} = a_{300},\ P_{12} = a_{111},\ \Re(P_{21}) = \Re(b_{210}),\ \Re(P_{22}) = \Re(b_{021}),$$

and

$$S_1 = a_{122} + a_{111}\left(\frac{\Re(b_{221})}{\Re(b_{210})} - 2\frac{\Re(b_{032})}{\Re(b_{021})} - \frac{a_{500}\Re(b_{021})}{a_{300}\Re(b_{210})}\right),$$
$$\Re(S_2) = \Re(b_{410}) + \Re(b_{210})\left(\frac{a_{311}}{a_{111}} - 2\frac{a_{500}}{a_{300}} - \frac{a_{300}\Re(b_{032})}{a_{111}\Re(b_{021})}\right),$$

(see page 356 in [67]).

[1] Unfortunately, there is also a minor misprint in our earlier 'correction' for the heteroclinic curve given in [71].

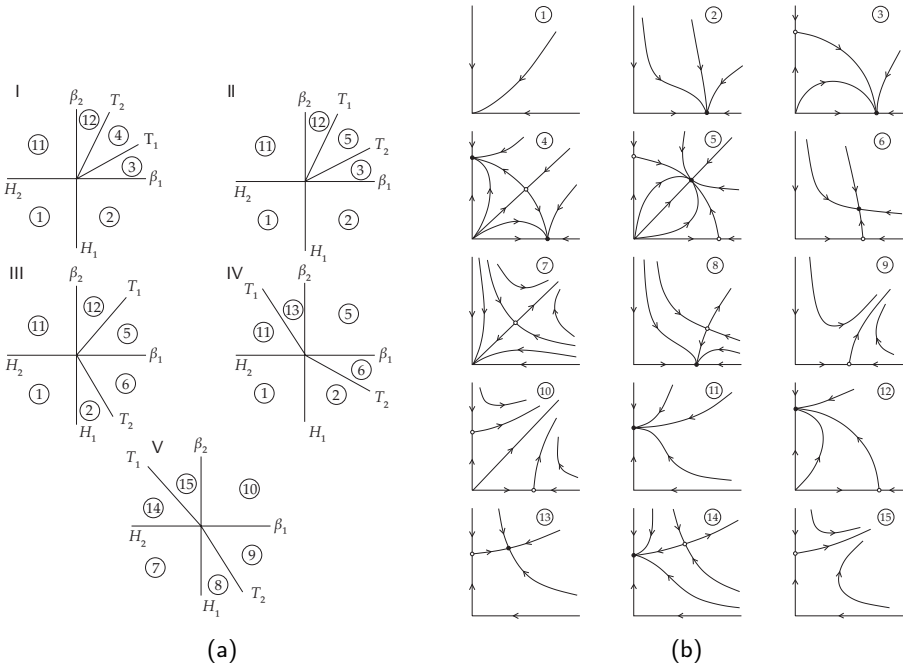

Figure 4.13: Bifurcation diagrams of the amplitude system (4.37) for the PDNS and NSNS bifurcations: (a) Parametric portraits in the 'simple' case. (b) Phase portraits in the 'simple' case.

The fifth order terms in (4.14) determine the stability of the tori in the 'difficult' cases. In fact, the sign of the first Lyapunov coefficient for the Neimark-Sacker bifurcation is given by (see Section 4.A)

$$\text{sign } l_1 = -\text{sign}\left(\delta(\theta(\theta-1)\Delta + \delta(\delta-1)\Theta)\right). \tag{4.38}$$

The output of MatCont is $(p_{11}, p_{22}, \theta, \delta, \text{sign } l_1)$.

For PDNS we have an interpretation analogous to LPNS, but the invariant sets may be 'doubled'. The origin always corresponds to the original limit cycle. Other fixed points on the vertical axis represent the period doubled limit cycles, while a fixed point on the horizontal axis corresponds to a $\mathbb{T}^2$. Fixed points off the coordinate axes correspond to doubled tori $\mathbb{T}^2$ and periodic orbits correspond to $\mathbb{T}^3$. As in the LPNS case, Figure 4.13 and Figure 4.14 present bifurcations of the

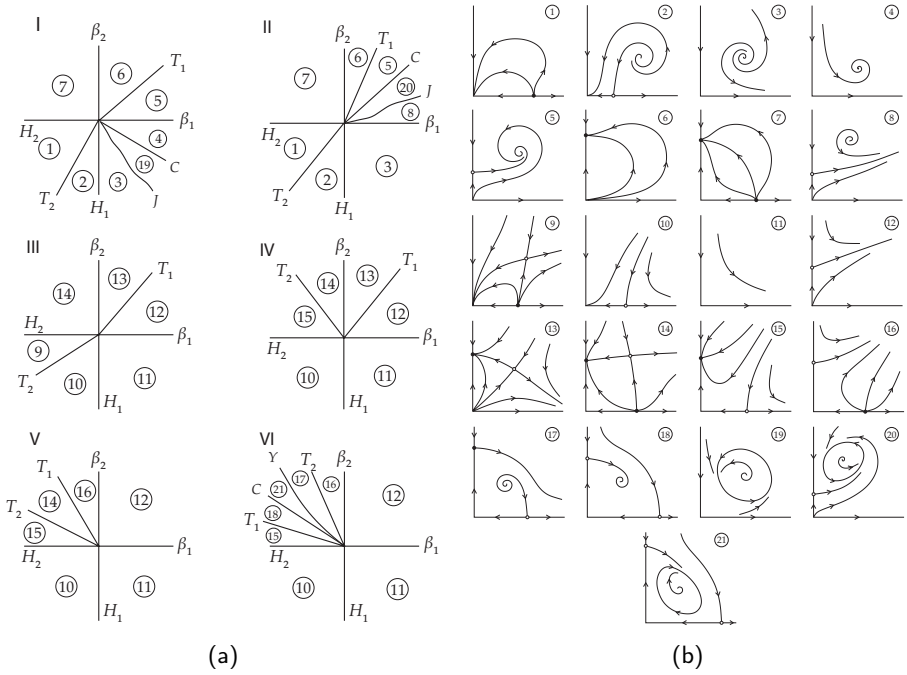

Figure 4.14: Bifurcation diagrams of the amplitude system (4.37) for the PDNS and NSNS bifurcations: (a) Parametric portraits in the 'difficult' case. (b) Phase portraits in the 'difficult' case.

truncated amplitude system that only approximates the full normalized unfolding. In particular, one has to be careful with 'torus doubling', which is in fact a complicated quasi-periodic bifurcation [79, 96].

4.4.4 Bifurcations with 5 critical eigenvalues

Double Neimark-Sacker bifurcation

Generically, a two-parameter unfolding of (4.1) near this bifurcation restricted to the center manifold is smoothly orbitally equivalent to a system in which the equations

for the transverse coordinates have the form (see Lemma 8.14 on page 354 of [67])

$$\begin{aligned}\frac{dv_1}{d\tau} &= (\beta_1 + i\omega_1)v_1 + P_{11}v_1|v_1|^2 + P_{12}v_1|v_2|^2 + iR_1v_1|v_1|^4 + S_1v_1|v_2|^4 \\ &\quad + O(|(v,\bar{v})|^6), \\ \frac{dv_2}{d\tau} &= (\beta_2 + i\omega_2)v_2 + P_{21}v_2|v_1|^2 + P_{22}v_2|v_2|^2 + S_2v_2|v_1|^4 + iR_2v_2|v_2|^4 \\ &\quad + O(|(v,\bar{v})|^6),\end{aligned} \tag{4.39}$$

where the O-terms are T-periodic in τ. Neglecting this periodicity, system (4.39) is the normal form for the Hopf-Hopf bifurcation of equilibria (cf. Theorem 8.8 on page 357 in [67]).

The truncated amplitude system for (4.39) is given by (4.37), where now

$$\begin{aligned}p_{11} = \Re(P_{11}) = \Re(a_{2100}),\ p_{12} = \Re(P_{12}) = \Re(a_{1011}), \\ p_{21} = \Re(P_{21}) = \Re(b_{1110}),\ p_{22} = \Re(P_{22}) = \Re(b_{0021}),\end{aligned}$$

and

$$\begin{aligned}s_1 &= \Re(S_1) \\ &= \Re(a_{1022}) + \Re(a_{1011})\left(\frac{\Re(b_{1121})}{\Re(b_{1110})} - 2\frac{\Re(b_{0032})}{\Re(b_{0021})} - \frac{\Re(a_{3200})\Re(b_{0021})}{\Re(a_{2100})\Re(b_{1110})}\right), \\ s_2 &= \Re(S_2) \\ &= \Re(b_{2210}) + \Re(b_{1110})\left(\frac{\Re(a_{2111})}{\Re(a_{1011})} - 2\frac{\Re(a_{3200})}{\Re(a_{2100})} - \frac{\Re(a_{2100})\Re(b_{0032})}{\Re(a_{1011})\Re(b_{0021})}\right).\end{aligned}$$

The output of MatCont is $(p_{11}, p_{22}, \theta, \delta, \text{sign } l_1)$.

Although the phase portraits of the truncated amplitude system are the same as for PDNS, their interpretation is slightly different, since they 'live' in the $(|v_1|, |v_2|)$-plane. Here, on both axes the fixed points correspond to invariant 2-dimensional tori $\mathbb{T}^2$ for the original system. Fixed points off the coordinate axes and limit cycles correspond to $\mathbb{T}^3$ and $\mathbb{T}^4$, respectively. The usual remark on the approximate nature of the bifurcation diagrams applies here as well.

4.5 Conclusion

In this chapter we discussed the normal forms of codim 2 bifurcations of limit cycles. Although in [17, 59] periodic normal forms for some codim 2 bifurcations

of limit cycles were presented, neither of these publications treated all 11 codim 2 local bifurcations of limit cycles. We have presented quantities in terms of the normal form coefficients that allow to pick the right bifurcation scenario for each specific case. Of course, we need explicit formulas for these critical coefficients. This problem will be tackled in the next chapter. There, we will propose an efficient method for the computation of the normal form coefficients.

4.A Bifurcations of the amplitude system for Hopf-Hopf bifurcation in the 'difficult' case

Here, we derive quadratic approximations of the Hopf and heteroclinic bifurcation curves for the Hopf-Hopf amplitude system (4.37). By introducing new phase variables and rescaling time, (4.37) can be rewritten as

$$\begin{pmatrix} x' \\ y' \end{pmatrix} = \begin{pmatrix} x(\beta_1 + x - \theta y + \Theta y^2) \\ y(\beta_2 + \delta x - y + \Delta x^2) \end{pmatrix}.$$

Remark that $'$ represents the derivative w.r.t. the rescaled time. The main results are

$$\begin{aligned} \beta_{1,Hopf} &= -\frac{\theta-1}{\delta-1}\beta_2 - \frac{(\delta-1)\Theta + (\theta-1)\Delta}{(\delta-1)^3}\beta_2^2, \\ \beta_{1,Het} &= -\frac{\theta-1}{\delta-1}\beta_2 + \frac{\theta\Theta(\delta-1)^3 + \delta\Delta(\theta-1)^3}{(\delta-1)^3(2\delta\theta-\delta-\theta)}\beta_2^2, \\ l_1 &= -\delta\left(\delta(\delta-1)\Theta + \theta(\theta-1)\Delta\right). \end{aligned}$$

For the Hopf bifurcation curve we impose the conditions $x' = 0, y' = 0$ and $\frac{\partial x'}{\partial x} + \frac{\partial y'}{\partial y} = 0$. Solving a series expansion yields the result for the Hopf curve. Next, the first Lyapunov coefficient l_1 is computed using the invariant formula (5.39) from [67], from which (4.38) follows.

For the heteroclinic curve we proceed as follows. We assume $\delta, \theta < 0$ and $\delta\theta - 1 > 0$ and we transform variables to obtain a system that is a perturbation of a Hamiltonian system. This enables us to formulate a Melnikov function. Setting this function to zero yields an equation from which we extract the quadratic approximation to the heteroclinic curve. Introducing the transformation $(\tau^*, x, y, \beta_1,$

$\beta_2) \to (\varepsilon x^{p-1}y^{q-1}\tau^*, \varepsilon x, \varepsilon y, c_1\varepsilon + c_2\varepsilon^2, \varepsilon)$ where

$$c_1 = -\frac{\theta-1}{\delta-1}, p = \frac{1-\delta}{\delta\theta-1}, q = \frac{1-\theta}{\delta\theta-1},$$

then we obtain

$$\begin{pmatrix} x' \\ y' \end{pmatrix} = x^{p-1}y^{q-1}\begin{pmatrix} x(c_1+x-\theta y) \\ y(1+\delta x-y) \end{pmatrix} + \varepsilon x^{p-1}y^{q-1}\begin{pmatrix} c_2x+\Theta xy^2 \\ \Delta yx^2 \end{pmatrix},$$

which for $\varepsilon = 0$ is a Hamiltonian system with Hamiltonian

$$H(x,y) = \frac{1}{p}x^p y^q\left(-1+\frac{\delta-1}{\theta-1}x+y\right).$$

Define $g_1 = x^p y^{q-1}(c_2+\Theta y^2)$ and $g_2 = \Delta x^{p+1}y^q$. The Melnikov function along the nontrivial critical curve $H(x,y)=0$ is given by the following integral

$$\begin{aligned} M(h) &= \int_{H=h} g_1 dy - g_2 dx \\ &= \int_{H=h} x^p y^{q-1}(c_2+\Theta y^2)dy - \Delta x^{p+1}y^q dx \\ &= \int_{H=h}\left(x^p y^{q-1}(c_2+\Theta y^2) + \frac{q\Delta}{p+2}x^{p+2}y^{q-1}\right)dy, \end{aligned}$$

where we have used Green's Theorem to convert the dx term to dy. Now along the nontrivial critical curve $H(x,y)=0$ we have $x = \frac{\theta-1}{\delta-1}(1-y)$ so that

$$\begin{aligned} M(0) &= \left(\frac{\theta-1}{\delta-1}\right)^p \int_0^1 (1-y)^p y^{q-1}\left(c_2+\Theta y^2 + \left(\frac{\theta-1}{\delta-1}\right)^2\frac{q\Delta}{p+2}(1-y)^2\right)dy \\ &\sim c_2 I_{p,q-1} + \Theta I_{p,q+1} + \left(\frac{\theta-1}{\delta-1}\right)^2\frac{q\Delta}{p+2}I_{p+2,q-1}, \end{aligned}$$

where we defined

$$I_{a,b} = \int_0^1 (1-y)^a y^b dy = \frac{\Gamma(1+a)\Gamma(1+b)}{\Gamma(2+a+b)}.$$

Solving $M(0)=0$ and substituting p,q we obtain

$$c_2 = \frac{\theta\Theta(\delta-1)^3 - \delta\Delta(1-\theta)^3}{(\delta-1)^3(2\delta\theta-\delta-\theta)}.$$

As a final check we consider the difference between the Hopf and heteroclinic curves

$$\beta_{1,HET} - \beta_{1,HOPF} = -\frac{(\delta\theta - 1)l_1}{\delta(\delta - 1)^3(2\delta\theta - \delta - \theta)}\beta_2^2.$$

We see that the curves coincide precisely when the Hopf bifurcation is degenerate.

5

Numerical Periodic Normalization for Codimension 2 Bifurcations of Limit Cycles – Computational Formulas

In this chapter we derive for all codimension 2 bifurcations of limit cycles the normal form coefficients that are needed to determine the bifurcation scenario near the bifurcation point.

5.1 Introduction

In generic systems of the form

$$\dot{x} = f(x, \alpha), \quad x \in \mathbb{R}^n, \ \alpha \in \mathbb{R}^p, \tag{5.1}$$

depending on one control parameter (i.e. with $p = 1$), a hyperbolic limit cycle exists for an open interval of parameter values α. At a boundary of such an interval, the

limit cycle may become nonhyperbolic, so that either a Limit Point of Cycles, or a Period-Doubling, or a Neimark-Sacker bifurcation occurs. In two-parameter generic systems (5.1) (i.e. with $p = 2$) these local bifurcations happen at certain curves in the parameter plane. These curves of codim 1 bifurcations can meet tangentially or intersect transversally at some codim 2 points characterized by a double degeneracy of the limit cycle. These codim 2 points play the role of organizing centers for local dynamics, i.e. near the critical cycle and for nearby parameter values. In some cases, such codim 2 bifurcations imply the appearance of nearby 'chaotic motions'.

The codim 2 bifurcations of limit cycles in generic systems (5.1) are well understood with the help of the corresponding Poincaré maps and their normal forms (see [3–5, 51, 58, 67]). Indeed, in the Poincaré map, the limit cycle is a fixed point and one can use techniques developed for maps to obtain the critical normal form [51, 71]. However, applications of these results to the analysis of concrete systems (5.1) are exceptional, since they require accurate higher-order derivatives of the Poincaré map that are hardly available numerically [55, 57, 70, 92].

This may be done by using software such as CAPD [1] and TIDES [2, 8]. These packages allow one to compute up to any precision level the solution of an ODE using a Taylor series method in a variable stepsize - variable order formulation. The software can also compute, up to any order, the partial derivatives of the solution with respect to the initial conditions. When applied to compute a periodic orbit by a shooting method, this will also provide the derivatives of the Poincaré map. Alternatively one could integrate the variational equations [90] or use automatic differentiation [57, 70] to obtain the derivatives of the Poincaré map.

All these methods, however, have some drawbacks that make them less (time) efficient. First, these are shooting methods that are difficult to use in a continuation context. Also, a shooting method does not have the high order convergence properties of the method of approximation by piecewise polynomials with collocation in the Gauss points (that is used in MatCont, as discussed in Section 2.8.2). Moreover, the number of derivatives of the Poincaré map to be computed is $O(n^k)$ if derivatives up to order k are needed (sometimes $k = 5$). Even for moderate values of n this involves a great deal of unnecessary work since in our situation the normal form itself is known in advance and we only need to compute its coefficients.

There is an alternative technique that is more suitable in the context of numerical continuation of periodic orbits using collocation and that avoids the computation of the Poincaré map and their derivatives. Indeed, recently a numerical method to analyse codim 1 limit cycle bifurcations has been developed in [68]. It is based on the periodic normalization proposed in [44, 59, 60]. The computation of the normal form

coefficients is reduced to solving certain linear boundary value problems, where only the partial derivatives of the right-hand side (**RHS**) of (5.1) are used, and evaluating certain integrals.

This chapter consists of the derivation of explicit formulas for the normal form coefficients for all codim 2 bifurcations of limit cycles (see Table 2.2). We order the different cases by the dimension n_c of the cycle center manifold. The formulas for the critical coefficients are independent of the dimension of the phase space and involve solutions of certain BVPs on the interval $[0, T]$, where T is the period of the critical cycle, as well as multilinear functions from the Taylor expansion of the right-hand side of (5.1) near the cycle.

In the LPNS, PDNS and NSNS cases, the critical coefficients impose a distinction between a 'simple' and a 'difficult' situation. In a 'simple' situation, terms up to the second order in the LPNS case and up to the third order in the PDNS and NSNS cases are sufficient to determine the bifurcation scenario. These terms are listed in the next section. However, in a 'difficult' situation, also the third order terms in the LPNS case and the fourth and fifth order terms in the PDNS and NSNS cases are needed. We have listed these higher order terms in Section 5.A.

5.2 Computation of critical coefficients

Our aim in this section is to derive expressions for the critical coefficients in the normal forms derived in the previous chapter. We first sketch the general idea that we will use in all the codim 2 bifurcations of limit cycles.

Assume that system (5.1) has a nonhyperbolic limit cycle Γ. Then, there exists an n_c-dimensional invariant center manifold, parametrized by $w \in \mathbb{R}^{n_c}$, such that

$$u = H(w), \quad H : \mathbb{R}^{n_c} \to \mathbb{R}^n. \tag{5.2}$$

The restriction of the differential equations to the center manifold is represented by some normal form

$$\dot{w} = G(w), \quad G : \mathbb{R}^{n_c} \to \mathbb{R}^{n_c}. \tag{5.3}$$

Substitution of (5.2) and (5.3) into

$$\dot{u} = F(u), \tag{5.4}$$

i.e. the restriction of (5.1) to the critical parameter values, gives the following **homological equation**

$$H_w(w)G(w) = F(H(w)). \tag{5.5}$$

To obtain an approximation to the solution, we expand the functions G and H in (5.5) into multivariate Taylor series, i.e.

$$G(w) = \sum_{|\nu|\geq 1} \frac{1}{\nu!} g_\nu w^\nu, \quad H(w) = \sum_{|\nu|\geq 1} \frac{1}{\nu!} h_\nu w^\nu.$$

Note that for a multi-index $\nu = (\nu_1, \nu_2, \ldots, \nu_k)$ it holds that $\nu! = \nu_1!\nu_2!\ldots\nu_k!$ and $|\nu| = \nu_1 + \nu_2 + \ldots + \nu_k$. The coefficients g_ν of the normal form and the coefficients h_ν of the Taylor expansion for $H(w)$ are unknown but they will be derived from the homological equation by a recursive procedure. Indeed, by collecting the coefficients corresponding to the w^ν-terms, we obtain a linear system for coefficient h_ν, i.e.

$$Lh_\nu = R_\nu,$$

where $L = \frac{d}{d\tau} - A + g(\mu)$ with $g(\mu)$ a function of the critical multipliers. The right-hand side R_ν depends on the coefficients of H and G of order less than or equal to $|\nu|$, as well as on terms of order less than or equal to $|\nu|$ of the Taylor expansion (4.3) of F. Now, there are two possibilities. Either L is nonsingular. Then, the order ν term is nonresonant, which means that g_ν does not appear in the normal form (5.3). Or L is singular. Then, the **Fredholm solvability condition** is involved, i.e.

$$\int_0^T \langle p, R_\nu \rangle d\tau = 0,$$

where p is a null-vector of the adjoint operator L^*. Indeed,

$$\int_0^T \langle p, R_\nu \rangle d\tau = \int_0^T \langle p, Lh_\nu \rangle d\tau = \int_0^T \langle L^* p, h_\nu \rangle d\tau = 0.$$

When R_ν depends on the unknown normal form coefficient g_ν, L is singular and the Fredholm solvability condition gives the expression for g_ν.

So following this **homological equation approach** [11], we can find the T-, $2T$-, $3T$- or $4T$-periodic unknown functions h_ν by solving appropriate BVPs on $[0, T]$. The coefficients of the normal forms arise from the Fredholm solvability conditions applied on the RHS of the ODEs as integrals of scalar products over

$[0, T]$, involving nonlinear terms of (5.4) near the periodic solution u_0, as well as the critical (generalized) eigenfunctions and already known expansion terms of the center manifold.

The linear parts in the homological equation determine the critical (generalized) eigenfunctions. The higher order terms lead to expressions for h_ν so that a better approximation for the center manifold is obtained. Note that the computation of an order k normal form coefficient demands only an order $k-1$ approximation of the center manifold. Of course, not all terms up to the order $k-1$ are needed. Note also that in the case of a complex multiplier the relation $h_{\nu_i\nu_j} = \overline{h_{\nu_j\nu_i}}$ holds for the appropriate positions ν_i and ν_j in the multi-index ν, corresponding with the positions of the complex conjugate multipliers.

The functions h_ν in the Taylor expansion are usually unique up to the addition of a multiple of a known eigenfunction. This can be fixed by adding an integral condition. Among other things this leads to the fact that normal form coefficients are not unique but implications for the underlying dynamical systems are independent of this. We also remark that the solvability of all the equations up to the maximal order of the normal form has to be checked. Also note that the coefficients in the equation for the cyclic variable will only be computed when needed for the computation of other critical coefficients. Finally, we remark that certain nondegeneracy conditions have to be fulfilled. If this is not the case, we are in a degenerate case.

In the codim 2 bifurcations where the center manifold is 4- or 5-dimensional, a distinction is made between 'simple' and 'difficult' cases in the bifurcation scenarios. The stability of the extra torus appearing in the 'difficult' cases is determined by up to third order terms for the LPNS bifurcation and up to fifth order terms for the PDNS and NSNS bifurcations. In the 'simple' cases, second order derivatives are sufficient to determine the behaviour in the LPNS bifurcations and third order derivatives are sufficient in the PDNS and NSNS bifurcations. Therefore, we restrict our computations in this section to second order terms in the LPNS case and up to and including third order terms in the PDNS and NSNS cases. The expressions of the third order coefficients for LPNS and fourth and fifth order coefficients for PDNS and NSNS are given in Section 5.A.

5.2.1 Bifurcations with a 2D center manifold

Cusp Point of Cycles bifurcation

The two-dimensional critical center manifold $W^c(\Gamma)$ at the CPC bifurcation can be parametrized locally by $(\tau,\xi)\in[0,T]\times\mathbb{R}$ as

$$u = u_0(\tau) + \xi v(\tau) + H(\tau,\xi), \tag{5.6}$$

where H satisfies $H(T,\xi) = H(0,\xi)$ and has the Taylor expansion

$$H(\tau,\xi) = \frac{1}{2}h_2(\tau)\xi^2 + \frac{1}{6}h_3(\tau)\xi^3 + O(|\xi|^4) \tag{5.7}$$

with $h_j(T) = h_j(0)$, for $j = 2,3$, while the generalized eigenfunction v is defined (as function of τ) by

$$\begin{cases} \dot v - A(\tau)v - F(u_0) = 0,\ \tau\in[0,T], \\ v(T) - v(0) = 0, \\ \displaystyle\int_0^T \langle v, F(u_0)\rangle d\tau = 0. \end{cases} \tag{5.8}$$

Note that in the rest of this chapter the dot denotes the derivative with respect to τ. The function v exists due to Proposition 2.26. Let φ^* be a nontrivial solution of the adjoint eigenvalue problem

$$\begin{cases} \dot\varphi^* + A^{\mathrm{T}}(\tau)\varphi^* = 0,\ \tau\in[0,T], \\ \varphi^*(T) - \varphi^*(0) = 0, \end{cases} \tag{5.9}$$

and the generalized adjoint eigenfunction v^* a solution of

$$\begin{cases} \dot v^* + A^{\mathrm{T}}(\tau)v^* + \varphi^* = 0,\ \tau\in[0,T], \\ v^*(T) - v^*(0) = 0, \end{cases} \tag{5.10}$$

which is now defined up to the addition of a multiple of φ^*. Note that the first equation of (5.8) implies

$$\int_0^T \langle \varphi^*, F(u_0)\rangle\, d\tau = \int_0^T \langle \varphi^*, \dot v - A(\tau)v\rangle\, d\tau = -\int_0^T \langle \dot\varphi^* + A^{\mathrm{T}}(\tau)\varphi^*, v\rangle\, d\tau = 0 \tag{5.11}$$

for φ^* satisfying (5.9). Moreover, due to spectral assumptions at the CPC-point, we can also assume

$$\int_0^T \langle \varphi^*, v \rangle d\tau = 1. \tag{5.12}$$

Notice that this assumption gives us another normalization condition for free, since taking into account (5.8) and (5.10) we have

$$\begin{aligned}\int_0^T \langle v^*, F(u_0) \rangle d\tau &= \int_0^T \langle v^*, \dot{v} - A(\tau)v \rangle \, d\tau \\ &= -\int_0^T \langle \dot{v}^* + A^{\mathrm{T}}(\tau)v^*, v \rangle \, d\tau \\ &= \int_0^T \langle \varphi^*, v \rangle d\tau \\ &= 1.\end{aligned}$$

So we have normalized the eigenfunction of the adjoint problem w.r.t. the generalized one of the original problem and the generalized eigenfunction of the adjoint problem w.r.t. the eigenfunction of the original problem. So φ^* is the unique solution of the BVP

$$\begin{cases} \dot{\varphi}^* + A^{\mathrm{T}}(\tau)\varphi^* = 0, \ \tau \in [0, T], \\ \varphi^*(T) - \varphi^*(0) = 0, \\ \int_0^T \langle \varphi^*, v \rangle d\tau - 1 = 0. \end{cases} \tag{5.13}$$

We still need an integral condition for the adjoint generalized eigenfunction v^*. In all cases, for the computation of an adjoint generalized eigenfunction we will require the inproduct with an original eigenfunction to be zero. Here, the inproduct with v is appropriate. Therefore, we obtain

$$\begin{cases} \dot{v}^* + A^{\mathrm{T}}(\tau)v^* + \varphi^* = 0, \ \tau \in [0, T], \\ v^*(T) - v^*(0) = 0, \\ \int_0^T \langle v^*, v \rangle d\tau = 0. \end{cases} \tag{5.14}$$

Now, we substitute (5.6) into (5.4), using (4.3), the CPC normal form (4.5), and

(5.7). This gives

$$\dot{u}_0 + \xi\,(\dot{v} - \dot{u}_0) + \xi^2\left(\alpha_1\dot{u}_0 - \dot{v} + \frac{1}{2}\dot{h}_2\right) + \xi^3\left(\alpha_2\dot{u}_0 + \alpha_1\dot{v} - \frac{1}{2}\dot{h}_2 + \frac{1}{6}\dot{h}_3 + cv\right)$$
$$+ O(|\xi|^4) = F(u_0) + \xi A(\tau)v + \frac{1}{2}\xi^2\,(A(\tau)h_2 + B(\tau;v,v)) + \frac{1}{6}\xi^3\,(A(\tau)h_3$$
$$+3B(\tau;h_2,v) + C(\tau;v,v,v)) + O(|\xi|^4).$$

Collecting the ξ^0-terms we get the identity $\dot{u}_0 = F(u_0)$, since u_0 is the periodic solution of (5.4). The ξ^1-terms provide another identity, namely $\dot{v} - \dot{u}_0 = A(\tau)v$, as stated in (5.8).

By collecting the ξ^2-terms we obtain an equation for h_2

$$\dot{h}_2 - A(\tau)h_2 = B(\tau;v,v) + 2\dot{v} - 2\alpha_1\dot{u}_0. \tag{5.15}$$

The differential operator $\frac{d}{d\tau} - A(\tau)$ in the left-hand side is singular in the space of vector functions on $[0,T]$ satisfying $h_2(T) = h_2(0)$, since $\dot{u}_0$ is in its kernel. Now, we project the left-hand side of (5.15) on the adjoint null-eigenfunction, i.e. we take the scalar product with φ^* pointwise and integrate the result over $[0,T]$ to obtain

$$\int_0^T \langle \varphi^*, \left(\frac{d}{d\tau} - A(\tau)\right) h_2\rangle\, d\tau = -\int_0^T \langle \left(\frac{d}{d\tau} + A^T(\tau)\right)\varphi^*, h_2\rangle\, d\tau = 0,$$

due to (5.9). Therefore, the projection of the right-hand side of (5.15) on φ^* also has to vanish, i.e.

$$\int_0^T \langle \varphi^*, B(\tau;v,v) + 2\dot{v} - 2\alpha_1\dot{u}_0\rangle\, d\tau = \int_0^T \langle \varphi^*, B(\tau;v,v) + 2A(\tau)v\rangle\, d\tau = 0,$$

due to (5.11). This represents the Fredholm solvability condition, discussed at the beginning of this section. Notice that this condition is actually trivially satisfied, due to the fact that we are at a CPC-point, for which holds that the second order normal form coefficient (see [68])

$$b = \frac{1}{2}\int_0^T \langle \varphi^*, B(\tau;v,v) + 2A(\tau)v\rangle\, d\tau$$

vanishes. Hence equation (5.15) is solvable, independent of the value of α_1. For any value of α_1 we get an equation for h_2 to be solved in the space of vector functions

on $[0,T]$ satisfying $h_2(T) = h_2(0)$. Notice that if h_2 satisfies (5.15), $h_2 + \varepsilon F(u_0)$ also satisfies (5.15), due to the fact that $F(u_0) = \dot{u}_0$. The orthogonality condition with v^* determines the value of ε such that we can define h_2 as the unique solution of

$$\begin{cases} \dot{h}_2 - A(\tau)h_2 - B(\tau;v,v) - 2Av - 2F(u_0) + 2\alpha_1 F(u_0) = 0, \ \tau \in [0,T], \\ h_2(T) - h_2(0) = 0, \\ \int_0^T \langle v^*, h_2 \rangle \, d\tau = 0. \end{cases} \tag{5.16}$$

Collecting the ξ^3-terms we obtain an equation in h_3 that allows us to determine the normal form coefficient c of the CPC normal form (4.5), namely

$$\dot{h}_3 - A(\tau)h_3 = -6\alpha_2\dot{u}_0 - 6\alpha_1\dot{v} + 3\dot{h}_2 - 6cv + 3B(\tau;h_2,v) + C(\tau;v,v,v).$$

The Fredholm solvability condition implies that

$$\int_0^T \langle \varphi^*, -6\alpha_2\dot{u}_0 - 6\alpha_1\dot{v} + 3\dot{h}_2 - 6cv + 3B(\tau;h_2,v) + C(\tau;v,v,v) \rangle \, d\tau = 0.$$

Making use of (5.8), (5.12) and (5.11), we then obtain the expression

$$\boxed{\begin{aligned} c = \frac{1}{6}\int_0^T \langle \varphi^*, &-6\alpha_1 A(\tau)v + 3A(\tau)h_2 + 3B(\tau;v,v) \\ &+ 6A(\tau)v + 3B(\tau;h_2,v) + C(\tau;v,v,v) \rangle \, d\tau \end{aligned}}$$

where v and φ^* are defined by (5.8) and (5.13), respectively, while h_2 satisfies (5.16).

Finally, let us prove that the choice of α_1 does not influence the value of the critical normal form coefficient c. Indeed, two solutions h_2 corresponding to $\alpha_1^{(1)} \neq \alpha_1^{(2)}$ in (5.16) differ by $h_2^{(2)} - h_2^{(1)} = -2(\alpha_1^{(2)} - \alpha_1^{(1)})v$, from which it follows that

$$\begin{aligned} c^{(2)} - c^{(1)} &= (\alpha_1^{(2)} - \alpha_1^{(1)}) \int_0^T \langle \varphi^*, -2A(\tau)v - B(\tau;v,v) \rangle \, d\tau \\ &= (\alpha_1^{(1)} - \alpha_1^{(2)}) \, b \\ &= 0, \end{aligned}$$

since $b = 0$. So, for simplicity, we take $\alpha_1 = 0$, that further simplifies the expression for c. The critical coefficient c in the periodic CPC normal form has thus been computed. The bifurcation is nondegenerate if $c \neq 0$.

Generalized Period-Doubling bifurcation

The two-dimensional critical center manifold $W^c(\Gamma)$ at the GPD bifurcation can be parametrized locally by $(\tau, \xi) \in [0, 2T] \times \mathbb{R}$ as

$$u = u_0(\tau) + \xi v(\tau) + H(\tau, \xi), \tag{5.17}$$

where the function H satisfies $H(2T, \xi) = H(0, \xi)$. It has the Taylor expansion

$$H(\tau, \xi) = \frac{1}{2}h_2(\tau)\xi^2 + \frac{1}{6}h_3(\tau)\xi^3 + \frac{1}{24}h_4(\tau)\xi^4 + \frac{1}{120}h_5(\tau)\xi^5 + O(|\xi|^6), \tag{5.18}$$

where $h_j(2T) = h_j(0)$, while

$$\begin{cases} \dot{v} - A(\tau)v = 0, \ \tau \in [0, T], \\ v(T) + v(0) = 0, \\ \int_0^T \langle v, v \rangle d\tau - 1 = 0, \end{cases} \tag{5.19}$$

and

$$v(\tau + T) = -v(\tau) \text{ for } \tau \in [0, T].$$

The function v exists due to Proposition 2.27.

The functions h_i, $i = 2, \ldots, 5$ can be found by solving appropriate BVPs, assuming that (5.4) restricted to $W^c(\Gamma)$ has the periodic GPD normal form (4.6). From (5.17) and (5.18) it follows that $h_i(\tau + T) = h_i(\tau)$ for i even and $h_i(\tau + T) = -h_i(\tau)$ for i odd, for $\tau \in [0, T]$. Indeed, since we are at the GPD point $u(\tau, \xi) = u(\tau + T, -\xi)$, so

$$\sum_i \frac{1}{i!}h_i(\tau)\xi^i = \sum_i \frac{1}{i!}h_i(\tau + T)(-1)^i\xi^i,$$

and thus

$$h_i(\tau) = (-1)^i h_i(\tau + T),$$

from which the stated follows. This makes it possible to restrict our considerations to the interval $[0, T]$ instead of $[0, 2T]$.

The coefficients α_1, α_2 and e arise from the solvability conditions for the BVPs as integrals of scalar products over the interval $[0, T]$. Specifically, these scalar

products involve among other things the terms up to the fifth order of (5.1) near the periodic solution u_0, the eigenfunction v, the adjoint eigenfunction φ^* satisfying

$$\begin{cases} \dot{\varphi}^* + A^{\mathrm{T}}(\tau)\varphi^* = 0, \ \tau \in [0,T], \\ \varphi^*(T) - \varphi^*(0) = 0, \\ \int_0^T \langle \varphi^*, F(u_0)\rangle \, d\tau - 1 = 0, \end{cases} \tag{5.20}$$

and a similar adjoint eigenfunction v^* satisfying

$$\begin{cases} \dot{v}^* + A^{\mathrm{T}}(\tau)v^* = 0, \ \tau \in [0,T], \\ v^*(T) + v^*(0) = 0, \\ \int_0^T \langle v^*, v\rangle d\tau - 1 = 0. \end{cases} \tag{5.21}$$

To derive the normal form coefficient, we proceed as in the CPC case, namely, we substitute (5.17) into (5.4) and use the GPD normal form (4.6), (5.18), as well as (4.3).

Collecting the ξ^0- and ξ^1-terms in the resulting equation gives the trivial identities, namely $\dot{u}_0 = F(u_0)$ and $\dot{v} = A(\tau)v$.

By collecting the ξ^2-terms, we obtain the following equation for h_2,

$$\dot{h}_2 - A(\tau)h_2 = B(\tau; v, v) - 2\alpha_1 \dot{u}_0, \tag{5.22}$$

to be solved in the space of functions satisfying $h_2(T) = h_2(0)$. In this space, the differential operator $\frac{d}{d\tau} - A(\tau)$ is singular with null-function $\dot{u}_0$. Thus, the following Fredholm solvability condition has to be satisfied

$$\int_0^T \langle \varphi^*, B(\tau; v, v) - 2\alpha_1 \dot{u}_0\rangle \, d\tau = 0,$$

which leads to the expression

$$\alpha_1 = \frac{1}{2}\int_0^T \langle \varphi^*, B(\tau; v, v)\rangle \, d\tau, \tag{5.23}$$

where v and φ^* are defined by (5.19) and (5.20), respectively.

With α_1 defined in this way, let h_2 be a solution of (5.22) in the space of functions satisfying $h_2(0) = h_2(T)$. Notice also that if h_2 is a solution of (5.22),

then also $h_2 + \varepsilon_1 F(u_0)$ satisfies (5.22), since $F(u_0)$ is in the kernel of the operator $\frac{d}{d\tau} - A(\tau)$. In order to obtain a unique solution (without projection on the null-eigenspace) we impose the following orthogonality condition that determines the value of ε_1:

$$\int_0^T \langle \varphi^*, h_2 \rangle \, d\tau = 0.$$

Thus h_2 is the unique solution of the BVP

$$\begin{cases} \dot{h}_2 - A(\tau)h_2 - B(\tau; v, v) + 2\alpha_1 F(u_0) = 0, \ \tau \in [0, T], \\ h_2(T) - h_2(0) = 0, \\ \int_0^T \langle \varphi^*, h_2 \rangle \, d\tau = 0. \end{cases} \tag{5.24}$$

By collecting the ξ^3-terms, we get the equation for h_3,

$$\dot{h}_3 - A(\tau)h_3 = C(\tau; v, v, v) + 3B(\tau; v, h_2) - 6\alpha_1 \dot{v}, \tag{5.25}$$

to be solved in the space of functions satisfying $h_3(T) = -h_3(0)$. In this space, the differential operator $\frac{d}{d\tau} - A(\tau)$ has a one-dimensional null-space, spanned by v, and (5.25) is solvable only if the RHS of this equation lies in the range of that operator. By using (5.19), we can rewrite the right-hand side as

$$C(\tau; v, v, v) + 3B(\tau; v, h_2) - 6\alpha_1 A(\tau)v.$$

Note that the Fredholm solvability condition

$$\int_0^T \langle v^*, C(\tau; v, v, v) + 3B(\tau; v, h_2) - 6\alpha_1 A(\tau)v \rangle \, d\tau = 0 \tag{5.26}$$

is trivially satisfied due to the fact that we are in a GPD point and so the cubic coefficient of the normal form (see [68])

$$c = \frac{1}{3} \int_0^T \langle v^*, C(\tau; v, v, v) + 3B(\tau; v, h_2) - 6\alpha_1 A(\tau)v \rangle \, d\tau$$

vanishes. Since the RHS of (5.25) is in the range space of the operator $\frac{d}{d\tau} - A(\tau)$, we can solve the equation in order to find h_3 as the unique solution of the BVP

$$\begin{cases} \dot{h}_3 - A(\tau)h_3 - C(\tau; v, v, v) - 3B(\tau; v, h_2) + 6\alpha_1 A(\tau)v = 0, \ \tau \in [0, T], \\ h_3(T) + h_3(0) = 0, \\ \int_0^T \langle v^*, h_3 \rangle \, d\tau = 0. \end{cases} \tag{5.27}$$

By collecting the ξ^4-terms, we get the equation for h_4,

$$\begin{aligned}\dot{h}_4 - A(\tau)h_4 = D(\tau;v,v,v,v) + 6C(\tau;v,v,h_2) + 3B(\tau;h_2,h_2)\\ + 4B(\tau;v,h_3) - 12\alpha_1\dot{h}_2 - 24\alpha_2\dot{u}_0,\end{aligned}$$

to be solved in the space of functions satisfying $h_4(T) = h_4(0)$. The Fredholm solvability condition gives us the following expression for α_2,

$$\begin{aligned}\alpha_2 = \frac{1}{24}\int_0^T \langle \varphi^*, D(\tau;v,v,v,v) + 6C(\tau;v,v,h_2)\\ + 3B(\tau;h_2,h_2) + 4B(\tau;v,h_3) - 12\alpha_1\dot{h}_2\rangle\, d\tau,\end{aligned}$$

which by considering (5.22) can be simplified into

$$\begin{aligned}\alpha_2 = \frac{1}{24}\int_0^T \langle \varphi^*, D(\tau;v,v,v,v) + 6C(\tau;v,v,h_2) + 3B(\tau;h_2,h_2)\\ + 4B(\tau;v,h_3) - 12\alpha_1(A(\tau)h_2 + B(\tau;v,v))\rangle\, d\tau \;+\; \alpha_1^2,\end{aligned}$$

where α_1 is given by (5.23), and h_2, h_3, v and φ^* are the solutions of the BVPs (5.24), (5.27), (5.19) and (5.20), respectively.

Using this value of α_2 we can find h_4 by solving

$$\begin{cases}\dot{h}_4 - A(\tau)h_4 - D(\tau;v,v,v,v) - 6C(\tau;v,v,h_2)\\ \quad -3B(\tau;h_2,h_2) - 4B(\tau;v,h_3) + 12\alpha_1(A(\tau)h_2\\ \qquad +B(\tau;v,v) - 2\alpha_1 F(u_0)) + 24\alpha_2 F(u_0) = 0,\ \tau\in[0,T],\\ \qquad\qquad h_4(T) - h_4(0) = 0,\\ \qquad\qquad \int_0^T \langle \varphi^*, h_4\rangle\, d\tau = 0.\end{cases} \tag{5.28}$$

Finally, by collecting the ξ^5-terms, we get the equation for h_5,

$$\begin{aligned}\dot{h}_5 - A(\tau)h_5 = E(\tau;v,v,v,v,v) + 10D(\tau;v,v,v,h_2) + 15C(\tau;v,h_2,h_2)\\ + 10C(\tau;v,v,h_3) + 10B(\tau;h_2,h_3) + 5B(\tau;v,h_4)\\ - 120\alpha_2\dot{v} - 20\alpha_1\dot{h}_3 - 120ev,\end{aligned}$$

which has to be solved in the space of functions satisfying $h_5(T) = -h_5(0)$. Since the operator $\frac{d}{d\tau} - A(\tau)$ has a one-dimensional null-space, we can apply the Fredholm solvability condition to compute the critical coefficient e in the GPD normal

form (4.6). Using the normalization of (5.21), (5.27), and (5.26), we get

$$\begin{aligned} e = \frac{1}{120}\int_0^T \langle v^*, E(\tau; v, v, v, v, v) + 10D(\tau; v, v, v, h_2) + 15C(\tau; v, h_2, h_2) \\ + 10C(\tau; v, v, h_3) + 10B(\tau; h_2, h_3) + 5B(\tau; v, h_4) \\ - 120\alpha_2 A(\tau)v - 20\alpha_1 A(\tau)h_3\rangle\, d\tau. \end{aligned}$$

If this quantity does not vanish, the codim 2 bifurcation is nondegenerate.

5.2.2 Bifurcations with a 3D center manifold

Chenciner bifurcation

The three-dimensional critical center manifold $W^c(\Gamma)$ at the CH bifurcation can be parametrized locally by $(\tau, \xi) \in [0, T] \times \mathbb{C}$ as

$$u = u_0(\tau) + \xi v(\tau) + \bar{\xi}\bar{v}(\tau) + H(\tau, \xi, \bar{\xi}), \tag{5.29}$$

where the real function H satisfies $H(T, \xi, \bar{\xi}) = H(0, \xi, \bar{\xi})$, and has the Taylor expansion

$$H(\tau, \xi, \bar{\xi}) = \sum_{\substack{i,j=0 \\ 2\le i+j\le 5}}^{5} \frac{1}{i!j!} h_{ij}(\tau)\xi^i\bar{\xi}^j + O(|\xi|^6), \tag{5.30}$$

with $h_{ij}(T) = h_{ij}(0)$ and $h_{ij} = \bar{h}_{ji}$ so that h_{ii} is real, while v and its conjugate $\bar{v}$ are defined as

$$\begin{cases} \dot{v}(\tau) - A(\tau)v + i\omega\, v = 0, \ \tau \in [0, T], \\ v(T) - v(0) = 0, \\ \int_0^T \langle v, v\rangle d\tau - 1 = 0. \end{cases} \tag{5.31}$$

These functions exist due to Proposition 2.26.

If we assume that (5.4) restricted to $W^c(\Gamma)$ has the CH periodic normal form (4.7), as in the previous cases we can find the functions $h_{ij}(\tau)$ by solving appropriate BVPs.

First, we introduce the two needed adjoint eigenfunctions. The first one, namely φ^*, satisfies

$$\begin{cases} \dot{\varphi}^* + A^{\mathrm{T}}(\tau)\varphi^* = 0, \ \tau \in [0,T], \\ \varphi^*(T) - \varphi^*(0) = 0, \\ \int_0^T \langle \varphi^*, F(u_0)\rangle \, d\tau - 1 = 0, \end{cases} \tag{5.32}$$

and the second one, namely v^*, satisfies

$$\begin{cases} \dot{v}^*(\tau) + A^{\mathrm{T}}(\tau)v^* + i\omega\, v^* = 0, \ \tau \in [0,T], \\ v^*(T) - v^*(0) = 0, \\ \int_0^T \langle v^*, v\rangle d\tau - 1 = 0. \end{cases} \tag{5.33}$$

Note that in [68] in the Neimark-Sacker bifurcation, the last term in the differential equation for v^* has the wrong sign. This error can have lead to wrong values of the cubic normal form coefficient at the torus bifurcation computed by earlier versions of MatCont.

As usual, we substitute (5.29) into (5.4), use the CH normal form (4.7), and (5.30), as well as (4.3), and collect the corresponding terms in order to find the needed normal form coefficients.

The ξ-independent and the linear terms give rise to the usual identities

$$\dot{u}_0 = F(u_0), \quad \dot{v} - A(\tau)v + i\omega v = 0, \quad \dot{\bar{v}} - A(\tau)\bar{v} - i\omega\bar{v} = 0.$$

Collecting the coefficients of the ξ^2- or $\bar{\xi}^2$-terms leads to the equation

$$\dot{h}_{20} - A(\tau)h_{20} + 2i\omega h_{20} = B(\tau; v, v)$$

or its complex-conjugate. This equation has a unique solution h_{20} satisfying $h_{20}(T) = h_{20}(0)$, since due to the spectral assumptions $e^{2i\omega T}$ is not a multiplier of the critical cycle. Thus, h_{20} can be found by solving

$$\begin{cases} \dot{h}_{20} - A(\tau)h_{20} + 2i\omega h_{20} - B(\tau; v, v) = 0, \ \tau \in [0,T], \\ h_{20}(T) - h_{20}(0) = 0. \end{cases}$$

By collecting the $|\xi|^2$-terms we obtain an equation for h_{11}, namely

$$\dot{h}_{11} - A(\tau)h_{11} = B(\tau; v, \bar{v}) - \alpha_1 \dot{u}_0,$$

to be solved in the space of the functions satisfying $h_{11}(T) = h_{11}(0)$. In this space the operator $\frac{d}{d\tau} - A(\tau)$ has a range space with codimension 1. As before, the null-eigenfunction of the adjoint operator $-\frac{d}{d\tau} - A^{\mathrm{T}}(\tau)$ is φ^*, given by (5.32), and thus because of the Fredholm solvability condition, we can easily obtain the needed value for α_1, i.e.

$$\alpha_1 = \int_0^T \langle \varphi^*, B(\tau; v, \bar{v}) \rangle d\tau.$$

With α_1 defined in this way, let h_{11} be the unique solution of the BVP

$$\begin{cases} \dot{h}_{11} - A(\tau)h_{11} - B(\tau; v, \bar{v}) + \alpha_1 \dot{u}_0 = 0, \ \tau \in [0, T], \\ h_{11}(T) - h_{11}(0) = 0, \\ \int_0^T \langle \varphi^*, h_{11} \rangle d\tau = 0. \end{cases}$$

The coefficient of the third order term in the CH normal form (4.7) is purely imaginary since the first Lyapunov coefficient vanishes at a Chenciner point. We are now ready to compute this coefficient. In fact, if we collect the $\xi |\xi|^2$-terms we obtain

$$\dot{h}_{21} - A(\tau)h_{21} + i\omega h_{21} = C(\tau; v, v, \bar{v}) + 2B(\tau; v, h_{11}) + B(\tau; \bar{v}, h_{20}) - 2icv - 2\alpha_1 \dot{v},$$

to be solved in the space of functions satisfying $h_{21}(T) = h_{21}(0)$. In this space the operator $\frac{d}{d\tau} - A(\tau) + i\omega$ is singular, since $e^{i\omega T}$ is a multiplier of the critical cycle. So we can impose the usual Fredholm solvability condition

$$\int_0^T \langle v^*, C(\tau; v, v, \bar{v}) + 2B(\tau; v, h_{11}) + B(\tau; \bar{v}, h_{20}) - 2icv - 2\alpha_1 \dot{v} \rangle d\tau = 0.$$

This allows us to find the value of the coefficient c of the CH normal form (4.7)

$$c = -\frac{i}{2} \int_0^T \langle v^*, C(\tau; v, v, \bar{v}) + 2B(\tau; v, h_{11}) + B(\tau; \bar{v}, h_{20}) - 2\alpha_1 A(\tau)v \rangle d\tau + \alpha_1 \omega$$

and, with c defined in this way, we can find h_{21} as the unique solution of the BVP

$$\begin{cases} \dot{h}_{21} - A(\tau)h_{21} + i\omega h_{21} - C(\tau; v, v, \bar{v}) - 2B(\tau; v, h_{11}) \\ \qquad -B(\tau; \bar{v}, h_{20}) + 2icv + 2\alpha_1 (A(\tau)v - i\omega v) = 0, \ \tau \in [0, T], \\ h_{21}(T) - h_{21}(0) = 0, \\ \int_0^T \langle v^*, h_{21} \rangle d\tau = 0. \end{cases} \tag{5.34}$$

Collecting the ξ^3-terms gives us an equation for h_{30}

$$\dot{h}_{30} - A(\tau)h_{30} + 3i\omega h_{30} = C(\tau; v, v, v) + 3B(\tau; v, h_{20}),$$

which has a unique solution h_{30} satisfying $h_{30}(T) = h_{30}(0)$, since $e^{3i\omega T}$ is not a multiplier of the critical cycle by the spectral assumptions. Thus, h_{30} is the unique solution of the BVP

$$\begin{cases} \dot{h}_{30} - A(\tau)h_{30} + 3i\omega h_{30} - C(\tau; v, v, v) - 3B(\tau; v, h_{20}) = 0, \ \tau \in [0, T], \\ h_{30}(T) - h_{30}(0) = 0. \end{cases}$$

By collecting the $\xi^2 |\xi|^2$-terms we obtain an equation for h_{31}

$$\begin{aligned} \dot{h}_{31} - A(\tau)h_{31} + 2i\omega h_{31} = {} & D(\tau; v, v, v, \bar{v}) + 3C(\tau; v, v, h_{11}) + 3C(\tau; v, \bar{v}, h_{20}) \\ & + 3B(\tau; h_{11}, h_{20}) + 3B(\tau; v, h_{21}) + B(\tau; \bar{v}, h_{30}) \\ & - 6ich_{20} - 3\alpha_1 \dot{h}_{20}, \end{aligned}$$

which has a unique solution h_{31} satisfying $h_{31}(T) = h_{31}(0)$, since $e^{2i\omega T}$ is not a multiplier of the critical cycle by the spectral assumptions. Thus, h_{31} is the unique solution of the BVP

$$\begin{cases} \dot{h}_{31} - A(\tau)h_{31} + 2i\omega h_{31} - D(\tau; v, v, v, \bar{v}) - 3C(\tau; v, v, h_{11}) \\ -3C(\tau; v, \bar{v}, h_{20}) - 3B(\tau; h_{11}, h_{20}) - 3B(\tau; v, h_{21})B(\tau; \bar{v}, h_{30}) \\ \qquad - + 6ich_{20} + 3\alpha_1(A(\tau)h_{20} - 2i\omega h_{20} + B(\tau; v, v)) = 0, \ \tau \in [0, T], \\ h_{31}(T) - h_{31}(0) = 0. \end{cases}$$

Taking the $|\xi|^4$-terms into account gives an equation for h_{22}

$$\begin{aligned} \dot{h}_{22} - A(\tau)h_{22} = {} & D(\tau; v, v, \bar{v}, \bar{v}) + C(\tau; v, v, h_{02}) + 4C(\tau; v, \bar{v}, h_{11}) \\ & + C(\tau; \bar{v}, \bar{v}, h_{20}) + 2B(\tau; h_{11}, h_{11}) + 2B(\tau; v, h_{12}) \\ & + B(\tau; h_{02}, h_{20}) + 2B(\tau; \bar{v}, h_{21}) - 4\alpha_1 \dot{h}_{11} - 4\alpha_2 \dot{u}_0, \end{aligned}$$

to be solved in the space of functions satisfying $h_{22}(T) = h_{22}(0)$. In this space the operator $\frac{d}{d\tau} - A(\tau)$ has a range space with codimension 1 that is orthogonal to φ^*. So one Fredholm solvability condition is involved, allowing to compute the value of

the coefficient α_2 of our normal form as follows

$$\begin{aligned}\alpha_2 = \frac{1}{4}\int_0^T \langle \varphi^*, D(\tau; v, v, \bar{v}, \bar{v}) + C(\tau; v, v, h_{02}) + 4C(\tau; v, \bar{v}, h_{11}) \\ + C(\tau; \bar{v}, \bar{v}, h_{20}) + 2B(\tau; h_{11}, h_{11}) + 2B(\tau; v, h_{12}) + B(\tau; h_{02}, h_{20}) \\ + 2B(\tau; \bar{v}, h_{21}) - 4\alpha_1(A(\tau)h_{11} + B(\tau; v, \bar{v}))\rangle d\tau + \alpha_1^2.\end{aligned}$$

Using this value for α_2 we can find h_{22} as the unique solution of the BVP

$$\begin{cases} \dot{h}_{22} - A(\tau)h_{22} - D(\tau; v, v, \bar{v}, \bar{v}) - C(\tau; v, v, h_{02}) \\ -4C(\tau; v, \bar{v}, h_{11}) - C(\tau; \bar{v}, \bar{v}, h_{20}) - 2B(\tau; h_{11}, h_{11}) \\ -2B(\tau; v, h_{12}) - B(\tau; h_{02}, h_{20}) - 2B(\tau; \bar{v}, h_{21}) \\ +4\alpha_1(A(\tau)h_{11} + B(\tau; v, \bar{v}) - \alpha_1 F(u_0)) + 4\alpha_2 F(u_0) = 0, \ \tau \in [0, T], \\ h_{22}(T) - h_{22}(0) = 0, \\ \int_0^T \langle \varphi^*, h_{22}\rangle d\tau = 0. \end{cases}$$

Finally, by collecting the $\xi\,|\xi|^4$-terms we obtain an equation for h_{32}

$$\begin{aligned}&\dot{h}_{32} - A(\tau)h_{32} + i\omega h_{32} \\ &\quad = E(\tau; v, v, v, \bar{v}, \bar{v}) + D(\tau; v, v, v, h_{02}) + 6D(\tau; v, v, \bar{v}, h_{11}) + 3D(\tau; v, \bar{v}, \bar{v}, h_{20}) \\ &\qquad + 6C(\tau; v, h_{11}, h_{11}) + 3C(\tau; v, v, h_{12}) + 3C(\tau; v, h_{02}, h_{20}) + 6C(\tau; \bar{v}, h_{11}, h_{20}) \\ &\qquad + 6C(\tau; v, \bar{v}, h_{21}) + C(\tau; \bar{v}, \bar{v}, h_{30}) + 3B(\tau; h_{12}, h_{20}) + 6B(\tau; h_{11}, h_{21}) \\ &\qquad + 3B(\tau; v, h_{22}) + B(\tau; h_{02}, h_{30}) + 2B(\tau; \bar{v}, h_{31}) \\ &\qquad - 12ev - 6ich_{21} - 12\alpha_2\dot{v} - 6\alpha_1\dot{h}_{21}\end{aligned}$$

that, since the operator is singular, allows us, using the first equation of (5.31) as well as the first and the last equation of (5.34), to compute the critical coefficient

e of the CH normal form by imposing the Fredholm solvability condition:

$$\begin{aligned} e = \frac{1}{12}\int_0^T \langle v^*, & E(\tau;v,v,v,\bar{v},\bar{v}) + D(\tau;v,v,v,h_{02}) + 6D(\tau;v,v,\bar{v},h_{11}) \\ & + \ 3D(\tau;v,\bar{v},\bar{v},h_{20}) + 6C(\tau;v,h_{11},h_{11}) + 3C(\tau;v,v,h_{12}) \\ & + 3C(\tau;v,h_{02},h_{20}) + 6C(\tau;\bar{v},h_{11},h_{20}) + 6C(\tau;v,\bar{v},h_{21}) + C(\tau;\bar{v},\bar{v},h_{30}) \\ & + 3B(\tau;h_{12},h_{20}) + 6B(\tau;h_{11},h_{21}) + 3B(\tau;v,h_{22}) + B(\tau;h_{02},h_{30}) \\ & + 2B(\tau;\bar{v},h_{31}) - 12\alpha_2 A(\tau)v - 6\alpha_1(A(\tau)h_{21} + 2B(\tau;v,h_{11}) \\ & + C(\tau;v,v,\bar{v}) + B(\tau;\bar{v},h_{20}) - 2\alpha_1 Av)\rangle d\tau + i\omega\alpha_2 + ic\alpha_1 - \alpha_1^2 i\omega. \end{aligned}$$

We define the **second Lyapunov coefficient** as

$$\boxed{L_2(0) = \Re(e)}.$$

If this coefficient does not vanish, the codim 2 point is nondegenerate.

Note that it can be checked that the equations for h_{40}, h_{50} and h_{41} are uniquely solvable. Since we are in a complex eigenvalue case, v is determined up to a factor γ, for which $\bar{\gamma}^{\mathrm{T}}\gamma = 1$. Then v^*, h_{20}, h_{21}, h_{30}, h_{31} are replaced by γv^*, $\gamma^2 h_{20}$, γh_{21}, $\gamma^3 h_{30}$, $\gamma^2 h_{31}$ respectively, but the values for α_1, α_2, c and e remain the same.

Strong Resonance 1:1 bifurcation

The three-dimensional critical center manifold $W^c(\Gamma)$ at the R1 bifurcation can be parameterized locally by $(\tau,\xi) = (\tau,\xi_1,\xi_2) \in [0,T]\times\mathbb{R}^2$ as

$$u = u_0(\tau) + \xi_1 v_1(\tau) + \xi_2 v_2(\tau) + H(\tau,\xi), \tag{5.35}$$

where H satisfies $H(T,\xi) = H(0,\xi)$ and has the Taylor expansion

$$H(\tau,\xi) = \frac{1}{2}h_{20}(\tau)\xi_1^2 + h_{11}(\tau)\xi_1\xi_2 + \frac{1}{2}h_{02}(\tau)\xi_2^2 + O(|\xi|^3). \tag{5.36}$$

Here, the functions h_{20}, h_{11} and h_{02} are T-periodic in τ, while v_1 and v_2 are the generalized eigenfunctions and are defined as the unique solutions of the BVPs

$$\begin{cases} \dot{v}_1 - A(\tau)v_1 - F(u_0) = 0, \ \tau\in[0,T], \\ \qquad v_1(T) - v_1(0) = 0, \\ \displaystyle\int_0^T \langle v_1, F(u_0)\rangle d\tau = 0, \end{cases} \tag{5.37}$$

and

$$\begin{cases} \dot{v}_2 - A(\tau)v_2 + v_1 = 0, \ \tau \in [0,T], \\ v_2(T) - v_2(0) = 0, \\ \int_0^T \langle v_2, F(u_0)\rangle d\tau = 0, \end{cases} \tag{5.38}$$

respectively. The functions v_1 and v_2 exist and are different due to Proposition 2.26. Following our approach to find the values of the normal form coefficients, we define φ^* as a solution of the adjoint eigenfunction problem (5.9), v_1^* as a solution of

$$\begin{cases} \dot{v_1}^*(\tau) + A^{\mathrm{T}}(\tau)v_1^* - \varphi^* = 0, \ \tau \in [0,T], \\ v_1^*(T) - v_1^*(0) = 0, \end{cases}$$

and v_2^* as a solution of

$$\begin{cases} \dot{v_2}^*(\tau) + A^{\mathrm{T}}(\tau)v_2^* + v_1^* = 0, \ \tau \in [0,T], \\ v_2^*(T) - v_2^*(0) = 0. \end{cases}$$

The above definitions immediately imply that

$$\int_0^T \langle \varphi^*, F(u_0)\rangle d\tau = \int_0^T \langle \varphi^*, v_1\rangle d\tau = \int_0^T \langle F(u_0), v_1^*\rangle d\tau = 0. \tag{5.39}$$

Due to the spectral assumptions at the R1-point we are free to assume that

$$\int_0^T \langle \varphi^*, v_2\rangle d\tau = 1. \tag{5.40}$$

Appending this condition to the eigenproblem, we can find the eigenfunction φ^* as the unique solution of the BVP

$$\begin{cases} \dot{\varphi}^* + A^{\mathrm{T}}(\tau)\varphi^* = 0, \ \tau \in [0,T], \\ \varphi^*(T) - \varphi^*(0) = 0, \\ \int_0^T \langle \varphi^*, v_2\rangle d\tau - 1 = 0. \end{cases} \tag{5.41}$$

As already mentioned in the CPC case, we will choose adjoint generalized eigenfunctions to be orthogonal to an original eigenfunction. Therefore, v_1^* and v_2^* are

obtained as the solution of

$$\begin{cases} \dot{v_1}^* + A^{\mathrm{T}}(\tau)v_1^* - \varphi^* = 0, \ \tau \in [0,T], \\ v_1^*(T) - v_1^*(0) = 0, \\ \displaystyle\int_0^T \langle v_1^*, v_2\rangle d\tau = 0, \end{cases} \tag{5.42}$$

and

$$\begin{cases} \dot{v_2}^*(\tau) + A^{\mathrm{T}}(\tau)v_2^* + v_1^* = 0, \ \tau \in [0,T], \\ v_2^*(T) - v_2^*(0) = 0, \\ \displaystyle\int_0^T \langle v_2^*, v_2\rangle d\tau = 0, \end{cases} \tag{5.43}$$

respectively. Notice that, as in the CPC case, we have normalized in (5.40) the adjoint eigenfunction with the last generalized eigenfunction, which gives us in addition

$$\int_0^T \langle v_1^*, v_1\rangle d\tau = \int_0^T \langle v_2^*, F(u_0)\rangle d\tau = 1.$$

As usual, to derive the value of the normal form coefficients we substitute (5.35) into (5.4), we use (4.3) as well as the R1 normal form (4.8) and (5.36) and get differential equations at every degree of ξ. Remark that in fact the solvability of all the equations up to the maximal order of the normal form has to be checked. We will pay extra attention to this in our discussion for the R1 case.

By collecting the ξ^0-terms we get the identity $\dot{u}_0 = F(u_0)$. The linear terms provide two other identities, namely

$$\dot{v_1} - A(\tau)v_1 - F(u_0) = 0 \qquad \text{and} \qquad \dot{v}_2 - Av_2 + v_1 = 0,$$

cf. (5.37) and (5.38).

By collecting the ξ_1^2-terms we find an equation for h_{20}, namely

$$\dot{h}_{20} - A(\tau)h_{20} = -2\alpha\dot{u}_0 + 2\dot{v}_1 + B(\tau; v_1, v_1) - 2av_2, \tag{5.44}$$

to be solved in the space of periodic functions on $[0,T]$. In this space, the differential operator $\frac{d}{d\tau} - A(\tau)$ is singular with a range orthogonal to φ^*. Using equations (5.39), (5.40), and (5.37), we obtain from the corresponding Fredholm solvability condition the following value for a

$$\boxed{a = \frac{1}{2}\int_0^T \langle \varphi^*, 2A(\tau)v_1 + B(\tau; v_1, v_1)\rangle d\tau.} \tag{5.45}$$

Notice that in the RHS of (5.44) we have no freedom to change the value of the coefficient a. This confirms the theoretically proven fact that the ξ_1^2-term of the R1 normal form (4.8) is resonant. Notice moreover that parameter α is undetermined, which gives us two degrees of freedom for h_{20}. In fact, if h_{20} is a solution of (5.44), then also $\tilde{h}_{20} = h_{20} + \varepsilon_{20}^{I} F(u_0) + \varepsilon_{20}^{II} v_1$ is a solution, due to the fact that $F(u_0)$ spans the null-space of the operator $\frac{d}{d\tau} - A(\tau)$ and that we can tune α as desired:

$$\begin{aligned} \frac{d\tilde{h}_{20}}{d\tau} - A(\tau)\tilde{h}_{20} &= \frac{dh_{20}}{d\tau} - A(\tau)h_{20} + \varepsilon_{20}^{II}\left(\frac{dv_1}{d\tau} - A(\tau)v_1\right) \\ &= \frac{dh_{20}}{d\tau} - A(\tau)h_{20} + \varepsilon_{20}^{II}\dot{u}_0. \end{aligned} \tag{5.46}$$

By collecting the $\xi_1\xi_2$-terms we find an equation for h_{11}

$$\dot{h}_{11} - A(\tau)h_{11} = B(\tau; v_1, v_2) + \dot{v}_2 - h_{20} - bv_2 + v_1, \tag{5.47}$$

to be solved in the space of T-periodic functions. As in the previous case, taking (5.40) into account, as well as (5.38) and (5.39), the corresponding solvability condition implies

$$b = \int_0^T \langle \varphi^*, B(\tau; v_1, v_2) + A(\tau)v_2 \rangle d\tau - \int_0^T \langle \varphi^*, h_{20} \rangle d\tau.$$

Using (5.42), (5.44), (5.39) and (5.37), we can rewrite this expression as

$$\boxed{\begin{aligned} b = &\int_0^T \langle \varphi^*, B(\tau; v_1, v_2) + A(\tau)v_2 \rangle d\tau \\ &+ \int_0^T \langle v_1^*, 2Av_1 + B(\tau; v_1, v_1) \rangle d\tau, \end{aligned}} \tag{5.48}$$

thus obtaining a formula for b that involves only the original and adjoint eigenfunctions.

Notice that the freedom that we have in h_{20} can not be used to change the value of coefficient b (and so the $\xi_1\xi_2$-term of the R1 normal form (4.8) is resonant). Indeed, h_{20} is defined up to a multiple of $F(u_0)$ and v_1, but both vectors are orthogonal to φ^*, see the first two orthogonality conditions in (5.39). However, the presence of h_{20} in the RHS gives us three degrees of freedom for h_{11}. In fact, if h_{11} is a solution of (5.47), also $\tilde{h}_{11} = h_{11} + \varepsilon_{11}^{I} F(u_0) - \varepsilon_{20}^{I} v_1 + \varepsilon_{20}^{II} v_2$ is a solution.

Collecting the ξ_2^2-terms gives us the following equation for h_{02}

$$\dot{h}_{02} - A(\tau)h_{02} = B(\tau, v_2, v_2) - 2h_{11},$$

to be solved in the space of T-periodic functions. This equation should be solvable, so the RHS should lay in the range of the operator $\frac{d}{dt} - A(\tau)$:

$$\int_0^T \langle \varphi^*, B(\tau, v_2, v_2) - 2h_{11} \rangle d\tau = 0.$$

This condition can be satisfied by tuning h_{11}. In fact, ε_{20}^{II} is not yet determined, so h_{11} can have a projection on v_2. Due to (5.40), v_2 does not lay in the range of the $\frac{d}{d\tau} - A(\tau)$ operator, and therefore we can require that

$$\int_0^T \langle \varphi^*, h_{11} \rangle d\tau = \frac{1}{2} \int_0^T \langle \varphi^*, B(\tau, v_2, v_2) \rangle d\tau.$$

This last solvability condition determines ε_{20}^{II} uniquely, and since ε_{20}^{II} determines the value of α, see (5.44) and (5.46), also α is now uniquely determined. So the center manifold expansion has now become unique. Note that in fact the value of α is not needed since it can be shown that it does not affect the bifurcation scenario. Remark also that in order to compute the necessary coefficients a and b by equations (5.45) and (5.48), the second order expansion of the center manifold is not needed. Indeed, we have rewritten the formulas of the normal form coefficients in terms of the original and adjoint eigenfunctions. Since h_{20} or h_{11} are not needed, we don't write down their defining BVPs.

Strong Resonance 1:2 bifurcation

The three-dimensional critical center manifold $W^c(\Gamma)$ at the R2 bifurcation can be parametrized locally by $(\tau, \xi) \in [0, 2T] \times \mathbb{R}^2$ as

$$u = u_0(\tau) + \xi_1 v_1(\tau) + \xi_2 v_2(\tau) + H(\tau, \xi), \quad \tau \in [0, 2T],\ \xi = (\xi_1, \xi_2) \in \mathbb{R}^2, \tag{5.49}$$

where H satisfies $H(2T, \xi) = H(0, \xi)$ and has the Taylor expansion

$$H(\tau, \xi) = \sum_{\substack{i,j=0 \\ 2 \le i+j \le 3}}^{3} \frac{1}{i!j!} h_{ij}(\tau) \xi_1^i \xi_2^j + O(|\xi|^4), \tag{5.50}$$

where all functions h_{ij} are $2T$-periodic, the eigenfunction corresponding to eigenvalue -1 is given by

$$\begin{cases} \dot{v}_1 - A(\tau)v_1 = 0, \ \tau \in [0,T], \\ v_1(T) + v_1(0) = 0, \\ \int_0^T \langle v_1, v_1 \rangle d\tau - 1 = 0, \end{cases} \tag{5.51}$$

and the generalized eigenfunction by

$$\begin{cases} \dot{v}_2 - A(\tau)v_2 + v_1 = 0, \ \tau \in [0,T], \\ v_2(T) + v_2(0) = 0, \\ \int_0^T \langle v_2, v_1 \rangle d\tau = 0, \end{cases} \tag{5.52}$$

with

$$v_1(\tau + T) := -v_1(\tau) \text{ and } v_2(\tau + T) := -v_2(\tau) \text{ for } \tau \in [0,T].$$

The functions v_1 and v_2 exist due to Proposition 2.27. The functions h_{ij} of (5.50) can be found by solving appropriate BVPs, assuming that (5.4) restricted to $W^c(\Gamma)$ has the R2 normal form (4.9). As in the Generalized Period-Doubling case, we first deduce periodicity properties of these functions h_{ij}. It holds that $u(\tau, \xi_1, \xi_2) = u(\tau + T, -\xi_1, -\xi_2)$. This implies that

$$\sum_{i,j} \frac{1}{i!j!} h_{ij}(\tau) \xi_1^i \xi_2^j = \sum_{i,j} \frac{1}{i!j!} h_{ij}(\tau + T)(-1)^{i+j} \xi_1^i \xi_2^j,$$

and thus

$$h_{ij}(\tau) = (-1)^{i+j} h_{ij}(\tau + T),$$

from which follows that $h_{ij}(\tau + T) = h_{ij}(\tau)$ for $i + j$ even and $h_{ij}(\tau + T) = -h_{ij}(\tau)$ for $i + j$ odd, for $\tau \in [0,T]$. Taking these (anti-)periodicity properties into account, we can reduce our analysis to the interval $[0,T]$ instead of $[0,2T]$.

The coefficients α, a and b arise from the solvability conditions for the BVPs as integrals of scalar products over the interval $[0,T]$. Specifically, those scalar products involve among other things the quadratic and cubic terms of (4.3) near the periodic solution u_0. The adjoint eigenfunction φ^* associated to the trivial multiplier is the T-periodic solution of (5.20). The adjoint eigenfunction v_1^* is the

unique solution of the problem

$$\begin{cases} \dot{v}_1^*(\tau) + A^{\mathrm{T}}(\tau)v_1^* = 0, \ \tau \in [0,T], \\ v_1^*(T) + v_1^*(0) = 0 \\ \int_0^T \langle v_1^*, v_2\rangle d\tau - 1 = 0. \end{cases} \tag{5.53}$$

Note that we can indeed require this normalization since v_2 is the last generalized eigenfunction of the original problem and therefore not orthogonal to all the eigenfunctions of the adjoint problem. We further define the generalized adjoint eigenfunction v_2^* as the unique solution of

$$\begin{cases} \dot{v}_2^*(\tau) + A^{\mathrm{T}}(\tau)v_2^* - v_1^* = 0, \ \tau \in [0,T], \\ v_2^*(T) + v_2^*(0) = 0 \\ \int_0^T \langle v_2^*, v_2\rangle d\tau = 0. \end{cases} \tag{5.54}$$

Moreover, we have

$$\int_0^T \langle v_2^*, v_1\rangle d\tau = 1$$

and

$$\int_0^T \langle v_1^*, v_1\rangle d\tau = 0. \tag{5.55}$$

To derive the normal form coefficients, we proceed as in the previous cases, namely, we substitute (5.49) into (5.4), and use (4.3) as well as the R2 normal form (4.9) and (5.50).

By collecting the ξ^0-terms we get the trivial identity $\dot{u}_0 = F(u_0)$. The linear terms provide two other identities, namely $\dot{v}_1 = A(\tau)v_1$ and $v_1 + \dot{v}_2 = A(\tau)v_2$, in accordance with (5.51) and (5.52).

Collecting the ξ_2^2-terms gives an equation for h_{02},

$$\dot{h}_{02} - A(\tau)h_{02} = B(\tau; v_2, v_2) - 2h_{11},$$

to be solved in the space of functions satisfying $h_{02}(T) = h_{02}(0)$. In this space, the differential operator $\frac{d}{d\tau} - A(\tau)$ is singular and the null-space of the adjoint operator

is spanned by φ^*. The Fredholm solvability condition gives a normalization condition for function h_{11}, namely

$$\int_0^T \langle \varphi^*, h_{11} \rangle \, d\tau = \frac{1}{2} \int_0^T \langle \varphi^*, B(\tau; v_2, v_2) \rangle \, d\tau.$$

By collecting the $\xi_1\xi_2$-terms we obtain the differential equation for h_{11}

$$\dot{h}_{11} - A(\tau)h_{11} = B(\tau; v_1, v_2) - h_{20},$$

which must be solved in the space of functions satisfying $h_{11}(T) = h_{11}(0)$. The Fredholm solvability condition gives in this case a normalization condition for h_{20}, i.e.

$$\int_0^T \langle \varphi^*, h_{20} \rangle \, d\tau = \int_0^T \langle \varphi^*, B(\tau; v_1, v_2) \rangle \, d\tau. \tag{5.56}$$

By collecting the ξ_1^2-terms we find an equation for h_{20}

$$\dot{h}_{20} - A(\tau)h_{20} = B(\tau; v_1, v_1) - 2\alpha\dot{u}_0, \tag{5.57}$$

to be solved in the space of functions satisfying $h_{20}(T) = h_{20}(0)$. In this space, the differential operator $\frac{d}{d\tau} - A(\tau)$ is singular and the null-space of its adjoint is spanned by φ^*. The Fredholm solvability condition leads to the expression

$$\alpha = \frac{1}{2} \int_0^T \langle \varphi^*, B(\tau; v_1, v_1) \rangle \, d\tau, \tag{5.58}$$

where v_1 is defined by (5.51).

With α defined in this way we have to find a normalization condition that makes the solution of (5.57) unique. Indeed, if h_{20} is a solution of (5.57) with $h_{20}(T) = h_{20}(0)$, also $\tilde{h}_{20} = h_{20} + \varepsilon_1\dot{u}_0$ is a solution, since $\dot{u}_0$ spans the kernel of the operator $\frac{d}{d\tau} - A(\tau)$ in the space of T-periodic functions. The projection along the space generated by $\dot{u}_0$ is fixed by solvability condition (5.56). So h_{20} can be found as the unique solution of the BVP

$$\begin{cases} \dot{h}_{20} - A(\tau)h_{20} - B(\tau; v_1, v_1) + 2\alpha F(u_0) = 0, \ \tau \in [0, T], \\ h_{20}(T) - h_{20}(0) = 0, \\ \displaystyle\int_0^T \langle \varphi^*, h_{20} \rangle \, d\tau = \int_0^T \langle \varphi^*, B(\tau; v_1, v_2) \rangle \, d\tau. \end{cases} \tag{5.59}$$

In the line of the previous observations, we can define h_{11} as the unique solution of the BVP

$$\begin{cases} \dot{h}_{11} - A(\tau)h_{11} - B(\tau; v_1, v_2) + h_{20} = 0, \ \tau \in [0, T] \\ h_{11}(T) - h_{11}(0) = 0, \\ \int_0^T \langle \varphi^*, h_{11} \rangle \, d\tau = \frac{1}{2} \int_0^T \langle \varphi^*, B(\tau; v_2, v_2) \rangle \, d\tau. \end{cases}$$

By collecting the ξ_1^3-terms we get an equation for h_{30}

$$\dot{h}_{30} - A(\tau)h_{30} = C(\tau; v_1, v_1, v_1) + 3B(\tau; v_1, h_{20}) - 6a v_2 - 6\alpha \dot{v}_1, \tag{5.60}$$

which must be solved in the space of functions satisfying $h_{30}(T) = -h_{30}(0)$. Taking the integral condition of (5.53) into account, we obtain

$$\boxed{a = \frac{1}{6} \int_0^T \langle v_1^*, C(\tau; v_1, v_1, v_1) + 3B(\tau; v_1, h_{20}) - 6\alpha A(\tau) v_1 \rangle \, d\tau}$$

where α is defined by (5.58), h_{20} is the solution of (5.59) and v_1 and v_1^* are defined in (5.51) and (5.53), respectively. As remarked before, it is important to note that if h_{30} is a solution of (5.60) with $h_{30}(T) = -h_{30}(0)$, also $\tilde{h}_{30} = h_{30} + \varepsilon_{30}^I v_1$ is a solution, since v_1 spans the null-space of the operator $\frac{d}{dt} - A(\tau)$ in the space of **anti-periodic functions** (i.e. functions v_1 for which holds that $v_1(T) = -v_1(0)$). By collecting the $\xi_1^2 \xi_2$-terms we get the equation for h_{21}

$$\begin{aligned} \dot{h}_{21} - A(\tau)h_{21} = &-h_{30} - 2b v_2 - 2\alpha \dot{v}_2 - 2\alpha v_1 + C(\tau; v_1, v_1, v_2) \\ &+ B(\tau; h_{20}, v_2) + 2B(\tau; h_{11}, v_1), \end{aligned} \tag{5.61}$$

to be solved in the space of functions satisfying $h_{21}(T) = -h_{21}(0)$. The solvability of this equation implies

$$\begin{aligned} \int_0^T \langle v_1^*, &-h_{30} - 2b v_2 - 2\alpha \dot{v}_2 - 2\alpha v_1 + C(\tau; v_1, v_1, v_2) \\ &+ B(\tau; h_{20}, v_2) + 2B(\tau; h_{11}, v_1) \rangle d\tau = 0. \end{aligned}$$

Notice that the $\xi_1^2 \xi_2$-term in the R2 normal form (4.9) is resonant: in fact we cannot use the freedom on h_{30} to make the normal form parameter b zero since

$$\int_0^T \langle v_1^*, \tilde{h}_{30} \rangle d\tau = \int_0^T \langle v_1^*, h_{30} + \varepsilon_{30}^I v_1 \rangle d\tau = \int_0^T \langle v_1^*, h_{30} \rangle d\tau,$$

because of (5.55). Using the normalization from (5.53) and (5.55) gives us the following expression for b:

$$b = \frac{1}{2}\int_0^T \langle v_1^*, -2\alpha A(\tau)v_2 + C(\tau; v_1, v_1, v_2) + B(\tau; h_{20}, v_2) + 2B(\tau; h_{11}, v_1)\rangle d\tau \\ - \frac{1}{2}\int_0^T \langle v_1^*, h_{30}\rangle d\tau.$$

However, there is no need to compute explicitly the cubic expansion of the center manifold since the last term of this sum can be rewritten. Indeed,

$$\begin{aligned} &- \frac{1}{2}\int_0^T \langle v_1^*, h_{30}\rangle d\tau \\ &\quad = -\frac{1}{2}\int_0^T \langle \dot{v}_2^* + A^{\mathrm{T}}(\tau)v_2^*, h_{30}\rangle d\tau \\ &\quad = \frac{1}{2}\int_0^T \langle v_2^*, \dot{h}_{30} - A(\tau)h_{30}\rangle d\tau \\ &\quad = \frac{1}{2}\int_0^T \langle v_2^*, C(\tau; v_1, v_1, v_1) + 3B(\tau; v_1, h_{20}) - 6av_2 - 6\alpha\dot{v}_1\rangle d\tau \\ &\quad = \frac{1}{2}\int_0^T \langle v_2^*, C(\tau; v_1, v_1, v_1) + 3B(\tau; v_1, h_{20}) - 6\alpha A(\tau)v_1\rangle d\tau, \end{aligned}$$

so that the formula for b takes the following form

$$\boxed{\begin{aligned} b = &\frac{1}{2}\int_0^T \langle v_1^*, -2\alpha A(\tau)v_2 + C(\tau; v_1, v_1, v_2) + B(\tau; h_{20}, v_2) + 2B(\tau; h_{11}, v_1)\rangle d\tau \\ &+ \frac{1}{2}\int_0^T \langle v_2^*, C(\tau; v_1, v_1, v_1) + 3B(\tau; v_1, h_{20}) - 6\alpha A v_1\rangle d\tau, \end{aligned}}$$

where h_{20} is defined in (5.59) and α calculated in (5.58). Notice that, since h_{30} appears on the RHS of equation (5.61), we have two degrees of freedom on h_{21}. In fact, if h_{21} is a solution of (5.61), also $\tilde{h}_{21} = h_{21} + \varepsilon_{21}^I v_1 + \varepsilon_{30}^I v_2$ is a solution since

$$\begin{aligned} \frac{d\tilde{h}_{21}}{d\tau} - A(\tau)\tilde{h}_{21} &= \frac{dh_{21}}{d\tau} - A(\tau)h_{21} + \varepsilon_{30}^I\left(\frac{dv_2}{d\tau} - A(\tau)v_2\right) \\ &= \frac{dh_{21}}{d\tau} - A(\tau)h_{21} - \varepsilon_{30}^I v_1. \end{aligned}$$

By collecting the $\xi_1\xi_2^2$-terms we get the equation for h_{12}

$$\dot{h}_{12} - A(\tau)h_{12} = C(\tau, v_1, v_2, v_2) + B(\tau, v_1, h_{02}) + 2B(\tau, v_2, h_{11}) - 2h_{21},$$

to be solved in the space of functions satisfying $h_{12}(T) = -h_{12}(0)$. The Fredholm solvability condition implies that

$$\int_0^T \langle v_1^*, C(\tau, v_1, v_2, v_2) + B(\tau, v_1, h_{02}) + 2B(\tau, v_2, h_{11}) - 2h_{21}\rangle d\tau = 0.$$

As mentioned before, h_{21} has a component in the direction of v_2 that is not orthogonal to the adjoint eigenfunction v_1^*, so it is possible to impose

$$\int_0^T \langle v_1^*, h_{21}\rangle d\tau = \frac{1}{2}\int_0^T \langle v_1^*, C(\tau, v_1, v_2, v_2) + B(\tau, v_1, h_{02}) + 2B(\tau, v_2, h_{11})\rangle d\tau.$$

This condition defines ε_{30}^I uniquely; the freedom of ε_{21}^I gives us as usual another freedom on h_{12} in the direction of v_2.

Finally, collecting the ξ_2^3-terms gives

$$\dot{h}_{03} - A(\tau)h_{03} = C(\tau, v_2, v_2, v_2) + 3B(v_2, h_{02}) - 3h_{12},$$

to be solved in the space of functions satisfying $h_{03}(T) = -h_{03}(0)$. The Fredholm solvability condition is

$$\int_0^T \langle v_1^*, C(\tau, v_2, v_2, v_2) + 3B(v_2, h_{02}) - 3h_{12}\rangle d\tau = 0,$$

which can be satisfied by imposing

$$\int_0^T \langle v_1^*, h_{12}\rangle d\tau = \frac{1}{3}\int_0^T \langle v_1^*, C(\tau, v_2, v_2, v_2) + 3B(v_2, h_{02})\rangle d\tau.$$

This last condition determines the value of ε_{21}^I and thus the third order center manifold expansion is uniquely determined. However, since this third order expansion of the center manifold is not needed for the computation of the critical coefficients, we do not write down those conditions explicitly.

Strong Resonance 1:3 bifurcation

The three-dimensional critical center manifold $W^c(\Gamma)$ at the R3 bifurcation can be parametrized locally by $(\tau, \xi) \in [0, 3T] \times \mathbb{C}$ as

$$u = u_0(\tau) + \xi v(\tau) + \bar{\xi}\bar{v}(\tau) + H(\tau, \xi, \bar{\xi}),$$

where the real function H satisfies $H(3T,\xi,\bar{\xi}) = H(0,\xi,\bar{\xi})$ and has the Taylor expansion

$$H(\tau,\xi,\bar{\xi}) = \sum_{\substack{i,j=0 \\ 2\le i+j\le 3}}^{3} \frac{1}{i!j!} h_{ij}(\tau)\xi^i\bar{\xi}^j + O(|\xi|^4),$$

with $h_{ij}(3T) = h_{ij}(0)$ and $h_{ij} = \bar{h}_{ji}$ so that h_{ii} is real. The eigenfunction v is defined as the unique solution of the BVP

$$\begin{cases} \dot{v}(\tau) - A(\tau)v = 0, \ \tau \in [0,T], \\ v(T) - e^{i\frac{2\pi}{3}}v(0) = 0, \\ \int_0^T \langle v, v\rangle d\tau - 1 = 0, \end{cases} \tag{5.62}$$

and extended on the interval $[0,3T]$ using the equivariance property of the normal form, i.e.

$$v(\tau+T) := e^{i\frac{2\pi}{3}}v(\tau) \text{ and } v(\tau+2T) := e^{i\frac{4\pi}{3}}v(\tau) \text{ for } \tau \in [0,T].$$

The definition of the conjugate eigenfunction $\bar{v}$ follows immediately. These functions exist due to Proposition 2.26.

As usual the functions h_{ij} can be found by solving appropriate BVPs, assuming that (5.4) restricted to $W^c(\Gamma)$ has the periodic R3 normal form (4.10). Also here we can deduce a property for the functions h_{ij}. The definition of $v(\tau)$ in $[0,3T]$ states that $u(\tau,\xi,\bar{\xi}) = u(\tau+T, e^{-i2\pi/3}\xi, e^{i2\pi/3}\bar{\xi})$. Therefore,

$$\sum_{k,l} \frac{1}{k!l!} h_{kl}(\tau)\xi^k\bar{\xi}^l = \sum_{k,l} \frac{1}{k!l!} h_{kl}(\tau+T)(e^{-i2\pi/3})^k\xi^k(e^{i2\pi/3})^l\bar{\xi}^l,$$

and thus

$$h_{kl}(\tau) = h_{kl}(\tau+T)(e^{-i2\pi/3})^k(e^{i2\pi/3})^l,$$

for $\tau \in [0,T]$. This implies that h_{kk} is T-periodic. These periodicity properties allow us to concentrate on the interval $[0,T]$.

The adjoint eigenfunction φ^* corresponding to the trivial multiplier is the unique

T-periodic solution of BVP (5.20). The adjoint eigenfunction v^* satisfies

$$\begin{cases} \dot{v}^*(\tau) + A^{\mathrm{T}}(\tau)v^* = 0, \ \tau \in [0,T], \\ v^*(T) - e^{i\frac{2\pi}{3}}v^*(0) = 0, \\ \displaystyle\int_0^T \langle v^*, v\rangle d\tau - 1 = 0. \end{cases} \tag{5.63}$$

Similarly, we obtain $\bar{v}^*$.

After the standard substitutions in (5.4), the constant and linear terms give us as usual

$$\dot{u}_0 = F(u_0), \qquad \dot{v} - A(\tau)v = 0, \qquad \dot{\bar{v}} - A(\tau)\bar{v} = 0.$$

From the ξ^2- or $\bar{\xi}^2$-terms we obtain the following equation (or its complex conjugate)

$$\dot{h}_{20} - A(\tau)h_{20} = B(\tau; v, v) - 2\bar{b}\bar{v},$$

to be solved in the space of functions satisfying $h_{20}(T) = e^{i\frac{4\pi}{3}}h_{20}(0)$. In this space the operator $\frac{d}{d\tau} - A(\tau)$ has a range space with codimension 1 that is orthogonal to $\bar{v}^*$. So only one Fredholm solvability condition is involved, from which we obtain

$$\boxed{b = \frac{1}{2}\int_0^T \langle v^*, B(\tau; \bar{v}, \bar{v})\rangle d\tau.}$$

Using this value for b we can find h_{20} as the unique solution of the BVP

$$\begin{cases} \dot{h}_{20} - A(\tau)h_{20} - B(\tau; v, v) + 2\bar{b}\bar{v} = 0, \ \tau \in [0,T], \\ h_{20}(T) - e^{i\frac{4\pi}{3}}h_{20}(0) = 0, \\ \displaystyle\int_0^T \langle \bar{v}^*, h_{20}\rangle d\tau = 0. \end{cases} \tag{5.64}$$

By collecting the $|\xi|^2$-terms we obtain an equation for h_{11}

$$\dot{h}_{11} - A(\tau)h_{11} = B(\tau; v, \bar{v}) - \alpha_1\dot{u}_0,$$

to be solved in the space of functions satisfying $h_{11}(T) = h_{11}(0)$. The Fredholm solvability condition implies

$$\alpha_1 = \int_0^T \langle \varphi^*, B(\tau; v, \bar{v})\rangle d\tau. \tag{5.65}$$

With α_1 defined in this way, let h_{11} be the unique solution of the BVP

$$\begin{cases} \dot{h}_{11} - A(\tau)h_{11} - B(\tau; v, \bar{v}) + \alpha_1 \dot{u}_0 = 0, \ \tau \in [0, T], \\ h_{11}(T) - h_{11}(0) = 0, \\ \int_0^T \langle \varphi^*, h_{11} \rangle d\tau = 0. \end{cases} \tag{5.66}$$

Finally, collecting the $\xi\,|\xi|^2$-terms gives an equation for h_{21}

$$\dot{h}_{21} - A(\tau)h_{21} = C(\tau; v, v, \bar{v}) + 2B(\tau; v, h_{11}) + B(\tau; \bar{v}, h_{20}) - 2cv - 2\bar{b}h_{02} - 2\alpha_1 \dot{v},$$

to be solved in the space of the functions satisfying $h_{21}(T) = e^{i\frac{2\pi}{3}} h_{21}(0)$. The Fredholm solvability condition implies that parameter c of the R3 normal form (4.10) is determined by

$$\boxed{c = \frac{1}{2} \int_0^T \langle v^*, C(\tau; v, v, \bar{v}) + 2B(\tau; v, h_{11}) + B(\tau; \bar{v}, h_{20}) - 2\alpha_1 Av \rangle d\tau}$$

where α_1 is defined by (5.65), and v, v^*, h_{11} and h_{20} are the unique solutions of the BVPs (5.62), (5.63), (5.66) and (5.64), respectively.

By collecting the ξ^3-terms we obtain

$$\dot{h}_{30} - A(\tau)h_{30} = C(\tau; v, v, v) + 3B(\tau; v, h_{20}) - 6\bar{b}h_{11} - 6\alpha_2 \dot{u}_0,$$

to be solved in the space of functions satisfying $h_{30}(T) = h_{30}(0)$. Therefore,

$$\alpha_2 = \int_0^T \langle \varphi^*, C(\tau; v, v, v) + 3B(\tau; v, h_{20}) \rangle d\tau.$$

Remark that as in the Chenciner case v is not uniquely determined. Indeed, when v is a solution of (5.62) and $\gamma \in \mathbb{C}$ with $\bar{\gamma}\gamma = 1$, then γv is also a solution. Then the adjoint function is given by γv^*, and b and h_{20} are replaced by $\bar{\gamma}^3 b$ and $\gamma^2 h_{20}$, respectively. The normal form coefficient c remains the same. However, the normal form coefficient b is multiplied with $\bar{\gamma}^3$. This doesn't affect the bifurcation analysis since there must just hold that this normal form coefficient is nonzero, and obviously $\gamma \neq 0$. Moreover, the analysis around the bifurcation point is independent from the sign of b.

Strong Resonance 1:4 bifurcation

The three-dimensional critical center manifold $W^c(\Gamma)$ at the R4 bifurcation can be parametrized locally by $(\tau, \xi) \in [0, 4T] \times \mathbb{C}$ as

$$u = u_0(\tau) + \xi v(\tau) + \bar{\xi}\bar{v}(\tau) + H(\tau, \xi, \bar{\xi}),$$

where the real function H satisfies $H(4T, \xi, \bar{\xi}) = H(0, \xi, \bar{\xi})$ and has the Taylor expansion

$$H(\tau, \xi, \bar{\xi}) = \sum_{\substack{i,j=0 \\ 2 \le i+j \le 3}}^{3} \frac{1}{i!j!} h_{ij}(\tau) \xi^i \bar{\xi}^j + O(|\xi|^4),$$

with $h_{ij}(4T) = h_{ij}(0)$ and $h_{ij} = \bar{h}_{ji}$ so that h_{ii} is real, while v is defined by

$$\begin{cases} \dot{v} - A(\tau)v = 0, \ \tau \in [0, T], \\ v(T) - e^{i\frac{\pi}{2}} v(0) = 0, \\ \int_0^T \langle v, v \rangle d\tau - 1 = 0, \end{cases} \tag{5.67}$$

extended on $[0, 4T]$ using the equivariance property of the normal form, i.e.

$$\begin{aligned} v(\tau + T) &:= e^{i\frac{\pi}{2}} v(\tau) = iv(\tau), \\ v(\tau + 2T) &:= e^{i\pi} v(\tau) = -v(\tau), \\ v(\tau + 3T) &:= e^{i\frac{3\pi}{2}} v(\tau) = -iv(\tau), \end{aligned}$$

for $\tau \in [0, T]$.

The definition of the conjugate $\bar{v}$ follows immediately. These functions exist due to Proposition 2.26. As usual the functions h_{ij} can be found by solving appropriate BVPs, assuming that (5.4) restricted to $W^c(\Gamma)$ has the periodic R4 normal form (4.11). Similar to the R3 case, it holds that

$$h_{kl}(\tau) = h_{kl}(\tau + T)(e^{-i\pi/2})^k (e^{i\pi/2})^l,$$

for $\tau \in [0, T]$.

The adjoint eigenfunction φ^* is defined by the T-periodic solution of (5.20) and v^* satisfies

$$\begin{cases} \dot{v}^*(\tau) + A^{\mathrm{T}}(\tau)v^* = 0, \ \tau \in [0,T], \\ v^*(T) - e^{i\frac{\pi}{2}}v^*(0) = 0, \\ \int_0^T \langle v^*, v\rangle d\tau - 1 = 0. \end{cases} \tag{5.68}$$

Similarly, we obtain $\bar{v}^*$.

The constant and the linear terms give the identities $\dot{u}_0 = F(u_0)$, $\dot{v} - A(\tau) = 0$, and $\dot{\bar{v}} - A(\tau)\bar{v} = 0$. From the ξ^2- or $\bar{\xi}^2$-terms the following equation (or its complex conjugate) follows

$$\dot{h}_{20} - A(\tau)h_{20} = B(\tau; v, v).$$

Notice that this equation is nonsingular in the space of functions satisfying $h_{20}(T) = -h_{20}(0)$. So h_{20} is obtained as the unique solution of the BVP

$$\begin{cases} \dot{h}_{20} - A(\tau)h_{20} - B(\tau; v, v) = 0, \ \tau \in [0,T], \\ h_{20}(T) + h_{20}(0) = 0. \end{cases} \tag{5.69}$$

By collecting the $|\xi|^2$-terms we obtain an equation for h_{11}

$$\dot{h}_{11} - A(\tau)h_{11} = B(\tau; v, \bar{v}) - \alpha_1 \dot{u}_0,$$

to be solved in the space of functions satisfying $h_{11}(T) = h_{11}(0)$. The Fredholm solvability condition gives exactly the same expression for α_1 as in the R3 case, namely

$$\alpha_1 = \int_0^T \langle \varphi^*, B(\tau; v, \bar{v})\rangle d\tau. \tag{5.70}$$

With this value of α_1, h_{11} is the unique solution of

$$\begin{cases} \dot{h}_{11} - A(\tau)h_{11} - B(\tau; v, \bar{v}) + \alpha_1 \dot{u}_0 = 0, \ \tau \in [0,T], \\ h_{11}(T) - h_{11}(0) = 0, \\ \int_0^T \langle \varphi^*, h_{11}\rangle d\tau = 0. \end{cases} \tag{5.71}$$

The $\bar{\xi}\,|\xi|^2$-terms give an equation for h_{12}

$$\dot{h}_{12} - A(\tau)h_{12} = C(\tau; v, \bar{v}, \bar{v}) + B(\tau; v, h_{02}) + 2B(\tau; \bar{v}, h_{11}) - 2\bar{c}\bar{v} - 2\alpha_1 \dot{\bar{v}},$$

to be solved in the space of functions satisfying $h_{12}(T) = -ih_{12}(0)$. The Fredholm solvability condition implies

$$\boxed{\bar{c} = \frac{1}{2}\int_0^T \langle \bar{v}^*, C(\tau; v, \bar{v}, \bar{v}) + B(\tau; v, h_{02}) + 2B(\tau; \bar{v}, h_{11}) - 2\alpha_1 A(\tau)\bar{v}\rangle d\tau,} \tag{5.72}$$

where α_1 is defined in (5.70), and v, h_{11} and h_{02} are the unique solutions of the BVPs (5.67), (5.71) and the complex conjugate of (5.69). The complex conjugate of (5.72) gives us the critical coefficient c in the R4 normal form (4.11). By collecting the $\bar{\xi}^3$-terms we obtain an equation for h_{03}

$$\dot{h}_{03} - A(\tau)h_{03} = C(\tau; \bar{v}, \bar{v}, \bar{v}) + 3B(\tau; \bar{v}, h_{02}) - 6dv,$$

to be solved in the space of functions satisfying $h_{03}(T) = ih_{03}(0)$. The nontrivial Fredholm solvability condition gives the value of the critical coefficient d in the R4 normal form, namely

$$\boxed{d = \frac{1}{6}\int_0^T \langle v^*, C(\tau; \bar{v}, \bar{v}, \bar{v}) + 3B(\tau; \bar{v}, h_{02})\rangle d\tau.}$$

So we finally obtain the value of

$$\boxed{A = \frac{c}{|d|}}$$

that can be used to determine the bifurcation scenario at the R4 point.

Also in this case v is not uniquely determined, since for every $\gamma \in \mathbb{C}$ with $\bar{\gamma}^{\mathrm{T}}\gamma = 1$, γv is also a solution. Then the adjoint eigenfunction is given by γv^*, and h_{20} is replaced by $\gamma^2 h_{20}$. The normal form coefficient c remains the same, but instead of d we get $\bar{\gamma}^4 d$. However, this again doesn't influence the bifurcation analysis since the study is determined by the above defined coefficient A for which we need only $|d|$.

Fold-Flip bifurcation

The three-dimensional critical center manifold $W^c(\Gamma)$ at the LPPD bifurcation can be parametrized locally by $(\tau, \xi) = (\tau, \xi_1, \xi_2) \in [0, 2T] \times \mathbb{R}^2$ as

$$u = u_0(\tau) + \xi_1 v_1(\tau) + \xi_2 v_2(\tau) + H(\tau, \xi),$$

where H satisfies $H(2T,\xi) = H(0,\xi)$ and has the Taylor expansion

$$H(\tau,\xi) = \sum_{\substack{i,j=0 \\ 2\le i+j\le 3}}^{3} \frac{1}{i!j!} h_{ij}(\tau)\xi_1^i\xi_2^j + O(|\xi|^4),$$

while the eigenfunctions v_1 and v_2 are given by

$$\begin{cases} \dot{v}_1 - A(\tau)v_1 - F(u_0) = 0, \ \tau \in [0,T], \\ v_1(T) - v_1(0) = 0, \\ \int_0^T \langle v_1, F(u_0)\rangle d\tau = 0, \end{cases} \tag{5.73}$$

and

$$\begin{cases} \dot{v}_2 - A(\tau)v_2 = 0, \ \tau \in [0,T], \\ v_2(T) + v_2(0) = 0, \\ \int_0^T \langle v_2, v_2\rangle d\tau - 1 = 0, \end{cases} \tag{5.74}$$

respectively, with

$$v_1(\tau+T) := v_1(\tau) \text{ and } v_2(\tau+T) := -v_2(\tau) \text{ for } \tau \in [0,T].$$

The functions v_1 and v_2 exist because of Proposition 2.26 and Proposition 2.27. The functions h_{ij} can be found by solving appropriate BVPs, assuming that (5.4) restricted to $W^c(\Gamma)$ has the periodic LPPD normal form (4.11). Moreover, similar as before, $u(\tau,\xi_1,\xi_2) = u(\tau+T,\xi_1,-\xi_2)$ such that

$$h_{ij}(\tau) = (-1)^j h_{ij}(\tau+T),$$

for $\tau \in [0,T]$. Therefore, we will reduce all computations to the interval $[0,T]$.

To compute the coefficients of the normal form, we need the generalized eigenfunction v_1 and eigenfunction v_2, and the adjoint eigenfunctions φ^*, v_1^* and v_2^*,

defined as solution of the BVPs

$$\begin{cases} \dot{\varphi}^* + A^{\mathrm{T}}(\tau)\varphi^* = 0, \ \tau \in [0,T], \\ \varphi^*(T) - \varphi^*(0) = 0, \\ \int_0^T \langle \varphi^*, v_1 \rangle d\tau - 1 = 0, \end{cases} \tag{5.75}$$

$$\begin{cases} \dot{v}_1^* + A^{\mathrm{T}}(\tau)v_1^* + \varphi^* = 0, \ \tau \in [0,T], \\ v_1^*(T) - v_1^*(0) = 0, \\ \int_0^T \langle v_1^*, v_1 \rangle d\tau = 0, \end{cases} \tag{5.76}$$

and

$$\begin{cases} \dot{v}_2^* + A^{\mathrm{T}}(\tau)v_2^* = 0, \ \tau \in [0,T], \\ v_2^*(T) + v_2^*(0) = 0, \\ \int_0^T \langle v_2^*, v_2 \rangle d\tau - 1 = 0. \end{cases} \tag{5.77}$$

Note that the integral conditions can be satisfied due to the spectral assumptions at the LPPD point. The following orthogonality conditions hold automatically

$$\begin{aligned} \int_0^T \langle \varphi^*, F(u_0) \rangle d\tau &= \int_0^T \langle \varphi^*, v_2 \rangle d\tau = \int_0^T \langle v_1^*, v_2 \rangle d\tau \\ &= \int_0^T \langle v_2^*, v_1 \rangle d\tau = \int_0^T \langle v_2^*, F(u_0) \rangle d\tau = 0, \end{aligned}$$

and since we have normalized the adjoint eigenfunction associated to multiplier 1 with the generalized eigenfunction, we also have

$$\int_0^T \langle v_1^*, F(u_0) \rangle d\tau = 1.$$

As usual, to derive the normal form coefficients we substitute the above expansions into (5.4) and compare term by term. By collecting the constant and linear terms we get the identities $\dot{u}_0 = F(u_0), \dot{v}_1 = A(\tau)v_1 + F(u_0)$, and $\dot{v}_2 = A(\tau)v_2$.

By collecting the ξ_1^2-terms we find an equation for h_{20}

$$\dot{h}_{20} - A(\tau)h_{20} = B(\tau; v_1, v_1) - 2a_{20}v_1 - 2\alpha_{20}\dot{u}_0 + 2\dot{v}_1, \tag{5.78}$$

to be solved in the space of functions satisfying $h_{20}(T) = h_{20}(0)$. In this space, the differential operator $\frac{d}{d\tau} - A(\tau)$ is singular and the null-space of the adjoint operator is spanned by φ^*. The corresponding Fredholm solvability condition implies

$$\boxed{a_{20} = \frac{1}{2}\int_0^T \langle \varphi^*, B(\tau; v_1, v_1) + 2A(\tau)v_1\rangle \, d\tau.}$$

With a_{20} tuned in this way, (5.78) is solvable for any value of parameter α_{20}. As in the Cusp Point of Cycles case, we are free to choose parameter α_{20} as we want; we take $\alpha_{20} = 0$. This choice will not influence our final conclusion about the possible bifurcation scenarios.

In order to make the solution of (5.78) unique, we have to fix the projection on the null-space of the operator, more specifically in the direction of $F(u_0)$. Therefore, we impose the orthogonality condition with the adjoint generalized eigenfunction v_1^*, and obtain h_{20} as the unique solution of the BVP

$$\begin{cases} \dot{h}_{20} - A(\tau)h_{20} - B(\tau; v_1, v_1) + 2a_{20}v_1 \\ \qquad +2\alpha_{20}F(u_0) - 2A(\tau)v_1 - 2F(u_0) = 0, \ \tau \in [0, T], \\ \qquad\qquad h_{20}(T) - h_{20}(0) = 0, \\ \qquad\qquad \int_0^T \langle v_1^*, h_{20}\rangle d\tau = 0. \end{cases}$$

By collecting the $\xi_1\xi_2$-terms we obtain a singular equation for h_{11}

$$\dot{h}_{11} - A(\tau)h_{11} = B(\tau; v_1, v_2) - b_{11}v_2 + \dot{v}_2,$$

to be solved in the space of the functions that satisfy $h_{11}(T) = -h_{11}(0)$. The Fredholm solvability condition gives

$$\boxed{b_{11} = \int_0^T \langle v_2^*, B(\tau; v_1, v_2) + A(\tau)v_2\rangle \, d\tau,}$$

due to (5.74) and (5.77). With b_{11} defined in this way, we can compute h_{11} as the unique solution of the BVP

$$\begin{cases} \dot{h}_{11} - A(\tau)h_{11} - B(\tau; v_1, v_2) + b_{11}v_2 - A(\tau)v_2 = 0, \ \tau \in [0, T], \\ \qquad\qquad h_{11}(T) + h_{11}(0) = 0, \\ \qquad\qquad \int_0^T \langle v_2^*, h_{11}\rangle d\tau = 0. \end{cases}$$

Collecting the ξ_2^2-terms gives a singular equation for h_{02}

$$\dot{h}_{02} - A(\tau)h_{02} = B(\tau; v_2, v_2) - 2a_{02}v_1 - 2\alpha_{02}\dot{u}_0, \tag{5.79}$$

where solvability gives in the standard way

$$\boxed{a_{02} = \frac{1}{2}\int_0^T \langle \varphi^*, B(\tau; v_2, v_2)\rangle \, d\tau.}$$

So (5.79) is solvable, for any value of the parameter α_{02}. For simplicity, we take $\alpha_{02} = 0$.

Notice that also here, the solution of (5.79) is orthogonal to the adjoint eigenfunction φ^*. Since we have to fix the projection in the direction of the eigenfunction $\dot{u}_0$, we define h_{02} as the unique solution of

$$\begin{cases} \dot{h}_{02} - A(\tau)h_{02} - B(\tau; v_2, v_2) + 2a_{02}v_1 + 2\alpha_{02}F(u_0) = 0, \ \tau \in [0, T], \\ h_{02}(T) - h_{02}(0) = 0, \\ \int_0^T \langle v_1^*, h_{02}\rangle d\tau = 0. \end{cases}$$

By applying the Fredholm solvability conditions to the singular equations for h_{ij} with $i + j = 3$, we obtain

$$\boxed{\begin{aligned} a_{30} &= \frac{1}{6}\int_0^T \langle \varphi^*, C(\tau; v_1, v_1, v_1) + 3B(\tau; h_{20}, v_1) - 6a_{20}h_{20} \\ &\quad + 3(A(\tau)h_{20} + B(\tau; v_1, v_1)) + 6(1 - \alpha_{20})A(\tau)v_1\rangle \, d\tau - a_{20}, \\ b_{21} &= \frac{1}{2}\int_0^T \langle v_2^*, C(\tau; v_1, v_1, v_2) + B(\tau; h_{20}, v_2) + 2B(\tau; h_{11}, v_1) - 2a_{20}h_{11} \\ &\quad - 2b_{11}h_{11} + 2(A(\tau)h_{11} + B(\tau; v_1, v_2)) + 2(1 - \alpha_{20})A(\tau)v_2\rangle \, d\tau - b_{11}, \\ a_{12} &= \frac{1}{2}\int_0^T \langle \varphi^*, C(\tau; v_1, v_2, v_2) + B(\tau; h_{02}, v_1) + 2B(\tau; h_{11}, v_2) - 2b_{11}h_{02} \\ &\quad - 2a_{02}h_{20} + A(\tau)h_{02} + B(\tau; v_2, v_2) - 2\alpha_{02}A(\tau)v_1\rangle \, d\tau - a_{02}, \\ b_{03} &= \frac{1}{6}\int_0^T \langle v_2^*, C(\tau; v_2, v_2, v_2) + 3B(\tau; h_{02}, v_2) - 6a_{02}h_{11} - 6\alpha_{02}A(\tau)v_2\rangle \, d\tau. \end{aligned}}$$

5.2.3 Bifurcations with a 4D center manifold

As discussed in the previous chapter, the representation of the normal forms for bifucations with a 4- or 5-dimensional center manifold is slightly different from

the ones corresponding with a 2- or 3-dimensional center manifold. Indeed, in the normal forms for LPNS, PDNS and NSNS we consider the derivative of the ξ-variable with respect to the phase coordinate τ instead of time t as in the first 8 cases. This, however, does not affect our homological equation approach. In fact, instead of looking at τ and ξ as functions of time t, we now consider ξ as a function of τ, which is in turn a function of time t. Both approaches are mathematically equivalent.

Limit Point-Neimark-Sacker bifurcation

The four-dimensional critical center manifold $W^c(\Gamma)$ at the LPNS bifurcation can be parametrized locally by $(\tau, \xi_1, \xi_2) \in [0,T] \times \mathbb{R} \times \mathbb{C}$ as

$$u = u_0(\tau) + \xi_1 v_1(\tau) + \xi_2 v_2(\tau) + \bar{\xi}_2 \bar{v}_2(\tau) + H(\tau, \xi_1, \xi_2, \bar{\xi}_2), \tag{5.80}$$

where the real function H satisfies $H(T, \xi_1, \xi_2, \bar{\xi}_2) = H(0, \xi_1, \xi_2, \bar{\xi}_2)$ and has the Taylor expansion

$$H(\tau, \xi_1, \xi_2, \bar{\xi}_2) = \sum_{2 \le i+j+k \le 3} \frac{1}{i!j!k!} h_{ijk}(\tau) \xi_1^i \xi_2^j \bar{\xi}_2^k + O(|\xi|^4), \tag{5.81}$$

where the eigenfunctions v_1 and v_2 are defined as

$$\begin{cases} \dot{v}_1 - A(\tau) v_1 - F(u_0) = 0, \ \tau \in [0,T], \\ v_1(T) - v_1(0) = 0, \\ \int_0^T \langle v_1, F(u_0) \rangle d\tau = 0, \end{cases} \tag{5.82}$$

and

$$\begin{cases} \dot{v}_2 - A(\tau) v_2 + i\omega v_2 = 0, \ \tau \in [0,T], \\ v_2(T) - v_2(0) = 0, \\ \int_0^T \langle v_2, v_2 \rangle d\tau - 1 = 0. \end{cases} \tag{5.83}$$

The functions v_1 and v_2 exist because of Proposition 2.26. The functions h_{ijk} can be found by solving appropriate BVPs, assuming that (5.4) restricted to $W^c(\Gamma)$ has the LPNS normal form (4.13).

The coefficients of the normal form arise from the solvability conditions for the BVPs as integrals of scalar products over the interval $[0,T]$. Specifically, those

scalar products involve among other things the quadratic and cubic terms of (4.3) near the periodic solution u_0, the generalized eigenfunction v_1 and the eigenfunction v_2, and the adjoint eigenfunctions φ^*, v_1^* and v_2^* as solutions of the problems

$$\begin{cases} \dot{\varphi}^* + A^{\mathrm{T}}(\tau)\varphi^* = 0, \ \tau \in [0,T], \\ \varphi^*(T) - \varphi^*(0) = 0, \\ \int_0^T \langle \varphi^*, v_1 \rangle d\tau - 1 = 0, \end{cases} \tag{5.84}$$

$$\begin{cases} \dot{v}_1^* + A^{\mathrm{T}}(\tau)v_1^* + \varphi^* = 0, \ \tau \in [0,T], \\ v_1^*(T) - v_1^*(0) = 0, \\ \int_0^T \langle v_1^*, v_1 \rangle d\tau = 0, \end{cases} \tag{5.85}$$

and

$$\begin{cases} \dot{v}_2^* + A^{\mathrm{T}}(\tau)v_2^* + i\omega v_2^* = 0, \ \tau \in [0,T], \\ v_2^*(T) - v_2^*(0) = 0, \\ \int_0^T \langle v_2^*, v_2 \rangle d\tau - 1 = 0. \end{cases} \tag{5.86}$$

In what follows we will make use of the orthogonality condition

$$\int_0^T \langle \varphi^*, F(u_0) \rangle d\tau = 0, \tag{5.87}$$

and the normalization condition

$$\int_0^T \langle v_1^*, F(u_0) \rangle d\tau = 1, \tag{5.88}$$

which can be easily obtained from (5.82), (5.84) and (5.85).

To derive the expressions for the normal form coefficients we write down the homological equation and compare term by term. We therefore substitute (5.80) into (5.4), using (4.3), (4.13) and (5.81). By collecting the constant and linear terms we get the identities

$$\dot{u}_0 = F(u_0), \qquad \dot{v}_1 - F(u_0) = A(\tau)v_1, \qquad \dot{v}_2 + i\omega v_2 = A(\tau)v_2,$$

and the complex conjugate of the last equation.

By collecting the ξ_1^2-terms we find an equation for h_{200}

$$\dot{h}_{200} - A(\tau)h_{200} = B(\tau; v_1, v_1) - 2a_{200}v_1 - 2\alpha_{200}\dot{u}_0 + 2\dot{v}_1, \tag{5.89}$$

to be solved in the space of functions satisfying $h_{200}(T) = h_{200}(0)$. In this space, the differential operator $\frac{d}{d\tau} - A(\tau)$ is singular and the null-space of its adjoint operator is spanned by φ^*. The Fredholm solvability condition

$$\int_0^T \langle \varphi^*, B(\tau; v_1, v_1) - 2a_{200}v_1 - 2\alpha_{200}\dot{u}_0 + 2\dot{v}_1 \rangle \, d\tau = 0$$

allows us to calculate coefficient a_{200} in (4.13) due to (5.82), (5.87) and the required normalization in (5.84), i.e.

$$\boxed{a_{200} = \frac{1}{2}\int_0^T \langle \varphi^*, B(\tau; v_1, v_1) + 2A(\tau)v_1 \rangle \, d\tau.} \tag{5.90}$$

With this expression for a_{200}, let h_{200} be a solution of (5.89) in the space of functions satisfying $h_{200}(0) = h_{200}(T)$. Notice that if h_{200} is a solution of (5.89), then also $h_{200} + \varepsilon_1 F(u_0)$ satisfies (5.89), since $F(u_0)$ lies in the kernel of the operator $\frac{d}{d\tau} - A(\tau)$. In order to obtain a unique solution (without a component along the null-eigenspace) we impose the following orthogonality condition

$$\int_0^T \langle v_1^*, h_{200} \rangle \, d\tau = 0,$$

which determines the value of ε_1 since (5.88) holds. Thus, h_{200} is the unique solution of the BVP

$$\begin{cases} \dot{h}_{200} - A(\tau)h_{200} - B(\tau; v_1, v_1) - 2A(\tau)v_1 \\ \qquad\qquad +2a_{200}v_1 + 2\alpha_{200}\dot{u}_0 - 2\dot{u}_0 = 0, \ \tau \in [0, T], \\ \qquad\qquad h_{200}(T) - h_{200}(0) = 0, \\ \qquad\qquad \int_0^T \langle v_1^*, h_{200} \rangle \, d\tau = 0. \end{cases}$$

By collecting the ξ_2^2-terms (or $\bar{\xi}_2^2$-terms) we find an equation for h_{020}

$$\dot{h}_{020} - A(\tau)h_{020} + 2i\omega h_{020} = B(\tau; v_2, v_2),$$

(or its complex conjugate). This equation has a unique solution satisfying $h_{020}(T) = h_{020}(0)$, since due to the spectral assumptions $e^{2i\omega T}$ is not a multiplier of the critical cycle. Thus, h_{020} can be found by solving

$$\begin{cases} \dot{h}_{020} - A(\tau)h_{020} + 2i\omega h_{020} - B(\tau; v_2, v_2) = 0, \ \tau \in [0, T], \\ h_{020}(T) - h_{020}(0) = 0. \end{cases}$$

By collecting the $\xi_1\xi_2$-terms we obtain an equation for h_{110}

$$\dot{h}_{110} - A(\tau)h_{110} + i\omega h_{110} = B(\tau; v_1, v_2) - b_{110}v_2 + \dot{v}_2 + i\omega v_2,$$

to be solved in the space of functions satisfying $h_{110}(T) = h_{110}(0)$. In this space, the differential operator $\frac{d}{d\tau} - A(\tau) + i\omega$ is singular, since $e^{i\omega T}$ is a critical multiplier. So we can impose the following Fredholm solvability condition

$$\int_0^T \langle v_2^*, B(\tau; v_1, v_2) - b_{110}v_2 + \dot{v}_2 + i\omega v_2 \rangle \, d\tau = 0,$$

which due to the normalization condition in (5.86) determines the value of the normal form coefficient b_{110}, yielding

$$\boxed{b_{110} = \int_0^T \langle v_2^*, B(\tau; v_1, v_2) + A(\tau)v_2 \rangle \, d\tau.} \tag{5.91}$$

The null-space of the operator $\frac{d}{d\tau} - A(\tau) + i\omega$ is one-dimensional and spanned by v_2. To determine h_{110} uniquely, we need to impose an orthogonality condition with a vector whose inproduct with v_2 is nonzero. v_2^* can be chosen because of the normalization condition in (5.86). Therefore, we obtain h_{110} as the unique solution of the BVP

$$\begin{cases} \dot{h}_{110} - A(\tau)h_{110} + i\omega h_{110} - B(\tau; v_1, v_2) + b_{110}v_2 - A(\tau)v_2 = 0, \ \tau \in [0, T], \\ h_{110}(T) - h_{110}(0) = 0, \\ \int_0^T \langle v_2^*, h_{110} \rangle \, d\tau = 0. \end{cases}$$

By collecting the $|\xi_2|^2$-terms we obtain a singular equation for h_{011}, namely

$$\dot{h}_{011} - A(\tau)h_{011} = B(\tau; v_2, \bar{v}_2) - a_{011}v_1 - \alpha_{011}\dot{u}_0,$$

to be solved in the space of functions satisfying $h_{011}(T) = h_{011}(0)$. The nontrivial kernel of the adjoint of the operator $\frac{d}{d\tau} - A(\tau)$ is spanned by φ^*. So, the following Fredholm solvability condition is involved

$$\int_0^T \langle \varphi^*, B(\tau; v_2, \bar{v}_2) - a_{011} v_1 - \alpha_{011} \dot{u}_0 \rangle \, d\tau = 0,$$

which gives us the expression for the normal form coefficient a_{011}, i.e.

$$\boxed{a_{011} = \int_0^T \langle \varphi^*, B(\tau; v_2, \bar{v}_2) \rangle \, d\tau.} \tag{5.92}$$

We impose the orthogonality condition with the adjoint generalized eigenfunction v_1^* to obtain h_{011} as the unique solution of

$$\begin{cases} \dot{h}_{011} - A(\tau) h_{011} - B(\tau; v_2, \bar{v}_2) + a_{011} v_1 + \alpha_{011} \dot{u}_0 = 0, \ \tau \in [0, T], \\ h_{011}(T) - h_{011}(0) = 0, \\ \int_0^T \langle v_1^*, h_{011} \rangle \, d\tau = 0. \end{cases}$$

Note that the values of α_{200} and α_{011} are not determined by the homological equation. We therefore put them equal to zero.

Third order coefficients are only needed to determine the stability of the torus, if it exists. We have listed these terms in Section 5.A.1.

Period-Doubling-Neimark-Sacker bifurcation

The four-dimensional critical center manifold $W^c(\Gamma)$ at the PDNS bifurcation can be parametrized locally by $(\tau, \xi_1, \xi_2) \in [0, 2T] \times \mathbb{R} \times \mathbb{C}$ as

$$u = u_0(\tau) + \xi_1 v_1(\tau) + \xi_2 v_2(\tau) + \bar{\xi}_2 \bar{v}_2(\tau) + H(\tau, \xi_1, \xi_2, \bar{\xi}_2),$$

where H satisfies $H(2T, \xi_1, \xi_2, \bar{\xi}_2) = H(0, \xi_1, \xi_2, \bar{\xi}_2)$ and has the Taylor expansion

$$H(\tau, \xi_1, \xi_2, \bar{\xi}_2) = \sum_{2 \le i+j+k \le 5} \frac{1}{i! j! k!} h_{ijk}(\tau) \xi_1^i \xi_2^j \bar{\xi}_2^k + O(|\xi|^6),$$

while the eigenfunctions v_1 and v_2 are defined by

$$\begin{cases} \dot{v}_1 - A(\tau) v_1 = 0, \ \tau \in [0, T], \\ v_1(T) + v_1(0) = 0, \\ \int_0^T \langle v_1, v_1 \rangle d\tau - 1 = 0, \end{cases} \tag{5.93}$$

with $v_1(\tau+T) = -v_1(\tau)$ for $\tau \in [0,T]$ and

$$\begin{cases} \dot{v}_2 - A(\tau)v_2 + i\omega v_2 = 0, \ \tau \in [0,T], \\ v_2(T) - v_2(0) = 0, \\ \int_0^T \langle v_2, v_2\rangle d\tau - 1 = 0. \end{cases} \tag{5.94}$$

The functions v_1 and v_2 exist because of Proposition 2.27 and Proposition 2.26. The functions h_{ijk} can be found by solving appropriate BVPs, assuming that (5.4) restricted to $W^c(\Gamma)$ has the normal form (4.14). Moreover, $u(\tau,\xi_1,\xi_2,\bar{\xi}_2) = u(\tau+T,-\xi_1,\xi_2,\bar{\xi}_2)$ so that

$$h_{ijk}(\tau) = (-1)^i h_{ijk}(\tau+T), \tag{5.95}$$

for $\tau \in [0,T]$. Therefore, we can restrict our computations to the interval $[0,T]$ instead of $[0,2T]$.

The coefficients of the normal form arise from the solvability conditions for the BVPs as integrals of scalar products over the interval $[0,T]$. Specifically, those scalar products involve among other things the quadratic up to quintic terms of (4.3) near the periodic solution u_0, v_1, v_2, and the adjoint eigenfunctions φ^*, v_1^* and v_2^* as solutions of the problems

$$\begin{cases} \dot{\varphi}^* + A^{\mathrm{T}}(\tau)\varphi^* = 0, \ \tau \in [0,T], \\ \varphi^*(T) - \varphi^*(0) = 0, \\ \int_0^T \langle \varphi^*, F(u_0)\rangle d\tau - 1 = 0, \end{cases} \tag{5.96}$$

$$\begin{cases} \dot{v}_1^* + A^{\mathrm{T}}(\tau)v_1^* = 0, \ \tau \in [0,T], \\ v_1^*(T) + v_1^*(0) = 0, \\ \int_0^T \langle v_1^*, v_1\rangle d\tau - 1 = 0, \end{cases} \tag{5.97}$$

and

$$\begin{cases} \dot{v}_2^* + A^{\mathrm{T}}(\tau)v_2^* + i\omega v_2^* = 0, \ \tau \in [0,T], \\ v_2^*(T) - v_2^*(0) = 0, \\ \int_0^T \langle v_2^*, v_2\rangle d\tau - 1 = 0. \end{cases} \tag{5.98}$$

By collecting the constant and linear terms in the homological equation we get the identities

$$\dot{u}_0 = F(u_0), \qquad \dot{v}_1 = A(\tau)v_1, \qquad \dot{v}_2 + i\omega v_2 = A(\tau)v_2,$$

and the complex conjugate of the last equation, which merely reflect the definition of u_0 and the differential equations in (5.93), (5.94).

By collecting the ξ_1^2-terms we find an equation for h_{200}

$$\dot{h}_{200} - A(\tau)h_{200} = B(\tau; v_1, v_1) - 2\alpha_{200}\dot{u}_0, \tag{5.99}$$

to be solved in the space of functions satisfying $h_{200}(T) = h_{200}(0)$. In this space, the differential operator $\frac{d}{d\tau} - A(\tau)$ is singular and the null-space of its adjoint is spanned by φ^*. The Fredholm solvability condition

$$\int_0^T \langle \varphi^*, B(\tau; v_1, v_1) - 2\alpha_{200}\dot{u}_0 \rangle \, d\tau = 0$$

together with the required normalization in (5.96) gives us the possibility to calculate α_{200} in (4.13), i.e.

$$\alpha_{200} = \frac{1}{2}\int_0^T \langle \varphi^*, B(\tau; v_1, v_1) \rangle \, d\tau. \tag{5.100}$$

As before, h_{200} is determined up to the addition of a multiple of $\dot{u}_0$, since $h_{200} + \varepsilon_1 F(u_0)$ is a solution of (5.99) for every value of ε_1. We fix the value of h_{200} by demanding the orthogonality with the adjoint eigenfunction corresponding with multiplier 1, i.e.

$$\int_0^T \langle \varphi^*, h_{200} \rangle \, d\tau = 0.$$

We then obtain h_{200} as the unique solution of the BVP

$$\begin{cases} \dot{h}_{200} - A(\tau)h_{200} - B(\tau; v_1, v_1) + 2\alpha_{200}\dot{u}_0 = 0, \ \tau \in [0, T], \\ h_{200}(T) - h_{200}(0) = 0, \\ \displaystyle\int_0^T \langle \varphi^*, h_{200} \rangle \, d\tau = 0. \end{cases} \tag{5.101}$$

By collecting the ξ_2^2-terms (or $\bar{\xi}_2^2$-terms) we obtain the differential equation for h_{020}

$$\dot{h}_{020} - A(\tau)h_{020} + 2i\omega h_{020} = B(\tau; v_2, v_2),$$

or its complex conjugate. Since $e^{2i\omega T}$ is not a critical multiplier, no Fredholm solvability condition has to be satisified. h_{020} can thus simply be found by solving

$$\begin{cases} \dot{h}_{020} - A(\tau)h_{020} + 2i\omega h_{020} - B(\tau; v_2, v_2) = 0, \ \tau \in [0, T], \\ h_{020}(T) - h_{020}(0) = 0. \end{cases}$$

The equation found by comparing the $\xi_1\xi_2$-terms is given by

$$\dot{h}_{110} - A(\tau)h_{110} + i\omega h_{110} = B(\tau; v_1, v_2).$$

From (5.95) it follows that h_{110} is anti-periodic. Now, since $-e^{i\omega T}$ is not a multiplier of the critical cycle, no solvability condition has to be satisfied. Therefore, we can immediately obtain h_{110} from

$$\begin{cases} \dot{h}_{110} - A(\tau)h_{110} + i\omega h_{110} - B(\tau; v_1, v_2) = 0, \ \tau \in [0, T], \\ h_{110}(T) + h_{110}(0) = 0. \end{cases}$$

The $|\xi_2|^2$-terms lead to a singular equation for h_{011}, namely

$$\dot{h}_{011} - A(\tau)h_{011} = B(\tau; v_2, \bar{v}_2) - \alpha_{011}\dot{u}_0,$$

to be solved in the space of T-periodic functions. The nontrivial kernel of the operator $\frac{d}{d\tau} - A(\tau)$ is spanned by $\dot{u}_0$. So, the Fredholm solvability condition with the corresponding T-periodic adjoint eigenfunction is involved, i.e.

$$\int_0^T \langle \varphi^*, B(\tau; v_2, \bar{v}_2) - \alpha_{011}\dot{u}_0 \rangle \, d\tau = 0,$$

from which the expression for the normal form coefficient α_{011} can be derived

$$\alpha_{011} = \int_0^T \langle \varphi^*, B(\tau; v_2, \bar{v}_2) \rangle \, d\tau.$$

Now, we still need to uniquely determine the multiple of $F(u_0)$ that can be added to function h_{011}, and will therefore impose the orthogonality condition with φ^* to obtain h_{011} as the unique solution of

$$\begin{cases} \dot{h}_{011} - A(\tau)h_{011} - B(\tau; v_2, \bar{v}_2) + \alpha_{011}\dot{u}_0 = 0, \ \tau \in [0, T], \\ h_{011}(T) - h_{011}(0) = 0, \\ \int_0^T \langle \varphi^*, h_{011} \rangle \, d\tau = 0. \end{cases}$$

We have now examined all order two terms, and continue with the order three terms. Collecting the ξ_1^3-terms determines an equation for h_{300} and will give us the possibility to compute the normal form coefficient a_{300} in (4.14). The differential equation

$$\dot{h}_{300} - A(\tau)h_{300} = C(\tau; v_1, v_1, v_1) + 3B(\tau; v_1, h_{200}) - 6\alpha_{200}\dot{v}_1 - 6a_{300}v_1$$

has to be solved in the space of functions satisfying $h_{300}(T) = -h_{300}(0)$. The nontrivial anti-periodic kernel of the operator $\frac{d}{d\tau} - A(\tau)$ is spanned by v_1. So, the Fredholm solvability condition with the anti-periodic adjoint eigenfunction v_1^* is involved, i.e.

$$\int_0^T \langle v_1^*, C(\tau; v_1, v_1, v_1) + 3B(\tau; v_1, h_{200}) - 6\alpha_{200}\dot{v}_1 - 6a_{300}v_1\rangle \, d\tau = 0$$

and thus

$$\boxed{a_{300} = \frac{1}{6}\int_0^T \langle v_1^*, C(\tau; v_1, v_1, v_1) + 3B(\tau; v_1, h_{200}) - 6\alpha_{200}A(\tau)v_1\rangle \, d\tau,}$$

due to the normalization condition from (5.97). The usual orthogonality condition with the adjoint eigenfunction v_1^* is imposed to obtain h_{300} as the unique solution of

$$\begin{cases} \dot{h}_{300} - A(\tau)h_{300} - C(\tau; v_1, v_1, v_1) - 3B(\tau; v_1, h_{200}) \\ \qquad\qquad +6\alpha_{200}A(\tau)v_1 + 6a_{300}v_1 = 0, \ \tau \in [0, T], \\ \qquad\qquad h_{300}(T) + h_{300}(0) = 0, \\ \qquad\qquad \int_0^T \langle v_1^*, h_{300}\rangle \, d\tau = 0. \end{cases}$$

The ξ_2^3 (or $\bar{\xi}_2^3$)-terms from the homological equation give the following expression for h_{030}

$$\dot{h}_{030} - A(\tau)h_{030} + 3i\omega h_{030} = C(\tau; v_2, v_2, v_2) + 3B(\tau; v_2, h_{020}),$$

or its complex conjugate. This equation has a unique solution h_{030} satisfying $h_{030}(T) = h_{030}(0)$, since due to the spectral assumptions $e^{3i\omega T}$ is not a multiplier of the critical cycle. Thus, h_{030} can be found by solving

$$\begin{cases} \dot{h}_{030} - A(\tau)h_{030} + 3i\omega h_{030} - C(\tau; v_2, v_2, v_2) - 3B(\tau; v_2, h_{020}) = 0, \ \tau \in [0, T], \\ \qquad\qquad h_{030}(T) - h_{030}(0) = 0. \end{cases}$$

By collecting the $\xi_1^2\xi_2$-terms we obtain an equation for h_{210}

$$\begin{aligned}\dot{h}_{210} - A(\tau)h_{210} + i\omega h_{210} = C(\tau; v_1, v_1, v_2) + B(\tau; v_2, h_{200}) + 2B(\tau; v_1, h_{110}) \\ - 2\alpha_{200}\dot{v}_2 - 2b_{210}v_2 - 2i\omega\alpha_{200}v_2,\end{aligned} \tag{5.102}$$

to be solved in the space of T-periodic functions. The nontrivial kernel of the adjoint of the operator $\frac{d}{d\tau} - A(\tau) + i\omega$ is spanned by the complex eigenfunction v_2^*. So, the following Fredholm solvability condition has to be imposed

$$\begin{aligned}\int_0^T \langle v_2^*, C(\tau; v_1, v_1, v_2) + B(\tau; v_2, h_{200}) + 2B(\tau; v_1, h_{110}) \\ -2\alpha_{200}\dot{v}_2 - 2b_{210}v_2 - 2i\omega\alpha_{200}v_2\rangle\, d\tau = 0,\end{aligned}$$

from which the expression for the normal form coefficient b_{210} can be derived, namely

$$\boxed{\begin{aligned}b_{210} = \frac{1}{2}\int_0^T \langle v_2^*, C(\tau; v_1, v_1, v_2) + B(\tau; v_2, h_{200}) \\ + 2B(\tau; v_1, h_{110}) - 2\alpha_{200}A(\tau)v_2\rangle d\tau,\end{aligned}}$$

taking the normalization from (5.98) into account. Now, h_{210} is defined by (5.102) up to the addition of a multiple of v_2. Therefore, we impose the orthogonality condition with the complex adjoint eigenfunction v_2^* to obtain h_{210} as the unique solution of

$$\begin{cases}\dot{h}_{210} - A(\tau)h_{210} + i\omega h_{210} - C(\tau; v_1, v_1, v_2) - B(\tau; v_2, h_{200}) \\ \qquad -2B(\tau; v_1, h_{110}) + 2\alpha_{200}A(\tau)v_2 + 2b_{210}v_2 = 0,\ \tau \in [0, T], \\ \qquad\qquad h_{210}(T) - h_{210}(0) = 0, \\ \qquad\qquad \int_0^T \langle v_2^*, h_{210}\rangle\, d\tau = 0.\end{cases}$$

Since no $\xi_1\xi_2^2$-term is present in the normal form (4.14), we will find a nonsingular equation for h_{120}. Moreover, because of property (5.95) h_{120} is anti-periodic and thus

$$\begin{cases}\dot{h}_{120} - A(\tau)h_{120} + 2i\omega h_{120} - C(\tau; v_1, v_2, v_2) \\ \qquad -B(\tau; v_1, h_{020}) - 2B(\tau; v_2, h_{110}) = 0,\ \tau \in [0, T], \\ \qquad\qquad h_{120}(T) + h_{120}(0) = 0.\end{cases}$$

The two remaining third order terms corresponding with $\xi_2 |\xi_2|^2$ and $\xi_1 |\xi_2|^2$ both give a singular equation, namely

$$\begin{aligned}\dot{h}_{021} - A(\tau)h_{021} + i\omega h_{021} = C(\tau; v_2, v_2, \bar{v}_2) + B(\tau; \bar{v}_2, h_{020}) + 2B(\tau; v_2, h_{011}) \\ - 2\alpha_{011}\dot{v}_2 - 2b_{021}v_2 - 2i\omega\alpha_{011}v_2\end{aligned}$$

and

$$\begin{aligned}\dot{h}_{111} - A(\tau)h_{111} = C(\tau; v_1, v_2, \bar{v}_2) + B(\tau; v_1, h_{011}) + B(\tau; v_2, h_{101}) \\ + B(\tau; \bar{v}_2, h_{110}) - \alpha_{011}\dot{v}_1 - a_{111}v_1.\end{aligned}$$

The first function is T-periodic, the second one is anti-periodic. Both involve a Fredholm solvability condition, which leads to the computation of the two remaining unknown third order normal form coefficients of (4.14), i.e.

$$\boxed{\begin{aligned}b_{021} = \frac{1}{2}\int_0^T \langle v_2^*, C(\tau; v_2, v_2, \bar{v}_2) + B(\tau; \bar{v}_2, h_{020}) \\ + 2B(\tau; v_2, h_{011}) - 2\alpha_{011}A(\tau)v_2\rangle \, d\tau\end{aligned}}$$

and

$$\boxed{\begin{aligned}a_{111} = \int_0^T \langle v_1^*, C(\tau; v_1, v_2, \bar{v}_2) + B(\tau; v_1, h_{011}) \\ + 2\Re(B(\tau; v_2, h_{101})) - \alpha_{011}A(\tau)v_1\rangle \, d\tau.\end{aligned}}$$

Since we need the functions h_{021} and h_{111} for the computation of higher order normal form coefficients, we write down their BVPs, yielding

$$\begin{cases}\dot{h}_{021} - A(\tau)h_{021} + i\omega h_{021} - C(\tau; v_2, v_2, \bar{v}_2) - B(\tau; \bar{v}_2, h_{020}) \\ \qquad -2B(\tau; v_2, h_{011}) + 2\alpha_{011}A(\tau)v_2 + 2b_{021}v_2 = 0, \ \tau \in [0, T], \\ \qquad\qquad h_{021}(T) - h_{021}(0) = 0, \\ \qquad\qquad \int_0^T \langle v_2^*, h_{021}\rangle \, d\tau = 0\end{cases}$$

and

$$\begin{cases}\dot{h}_{111} - A(\tau)h_{111} - C(\tau; v_1, v_2, \bar{v}_2) - B(\tau; v_1, h_{011}) \\ \qquad -2\Re(B(\tau; v_2, h_{101})) + \alpha_{011}A(\tau)v_1 + a_{111}v_1 = 0, \ \tau \in [0, T], \\ \qquad\qquad h_{111}(T) + h_{111}(0) = 0, \\ \qquad\qquad \int_0^T \langle v_1^*, h_{111}\rangle \, d\tau = 0.\end{cases}$$

The stability of a possibly existing extra torus depends on the fourth and fifth order coefficients, which we have listed in Section 5.A.2.

5.2.4 Bifurcations with a 5D center manifold

Double Neimark-Sacker bifurcation

The five-dimensional critical center manifold $W^c(\Gamma)$ at the NSNS bifurcation can be parametrized locally by $(\tau, \xi_1, \xi_2) \in [0,T] \times \mathbb{C}^2$ as

$$u = u_0(\tau) + \xi_1 v_1(\tau) + \bar{\xi}_1 \bar{v}_1(\tau) + \xi_2 v_2(\tau) + \bar{\xi}_2 \bar{v}_2(\tau) + H(\tau, \xi_1, \bar{\xi}_1, \xi_2, \bar{\xi}_2),$$

where H satisfies $H(T, \xi_1, \bar{\xi}_1, \xi_2, \bar{\xi}_2) = H(0, \xi_1, \bar{\xi}_1, \xi_2, \bar{\xi}_2)$ and has the Taylor expansion

$$H(\tau, \xi_1, \bar{\xi}_1, \xi_2, \bar{\xi}_2) = \sum_{2 \le i+j+k+l \le 5} \frac{1}{i!j!k!l!} h_{ijkl}(\tau) \xi_1^i \bar{\xi}_1^j \xi_2^k \bar{\xi}_2^l + O(|\xi|^6),$$

where the complex eigenfunctions v_1 and v_2 are given by

$$\begin{cases} \dot{v}_1 - A(\tau) v_1 + i\omega_1 v_1 = 0, \ \tau \in [0,T], \\ v_1(T) - v_1(0) = 0, \\ \int_0^T \langle v_1, v_1 \rangle d\tau - 1 = 0, \end{cases} \tag{5.103}$$

and

$$\begin{cases} \dot{v}_2 - A(\tau) v_2 + i\omega_2 v_2 = 0, \ \tau \in [0,T], \\ v_2(T) - v_2(0) = 0, \\ \int_0^T \langle v_2, v_2 \rangle d\tau - 1 = 0. \end{cases} \tag{5.104}$$

The functions v_1 and v_2 exist because of Proposition 2.26. The functions h_{ijkl} will be found by solving appropriate BVPs, assuming that (5.4) restricted to $W^c(\Gamma)$ has the normal form (4.15).

The coefficients of the normal form arise from the solvability conditions for the BVPs as integrals of scalar products over the interval $[0,T]$. Specifically, those scalar products involve among other things the quadratic up to quintic terms of

(4.3) near the periodic solution u_0, the eigenfunctions v_1 and v_2, and the adjoint eigenfunctions φ^*, v_1^* and v_2^* as solution of the problems

$$\begin{cases} \dot{\varphi}^* + A^{\mathrm{T}}(\tau)\varphi^* = 0, \ \tau \in [0,T], \\ \varphi^*(T) - \varphi^*(0) = 0, \\ \int_0^T \langle \varphi^*, F(u_0)\rangle d\tau - 1 = 0, \end{cases} \tag{5.105}$$

$$\begin{cases} \dot{v}_1^* + A^{\mathrm{T}}(\tau)v_1^* + i\omega_1 v_1^* = 0, \ \tau \in [0,T], \\ v_1^*(T) - v_1^*(0) = 0, \\ \int_0^T \langle v_1^*, v_1\rangle d\tau - 1 = 0, \end{cases} \tag{5.106}$$

and

$$\begin{cases} \dot{v}_2^* + A^{\mathrm{T}}(\tau)v_2^* + i\omega_2 v_2^* = 0, \ \tau \in [0,T], \\ v_2^*(T) - v_2^*(0) = 0, \\ \int_0^T \langle v_2^*, v_2\rangle d\tau - 1 = 0. \end{cases} \tag{5.107}$$

By collecting the constant and linear terms in the homological equation we get the identities

$$\dot{u}_0 = F(u_0), \qquad \dot{v}_1 + i\omega_1 v_1 = A(\tau)v_1, \qquad \dot{v}_2 + i\omega_2 v_2 = A(\tau)v_2, \tag{5.108}$$

and the complex conjugates of the last two equations. (5.108) merely reflects the definition of u_0 and the differential equations in (5.103) and (5.104).

By collecting the ξ_1^2 (or $\bar{\xi}_1^2$)-terms we find an equation for h_{2000}

$$\dot{h}_{2000} - A(\tau)h_{2000} + 2i\omega_1 h_{2000} = B(\tau; v_1, v_1),$$

(or its complex conjugate). This equation has a unique solution h_{2000} satisfying $h_{2000}(T) = h_{2000}(0)$, since due to the spectral assumptions $e^{2i\omega_1 T}$ is not a multiplier of the critical cycle. Thus, h_{2000} can be found by solving

$$\begin{cases} \dot{h}_{2000} - A(\tau)h_{2000} + 2i\omega_1 h_{2000} - B(\tau; v_1, v_1) = 0, \ \tau \in [0,T], \\ h_{2000}(T) - h_{2000}(0) = 0. \end{cases} \tag{5.109}$$

The function h_{0200} is just the complex conjugate of the function h_{2000}. Analogously, by comparing the ξ_2^2-terms, we obtain h_{0020} as the unique solution of

$$\begin{cases} \dot{h}_{0020} - A(\tau)h_{0020} + 2i\omega_2 h_{0020} - B(\tau; v_2, v_2) = 0, \ \tau \in [0,T], \\ h_{0020}(T) - h_{0020}(0) = 0. \end{cases} \tag{5.110}$$

Notice the symmetry between (5.109) and (5.110).

By collecting the $|\xi_1|^2$-terms we obtain a singular equation, as expected since this term is present in the NSNS normal form (4.15), namely

$$\dot{h}_{1100} - A(\tau)h_{1100} = B(\tau; v_1, \bar{v}_1) - \alpha_{1100}\dot{u}_0,$$

to be solved in the space of functions satisfying $h_{1100}(T) = h_{1100}(0)$. Since the null-space of the adjoint operator is spanned by φ^*, the Fredholm solvability condition

$$\int_0^T \langle \varphi^*, B(\tau; v_1, \bar{v}_1) - \alpha_{1100}\dot{u}_0 \rangle \, d\tau = 0$$

gives us the possibility to calculate parameter α_{1100} due to the normalization condition in (5.105), i.e.

$$\alpha_{1100} = \int_0^T \langle \varphi^*, B(\tau; v_1, \bar{v}_1) \rangle \, d\tau.$$

The function h_{1100} is now determined up to the addition of a multiple of $\dot{u}_0$. As always, we will add an orthogonality condition, in this case with the adjoint eigenfunction corresponding with multiplier 1. Therefore, we obtain h_{1100} as the unique solution of the BVP

$$\begin{cases} \dot{h}_{1100} - A(\tau)h_{1100} - B(\tau; v_1, \bar{v}_1) + \alpha_{1100}\dot{u}_0 = 0, \ \tau \in [0,T], \\ h_{1100}(T) - h_{1100}(0) = 0, \\ \displaystyle\int_0^T \langle \varphi^*, h_{1100} \rangle \, d\tau = 0. \end{cases}$$

Analogously, the function h_{0011} can be obtained by solving

$$\begin{cases} \dot{h}_{0011} - A(\tau)h_{0011} - B(\tau; v_2, \bar{v}_2) + \alpha_{0011}\dot{u}_0 = 0, \ \tau \in [0,T], \\ h_{0011}(T) - h_{0011}(0) = 0, \\ \displaystyle\int_0^T \langle \varphi^*, h_{0011} \rangle \, d\tau = 0, \end{cases}$$

where

$$\alpha_{0011} = \int_0^T \langle \varphi^*, B(\tau; v_2, \bar{v}_2) \rangle \, d\tau.$$

By collecting the $\xi_1\xi_2$-terms we find the following differential equation for h_{1010}

$$\dot{h}_{1010} - A(\tau)h_{1010} + i\omega_1 h_{1010} + i\omega_2 h_{1010} = B(\tau; v_1, v_2).$$

This equation has a unique solution satisfying $h_{1010}(T) = h_{1010}(0)$, since due to the spectral assumptions $e^{i(\omega_1+\omega_2)T}$ is not a multiplier of the critical cycle. Thus, h_{1010} can be found by solving

$$\begin{cases} \dot{h}_{1010} - A(\tau)h_{1010} + i\omega_1 h_{1010} + i\omega_2 h_{1010} - B(\tau; v_1, v_2) = 0, \ \tau \in [0, T], \\ h_{1010}(T) - h_{1010}(0) = 0. \end{cases}$$

Note that $h_{0101} = \overline{h_{1010}}$.

The last second order derivative corresponding with the $\xi_1\bar{\xi}_2$-terms results in a nonsingular differential equation, such that

$$\begin{cases} \dot{h}_{1001} - A(\tau)h_{1001} + i\omega_1 h_{1001} - i\omega_2 h_{1001} - B(\tau; v_1, \bar{v}_2) = 0, \ \tau \in [0, T], \\ h_{1001}(T) - h_{1001}(0) = 0. \end{cases}$$

We now investigate the third order terms. From the ξ_1^3- and ξ_2^3-terms we immediately get the BVPs for h_{3000} and h_{0030}, namely

$$\begin{cases} \dot{h}_{3000} - A(\tau)h_{3000} + 3i\omega_1 h_{3000} \\ -C(\tau; v_1, v_1, v_1) - 3B(\tau; v_1, h_{2000}) = 0, \ \tau \in [0, T], \\ h_{3000}(T) - h_{3000}(0) = 0 \end{cases}$$

and

$$\begin{cases} \dot{h}_{0030} - A(\tau)h_{0030} + 3i\omega_2 h_{0030} \\ -C(\tau; v_2, v_2, v_2) - 3B(\tau; v_2, h_{0020}) = 0, \ \tau \in [0, T], \\ h_{0030}(T) - h_{0030}(0) = 0. \end{cases}$$

Since the $\xi_1 |\xi_1|^2$-term is present in the NSNS normal form, a Fredholm solvability condition is applied to the RHS of the differential equation for h_{2100}

$$\begin{aligned} &\dot{h}_{2100} - A(\tau)h_{2100} + i\omega_1 h_{2100} \\ &\quad = C(\tau; v_1, v_1, \bar{v}_1) + 2B(\tau; v_1, h_{1100}) + B(\tau; \bar{v}_1, h_{2000}) \\ &\quad - 2a_{2100}v_1 - 2i\omega_1\alpha_{1100}v_1 - 2\alpha_{1100}\dot{v}_1, \end{aligned}$$

namely

$$\int_0^T \langle v_1^*, C(\tau; v_1, v_1, \bar{v}_1) + 2B(\tau; v_1, h_{1100}) + B(\tau; \bar{v}_1, h_{2000}) \\ -2a_{2100}v_1 - 2\alpha_{1100}\dot{v}_1 - 2i\omega_1\alpha_{1100}v_1\rangle \, d\tau = 0.$$

Taking the normalization condition from (5.106) and the differential equation from (5.103) into account, we get

$$\boxed{a_{2100} = \frac{1}{2}\int_0^T \langle v_1^*, C(\tau; v_1, v_1, \bar{v}_1) + 2B(\tau; v_1, h_{1100}) \\ + B(\tau; \bar{v}_1, h_{2000}) - 2\alpha_{1100}A(\tau)v_1\rangle \, d\tau.}$$

We can then compute h_{2100} as the unique solution of the BVP

$$\begin{cases} \dot{h}_{2100} - A(\tau)h_{2100} + i\omega_1 h_{2100} - C(\tau; v_1, v_1, \bar{v}_1) \\ \qquad -2B(\tau; v_1, h_{1100}) - B(\tau; \bar{v}_1, h_{2000}) \\ \qquad +2a_{2100}v_1 + 2\alpha_{1100}A(\tau)v_1 = 0, \ \tau \in [0, T], \\ \qquad h_{2100}(T) - h_{2100}(0) = 0, \\ \qquad \int_0^T \langle v_1^*, h_{2100}\rangle \, d\tau = 0. \end{cases}$$

We now immediately list the following BVPs

$$\begin{cases} \dot{h}_{2010} - A(\tau)h_{2010} + 2i\omega_1 h_{2010} + i\omega_2 h_{2010} - C(\tau; v_1, v_1, v_2) \\ \qquad -B(\tau; v_2, h_{2000}) - 2B(\tau; v_1, h_{1010}) = 0, \ \tau \in [0, T], \\ \qquad h_{2010}(T) - h_{2010}(0) = 0, \end{cases}$$

$$\begin{cases} \dot{h}_{2001} - A(\tau)h_{2001} + 2i\omega_1 h_{2001} - i\omega_2 h_{2001} - C(\tau; v_1, v_1, \bar{v}_2) \\ \qquad -B(\tau; \bar{v}_2, h_{2000}) - 2B(\tau; v_1, h_{1001}) = 0, \ \tau \in [0, T], \\ \qquad h_{2001}(T) - h_{2001}(0) = 0, \end{cases}$$

$$\begin{cases} \dot{h}_{1020} - A(\tau)h_{1020} + i\omega_1 h_{1020} + 2i\omega_2 h_{1020} - C(\tau; v_1, v_2, v_2) \\ \qquad -B(\tau; v_1, h_{0020}) - 2B(\tau; v_2, h_{1010}) = 0, \ \tau \in [0, T], \\ \qquad h_{1020}(T) - h_{1020}(0) = 0, \end{cases}$$

and

$$\begin{cases} \dot{h}_{0120} - A(\tau)h_{0120} - i\omega_1 h_{0120} + 2i\omega_2 h_{0120} - C(\tau; \bar{v}_1, v_2, v_2) \\ \qquad -B(\tau; \bar{v}_1, h_{0020}) - 2B(\tau; v_2, h_{0110}) = 0, \ \tau \in [0, T], \\ \qquad h_{0120}(T) - h_{0120}(0) = 0, \end{cases}$$

corresponding with a nonsingular differential equation. The $\xi_2 |\xi_2|^2$-terms from the homological equation make it possible to compute b_{0021}. Indeed, the differential equation

$$\begin{aligned}\dot{h}_{0021} - A(\tau)h_{0021} + i\omega_2 h_{0021} \\ = C(\tau; v_2, v_2, \bar{v}_2) + B(\tau; \bar{v}_2, h_{0020}) + 2B(\tau; v_2, h_{0011}) \\ - 2b_{0021}v_2 - 2\alpha_{0011}\dot{v}_2 - 2i\omega_2\alpha_{0011}v_2\end{aligned}$$

results in a solvability condition with v_2^*, i.e.

$$\begin{aligned}\int_0^T \langle v_2^*, C(\tau; v_2, v_2, \bar{v}_2) + B(\tau; \bar{v}_2, h_{0020}) + 2B(\tau; v_2, h_{0011}) \\ -2b_{0021}v_2 - 2\alpha_{0011}\dot{v}_2 - 2i\omega_2\alpha_{0011}v_2\rangle \, d\tau = 0.\end{aligned}$$

Therefore, considering the normalization condition from (5.107) and the differential equation from (5.104), we can calculate coefficient b_{0021} as

$$\boxed{\begin{aligned}b_{0021} = \frac{1}{2}\int_0^T \langle v_2^*, C(\tau; v_2, v_2, \bar{v}_2) + B(\tau; \bar{v}_2, h_{0020}) \\ + 2B(\tau; v_2, h_{0011}) - 2\alpha_{0011}A(\tau)v_2\rangle \, d\tau,\end{aligned}}$$

with h_{0021} the unique solution of the BVP

$$\begin{cases} \dot{h}_{0021} - A(\tau)h_{0021} + i\omega_2 h_{0021} - C(\tau; v_2, v_2, \bar{v}_2) \\ \quad -B(\tau; \bar{v}_2, h_{0020}) - 2B(\tau; v_2, h_{0011}) \\ \quad +2b_{0021}v_2 + 2\alpha_{0011}A(\tau)v_2 = 0, \ \tau \in [0, T], \\ \quad h_{0021}(T) - h_{0021}(0) = 0, \\ \quad \int_0^T \langle v_2^*, h_{0021}\rangle \, d\tau = 0. \end{cases}$$

The last two to be examined third order terms give us both an expression for a normal form coefficient. The first one, obtained from the $|\xi_1|^2 \xi_2$-terms, leads to the BVP

$$\begin{cases} \dot{h}_{1110} - A(\tau)h_{1110} + i\omega_2 h_{1110} - C(\tau; v_1, \bar{v}_1, v_2) \\ -B(\tau; v_1, h_{0110}) - B(\tau; \bar{v}_1, h_{1010}) - B(\tau; v_2, h_{1100}) \\ \quad +b_{1110}v_2 + \alpha_{1100}A(\tau)v_2 = 0, \ \tau \in [0, T], \\ \quad h_{1110}(T) - h_{1110}(0) = 0, \\ \quad \int_0^T \langle v_2^*, h_{1110}\rangle \, d\tau = 0, \end{cases}$$

where from the solvability condition follows that

$$\boxed{\begin{aligned} b_{1110} = \int_0^T \langle v_2^*, C(\tau; v_1, \bar{v}_1, v_2) + B(\tau; v_1, h_{0110}) + B(\tau; \bar{v}_1, h_{1010}) \\ + B(\tau; v_2, h_{1100}) - \alpha_{1100} A(\tau) v_2 \rangle \, d\tau. \end{aligned}}$$

Analogously, we obtain the following BVP

$$\begin{cases} \dot{h}_{1011} - A(\tau) h_{1011} + i\omega_1 h_{1011} - C(\tau; v_1, v_2, \bar{v}_2) \\ -B(\tau; v_1, h_{0011}) - B(\tau; v_2, h_{1001}) - B(\tau; \bar{v}_2, h_{1010}) \\ \qquad + a_{1011} v_1 + \alpha_{0011} A(\tau) v_1 = 0, \ \tau \in [0, T], \\ \qquad\qquad h_{1011}(T) - h_{1011}(0) = 0, \\ \qquad\qquad \int_0^T \langle v_1^*, h_{1011} \rangle \, d\tau = 0, \end{cases}$$

where

$$\boxed{\begin{aligned} a_{1011} = \int_0^T \langle v_1^*, C(\tau; v_1, v_2, \bar{v}_2) + B(\tau; v_1, h_{0011}) + B(\tau; v_2, h_{1001}) \\ + B(\tau; \bar{v}_2, h_{1010}) - \alpha_{0011} A(\tau) v_1 \rangle \, d\tau. \end{aligned}}$$

We still need the coefficients b_{1101} and a_{0111}, determined by

$$\begin{aligned} b_{1101} = \int_0^T \langle \bar{v}_2^*, C(\tau; v_1, \bar{v}_1, \bar{v}_2) + B(\tau; v_1, h_{0101}) + B(\tau; \bar{v}_1, h_{1001}) \\ + B(\tau; \bar{v}_2, h_{1100}) - \alpha_{1100} A(\tau) \bar{v}_2 \rangle \, d\tau \end{aligned}$$

and

$$\begin{aligned} a_{0111} = \int_0^T \langle \bar{v}_1^*, C(\tau; \bar{v}_1, v_2, \bar{v}_2) + B(\tau; \bar{v}_1, h_{0011}) + B(\tau; v_2, h_{0101}) \\ + B(\tau; \bar{v}_2, h_{0110}) - \alpha_{0011} A(\tau) \bar{v}_1 \rangle \, d\tau. \end{aligned}$$

As before, the higher order terms (fourth and fifth order) that determine the stability of the extra torus can be found in Section 5.A.3.

5.3 Conclusion

This chapter completes the development of efficient methods for the computation of the critical normal form coefficients for all codim 1 and 2 local bifurcations

of limit cycles, started in [68] and based on [59]. Together with the papers on the computation of the critical normal form coefficients for codim 1 and 2 local bifurcations of equilibria in ODEs [66] and fixed points of maps [70,71], it contributes to the development of methods, algorithms, and software tools for multiparameter bifurcation analysis of smooth finite-dimensional dynamical systems.

In this chapter, we have provided the explicit formulas for the normal form coefficients for codim 2 local bifurcations of limit cycles. The approach perfectly fits into the continuation context, where limit cycles and their bifurcations are computed using the BVP-approach, without numerical approximation of Poincaré maps. The resulting formulas are independent of the phase space dimension and are applied in the original basis. In the next chapter, full details are given of the implementation of the developed methods, together with a discussion of several numerical examples in which the validity of the values of the normal form coefficients is checked for.

5.A Higher order coefficients

In this appendix we list the third order normal form coefficients for the LPNS bifurcation and the fourth and fifth order coefficients for PDNS and NSNS, which are necessary to determine the stability of the extra torus (if it exists). Remark that we have not listed the coefficients that can be obtained by complex conjugacy or the similar expressions for ω_2 instead of ω_1 in the case of NSNS.

5.A.1 Third order coefficients for LPNS

The third order normal form coefficients in (4.13) are determined by

$$\begin{aligned}
a_{300} &= \frac{1}{6}\int_0^T \langle \varphi^*, C(\tau; v_1, v_1, v_1) + 3B(\tau; v_1, h_{200}) + 3\dot{h}_{200} \\
&\quad - 6a_{200}h_{200} - 6\alpha_{200}A(\tau)v_1\rangle \, d\tau + a_{200}, \\
b_{210} &= \frac{1}{2}\int_0^T \langle v_2^*, C(\tau; v_1, v_1, v_2) + B(\tau; v_2, h_{200}) + 2B(\tau; v_1, h_{110}) \\
&\quad + 2\dot{h}_{110} - 2\alpha_{200}A(\tau)v_2\rangle \, d\tau + b_{110}, \\
b_{021} &= \frac{1}{2}\int_0^T \langle v_2^*, C(\tau; v_2, v_2, \bar{v}_2) + B(\tau; \bar{v}_2, h_{020}) \\
&\quad + 2B(\tau; v_2, h_{011}) - 2\alpha_{011}A(\tau)v_2\rangle \, d\tau,
\end{aligned}$$

$$a_{111} = \int_0^T \langle \varphi^*, C(\tau; v_1, v_2, \bar{v}_2) + 2\Re(B(\tau; v_2, h_{101})) + B(\tau; v_1, h_{011}) + \dot{h}_{011} - \alpha_{011} A(\tau) v_1 - 2\Re(b_{110}) h_{011} - a_{011} h_{200} \rangle \, d\tau + a_{011}.$$

5.A.2 Fourth and fifth order coefficients for PDNS

The fourth order normal form coefficients in (4.14) are determined by

$$\begin{aligned}
\alpha_{400} &= \frac{1}{24} \int_0^T \langle \varphi^*, D(\tau; v_1, v_1, v_1, v_1) + 6C(\tau; v_1, v_1, h_{200}) \\
&\quad + 3B(\tau; h_{200}, h_{200}) + 4B(\tau; v_1, h_{300}) - 12\alpha_{200}\dot{h}_{200} \rangle \, d\tau, \\
\alpha_{211} &= \frac{1}{2} \int_0^T \langle \varphi^*, D(\tau; v_1, v_1, v_2, \bar{v}_2) + C(\tau; v_1, v_1, h_{011}) + C(\tau; v_2, \bar{v}_2, h_{200}) \\
&\quad + 4\Re(C(\tau; v_1, v_2, h_{101})) + 2\Re(B(\tau; v_2, h_{201})) + B(\tau; h_{200}, h_{011}) \\
&\quad + 2B(\tau; h_{101}, h_{110}) + 2B(\tau; v_1, h_{111}) - \alpha_{011}\dot{h}_{200} - 2\alpha_{200}\dot{h}_{011} \rangle \, d\tau, \\
\alpha_{022} &= \frac{1}{4} \int_0^T \langle \varphi^*, D(\tau; v_2, v_2, \bar{v}_2, \bar{v}_2) + 4C(\tau; v_2, \bar{v}_2, h_{011}) + 2\Re(C(\tau; v_2, v_2, h_{002})) \\
&\quad + B(\tau; h_{020}, h_{002}) + 2B(\tau; h_{011}, h_{011}) + 4\Re(B(\tau; v_2, h_{012})) - 4\alpha_{011}\dot{h}_{011} \rangle \, d\tau.
\end{aligned}$$

The fourth order functions of the expansion of the critical center manifold can be computed by solving the following BVPs on $[0, T]$

$$\begin{cases}
\dot{h}_{400} - A(\tau) h_{400} - D(\tau; v_1, v_1, v_1, v_1) - 6C(\tau; v_1, v_1, h_{200}) \\
\qquad -3B(\tau; h_{200}, h_{200}) - 4B(\tau; v_1, h_{300}) + 12\alpha_{200}\dot{h}_{200} \\
\qquad +24\alpha_{400}\dot{u}_0 + 24a_{300}h_{200} = 0, \\
h_{400}(T) - h_{400}(0) = 0, \\
\int_0^T \langle \varphi^*, h_{400} \rangle \, d\tau = 0,
\end{cases}$$

$$\begin{cases}
\dot{h}_{040} - A(\tau) h_{040} + 4i\omega h_{040} - D(\tau; v_2, v_2, v_2, v_2) \\
-6C(\tau; v_2, v_2, h_{020}) - 4B(\tau; v_2, h_{030}) - 3B(\tau; h_{020}, h_{020}) = 0, \\
h_{040}(T) - h_{040}(0) = 0,
\end{cases}$$

$$\begin{cases} \dot{h}_{310} - A(\tau)h_{310} + i\omega h_{310} - D(\tau; v_1, v_1, v_1, v_2) \\ -3C(\tau; v_1, v_1, h_{110}) - 3C(\tau; v_1, v_2, h_{200}) - B(\tau; v_2, h_{300}) \\ -3B(\tau; v_1, h_{210}) - 3B(\tau; h_{200}, h_{110}) + 6\alpha_{200}\dot{h}_{110} \\ +6a_{300}h_{110} + 6b_{210}h_{110} + 6i\omega\alpha_{200}h_{110} = 0, \\ h_{310}(T) + h_{310}(0) = 0, \end{cases}$$

$$\begin{cases} \dot{h}_{130} - A(\tau)h_{130} + 3i\omega h_{130} - D(\tau; v_1, v_2, v_2, v_2) \\ -3C(\tau; v_2, v_2, h_{110}) - 3C(\tau; v_1, v_2, h_{020}) - B(\tau; v_1, h_{030}) \\ -3B(\tau; h_{020}, h_{110}) - 3B(\tau; v_2, h_{120}) = 0, \\ h_{130}(T) + h_{130}(0) = 0, \end{cases}$$

$$\begin{cases} \dot{h}_{031} - A(\tau)h_{031} + 2i\omega h_{031} - D(\tau; v_2, v_2, v_2, \bar{v}_2) \\ -3C(\tau; v_2, v_2, h_{011}) - 3C(\tau; v_2, \bar{v}_2, h_{020}) - B(\tau; \bar{v}_2, h_{030}) \\ -3B(\tau; h_{020}, h_{011}) - 3B(\tau; v_2, h_{021}) + 3\alpha_{011}\dot{h}_{020} \\ +6b_{021}h_{020} + 6i\omega\alpha_{011}h_{020} = 0, \\ h_{031}(T) - h_{031}(0) = 0, \end{cases}$$

$$\begin{cases} \dot{h}_{211} - A(\tau)h_{211} - D(\tau; v_1, v_1, v_2, \bar{v}_2) - C(\tau; v_1, v_1, h_{011}) \\ -C(\tau; v_2, \bar{v}_2, h_{200}) - 4\Re(C(\tau; v_1, v_2, h_{101})) - 2\Re(B(\tau; v_2, h_{201})) \\ -B(\tau; h_{200}, h_{011}) - 2B(\tau; h_{101}, h_{110}) - 2B(\tau; v_1, h_{111}) + \alpha_{011}\dot{h}_{200} \\ +2\alpha_{200}\dot{h}_{011} + 2\alpha_{211}\dot{u}_0 + 2a_{111}h_{200} + 4\Re(b_{210})h_{011} = 0, \\ h_{211}(T) - h_{211}(0) = 0, \\ \int_0^T \langle \varphi^*, h_{211} \rangle \, d\tau = 0, \end{cases}$$

$$\begin{cases} \dot{h}_{121} - A(\tau)h_{121} + i\omega h_{121} - D(\tau; v_1, v_2, v_2, \bar{v}_2) \\ -C(\tau; v_1, \bar{v}_2, h_{020}) - 2C(\tau; v_1, v_2, h_{011}) - C(\tau; v_2, v_2, h_{101}) \\ -2C(\tau; v_2, \bar{v}_2, h_{110}) - B(\tau; v_1, h_{021}) - B(\tau; h_{020}, h_{101}) \\ -2B(\tau; h_{011}, h_{110}) - 2B(\tau; v_2, h_{111}) - B(\tau; \bar{v}_2, h_{120}) \\ +2\alpha_{011}\dot{h}_{110} + 2b_{021}h_{110} + 2a_{111}h_{110} + 2i\omega\alpha_{011}h_{110} = 0, \\ h_{121}(T) + h_{121}(0) = 0, \end{cases}$$

$$\begin{cases} \dot{h}_{220} - A(\tau)h_{220} + 2i\omega h_{220} - D(\tau; v_1, v_1, v_2, v_2) \\ -C(\tau; v_2, v_2, h_{200}) - 4C(\tau; v_1, v_2, h_{110}) - C(\tau; v_1, v_1, h_{020}) \\ -B(\tau; h_{200}, h_{020}) - 2B(\tau; v_2, h_{210}) - 2B(\tau; h_{110}, h_{110}) \\ -2B(\tau; v_1, h_{120}) + 2\alpha_{200}\dot{h}_{020} + 4b_{210}h_{020} + 4i\omega\alpha_{200}h_{020} = 0, \\ h_{220}(T) - h_{220}(0) = 0, \end{cases}$$

$$\begin{cases} \dot{h}_{022} - A(\tau)h_{022} - D(\tau; v_2, v_2, \bar{v}_2, \bar{v}_2) - 4C(\tau; v_2, \bar{v}_2, h_{011}) \\ -2\Re(C(\tau; v_2, v_2, h_{002})) - B(\tau; h_{020}, h_{002}) - 2B(\tau; h_{011}, h_{011}) \\ -4\Re(B(\tau; v_2, h_{012})) + 4\alpha_{011}\dot{h}_{011} + 4\alpha_{022}\dot{u}_0 + 8\Re(b_{021})h_{011} = 0, \\ h_{022}(T) - h_{022}(0) = 0, \\ \int_0^T \langle \varphi^*, h_{022} \rangle \, d\tau = 0. \end{cases}$$

The fifth order normal form coefficients in (4.14) are determined by

$$\begin{aligned} a_{500} = \frac{1}{120}\int_0^T \langle v_1^*, & E(\tau; v_1, v_1, v_1, v_1, v_1) + 10D(\tau; v_1, v_1, v_1, h_{200}) \\ & + 10C(\tau; v_1, v_1, h_{300}) + 15C(\tau; v_1, h_{200}, h_{200}) + 10B(\tau; h_{200}, h_{300}) \\ & + 5B(\tau; v_1, h_{400}) - 20\alpha_{200}\dot{h}_{300} - 120\alpha_{400}A(\tau)v_1 \rangle \, d\tau - \alpha_{200}a_{300}, \\ b_{410} = \frac{1}{24}\int_0^T \langle v_2^*, & E(\tau; v_1, v_1, v_1, v_1, v_2) + 6D(\tau; v_1, v_1, v_2, h_{200}) \\ & + 4D(\tau; v_1, v_1, v_1, h_{110}) + 4C(\tau; v_1, v_2, h_{300}) + 6C(\tau; v_1, v_1, h_{210}) \\ & + 3C(\tau; v_2, h_{200}, h_{200}) + 12C(\tau; v_1, h_{200}, h_{110}) + 4B(\tau; v_1, h_{310}) \\ & + 4B(\tau; h_{110}, h_{300}) + 6B(\tau; h_{200}, h_{210}) + B(\tau; v_2, h_{400}) \\ & - 24\alpha_{400}A(\tau)v_2 - 12\alpha_{200}\dot{h}_{210} \rangle \, d\tau - \alpha_{200}b_{210}, \\ a_{311} = \frac{1}{6}\int_0^T \langle v_1^*, & E(\tau; v_1, v_1, v_1, v_2, \bar{v}_2) + D(\tau; v_1, v_1, v_1, h_{011}) \\ & + 6\Re(D(\tau; v_1, v_1, v_2, h_{101})) + 3D(\tau; v_1, v_2, \bar{v}_2, h_{200}) + 3C(\tau; v_1, h_{200}, h_{011}) \\ & + 6\Re(C(\tau; v_2, h_{200}, h_{101})) + 6\Re(C(\tau; v_1, v_2, h_{201})) + C(\tau; v_2, \bar{v}_2, h_{300}) \\ & + 3C(\tau; v_1, v_1, h_{111}) + 6C(\tau; v_1, h_{101}, h_{110}) + 3B(\tau; h_{200}, h_{111}) \\ & + 6\Re(B(\tau; h_{201}, h_{110})) + 2\Re(B(\tau; v_2, h_{301})) + B(\tau; h_{011}, h_{300}) \\ & + 3B(\tau; h_{211}, v_1) - 6\alpha_{211}A(\tau)v_1 - \alpha_{011}\dot{h}_{300} \\ & - 6\alpha_{200}\dot{h}_{111} \rangle \, d\tau - \alpha_{200}a_{111} - \alpha_{011}a_{300}, \end{aligned}$$

$$
\begin{aligned}
b_{221} = \frac{1}{4}\int_0^T \langle v_2^*, & E(\tau; v_1, v_1, v_2, v_2, \bar{v}_2) + D(\tau; v_2, v_2, \bar{v}_2, h_{200}) \\
& + 2D(\tau; v_1, v_2, v_2, h_{101}) + 2D(\tau; v_1, v_1, v_2, h_{011}) \\
& + D(\tau; v_1, v_1, \bar{v}_2, h_{020}) + 4D(\tau; v_1, v_2, \bar{v}_2, h_{110}) + 2C(\tau; \bar{v}_2, h_{110}, h_{110}) \\
& + C(\tau; v_1, v_1, h_{021}) + C(\tau; v_2, v_2, h_{201}) + C(\tau; \bar{v}_2, h_{200}, h_{020}) \\
& + 2C(\tau; v_2, \bar{v}_2, h_{210}) + 2C(\tau; v_1, \bar{v}_2, h_{120}) + 2C(\tau; v_1, h_{020}, h_{101}) \\
& + 4C(\tau; v_1, v_2, h_{111}) + 4C(\tau; v_2, h_{101}, h_{110}) + 2C(\tau; v_2, h_{200}, h_{011}) \\
& + 4C(\tau; v_1, h_{110}, h_{011}) + B(\tau; \bar{v}_2, h_{220}) + 2B(\tau; v_1, h_{121}) + 2B(\tau; h_{120}, h_{101}) \\
& + 4B(\tau; h_{110}, h_{111}) + 2B(\tau; h_{210}, h_{011}) + 2B(\tau; v_2, h_{211}) + B(\tau; h_{200}, h_{021}) \\
& + B(\tau; h_{201}, h_{020}) - 2\alpha_{011}\dot{h}_{210} - 4\alpha_{211}A(\tau)v_2 - 2\alpha_{200}\dot{h}_{021}\rangle \, d\tau \\
& - \alpha_{200}b_{021} - \alpha_{011}b_{210}, \\
a_{122} = \frac{1}{4}\int_0^T \langle v_1^*, & E(\tau; v_1, v_2, v_2, \bar{v}_2, \bar{v}_2) + 4\Re(D(\tau; v_2, v_2, \bar{v}_2, h_{101})) \\
& + 2\Re(D(\tau; v_1, v_2, v_2, h_{002})) + 4D(\tau; v_1, v_2, \bar{v}_2, h_{011}) + 2C(\tau; v_1, h_{011}, h_{011}) \\
& + 8\Re(C(\tau; v_2, h_{011}, h_{101})) + 4\Re(C(\tau; v_2, h_{002}, h_{110})) + C(\tau; v_1, h_{020}, h_{002}) \\
& + 4\Re(C(\tau; v_1, v_2, h_{012})) + 4C(\tau; v_2, \bar{v}_2, h_{111}) + 2\Re(C(\tau; v_2, v_2, h_{102})) \\
& + 4B(\tau; h_{011}, h_{111}) + 2\Re(B(\tau; h_{020}, h_{102})) + 4\Re(B(\tau; v_2, h_{112})) \\
& + B(\tau; v_1, h_{022}) + 4\Re(B(\tau; h_{110}, h_{012})) - 4\alpha_{011}\dot{h}_{111} \\
& - 4\alpha_{022}A(\tau)v_1\rangle \, d\tau - \alpha_{011}a_{111}, \\
b_{032} = \frac{1}{12}\int_0^T \langle v_2^*, & E(\tau; v_2, v_2, v_2, \bar{v}_2, \bar{v}_2) + D(\tau; v_2, v_2, v_2, h_{002}) \\
& + 3D(\tau; v_2, \bar{v}_2, \bar{v}_2, h_{020}) + 6D(\tau; v_2, v_2, \bar{v}_2, h_{011}) + 6C(\tau; \bar{v}_2, h_{020}, h_{011}) \\
& + 6C(\tau; v_2, \bar{v}_2, h_{021}) + C(\tau; \bar{v}_2, \bar{v}_2, h_{030}) + 3C(\tau; v_2, h_{002}, h_{020}) \\
& + 3C(\tau; v_2, v_2, h_{012}) + 6C(\tau; v_2, h_{011}, h_{011}) + 3B(\tau; h_{020}, h_{021}) \\
& + 6B(\tau; h_{021}, h_{011}) + 3B(\tau; v_2, h_{022}) + 2B(\tau; \bar{v}_2, h_{031}) \\
& + B(\tau; h_{002}, h_{030}) - 6\alpha_{011}\dot{h}_{021} - 12\alpha_{022}A(\tau)v_2\rangle \, d\tau - \alpha_{011}b_{021}.
\end{aligned}
$$

5.A.3 Fourth and fifth order coefficients for NSNS

The fourth order normal form coefficients for (4.15) are determined by

$$\begin{aligned}\alpha_{2200} = \frac{1}{4}\int_0^T \langle \varphi^*, & D(\tau; v_1, v_1, \bar{v}_1, \bar{v}_1) + 2\Re(C(\tau; v_1, v_1, h_{0200})) \\ & + 4C(\tau; v_1, \bar{v}_1, h_{1100}) + B(\tau; h_{2000}, h_{0200}) + 2B(\tau; h_{1100}, h_{1100}) \\ & + 4\Re(B(\tau; v_1, h_{1200})) - 4\alpha_{1100}\dot{h}_{1100}\rangle \, d\tau, \\ \alpha_{1111} = \int_0^T \langle \varphi^*, & D(\tau; v_1, \bar{v}_1, v_2, \bar{v}_2) + C(\tau; v_1, \bar{v}_1, h_{0011}) + 2\Re(C(\tau; v_1, v_2, h_{0101})) \\ & + 2\Re(C(\tau; v_1, \bar{v}_2, h_{0110})) + C(\tau; v_2, \bar{v}_2, h_{1100}) + 2\Re(B(\tau; v_1, h_{0111})) \\ & + B(\tau; h_{0110}, h_{1001}) + B(\tau; h_{0101}, h_{1010}) + B(\tau; h_{0011}, h_{1100}) \\ & + 2\Re(B(\tau; v_2, h_{1101})) - \alpha_{0011}\dot{h}_{1100} - \alpha_{1100}\dot{h}_{0011}\rangle \, d\tau.\end{aligned}$$

The fourth order functions of the expansion of the critical center manifold can be computed by solving the following BVPs on $[0, T]$

$$\begin{cases} \dot{h}_{4000} - A(\tau)h_{4000} + 4i\omega_1 h_{4000} - D(\tau; v_1, v_1, v_1, v_1) \\ -6C(\tau; v_1, v_1, h_{2000}) - 3B(\tau; h_{2000}, h_{2000}) - 4B(\tau; v_1, h_{3000}) = 0, \\ h_{4000}(T) - h_{4000}(0) = 0, \end{cases}$$

$$\begin{cases} \dot{h}_{3100} - A(\tau)h_{3100} + 2i\omega_1 h_{3100} - D(\tau; v_1, v_1, v_1, \bar{v}_1) \\ -3C(\tau; v_1, v_1, h_{1100}) - 3C(\tau; v_1, \bar{v}_1, h_{2000}) - B(\tau; \bar{v}_1, h_{3000}) \\ -3B(\tau; v_1, h_{2100}) - 3B(\tau; h_{2000}, h_{1100}) + 3\alpha_{1100}\dot{h}_{2000} \\ +6a_{2100}h_{2000} + i\omega_1\alpha_{1100}h_{2000} = 0, \\ h_{3100}(T) - h_{3100}(0) = 0, \end{cases}$$

$$\begin{cases} \dot{h}_{3010} - A(\tau)h_{3010} + 3i\omega_1 h_{3010} + i\omega_2 h_{3010} - D(\tau; v_1, v_1, v_1, v_2) \\ -3C(\tau; v_1, v_1, h_{1010}) - 3C(\tau; v_1, v_2, h_{2000}) - B(\tau; v_2, h_{3000}) \\ -3B(\tau; v_1, h_{2010}) - 3B(\tau; h_{2000}, h_{1010}) = 0, \\ h_{3010}(T) - h_{3010}(0) = 0, \end{cases}$$

$$\begin{cases} \dot{h}_{3001} - A(\tau)h_{3001} + 3i\omega_1 h_{3001} - i\omega_2 h_{3001} - D(\tau; v_1, v_1, v_1, \bar{v}_2) \\ -3C(\tau; v_1, v_1, h_{1001}) - 3C(\tau; v_1, \bar{v}_2, h_{2000}) - B(\tau; \bar{v}_2, h_{3000}) \\ -3B(\tau; v_1, h_{2001}) - 3B(\tau; h_{2000}, h_{1001} = 0, \\ h_{3001}(T) - h_{3001}(0) = 0, \end{cases}$$

$$\begin{cases} \dot{h}_{2200} - A(\tau)h_{2200} - D(\tau; v_1, v_1, \bar{v}_1, \bar{v}_1) - 2\Re(C(\tau; v_1, v_1, h_{0200})) \\ \quad -4C(\tau; v_1, \bar{v}_1, h_{1100}) - B(\tau; h_{2000}, h_{0200}) - 2B(\tau; h_{1100}, h_{1100}) \\ -4\Re(B(\tau; v_1, h_{1200})) + 8\Re(a_{2100})h_{1100} + 4\alpha_{2200}\dot{u}_0 + 4\alpha_{1100}\dot{h}_{1100} = 0, \\ h_{2200}(T) - h_{2200}(0) = 0, \\ \int_0^T \langle \varphi^*, h_{2200} \rangle \, d\tau = 0, \end{cases}$$

$$\begin{cases} \dot{h}_{2020} - A(\tau)h_{2020} + 2i\omega_1 h_{2020} + 2i\omega_2 h_{2020} - D(\tau; v_1, v_1, v_2, v_2) \\ \quad -C(\tau; v_1, v_1, h_{0020}) - C(\tau; v_2, v_2, h_{2000}) - 4C(\tau; v_1, v_2, h_{1010}) \\ \quad -B(\tau; h_{2000}, h_{0020}) - 2B(\tau; v_2, h_{2010}) \\ \quad -2B(\tau; h_{1010}, h_{1010}) - 2B(\tau; v_1, h_{1020}) = 0, \\ h_{2020}(T) - h_{2020}(0) = 0, \end{cases}$$

$$\begin{cases} \dot{h}_{2002} - A(\tau)h_{2002} + 2i\omega_1 h_{2002} - 2i\omega_2 h_{2002} - D(\tau; v_1, v_1, \bar{v}_2, \bar{v}_2) \\ \quad -C(\tau; \bar{v}_2, \bar{v}_2, h_{2000}) - 4C(\tau; v_1, \bar{v}_2, h_{1001}) - C(\tau; v_1, v_1, h_{0002}) \\ \quad -2B(\tau; \bar{v}_2, h_{2001}) - B(\tau; h_{2000}, h_{0002}) \\ \quad -2B(\tau; h_{1001}, h_{1001}) - 2B(\tau; v_1, h_{1002}) = 0, \\ h_{2002}(T) - h_{2002}(0) = 0, \end{cases}$$

$$\begin{cases} \dot{h}_{2110} - A(\tau)h_{2110} + i\omega_1 h_{2110} + i\omega_2 h_{2110} - D(\tau; v_1, v_1, \bar{v}_1, v_2) \\ \quad -C(\tau; v_1, v_1, h_{0110}) - 2C(\tau; v_1, \bar{v}_1, h_{1010}) - C(\tau; \bar{v}_1, v_2, h_{2000}) \\ \quad -2C(\tau; v_1, v_2, h_{1100}) - B(\tau; \bar{v}_1, h_{2010}) - 2B(\tau; h_{1010}, h_{1100}) \\ -B(\tau; v_2, h_{2100}) - B(\tau; h_{2000}, h_{0110}) - 2B(\tau; v_1, h_{1110}) + 2a_{2100}h_{1010} \\ \quad +2b_{1110}h_{1010} + 2\alpha_{1100}\dot{h}_{1010} + 2i(\omega_1 + \omega_2)\alpha_{1100}h_{1010} = 0, \\ h_{2110}(T) - h_{2110}(0) = 0, \end{cases}$$

$$\begin{cases} \dot{h}_{2101} - A(\tau)h_{2101} + i\omega_1 h_{2101} - i\omega_2 h_{2101} - D(\tau; v_1, v_1, \bar{v}_1, \bar{v}_2) \\ \quad -C(\tau; v_1, v_1, h_{0101}) - 2C(\tau; v_1, \bar{v}_1, h_{1001}) - C(\tau; \bar{v}_1, \bar{v}_2, h_{2000}) \\ \quad -2C(\tau; v_1, \bar{v}_2, h_{1100}) - 2B(\tau; h_{1001}, h_{1100}) - 2B(\tau; v_1, h_{1101}) \\ \quad -B(\tau; \bar{v}_2, h_{2100}) - B(\tau; \bar{v}_1, h_{2001}) - B(\tau; h_{2000}, h_{0101}) \\ +2a_{2100}h_{1001} + 2b_{1101}h_{1001} + 2\alpha_{1100}\dot{h}_{1001} + 2i(\omega_1 - \omega_2)\alpha_{1100}h_{1001} = 0, \\ h_{2101}(T) - h_{2101}(0) = 0, \end{cases}$$

$$\begin{cases} \dot{h}_{2011} - A(\tau)h_{2011} + 2i\omega_1 h_{2011} - D(\tau; v_1, v_1, v_2, \bar{v}_2) \\ -C(\tau; v_1, v_1, h_{0011}) - 2C(\tau; v_1, v_2, h_{1001}) - C(\tau; v_2, \bar{v}_2, h_{2000}) \\ -2C(\tau; v_1, \bar{v}_2, h_{1010}) - B(\tau; \bar{v}_2, h_{2010}) - B(\tau; v_2, h_{2001}) \\ -B(\tau; h_{2000}, h_{0011}) - 2B(\tau; h_{1001}, h_{1010}) - 2B(\tau; v_1, h_{1011}) \\ +2a_{1011}h_{2000} + \alpha_{0011}\dot{h}_{2000} + 2i\omega_1\alpha_{0011}h_{2000} = 0, \\ h_{2011}(T) - h_{2011}(0) = 0, \end{cases}$$

$$\begin{cases} \dot{h}_{1111} - A(\tau)h_{1111} - D(\tau; v_1, \bar{v}_1, v_2, \bar{v}_2) - C(\tau; v_1, \bar{v}_1, h_{0011}) \\ -2\Re(C(\tau; v_1, v_2, h_{0101})) - 2\Re(C(\tau; v_1, \bar{v}_2, h_{0110})) \\ -C(\tau; v_2, \bar{v}_2, h_{1100}) - 2\Re(B(\tau; v_1, h_{0111})) - B(\tau; h_{0110}, h_{1001}) \\ -B(\tau; h_{0101}, h_{1010}) - B(\tau; h_{0011}, h_{1100}) - 2\Re(B(\tau; v_2, h_{1101})) \\ +2\Re(a_{0111})h_{1100} + \alpha_{0011}\dot{h}_{1100} + 2\Re(b_{1101})h_{0011} \\ +\alpha_{1111}\dot{u}_0 + \alpha_{1100}\dot{h}_{0011} = 0, \\ h_{1111}(T) - h_{1111}(0) = 0, \\ \int_0^T \langle \varphi^*, h_{1111} \rangle \, d\tau = 0. \end{cases}$$

The fifth order normal form coefficients for (4.15) are given by

$$\begin{aligned} a_{3200} = \frac{1}{12}\int_0^T \langle v_1^*, & E(\tau; v_1, v_1, v_1, \bar{v}_1, \bar{v}_1) + D(\tau; v_1, v_1, v_1, h_{0200}) \\ & + 3D(\tau; v_1, \bar{v}_1, \bar{v}_1, h_{2000}) + 6D(\tau; v_1, v_1, \bar{v}_1, h_{1100}) + 6C(\tau; v_1, h_{1100}, h_{1100}) \\ & + 3C(\tau; v_1, v_1, h_{1200}) + C(\tau; \bar{v}_1, \bar{v}_1, h_{3000}) + 6C(\tau; v_1, \bar{v}_1, h_{2100}) \\ & + 6C(\tau; \bar{v}_1, h_{2000}, h_{1100}) + 3C(\tau; v_1, h_{0200}, h_{2000}) + B(\tau; h_{0200}, h_{3000}) \\ & + 2B(\tau; \bar{v}_1, h_{3100}) + 3B(\tau; v_1, h_{2200}) + 6B(\tau; h_{2100}, h_{1100}) \\ & + 3B(\tau; h_{2000}, h_{1200}) - 6\alpha_{1100}\dot{h}_{2100} - 12\alpha_{2200}A(\tau)v_1\rangle \, d\tau - \alpha_{1100}a_{2100}, \end{aligned}$$

$$\begin{aligned} b_{0032} = \frac{1}{12}\int_0^T \langle v_2^*, & E(\tau; v_2, v_2, v_2, \bar{v}_2, \bar{v}_2) + D(\tau; v_2, v_2, v_2, h_{0002}) \\ & + 3D(\tau; v_2, \bar{v}_2, \bar{v}_2, h_{0020}) + 6D(\tau; v_2, v_2, \bar{v}_2, h_{0011}) + 6C(\tau; v_2, h_{0011}, h_{0011}) \\ & + 3C(\tau; v_2, v_2, h_{0012}) + C(\tau; \bar{v}_2, \bar{v}_2, h_{0030}) + 6C(\tau; v_2, \bar{v}_2, h_{0021}) \\ & + 6C(\tau; \bar{v}_2, h_{0020}, h_{0011}) + 3C(\tau; v_2, h_{0002}, h_{0020}) + B(\tau; h_{0002}, h_{0030}) \\ & + 2B(\tau; \bar{v}_2, h_{0031}) + 3B(\tau; v_2, h_{0022}) + 6B(\tau; h_{0021}, h_{0011}) \\ & + 3B(\tau; h_{0020}, h_{0012}) - 6\alpha_{0011}\dot{h}_{0021} - 12\alpha_{0022}A(\tau)v_2\rangle \, d\tau - \alpha_{0011}b_{0021}, \end{aligned}$$

$$
\begin{aligned}
a_{1022} = \frac{1}{4}\int_0^T \langle v_1^*, & E(\tau; v_1, v_2, v_2, \bar{v}_2, \bar{v}_2) + D(\tau; v_1, \bar{v}_2, \bar{v}_2, h_{0020}) \\
& + D(\tau; v_1, v_2, v_2, h_{0002}) + 2D(\tau; v_2, v_2, \bar{v}_2, h_{1001}) + 2D(\tau; v_2, \bar{v}_2, \bar{v}_2, h_{1010}) \\
& + 4D(\tau; v_1, v_2, \bar{v}_2, h_{0011}) + 2C(\tau; v_1, \bar{v}_2, h_{0021}) + C(\tau; v_1, h_{0020}, h_{0002}) \\
& + 2C(\tau; v_1, v_2, h_{0012}) + 2C(\tau; \bar{v}_2, h_{1001}, h_{0020}) + 4C(\tau; v_2, h_{1001}, h_{0011}) \\
& + 2C(\tau; v_2, h_{1010}, h_{0002}) + C(\tau; v_2, v_2, h_{1002}) + 4C(\tau; \bar{v}_2, h_{1010}, h_{0011}) \\
& + 4C(\tau; v_2, \bar{v}_2, h_{1011}) + C(\tau; \bar{v}_2, \bar{v}_2, h_{1020}) + 2C(\tau; v_1, h_{0011}, h_{0011}) \\
& + B(\tau; v_1, h_{0022}) + 2B(\tau; h_{0021}, h_{1001}) + B(\tau; h_{0020}, h_{1002}) \\
& + 2B(\tau; h_{0012}, h_{1010}) + 4B(\tau; h_{0011}, h_{1011}) + 2B(\tau; v_2, h_{1012}) \\
& + B(\tau; h_{0002}, h_{1020}) + 2B(\tau; \bar{v}_2, h_{1021}) - 4\alpha_{0011}\dot{h}_{1011} \\
& - 4\alpha_{0022}A(\tau)v_1\rangle \, d\tau - \alpha_{0011}a_{1011},
\end{aligned}
$$

$$
\begin{aligned}
b_{2210} = \frac{1}{4}\int_0^T \langle v_2^*, & E(\tau; v_1, v_1, \bar{v}_1, \bar{v}_1, v_2) + D(\tau; \bar{v}_1, \bar{v}_1, v_2, h_{2000}) \\
& + D(\tau; v_1, v_1, v_2, h_{0200}) + 2D(\tau; v_1, v_1, \bar{v}_1, h_{0110}) + 2D(\tau; v_1, \bar{v}_1, \bar{v}_1, h_{1010}) \\
& + 4D(\tau; v_1, \bar{v}_1, v_2, h_{1100}) + 2C(\tau; \bar{v}_1, v_2, h_{2100}) + C(\tau; v_2, h_{2000}, h_{0200}) \\
& + 2C(\tau; v_1, v_2, h_{1200}) + 2C(\tau; \bar{v}_1, h_{0110}, h_{2000}) + 4C(\tau; v_1, h_{0110}, h_{1100}) \\
& + 2C(\tau; v_1, h_{1010}, h_{0200}) + C(\tau; v_1, v_1, h_{0210}) + 4C(\tau; \bar{v}_1, h_{1010}, h_{1100}) \\
& + 4C(\tau; v_1, \bar{v}_1, h_{1110}) + C(\tau; \bar{v}_1, \bar{v}_1, h_{2010}) + 2C(\tau; v_2, h_{1100}, h_{1100}) \\
& + B(\tau; v_2, h_{2200}) + 2B(\tau; h_{2100}, h_{0110}) + B(\tau; h_{2000}, h_{0210}) \\
& + 2B(\tau; h_{1200}, h_{1010}) + 4B(\tau; h_{1100}, h_{1110}) + 2B(\tau; v_1, h_{1210}) \\
& + B(\tau; h_{0200}, h_{2010}) + 2B(\tau; \bar{v}_1, h_{2110}) - 4\alpha_{1100}\dot{h}_{1110} \\
& - 4\alpha_{2200}A(\tau)v_2\rangle \, d\tau - \alpha_{1100}b_{1110},
\end{aligned}
$$

$$
\begin{aligned}
a_{2111} = \frac{1}{2}\int_0^T \langle v_1^*, & E(\tau; v_1, v_1, \bar{v}_1, v_2, \bar{v}_2) + D(\tau; v_1, v_1, v_2, h_{0101}) \\
& + D(\tau; v_1, v_1, \bar{v}_1, h_{0011}) + D(\tau; v_1, v_1, \bar{v}_2, h_{0110}) + 2D(\tau; v_1, \bar{v}_1, \bar{v}_2, h_{1010}) \\
& + 2D(\tau; v_1, v_2, \bar{v}_2, h_{1100}) + D(\tau; \bar{v}_1, v_2, \bar{v}_2, h_{2000}) + 2D(\tau; v_1, \bar{v}_1, v_2, h_{1001}) \\
& + 2C(\tau; v_1, h_{1001}, h_{0110}) + C(\tau; v_2, \bar{v}_2, h_{2100}) + 2C(\tau; v_2, h_{1001}, h_{1100}) \\
& + 2C(\tau; v_1, h_{1100}, h_{0011}) + 2C(\tau; v_1, h_{1010}, h_{0101}) + C(\tau; \bar{v}_1, \bar{v}_2, h_{2010}) \\
& + C(\tau; \bar{v}_1, v_2, h_{2001}) + 2C(\tau; v_1, \bar{v}_2, h_{1110}) + 2C(\tau; \bar{v}_2, h_{1010}, h_{1100}) \\
& + 2C(\tau; v_1, v_2, h_{1101}) + C(\tau; v_2, h_{2000}, h_{0101}) + 2C(\tau; \bar{v}_1, h_{1001}, h_{1010}) \\
& + C(\tau; \bar{v}_1, h_{2000}, h_{0011}) + C(\tau; \bar{v}_2, h_{2000}, h_{0110}) + 2C(\tau; v_1, \bar{v}_1, h_{1011}) \\
& + C(\tau; v_1, v_1, h_{0111}) + B(\tau; v_2, h_{2101}) + B(\tau; h_{2100}, h_{0011}) \\
& + 2B(\tau; v_1, h_{1111}) + B(\tau; \bar{v}_1, h_{2011}) + B(\tau; h_{0101}, h_{2010}) \\
& + B(\tau; h_{2001}, h_{0110}) + B(\tau; h_{2000}, h_{0111}) + B(\tau; \bar{v}_2, h_{2110}) \\
& + 2B(\tau; h_{1011}, h_{1100}) + 2B(\tau; h_{1010}, h_{1101}) + 2B(\tau; h_{1001}, h_{1110}) \\
& - 2\alpha_{1111}A(\tau)v_1 - 2\alpha_{1100}\dot{h}_{1011} - \alpha_{0011}\dot{h}_{2100}\rangle\, d\tau - \alpha_{0011}a_{2100} - \alpha_{1100}a_{1011},
\end{aligned}
$$

$$
\begin{aligned}
b_{1121} = \frac{1}{2}\int_0^T \langle v_2^*, & E(\tau; v_1, \bar{v}_1, v_2, v_2, \bar{v}_2) + D(\tau; v_1, v_2, v_2, h_{0101}) \\
& + D(\tau; v_2, v_2, \bar{v}_2, h_{1100}) + D(\tau; \bar{v}_1, v_2, v_2, h_{1001}) + 2D(\tau; \bar{v}_1, v_2, \bar{v}_2, h_{1010}) \\
& + 2D(\tau; v_1, \bar{v}_1, v_2, h_{0011}) + D(\tau; v_1, \bar{v}_1, \bar{v}_2, h_{0020}) + 2D(\tau; v_1, v_2, \bar{v}_2, h_{0110}) \\
& + 2C(\tau; v_2, h_{0110}, h_{1001}) + C(\tau; v_1, \bar{v}_1, h_{0021}) + 2C(\tau; v_1, h_{0110}, h_{0011}) \\
& + 2C(\tau; v_2, h_{0011}, h_{1100}) + 2C(\tau; v_2, h_{1010}, h_{0101}) + C(\tau; \bar{v}_1, \bar{v}_2, h_{1020}) \\
& + C(\tau; v_1, \bar{v}_2, h_{0120}) + 2C(\tau; \bar{v}_1, v_2, h_{1011}) + 2C(\tau; \bar{v}_1, h_{1010}, h_{0011}) \\
& + 2C(\tau; v_1, v_2, h_{0111}) + C(\tau; v_1, h_{0020}, h_{0101}) + 2C(\tau; \bar{v}_2, h_{0110}, h_{1010}) \\
& + C(\tau; \bar{v}_2, h_{0020}, h_{1100}) + C(\tau; \bar{v}_1, h_{0020}, h_{1001}) + 2C(\tau; v_2, \bar{v}_2, h_{1110}) \\
& + C(\tau; v_2, v_2, h_{1101}) + B(\tau; v_1, h_{0121}) + B(\tau; h_{0021}, h_{1100}) \\
& + 2B(\tau; v_2, h_{1111}) + B(\tau; \bar{v}_2, h_{1120}) + B(\tau; h_{0101}, h_{1020}) \\
& + B(\tau; h_{0120}, h_{1001}) + B(\tau; h_{0020}, h_{1101}) + B(\tau; \bar{v}_1, h_{1021}) \\
& + 2B(\tau; h_{1110}, h_{0011}) + 2B(\tau; h_{1010}, h_{0111}) + 2B(\tau; h_{0110}, h_{1011}) \\
& - 2\alpha_{1111}A(\tau)v_2 - 2\alpha_{0011}\dot{h}_{1110} - \alpha_{1100}\dot{h}_{0021}\rangle\, d\tau - \alpha_{1100}b_{0021} - \alpha_{0011}b_{1110}.
\end{aligned}
$$

6

Numerical Periodic Normalization for Codimension 2 Bifurcations of Limit Cycles – Implementation and Examples

In this chapter we concentrate on the implementation details for the critical coefficients and demonstrate the correctness of the normal form analysis by numerous examples.

6.1 Introduction

Consider a smooth system of ODEs

$$\dot{x} = f(x, \alpha), \quad x \in \mathbb{R}^n, \ \alpha \in \mathbb{R}^p, \tag{6.1}$$

smoothly depending on a parameter α. Typically, the dynamics of such systems show qualitative transitions upon variation of the parameter. At these bifurcation

points, the normal form coefficients allow one to distinguish between the complicated bifurcation scenarios that can happen near the codim 2 bifurcations of limit cycles, where 3-tori and 4-tori can be present. The formulas for these critical coefficients were theoretically derived in the previous chapter. In this chapter, we check the validity of the obtained expressions for the normal form coefficients by means of several examples.

Numerical continuation software, such as MatCont, may be used to track bifurcations from a stable equilibrium to a periodic oscillation by a Hopf bifurcation. Once a limit cycle is obtained, first codim 1 bifurcations of limit cycles and then codim 2 bifurcations can be detected. The neighbourhood of the codim 2 point is then scanned to determine the position of local bifurcations with respect to the bifurcation point and to each other. Global bifurcations, however, are more difficult to detect. Some global bifurcations as the appearance of (un)stable invariant tori with multi-frequency oscillations can be found from a Hopf-Hopf or a Neimark-Sacker bifurcation. Bifurcations of these invariant tori $\mathbb{T}^{m\geq 2}$ into other tori or chaos, however, are out of reach of the standard numerical analysis.

One possibility to study bifurcations of tori – if they are stable – is to compute **Lyapunov exponents**. The dimension of the torus for a given parameter value then equals the number of exponents equal to zero. Varying one parameter one can observe that exponents become zero and this indicates a bifurcation. Lyapunov exponents will be used to check whether the obtained values of the critical coefficients are acceptable in the three most complex codim 2 bifurcations of limit cycles where the dimension of the center manifold equals 4 or 5, i.e. LPNS, PDNS and NSNS.

In Chapter 4 we have computed the normal forms for all codim 2 bifurcations of limit cycles and in Chapter 5 its coefficients by a method based on periodic normalization. The computation of the normal form coefficients was reduced to solving certain linear boundary value problems, where only the partial derivatives of the RHS of (6.1) are used. In our implementation in MatCont, we discretize these BVPs by orthogonal collocation with piecewise-polynomial functions. Note that all appearing integrals can also be easily computed using this discretization. MatCont automatically invokes the algorithm of the calculation of the critical coefficients whenever the corresponding bifurcation is detected. Hence, any user is able to use it and to take advantage of the automated normal form analysis. In this chapter we document precisely on the implementation details and we numerically confirm the results of the normal form analysis by means of several examples.

Similar to the formulation of the BVP for periodic solutions on the unit interval

instead of $[0,T]$, we redefine the critical coefficients and the BVPs for the functions in the expansion of the center manifold, derived in Chapter 5, to the interval $[0,1]$. In Section 6.2 we give the explicit formulas for all needed functions and coefficients on $[0,1]$ and discuss their implementation in MatCont. In Section 6.3 we analyse seven models that exhibit all 11 codim 2 bifurcations of limit cycles. We consider two models from population biology, the Steinmetz-Larter model, the Lorenz-84 and the extended Lorenz-84 model, a laser model and one for mechanical vibrations. In these models, we discuss in detail what type of codim 2 bifurcation is detected and check the correspondence with the value/sign of the normal form coefficients. In the LPNS, PDNS and NSNS cases we corroborate the predictions using Lyapunov exponents to verify the existence of stable invariant tori of various dimensions and chaos. In fact, we argue that the classification from the critical normal forms guides the correct interpretation of the Lyapunov exponents. Finally, in Section 6.A some results on differential-difference operators used in Section 6.2, are formulated.

6.2 Implementation issues

Numerical implementation of the formulas derived in Chapter 5 requires the evaluation of integrals of scalar functions over $[0,T]$ and the solution of nonsingular linear BVPs with integral constraints. In MatCont, periodic solutions to (6.1) are computed with the method of orthogonal collocation with piecewise polynomials applied to properly formulated BVPs, as discussed in Section 2.8.2. In this section we first fix notation concerning the discretization of the BVPs and the integral expressions for the normal form coefficients. We then discuss the implementation details for all needed critical coefficients and functions for each codim 2 bifurcation of limit cycles.

6.2.1 Discretization notation

The standard BVP for the periodic solutions is formulated on the unit interval $[0,1]$ so that the period T becomes a parameter, and it involves an integral phase condition. The system that we typically use is (2.5). In the orthogonal collocation

method [6], problem (2.5) is replaced by the following discretization:

$$\begin{cases} \sum_{j=0}^{m} x_{i,j}\dot{\ell}_{i,j}(\zeta_{i,k}) - Tf\left(\sum_{j=0}^{m} x_{i,j}\ell_{i,j}(\zeta_{i,k}), \alpha\right) = 0, \\ x_{0,0} - x_{N-1,m} = 0, \\ \sum_{i=0}^{N-1}\sum_{j=0}^{m-1} \sigma_{i,j}\langle x_{i,j}, \dot{\xi}_{i,j}\rangle + \sigma_{N,0}\langle x_{N,0}, \dot{\xi}_{N,0}\rangle = 0. \end{cases} \tag{6.2}$$

The points $x_{i,j}\,(i = 0,\ldots,N-1, j = 0,\ldots m)$ form the approximation of the exact solution x in the equidistant mesh points $\tau_{i,j}$. The $\ell_{i,j}$'s are the Lagrange basis polynomials, while the points $\zeta_{i,j}$ are the Gauss points. Function ξ is a previously calculated periodic solution, with function values in $[0,1]$. The integration weight $\sigma_{i,j}$ of $\tau_{i,j}$ is given by $w_{j+1}h_i$ for $0 \le i \le N-1$ and $0 < j < m$. Recall that $h_i = \tau_{i+1} - \tau_i$. For $i = 0,\ldots,N-2$, the integration weight of $\tau_{i,m}$ ($\tau_{i,m} = \tau_{i+1,0}$) is given by $\sigma_{i,m} = w_{m+1}h_i + w_1 h_{i+1}$, and the integration weights of τ_0 and τ_N are given by $w_1 h_0$ and $w_{m+1}h_{N-1}$, respectively. In the above expressions, w_{j+1} is the Lagrange quadrature coefficient.

It is convenient to discretize all needed functions by using the same mesh as in (6.2). Consider a vector function $\eta \in \mathcal{C}^1([0,1],\mathbb{R}^n)$. In Section 2.8.2 we introduced η_M as the vector of the function values at the mesh points and η_C as the vector of the function values at the collocation points. We now also consider $\eta_W = \begin{bmatrix} \eta_{W_1} \\ \eta_{W_2} \end{bmatrix} \in \mathbb{R}^{Nmn} \times \mathbb{R}^n$, where η_{W_1} is the vector of the function values at the collocation points multiplied by the Gauss-Legendre weights and the lengths of the corresponding mesh intervals, and $\eta_{W_2} = \eta(0)$.

Formally, we also introduce the structured sparse matrix $L_{C\times M}$ that converts a vector η_M into a vector η_C, i.e. $\eta_C = L_{C\times M}\eta_M$. This matrix is never formed explicitly; its entries are the $\ell_{i,j}(\zeta_{i,k})$-coefficients in (6.2). We also need a matrix $A_{C\times M}$ such that $A_{C\times M}\eta_M = (A(t)\eta(t))_C$. Again this matrix need not be formed explicitly. On the other hand, we need the matrix $(D - TA(t))_{C\times M}$ explicitly; it is defined by $(D - TA(t))_{C\times M}\eta_M = (\dot{\eta}(t) - TA(t)\eta(t))_C$. Finally, let the tensors $B_{C\times M\times M}$ and $C_{C\times M\times M\times M}$ be defined by $B_{C\times M\times M}\eta_{1M}\eta_{2M} = (B(t;\eta_1(t), \eta_2(t)))_C$ and

$$C_{C\times M\times M\times M}\eta_{1M}\eta_{2M}\eta_{3M} = (C(t;\eta_1(t),\eta_2(t),\eta_3(t)))_C$$

for all $\eta_i \in \mathcal{C}^1([0,1],\mathbb{R}^n)$. An analogous notation is used for the fourth and fifth order derivatives. Note that these tensors are not formed explicitly.

Let $f(t)$ and $g(t) \in \mathcal{C}^0([0,1],\mathbb{R})$ be two scalar functions. Then the integral $\int_0^1 f(t)dt$ is represented by $\sum_{i=0}^{N-1}\sum_{j=1}^{m}\omega_j(f_C)_{i,j}h_i = \sum_{i=0}^{N-1}\sum_{j=1}^{m}(f_{W_1})_{i,j}$, where $(f_C)_{i,j} = f(\zeta_{i,j})$ and ω_j is the Gauss-Legendre quadrature coefficient. The integral $\int_0^1 f(t)g(t)dt$ is approximated with Gauss-Legendre by $f_{W_1}^{\mathrm{T}} g_C = f_{W_1}^{\mathrm{T}} L_{C\times M} g_M$. For vector functions $f(t), g(t) \in \mathcal{C}^0([0,1],\mathbb{R}^n)$, the integral $\int_0^1 \langle f(t), g(t)\rangle dt$ is formally approximated by the same expression: $f_{W_1}^{\mathrm{T}} g_C = f_{W_1}^{\mathrm{T}} L_{C\times M} g_M$. Concerning the accuracy of the quadrature formulas, we first note that accuracy is not an important issue for the phase integral in (2.5), as this equation only selects a specific solution from the continuum of solutions obtained by phase shifts. Similarly, the discretization of the normalization integrals does not affect the inherent accuracy, including superconvergence at the coarse mesh points τ_i of the solution of the discretized BVP. Discretization of integrals follows the standard Gauss quadrature error, which has order of accuracy $2m$. Otherwise, still assuming sufficient piecewise smoothness, the order of accuracy of the numerical integrals is $m+1$ if m is odd, and $m+2$ if m is even. In particular, for the often used choice $m = 4$, the integrals would then have order of accuracy 6.

Since in the rest of this section we will often deal with equations of the form $Mx = r$, with M a singular matrix, we first discuss a **bordering technique** that allows us to determine the solution to this problem. Let q be a right null-vector of M, i.e. $Mq = 0$, and p be a left null-vector of M, i.e. $p^{\mathrm{H}}M = 0$. Then, the matrix

$$\begin{pmatrix} M & p \\ q^{\mathrm{H}} & 0 \end{pmatrix}$$

is nonsingular. Therefore, x can be obtained by solving the system

$$\begin{pmatrix} M & p \\ q^{\mathrm{H}} & 0 \end{pmatrix}\begin{pmatrix} x \\ s \end{pmatrix} = \begin{pmatrix} r \\ 0 \end{pmatrix}. \tag{6.3}$$

Indeed, (6.3) corresponds with the equations $Mx + sp = r$ and $\langle q, x\rangle = 0$. Now, from the Fredholm solvability condition follows that $\langle p, r\rangle = 0$. Therefore,

$$\begin{aligned} 0 &= \langle p, r\rangle \\ &= \langle p, Mx + sp\rangle \\ &= \langle M^{\mathrm{H}}p, x\rangle + s\langle p, p\rangle \\ &= s\langle p, p\rangle, \end{aligned}$$

and thus $s = 0$, so that $Mx = r$. Equation $\langle q, x\rangle = 0$ just selects one from the many solutions.

In Chapter 5 we derived the coefficients of the critical normal forms and the functions needed for their computation using the coordinate $\tau \in [0, T]$. Regarding the implementation, in all cases we will rescale to the interval $[0, 1]$. Therefore, define $u_1(t) = u_0(Tt) = u_0(\tau)$ for $t \in [0, 1]$, where u_0 corresponds with the original limit cycle (as defined in Section 4.2). In this chapter, the dot then denotes the derivative with respect to $t \in [0, 1]$. In what follows, the rescaled vector functions will have an extra lower index 1.

6.2.2 Bifurcations with a 2D center manifold

Cusp Point of Cycles bifurcation

The rescalings of the linear BVP's (5.8), (5.13) and (6.4) defining the generalized eigenfunction, the adjoint and generalized adjoint eigenfunction respectively, are given by

$$\begin{cases} \dot{v}_1(t) - TA(t)v_1(t) - TF(u_1(t)) = 0, \ t \in [0,1], \\ v_1(1) - v_1(0) = 0, \\ \int_0^1 \langle v_1(t), F(u_1(t))\rangle dt = 0, \end{cases} \tag{6.4}$$

with $v(\tau) = v_1(\tau/T)$,

$$\begin{cases} \dot{\varphi}_1^*(t) + TA^{\mathrm{T}}(t)\varphi_1^*(t) = 0, \ t \in [0,1], \\ \varphi_1^*(1) - \varphi_1^*(0) = 0, \\ \int_0^1 \langle \varphi_1^*(t), v_1(t)\rangle dt - 1 = 0, \end{cases} \tag{6.5}$$

where $\varphi^*(\tau) = \varphi_1^*(\tau/T)/T$ and

$$\begin{cases} \dot{v}_1^*(t) + TA^{\mathrm{T}}(t)v_1^*(t) + T\varphi_1^*(t) = 0, \ t \in [0,1], \\ v_1^*(1) - v_1^*(0) = 0, \\ \int_0^1 \langle v_1^*(t), v_1(t)\rangle dt = 0, \end{cases} \tag{6.6}$$

with $v^*(\tau) = v_1^*(\tau/T)/T$. Function $h_{2,1}$ is the rescaled version of h_2, defined by (5.16), and can be found as the unique solution of

$$\begin{cases} \dot{h}_{2,1}(t) - TA(t)h_{2,1}(t) - TB(t; v_1(t), v_1(t)) \\ \qquad -2TA(t)v_1(t) - 2TF(u_1(t)) = 0, \ t \in [0,1], \\ \qquad h_{2,1}(1) - h_{2,1}(0) = 0, \\ \qquad \int_0^1 \langle v_1^*(t), h_{2,1}(t) \rangle \, dt = 0, \end{cases} \tag{6.7}$$

where $h_2(\tau) = h_{2,1}(\tau/T)$. Normal form coefficient c is then given by the following expression

$$\begin{aligned} c = \frac{1}{6} \int_0^1 \langle \varphi_1^*(t), 3A(t)h_{2,1}(t) + 3B(t; v_1(t), v_1(t)) + 6A(t)v_1(t) \\ + 3B(t; h_{2,1}(t), v_1(t)) + C(t; v_1(t), v_1(t), v_1(t)) \rangle \, dt. \end{aligned} \tag{6.8}$$

We now concentrate on how the functions and coefficients can efficiently be implemented in Matlab. The approximation v_{1M} to v_1 can be computed by solving the discretization of (6.4), i.e.

$$\begin{bmatrix} (D - TA(t))_{C\times M} & p \\ \delta_0 - \delta_1 & 0 \\ g_{W_1}^{\mathrm{T}} L_{C\times M} & 0 \end{bmatrix} \begin{bmatrix} v_{1M} \\ a_1 \end{bmatrix} = \begin{bmatrix} Tf_C \\ 0_{n\times 1} \\ 0 \end{bmatrix}, \tag{6.9}$$

where a_1 equals zero since the $M \times M$ upper left part of the big matrix is singular, $g(t) = F(u_1(t))$, and p is obtained by solving the following system

$$\begin{bmatrix} p^{\mathrm{T}} & a_2 \end{bmatrix} \begin{bmatrix} (D - TA(t))_{C\times M} & r_1 \\ \delta_0 - \delta_1 & \\ r_2^{\mathrm{T}} & 0 \end{bmatrix} = \begin{bmatrix} 0_{1\times M} & 1 \end{bmatrix}, \tag{6.10}$$

where r_1 and r_2 are any $M \times 1$ vectors that make the $(M+1) \times (M+1)$-matrix in (6.10) nonsingular. Here, $a_2 = 0$ such that p is then the left null-vector of $\begin{bmatrix} (D - TA(t))_{C\times M} \\ \delta_0 - \delta_1 \end{bmatrix}$; in (6.9) the normalized p is used. This technique guarantees that we always deal with nonsingular systems. Note that $\delta_0 v_{1M}$ corresponds with the first n components of v_{1M} and $\delta_1 v_{1M}$ with the last n components of v_{1M}.

Concerning the adjoint eigenfuntion, we will compute φ_{1W}^* instead of φ_{1M}^* since φ_{1W}^* can be calculated by a system very similar to (6.9). Formally, the computation

of φ^*_{1W} is based on Proposition 6.1 on page 255 from the appendix, i.e. since $\varphi \in \mathrm{Ker}(\phi_2)$, with ϕ_2 defined in Proposition 6.1, $\begin{pmatrix} \varphi_1^* \\ \varphi_1^*(0) \end{pmatrix}$ is orthogonal to the range of $\begin{bmatrix} D - TA(t) \\ \delta_0 - \delta_1 \end{bmatrix}$. By discretization we obtain

$$(\varphi_1^*)_W^{\mathrm{T}} \begin{bmatrix} (D - TA(t))_{C\times M} \\ \delta_0 - \delta_1 \end{bmatrix} = 0.$$

Therefore, φ^*_{1W} can be obtained by solving

$$\begin{bmatrix} (\varphi_1^*)_W^{\mathrm{T}} & a \end{bmatrix} \begin{bmatrix} (D - TA(t))_{C\times M} & p \\ \delta_0 - \delta_1 & \\ q^{\mathrm{T}} & 0 \end{bmatrix} = \begin{bmatrix} 0_{1\times M} & 1 \end{bmatrix}, \tag{6.11}$$

where a equals zero and q is the normalized right null-vector of $\begin{bmatrix} (D - TA(t))_{C\times M} \\ \delta_0 - \delta_1 \end{bmatrix}$. Such a null-vector is obtained by solving the following system

$$\begin{bmatrix} (D - TA(t))_{C\times M} & r_1 \\ \delta_0 - \delta_1 & \\ r_2^{\mathrm{T}} & 0 \end{bmatrix} \begin{bmatrix} q \\ a_1 \end{bmatrix} = \begin{bmatrix} 0_{M\times 1} \\ 1 \end{bmatrix}, \tag{6.12}$$

with r_1 and r_2 random vectors. We then approximate $I = \int_0^1 \langle \varphi_1^*(t), v_1(t)\rangle dt$ by $I_1 = (\varphi_1^*)_{W_1}^{\mathrm{T}} L_{C\times M} v_{1M}$. The obtained φ^*_{1W} from (6.11) is then rescaled to ensure that $I_1 = 1$.

It is more efficient to compute v^*_{1W} instead of v^*_{1M}, since v_1^* will only be used to compute integrals of the form $\int_0^1 \langle v_1^*(t), \zeta(t)\rangle dt$. From Proposition 6.5 on page 258 we can conclude that

$$\left\langle \begin{bmatrix} v_1^* \\ v_1^*(0) \end{bmatrix}, \begin{bmatrix} \dot{h} - TA(t)h \\ h(0) - h(1) \end{bmatrix} \right\rangle = -\left\langle \begin{bmatrix} -T\varphi_1^* \\ 0 \end{bmatrix}, \begin{bmatrix} h \\ 0 \end{bmatrix} \right\rangle,$$

for all appropriate functions h, such that v_1^* can be obtained by solving

$$\begin{bmatrix} (v_1^*)_W^{\mathrm{T}} & a \end{bmatrix} \begin{bmatrix} (D - TA(t))_{C\times M} & v_{1C} \\ \delta_0 - \delta_1 & 0_{n\times 1} \\ q^{\mathrm{T}} & 0 \end{bmatrix} = \begin{bmatrix} T(\varphi_1^*)_{W_1}^{\mathrm{T}} L_{C\times M} & 0 \end{bmatrix},$$

where a equals zero and q is the normalized solution of (6.12).

Next, $h_{2,1M}$ is found by solving the discretization of (6.7), namely

$$\begin{bmatrix} (D - TA(t))_{C\times M} & p \\ \delta_0 - \delta_1 & 0 \\ (v_1^*)_{W_1}^{\mathrm{T}} L_{C\times M} & 0 \end{bmatrix} \begin{bmatrix} h_{2,1M} \\ a \end{bmatrix} = \begin{bmatrix} \mathrm{R} \\ 0_{n\times 1} \\ 0 \end{bmatrix},$$

with $\mathrm{R} = TB_{C\times M\times M} v_{1M} v_{1M} + 2TA_{C\times M} v_{1M} + 2Tg_C$, $a = 0$ and p is obtained by normalizing the solution of (6.10).

Finally, the normal form coefficient of interest (6.8) is approximated by

$$\begin{aligned} c = \frac{1}{6}(\varphi_1^*)_{W_1}^{\mathrm{T}} \, (&3A_{C\times M} h_{2,1M} + 3B_{C\times M\times M} v_{1M} v_{1M} + 6A_{C\times M} v_{1M} \\ &+3B_{C\times M\times M} h_{2,1M} v_{1M} + C_{C\times M\times M\times M} v_{1M} v_{1M} v_{1M}) \, . \end{aligned}$$

Remark that since we have a CPC bifurcation, the quadratic coefficient appearing in the ξ-equation of the normal form has to be equal to zero. We have provided in MatCont an extra check whether this coefficient (see [68]), determined by

$$b = \frac{1}{2}(\varphi_1^*)_{W_1}^{\mathrm{T}} (B_{C\times M\times M} v_{1M} v_{1M} + 2A_{C\times M} v_{1M}),$$

is indeed small enough.

Generalized Period-Doubling bifurcation

The rescaled linear BVPs for the eigenfunction v associated to multiplier -1, defined by (5.19), and the adjoint eigenfunctions φ^* and v^*, respectively defined by (5.20) and (5.21), are given by

$$\begin{cases} \dot{v}_1(t) - TA(t) v_1(t) = 0, \ t \in [0,1], \\ v_1(1) + v_1(0) = 0, \\ \int_0^1 \langle v_1(t), v_1(t) \rangle dt - 1 = 0, \end{cases} \tag{6.13}$$

where $v(\tau) = v_1(\tau/T)/\sqrt{T}$,

$$\begin{cases} \dot{\varphi}_1^*(t) + TA^{\mathrm{T}}(t) \varphi_1^*(t) = 0, \ t \in [0,1], \\ \varphi_1^*(1) - \varphi_1^*(0) = 0, \\ \int_0^1 \langle \varphi_1^*(t), F(u_1(t)) \rangle \, dt - 1 = 0, \end{cases} \tag{6.14}$$

with $\varphi^*(\tau) = \varphi_1^*(\tau/T)/T$ and

$$\begin{cases} \dot{v}_1^*(t) + TA^{\mathrm{T}}(t)v_1^*(t) = 0, \ t \in [0,1], \\ v_1^*(1) + v_1^*(0) = 0, \\ \int_0^1 \langle v_1^*(t), v_1(t)\rangle dt - 1 = 0, \end{cases} \tag{6.15}$$

with $v^*(\tau) = v_1^*(\tau/T)/\sqrt{T}$.

Let $h_{2,1}$ be the unique solution of the BVP

$$\begin{cases} \dot{h}_{2,1}(t) - TA(t)h_{2,1}(t) - TB(t; v_1(t), v_1(t)) + 2\alpha_{1,1}TF(u_1(t)) = 0, \ t \in [0,1], \\ h_{2,1}(1) - h_{2,1}(0) = 0, \\ \int_0^1 \langle \varphi_1^*(t), h_{2,1}(t)\rangle \, dt = 0, \end{cases}$$

with $h_2(\tau) = h_{2,1}(\tau/T)/T$, and $h_{3,1}$ the unique solution of

$$\begin{cases} \dot{h}_{3,1}(t) - TA(t)h_{3,1}(t) - TC(t; v_1(t), v_1(t), v_1(t)) \\ \quad -3TB(t; v_1(t), h_{2,1}(t)) + 6\alpha_{1,1}TA(t)v_1(t) = 0, \ t \in [0,1], \\ h_{3,1}(1) + h_{3,1}(0) = 0, \\ \int_0^1 \langle v_1^*(t), h_{3,1}(t)\rangle \, dt = 0, \end{cases}$$

with $h_3(\tau) = h_{3,1}(\tau/T)/(\sqrt{T}T)$, where

$$\alpha_{1,1} = \frac{1}{2}\int_0^1 \langle \varphi_1^*(t), B(t; v_1(t), v_1(t))\rangle \, dt,$$

and $\alpha_{1,1} = T\alpha_1$.

The rescaled version of function h_4, defined by (5.28), is the unique solution of the following BVP

$$\begin{cases} \dot{h}_{4,1}(t) - TA(t)h_{4,1}(t) - TD(t; v_1(t), v_1(t), v_1(t), v_1(t)) \\ \quad -6TC(t; v_1(t), v_1(t), h_{2,1}(t)) - 3TB(t; h_{2,1}(t), h_{2,1}(t)) \\ \quad -4TB(t; v_1(t), h_{3,1}(t)) + 12\alpha_{1,1}T(A(t)h_{2,1}(t) \\ +B(t; v_1(t), v_1(t)) - 2\alpha_{1,1}F(u_1(t))) + 24\alpha_{2,1}TF(u_1(t)) = 0, \ t \in [0,1], \\ h_{4,1}(1) - h_{4,1}(0) = 0, \\ \int_0^1 \langle \varphi_1^*(t), h_{4,1}(t)\rangle \, dt = 0, \end{cases}$$

with $h_4(\tau) = h_{4,1}(\tau/T)/T^2$, and where

$$\begin{aligned}\alpha_{2,1} = \frac{1}{24}\int_0^1 \langle \varphi_1^*(t), D(t; v_1(t), v_1(t), v_1(t), v_1(t)) + 6C(t; v_1(t), v_1(t), h_{2,1}(t)) \\ + 3B(t; h_{2,1}(t), h_{2,1}(t)) + 4B(t; v_1(t), h_{3,1}(t)) - 12\alpha_{1,1}(A(t)h_{2,1}(t) \\ + B(t; v_1(t), v_1(t)))\rangle\, dt \;+\; \alpha_{1,1}^2,\end{aligned}$$

with $\alpha_{2,1} = T^2\alpha_2$.

Finally, we can write down the critical coefficient

$$\begin{aligned}e = \frac{1}{120\,T^2}\int_0^1 \langle v_1^*(t), E(t; v_1(t), v_1(t), v_1(t), v_1(t), v_1(t)) \\ + 10D(t; v_1(t), v_1(t), v_1(t), h_{2,1}(t)) + 15C(t; v_1(t), h_{2,1}(t), h_{2,1}(t)) \\ + 10C(t; v_1(t), v_1(t), h_{3,1}(t)) + 10B(t; h_{2,1}(t), h_{3,1}(t)) \\ + 5B(t; v_1(t), h_{4,1}(t)) - 120\alpha_{2,1}A(t)v_1(t) - 20\alpha_{1,1}A(t)h_{3,1}(t)\rangle\, dt.\end{aligned}$$

We now concentrate on the implementation details in MatCont. We compute the approximation v_{1M} to v_1 given by (6.13) by solving

$$\begin{bmatrix} (D - TA(t))_{C\times M} & p_1 \\ \delta_0 + \delta_1 & \\ q_1^{\mathrm{T}} & 0 \end{bmatrix} \begin{bmatrix} v_{1M} \\ a_1 \end{bmatrix} = \begin{bmatrix} 0_{M\times 1} \\ 1 \end{bmatrix}, \tag{6.16}$$

with p_1 and q_1 the normalized solutions of

$$\begin{bmatrix} (D - TA(t))_{C\times M} & r_1 \\ \delta_0 + \delta_1 & \\ r_2^{\mathrm{T}} & 0 \end{bmatrix} \begin{bmatrix} q_1 \\ a_2 \end{bmatrix} = \begin{bmatrix} 0_{M\times 1} \\ 1 \end{bmatrix}$$

and

$$\begin{bmatrix} p_1^{\mathrm{T}} & a_3 \end{bmatrix} \begin{bmatrix} (D - TA(t))_{C\times M} & r_1 \\ \delta_0 + \delta_1 & \\ r_2^{\mathrm{T}} & 0 \end{bmatrix} = \begin{bmatrix} 0_{1\times M} & 1 \end{bmatrix},$$

where r_1 and r_2 are random vectors. Every a_i equals zero. v_{1M} is then uniquely determined by the normalization $\sum_{i=0}^{N-1}\sum_{j=0}^{m}\sigma_j\langle (v_{1M})_{i,j}, (v_{1M})_{i,j}\rangle = 1$, where σ_j is the Lagrange quadrature coefficient.

As in the CPC case, φ^*_{1W} is computed instead of φ^*_{1M}, which can be done by making use of (6.11). We approximate $I = \int_0^1 \langle \varphi^*_1(t), F(u_1(t))\rangle dt$ by $I_1 = (\varphi^*_1)^{\mathrm{T}}_{W_1} g_C$ and normalize φ^*_{1W} to ensure that $I_1 = 1$.

This then makes it possible to compute $\alpha_{1,1}$ as

$$\alpha_{1,1} = \frac{1}{2}(\varphi^*_1)^{\mathrm{T}}_{W_1} B_{C\times M\times M} v_{1M} v_{1M}. \tag{6.17}$$

The discretization of (6.15) can be computed with the matrix from (6.16), see Proposition 6.2 on page 256 in Section 6.A,

$$\begin{bmatrix} (v^*_1)^{\mathrm{T}}_W & a \end{bmatrix} \begin{bmatrix} (D - TA(t))_{C\times M} & p_1 \\ \delta_0 + \delta_1 & \\ q_1^{\mathrm{T}} & 0 \end{bmatrix} = \begin{bmatrix} 0_{1\times M} & 1 \end{bmatrix},$$

where $a = 0$. We approximate $I = \int_0^1 \langle v^*_1(t), v_1(t)\rangle dt$ by $I_1 = (v^*_1)^{\mathrm{T}}_{W_1} L_{C\times M} v_{1M}$. v^*_{1W} is rescaled to ensure that $I_1 = 1$.

Now, $h_{2,1}, h_{3,1}$ and $h_{4,1}$ are found by solving the following systems

$$\begin{bmatrix} (D - TA(t))_{C\times M} & p \\ \delta_0 - \delta_1 & \\ (\varphi^*_1)^{\mathrm{T}}_{W_1} L_{C\times M} & 0 \end{bmatrix} \begin{bmatrix} h_{2,1M} \\ a_1 \end{bmatrix} = \begin{bmatrix} TB_{C\times M\times M} v_{1M} v_{1M} - 2\alpha_{1,1} T g_C \\ 0_{n\times 1} \\ 0 \end{bmatrix},$$

$$\begin{bmatrix} (D - TA(t))_{C\times M} & p_1 \\ \delta_0 + \delta_1 & \\ (v^*_1)^{\mathrm{T}}_{W_1} L_{C\times M} & 0 \end{bmatrix} \begin{bmatrix} h_{3,1M} \\ a_2 \end{bmatrix} = \begin{bmatrix} \mathsf{R} \\ 0_{n\times 1} \\ 0 \end{bmatrix},$$

with

$$\mathsf{R} = TC_{C\times M\times M\times M} v_{1M} v_{1M} v_{1M} + 3TB_{C\times M\times M} v_{1M} h_{2,1M} - 6\alpha_{1,1} TA_{C\times M} v_{1M},$$

and

$$\begin{bmatrix} (D - TA(t))_{C\times M} & p \\ \delta_0 - \delta_1 & \\ (\varphi^*_1)^{\mathrm{T}}_{W_1} L_{C\times M} & 0 \end{bmatrix} \begin{bmatrix} h_{4,1M} \\ a_3 \end{bmatrix} = \begin{bmatrix} \mathsf{R} \\ 0_{n\times 1} \\ 0 \end{bmatrix},$$

where

$$\begin{aligned} \mathsf{R} = {} & TD_{C\times M\times M\times M\times M} v_{1M} v_{1M} v_{1M} v_{1M} + 6TC_{C\times M\times M\times M} v_{1M} v_{1M} h_{2,1M} \\ & + 3TB_{C\times M\times M} h_{2,1M} h_{2,1M} + 4TB_{C\times M\times M} v_{1M} h_{3,1M} \\ & - 12\alpha_{1,1} T(A_{C\times M} h_{2,1M} + B_{C\times M\times M} v_{1M} v_{1M} - 2\alpha_{1,1} g_C) - 24\alpha_{2,1} T g_C \end{aligned}$$

and

$$\alpha_{2,1} = \frac{1}{24}(\varphi_1^*)^{\mathrm{T}}_{W_1}(D_{C\times M\times M\times M\times M}v_{1M}v_{1M}v_{1M}v_{1M} + 6C_{C\times M\times M\times M}v_{1M}v_{1M}h_{2,1M} + 3B_{C\times M\times M}h_{2,1M}h_{2,1M} + 4B_{C\times M\times M}v_{1M}h_{3,1M} - 12\alpha_{1,1}(A_{C\times M}h_{2,1M} + B_{C\times M\times M}v_{1M}v_{1M})) + \alpha_{1,1}^2. \tag{6.18}$$

Here, q is the normalized right null-vector and p the normalized left null-vector of the $M \times M$-matrix corresponding with the T-periodic boundary condition (as in the CPC case). In what follows, p, q, p_1 and q_1 will denote the previously defined null-vectors. Note that every a_i equals zero.

Now, we have all ingredients for the computation of the normal form coefficient

$$e = \frac{1}{120T^2}(v_1^*)^{\mathrm{T}}_{W_1}(E_{C\times M\times M\times M\times M\times M}v_{1M}v_{1M}v_{1M}v_{1M}v_{1M} + 10D_{C\times M\times M\times M\times M}v_{1M}v_{1M}v_{1M}h_{2,1M} + 15C_{C\times M\times M\times M}v_{1M}h_{2,1M}h_{2,1M} + 10C_{C\times M\times M\times M}v_{1M}v_{1M}h_{3,1M} + 10B_{C\times M\times M}h_{2,1M}h_{3,1M} + 5B_{C\times M\times M}v_{1M}h_{4,1M} - 120\alpha_{2,1}A_{C\times M}v_{1M} - 20\alpha_{1,1}A_{C\times M}h_{3,1M}). \tag{6.19}$$

Remark that since we are in a GPD point, the cubic coefficient of the ξ-equation in the corresponding normal form has to vanish. MatCont makes an extra check to verify whether this coefficient, computed as (see [68])

$$c = \frac{1}{3T}(v_1^*)^{\mathrm{T}}_{W_1}(C_{C\times M\times M}v_{1M}v_{1M}v_{1M} + 3B_{C\times M\times M}v_{1M}h_{2,1M} - 6\alpha_{1,1}A_{C\times M}v_{1M}),$$

is indeed small enough.

6.2.3 Bifurcations with a 3D center manifold

Chenciner bifurcation

When rescaling, the linear BVP (5.31) defining the eigenfunction associated to the complex multiplier and the BVPs (5.32) and (5.33) defining the adjoint eigenfunctions are replaced by

$$\begin{cases} \dot{v}_1(t) - TA(t)v_1(t) + i\omega T\, v_1(t) = 0, \ t \in [0,1], \\ v_1(1) - v_1(0) = 0, \\ \int_0^1 \langle v_1(t), v_1(t)\rangle dt - 1 = 0, \end{cases} \tag{6.20}$$

with $v(\tau) = v_1(\tau/T)/\sqrt{T}$, (6.14) and

$$\begin{cases} \dot{v}_1^*(t) + TA^{\mathrm{T}}(t)v_1^*(t) + i\omega T\, v_1^*(t) = 0,\ t \in [0,1], \\ v_1^*(1) - v_1^*(0) = 0, \\ \int_0^1 \langle v_1^*(t), v_1(t)\rangle dt - 1 = 0, \end{cases}$$

where $v^*(\tau) = v_1^*(\tau/T)/\sqrt{T}$, respectively.

The second order terms are defined by

$$\begin{cases} \dot{h}_{20,1}(t) - TA(t)h_{20,1}(t) + 2i\omega T h_{20,1}(t) - TB(t; v_1(t), v_1(t)) = 0,\ t \in [0,1], \\ h_{20,1}(1) - h_{20,1}(0) = 0, \end{cases}$$

with $h_{20}(\tau) = h_{20,1}(\tau/T)/T$, and

$$\begin{cases} \dot{h}_{11,1}(t) - TA(t)h_{11,1}(t) - TB(t; v_1(t), \bar{v}_1(t)) + \alpha_{1,1}TF(u_1(t)) = 0,\ t \in [0,1], \\ h_{11,1}(1) - h_{11,1}(0) = 0, \\ \int_0^1 \langle \varphi_1^*(t), h_{11,1}(t)\rangle dt = 0, \end{cases}$$

with $h_{11}(\tau) = h_{11,1}(\tau/T)/T$, where

$$\alpha_{1,1} = \int_0^1 \langle \varphi_1^*(t), B(t; v_1(t), \bar{v}_1(t))\rangle dt,$$

for $\alpha_{1,1} = T\alpha_1$.

Now, we can compute

$$\begin{aligned} c_1 = -\frac{i}{2}\int_0^1 \langle v_1^*(t), C(t; v_1(t), v_1(t), \bar{v}_1(t)) + 2B(t; v_1(t), h_{11,1}(t)) \\ + B(t; \bar{v}_1(t), h_{20,1}(t)) - 2\alpha_{1,1}A(t)v_1(t)\rangle dt + \alpha_{1,1}\omega, \end{aligned}$$

for $c_1 = Tc$. With c_1 defined in this way, h_{21M} can be computed as the solution of

$$\begin{cases} \dot{h}_{21,1}(t) - TA(t)h_{21,1}(t) + i\omega T h_{21,1}(t) \\ -TC(t; v_1(t), v_1(t), \bar{v}_1(t)) - 2TB(t; v_1(t), h_{11,1}(t)) \\ -TB(t; h_{20,1}(t), \bar{v}_1(t)) + 2ic_1 T v_1(t) \\ +2\alpha_{1,1}T(A(t)v_1(t) - i\omega v_1(t)) = 0,\ t \in [0,1], \\ h_{21,1}(1) - h_{21,1}(0) = 0, \\ \int_0^1 \langle v_1^*(t), h_{21,1}(t)\rangle dt = 0, \end{cases}$$

where $h_{21}(\tau) = h_{21,1}(\tau/T)/(\sqrt{T}T)$.

Next, the rescaling of h_{30} gives

$$\begin{cases} \dot{h}_{30,1}(t) - TA(t)h_{30,1}(t) + 3i\omega T h_{30,1}(t) \\ -TC(t; v_1(t), v_1(t), v_1(t)) - 3TB(t; v_1(t), h_{20,1}(t)) = 0, \ t \in [0,1], \\ h_{30,1}(1) - h_{30,1}(0) = 0, \end{cases}$$

with $h_{30}(\tau) = h_{30,1}(\tau/T)/(\sqrt{T}T)$.

Now, we come to the fourth order terms where the rescaled $h_{31,1}$ is the solution of

$$\begin{cases} \dot{h}_{31,1}(t) - TA(t)h_{31,1}(t) + 2i\omega T h_{31,1}(t) \\ -TD(t; v_1(t), v_1(t), v_1(t), \bar{v}_1(t)) - 3TC(t; v_1(t), v_1(t), h_{11,1}(t)) \\ -3TC(t; v_1(t), \bar{v}_1(t), h_{20,1}(t)) - 3TB(t; h_{11,1}(t), h_{20,1}(t)) \\ -3TB(t; v_1(t), h_{21,1}(t)) - TB(t; \bar{v}_1(t), h_{30,1}(t)) \\ +6ic_1 T h_{20,1}(t) + 3\alpha_{1,1} T(A(t)h_{20,1}(t) \\ -2i\omega h_{20,1}(t) + B(t; v_1(t), v_1(t))) = 0, \ t \in [0,1], \\ h_{31,1}(1) - h_{31,1}(0) = 0, \end{cases} \tag{6.21}$$

with $h_{31}(\tau) = h_{31,1}(\tau/T)/T^2$, and the rescaled $h_{22,1}$ the solution of

$$\begin{cases} \dot{h}_{22,1}(t) - TA(t)h_{22,1}(t) - TD(t; v_1(t), v_1(t), \bar{v}_1(t), \bar{v}_1(t)) \\ -TC(t; v_1(t), v_1(t), h_{02,1}(t)) - 4TC(t; v_1(t), \bar{v}_1(t), h_{11,1}(t)) \\ -TC(t; \bar{v}_1(t), \bar{v}_1(t), h_{20,1}(t)) - 2TB(t; h_{11,1}(t), h_{11,1}(t)) \\ -2TB(t; v_1(t), h_{12,1}(t)) - TB(t; h_{02,1}(t), h_{20,1}(t)) \\ -2TB(t; \bar{v}_1(t), h_{21,1}(t)) + 4\alpha_{1,1} T(A(t)h_{11,1}(t) \\ +B(t; v_1(t), \bar{v}_1(t)) - \alpha_{1,1} F(u_1(t))) + 4\alpha_{2,1} TF(u_1(t)) = 0, \ t \in [0,1], \\ h_{22,1}(1) - h_{22,1}(0) = 0, \\ \int_0^1 \langle \varphi_1^*(t), h_{22,1}(t) \rangle dt = 0, \end{cases}$$

with $h_{22}(\tau) = h_{22,1}(\tau/T)/T^2$, and

$$\begin{aligned}\alpha_{2,1} = \frac{1}{4}\int_0^1 \langle \varphi_1^*(t), D(t; v_1(t), v_1(t), \bar{v}_1(t), \bar{v}_1(t)) + C(t; v_1(t), v_1(t), h_{02,1}(t))\\ + 4C(t; v_1(t), \bar{v}_1(t), h_{11,1}(t)) + C(t; \bar{v}_1(t), \bar{v}_1(t), h_{20,1}(t))\\ + 2B(t; h_{11,1}(t), h_{11,1}(t)) + 2B(t; v_1(t), h_{12,1}(t)) + B(t; h_{02,1}(t), h_{20,1}(t))\\ + 2B(t; \bar{v}_1(t), h_{21,1}(t)) - 4\alpha_{1,1}(A(t)h_{11,1}(t) + B(t; v_1(t), \bar{v}_1(t)))\rangle dt + \alpha_{1,1}^2,\end{aligned}$$

for $\alpha_{2,1} = T^2\alpha_2$.

At last, the critical coefficient e is determined by

$$\begin{aligned}e = \frac{1}{12T^2}\int_0^1 \langle v_1^*(t), E(t; v_1(t), v_1(t), v_1(t), \bar{v}_1(t), \bar{v}_1(t))\\ + D(t; v_1(t), v_1(t), v_1(t), h_{02,1}(t)) + 6D(t; v_1(t), v_1(t), \bar{v}_1(t), h_{11,1}(t))\\ + 3D(t; v_1(t), \bar{v}_1(t), \bar{v}_1(t), h_{20,1}(t)) + 6C(t; v_1(t), h_{11,1}(t), h_{11,1}(t))\\ + 3C(t; v_1(t), v_1(t), h_{12,1}(t)) + 3C(t; v_1(t), h_{02,1}(t), h_{20,1}(t))\\ + 6C(t; \bar{v}_1(t), h_{11,1}(t), h_{20,1}(t)) + 6C(t; v_1(t), \bar{v}_1(t), h_{21,1}(t))\\ + C(t; \bar{v}_1(t), \bar{v}_1(t), h_{30,1}(t)) + 3B(t; h_{12,1}(t), h_{20,1}(t))\\ + 6B(t; h_{11,1}(t), h_{21,1}(t)) + 3B(t; v_1(t), h_{22,1}(t)) + B(t; h_{02,1}(t), h_{30,1}(t))\\ + 2B(t; \bar{v}_1(t), h_{31,1}(t)) - 12\alpha_{2,1}A(t)v_1(t) - 6\alpha_{1,1}(A(t)h_{21,1}(t)\\ + 2B(t; v_1(t), h_{11,1}(t)) + C(t; v_1(t), v_1(t), \bar{v}_1(t)) + B(t; h_{20,1}(t), \bar{v}_1(t))\\ - 2\alpha_{1,1}A(t)v_1(t))\rangle dt + \alpha_{2,1}i\frac{\omega}{T^2} + \alpha_{1,1}i\frac{c_1}{T^2} - \alpha_{1,1}^2 i\frac{\omega}{T^2}.\end{aligned}$$

We now concentrate on the computation of the vector approximations for the previously defined functions. We compute v_{1M} by solving the discretization of (6.20)

$$\begin{bmatrix} (D - TA(t) + i\omega TL)_{C\times M} & p_2 \\ \delta_0 - \delta_1 & \\ q_2^{\mathrm{H}} & 0 \end{bmatrix} \begin{bmatrix} v_{1M} \\ a \end{bmatrix} = \begin{bmatrix} 0_{M\times 1} \\ 1 \end{bmatrix},$$

with $a = 0$, and where q_2 is the normalized right null-vector of the complex matrix $K = \begin{bmatrix} (D - TA(t) + i\omega TL)_{C\times M} \\ \delta_0 - \delta_1 \end{bmatrix}$ and p_2 the normalized right null-vector of K^{H}. This vector is then rescaled to ensure that $\sum_{i=0}^{N-1}\sum_{j=0}^{m}\sigma_j\langle(v_{1M})_{i,j}, (v_{1M})_{i,j}\rangle = 1$.

The approximation $(\varphi_1^*)_{W_1}$ to the adjoint eigenfunction φ_1^* is computed as in the GPD case. For the calculation of v_1^* we apply Proposition 6.3 on page 257 from

the appendix. Since v_1^* lies in the kernel of the operator ϕ_2, it holds that $\begin{bmatrix} v_1^* \\ v_1^*(0) \end{bmatrix}$ is orthogonal to the range of $\begin{bmatrix} D - TA^{\mathrm{T}}(t) + i\omega T \\ \delta_0 - \delta_1 \end{bmatrix}$. By discretization we obtain

$$\begin{bmatrix} (v_1^*)_W^{\mathrm{H}} & a \end{bmatrix} \begin{bmatrix} (D - TA(t) + i\omega TL)_{C\times M} & p_2 \\ \delta_0 - \delta_1 & \\ q_2^{\mathrm{H}} & 0 \end{bmatrix} = \begin{bmatrix} 0_{1\times M} & 1 \end{bmatrix}.$$

We then approximate $I = \int_0^1 \langle v_1^*(t), v_1(t)\rangle dt$ by $I_1 = (v_1^*)_{W_1}^{\mathrm{H}} L_{C\times M} v_{1M}$ and rescale v_{1W}^* so that $I_1 = 1$.

The second order terms are approximated by

$$\begin{bmatrix} (D - TA(t) + 2\,i\omega TL)_{C\times M} \\ \delta_0 - \delta_1 \end{bmatrix} h_{20,1M} = \begin{bmatrix} TB_{C\times M\times M} v_{1M} v_{1M} \\ 0_{n\times 1} \end{bmatrix}$$

and

$$\begin{bmatrix} (D - TA(t))_{C\times M} & p \\ \delta_0 - \delta_1 & \\ (\varphi_1^*)_{W_1}^{\mathrm{T}} L_{C\times M} & 0 \end{bmatrix} \begin{bmatrix} h_{11,1M} \\ a \end{bmatrix} = \begin{bmatrix} TB_{C\times M\times M} v_{1M} \bar{v}_{1M} - \alpha_{1,1} T g_C \\ 0_{n\times 1} \\ 0 \end{bmatrix},$$

with $a = 0$ and $\alpha_{1,1}$ computed as

$$\alpha_{1,1} = (\varphi_1^*)_{W_1}^{\mathrm{T}} B_{C\times M\times M} v_{1M} \bar{v}_{1M}.$$

An approximation to the rescaled normal form coefficient c_1 is given by

$$\begin{aligned} c_1 = -\frac{i}{2}(v_1^*)_{W_1}^{\mathrm{H}} (&C_{C\times M\times M\times M} v_{1M} v_{1M} \bar{v}_{1M} + 2B_{C\times M\times M} v_{1M} h_{11,1M} \\ &+ B_{C\times M\times M} \bar{v}_{1M} h_{20,1M} - 2\alpha_{1,1} A_{C\times M} v_{1M}) + \alpha_{1,1}\omega, \end{aligned}$$

where MatCont provides an extra check to ensure that this coefficient is indeed purely imaginary.

Next, we determine the third order coefficients of the center manifold expansion, namely

$$\begin{bmatrix} (D - TA(t) + i\omega TL)_{C\times M} & p_2 \\ \delta_0 - \delta_1 & \\ (v_1^*)_{W_1}^{\mathrm{H}} L_{C\times M} & 0 \end{bmatrix} \begin{bmatrix} h_{21,1M} \\ a \end{bmatrix} = \begin{bmatrix} \mathsf{R} \\ 0_{n\times 1} \\ 0 \end{bmatrix},$$

where

$$\begin{aligned}\mathsf{R} = {} & TC_{C\times M\times M\times M}v_{1M}v_{1M}\bar{v}_{1M} + 2TB_{C\times M\times M}v_{1M}h_{11,1M} \\ & + TB_{C\times M\times M}h_{20,1M}\bar{v}_{1M} - 2ic_1TL_{C\times M}v_{1M} \\ & - 2\alpha_{1,1}T(A_{C\times M}v_{1M} - i\omega L_{C\times M}v_{1M})\end{aligned}$$

and $a = 0$, and

$$\begin{bmatrix} (D - TA(t) + 3i\omega TL)_{C\times M} \\ \delta_0 - \delta_1 \end{bmatrix} h_{30,1M} = \begin{bmatrix} \mathsf{R} \\ 0_{n\times 1} \end{bmatrix},$$

with $\mathsf{R} = TC_{C\times M\times M\times M}v_{1M}v_{1M}v_{1M} + 3TB_{C\times M\times M}v_{1M}h_{20,1M}$.

The approximation to (6.21) is given by

$$\begin{bmatrix} (D - TA(t) + 2i\omega TL)_{C\times M} \\ \delta_0 - \delta_1 \end{bmatrix} h_{31,1M} = \begin{bmatrix} \mathsf{R} \\ 0_{n\times 1} \end{bmatrix},$$

with

$$\begin{aligned}\mathsf{R} = {} & TD_{C\times M\times M\times M\times M}v_{1M}v_{1M}v_{1M}\bar{v}_{1M} + 3TC_{C\times M\times M\times M}v_{1M}v_{1M}h_{11,1M} \\ & + 3TC_{C\times M\times M\times M}v_{1M}\bar{v}_{1M}h_{20,1M} + 3TB_{C\times M\times M}h_{11,1M}h_{20,1M} \\ & + 3TB_{C\times M\times M}v_{1M}h_{21,1M} + TB_{C\times M\times M}\bar{v}_{1M}h_{30,1M} - 6ic_1TL_{C\times M}h_{20,1M} \\ & - 3\alpha_{1,1}T(A_{C\times M}h_{20,1M} - 2i\omega L_{C\times M}h_{20,1M} + B_{C\times M\times M}v_{1M}v_{1M})\end{aligned}$$

while

$$\begin{aligned}\alpha_{2,1} = {} & \frac{1}{4}(\varphi_1^*)^{\mathrm{T}}_{W_1}(D_{C\times M\times M\times M\times M}v_{1M}v_{1M}\bar{v}_{1M}\bar{v}_{1M} + C_{C\times M\times M\times M}v_{1M}v_{1M}h_{02,1M} \\ & + 4C_{C\times M\times M\times M}v_{1M}\bar{v}_{1M}h_{11,1M} + C_{C\times M\times M\times M}\bar{v}_{1M}\bar{v}_{1M}h_{20,1M} \\ & + 2B_{C\times M\times M}h_{11,1M}h_{11,1M} + 2B_{C\times M\times M}v_{1M}h_{12,1M} + B_{C\times M\times M}h_{02,1M}h_{20,1M} \\ & + 2B_{C\times M\times M}\bar{v}_{1M}h_{21,1M} - 4\alpha_{1,1}(A_{C\times M}h_{11,1M} + B_{C\times M\times M}v_{1M}\bar{v}_{1M})) + \alpha_{1,1}^2.\end{aligned}$$

The other needed fourth order term is given by

$$\begin{bmatrix} (D - TA(t))_{C\times M} & p \\ \delta_0 - \delta_1 & \\ (\varphi_1^*)^{\mathrm{T}}_{W_1}L_{C\times M} & 0 \end{bmatrix} \begin{bmatrix} h_{22,1M} \\ a \end{bmatrix} = \begin{bmatrix} \mathsf{R} \\ 0_{n\times 1} \\ 0 \end{bmatrix},$$

with

$$\begin{aligned}\mathrm{R} = {} & TD_{C\times M\times M\times M\times M}v_{1M}v_{1M}\bar{v}_{1M}\bar{v}_{1M} + TC_{C\times M\times M\times M}v_{1M}v_{1M}h_{02,1M}\\ & + 4TC_{C\times M\times M\times M}v_{1M}\bar{v}_{1M}h_{11,1M} + TC_{C\times M\times M\times M}\bar{v}_{1M}\bar{v}_{1M}h_{20,1M}\\ & + 2TB_{C\times M\times M}h_{11,1M}h_{11,1M} + 2TB_{C\times M\times M}v_{1M}h_{12,1M}\\ & + TB_{C\times M\times M}h_{02,1M}h_{20,1M} + 2TB_{C\times M\times M}\bar{v}_{1M}h_{21,1M}\\ & - 4\alpha_{1,1}T(A_{C\times M}h_{11,1M} + B_{C\times M\times M}v_{1M}\bar{v}_{1M} - \alpha_1 g_C) - 4\alpha_{2,1}Tg_C\end{aligned}$$

and $a = 0$. Now, we have all information needed to compute the fifth order coefficient of the normal form, namely

$$\begin{aligned}e = {} & \frac{1}{12T^2}(v_1^*)^{\mathrm{H}}_{W_1}(E_{C\times M\times M\times M\times M\times M}v_{1M}v_{1M}v_{1M}\bar{v}_{1M}\bar{v}_{1M}\\ & + D_{C\times M\times M\times M\times M}v_{1M}v_{1M}v_{1M}h_{02,1M} + 6D_{C\times M\times M\times M\times M}v_{1M}v_{1M}\bar{v}_{1M}h_{11,1M}\\ & + 3D_{C\times M\times M\times M\times M}v_{1M}\bar{v}_{1M}\bar{v}_{1M}h_{20,1M} + 6C_{C\times M\times M\times M}v_{1M}h_{11,1M}h_{11,1M}\\ & + 3C_{C\times M\times M\times M}v_{1M}v_{1M}h_{12,1M} + 3C_{C\times M\times M\times M}v_{1M}h_{02,1M}h_{20,1M}\\ & + 6C_{C\times M\times M\times M}\bar{v}_{1M}h_{11,1M}h_{20,1M} + 6C_{C\times M\times M\times M}v_{1M}\bar{v}_{1M}h_{21,1M}\\ & + C_{C\times M\times M\times M}\bar{v}_{1M}\bar{v}_{1M}h_{30,1M} + 3B_{C\times M\times M}h_{12,1M}h_{20,1M}\\ & + 6B_{C\times M\times M}h_{11,1M}h_{21,1M} + 3B_{C\times M\times M}v_{1M}h_{22,1M}\\ & + B_{C\times M\times M}h_{02,1M}h_{30,1M} + 2B_{C\times M\times M}\bar{v}_{1M}h_{31,1M} - 12\alpha_{2,1}A_{C\times M}v_{1M}\\ & - 6\alpha_{1,1}(A_{C\times M}h_{21,1M} + 2B_{C\times M\times M}v_{1M}h_{11,1M} + C_{C\times M\times M\times M}v_{1M}v_{1M}\bar{v}_{1M}\\ & + B_{C\times M\times M}h_{20,1M}\bar{v}_{1M} - 2\alpha_{1,1}A_{C\times M}v_{1M})) + \alpha_{2,1}i\frac{\omega}{T^2} + \alpha_{1,1}i\frac{c_1}{T^2} - \alpha_{1,1}^2 i\frac{\omega}{T^2}.\end{aligned}$$

Strong Resonance 1:1 bifurcation

Next to the generalized eigenfunction $v_{1,1}$ defined by (6.4), the second generalized eigenfunction associated to multiplier 1 is given by

$$\begin{cases}\dot{v}_{2,1}(t) - TA(t)v_{2,1}(t) + Tv_{1,1}(t) = 0, \ t\in[0,1],\\ v_{2,1}(1) - v_{2,1}(0) = 0,\\ \int_0^1 \langle v_{2,1}(t), F(u_1(t))\rangle dt = 0,\end{cases}$$

with $v_2(\tau) = v_{2,1}(\tau/T)$.

The adjoint eigenfunction φ_1^* is determined by the first two equations of (6.5) and the normalization condition

$$\int_0^1 \langle \varphi_1^*(t), v_{2,1}(t)\rangle dt - 1 = 0.$$

We also need the rescaled first generalized adjoint eigenfunction that is the solution of

$$\begin{cases} \dot{v}_{1,1}^*(t) + TA^{\mathrm{T}}(t)v_{1,1}^*(t) - T\varphi_1^*(t) = 0,\ t \in [0,1], \\ v_{1,1}^*(1) - v_{1,1}^*(0) = 0, \\ \int_0^1 \langle v_{1,1}^*(t), v_{2,1}(t)\rangle dt = 0, \end{cases}$$

with $v_1^*(\tau) = v_{1,1}^*(\tau/T)/T$. Now, we have all information needed to write down the expression of the two rescaled critical coefficients, namely

$$a = \frac{1}{2}\int_0^1 \langle \varphi_1^*(t), 2A(t)v_{1,1}(t) + B(t; v_{1,1}(t), v_{1,1}(t))\rangle dt$$

and

$$\begin{aligned} b = &\int_0^1 \langle \varphi_1^*(t), B(t; v_{1,1}(t), v_{2,1}(t)) + A(t)v_{2,1}(t)\rangle dt \\ &+ \int_0^1 \langle v_{1,1}^*(t), 2A(t)v_{1,1}(t) + B(t; v_{1,1}(t), v_{1,1}(t))\rangle dt. \end{aligned}$$

The implementation in MatCont is straightforward and relies on earlier explained techniques so we will omit further details.

Strong Resonance 1:2 bifurcation

Eigenfunction $v_{1,1}$ associated to multiplier -1 is given by the solution of (6.13), where $v_1(\tau) = v_{1,1}(\tau/T)/\sqrt{T}$, and the generalized eigenfunction $v_{2,1}$ defined on the interval $[0,1]$ is the solution of

$$\begin{cases} \dot{v}_{2,1}(t) - TA(t)v_{2,1}(t) + Tv_{1,1}(t) = 0,\ t \in [0,1], \\ v_{2,1}(1) + v_{2,1}(0) = 0, \\ \int_0^1 \langle v_{2,1}(t), v_{1,1}(t)\rangle dt = 0, \end{cases}$$

where $v_2(\tau) = v_{2,1}(\tau/T)/\sqrt{T}$.

The rescaled adjoint eigenfunctions are determined by (6.14), the first two equation of (6.15) with normalization condition $\int_0^1 \langle v_{1,1}^*(t), v_{2,1}(t)\rangle dt = 1$ and

$$\begin{cases} \dot{v}_{2,1}^*(t) + TA^{\mathrm{T}}(t)v_{2,1}^*(t) - Tv_{1,1}^*(t) = 0, \ t \in [0,1], \\ v_{2,1}^*(1) + v_{2,1}^*(0) = 0, \\ \int_0^1 \langle v_{2,1}(t), v_{2,1}^*(t)\rangle \, dt = 0, \end{cases}$$

where $v_2^*(\tau) = v_{2,1}^*(\tau/T)/\sqrt{T}$.

With α_1 defined as

$$\alpha_1 = \frac{1}{2}\int_0^1 \langle \varphi_1^*(t), B(t; v_{1,1}(t), v_{1,1}(t))\rangle \, dt,$$

for $\alpha_1 = T\alpha$, let $h_{20,1}$ be the unique solution of the BVP

$$\begin{cases} \dot{h}_{20,1}(t) - TA(t)h_{20,1}(t) - TB(t; v_{1,1}(t), v_{1,1}(t)) + 2\alpha_1 TF(u_1(t)) = 0, \ t \in [0,1], \\ h_{20,1}(1) - h_{20,1}(0) = 0, \\ \int_0^1 \langle \varphi_1^*(t), h_{20,1}(t)\rangle \, dt - \int_0^1 \langle \varphi_1^*(t), B(v_{1,1}(t), v_{2,1}(t))\rangle \, dt = 0, \end{cases} \tag{6.22}$$

where $h_{20}(\tau) = h_{20,1}(\tau/T)/T$.

With $h_{11,1}$, being the rescaling of the function h_{11}, the solution of

$$\begin{cases} \dot{h}_{11,1}(t) - TA(t)h_{11,1}(t) - TB(t; v_{1,1}(t), v_{2,1}(t)) + Th_{20,1}(t) = 0, \ t \in [0,1], \\ h_{11,1}(1) - h_{11,1}(0) = 0, \\ \int_0^1 \langle \varphi_1^*(t), h_{11,1}(t)\rangle \, dt - \frac{1}{2}\int_0^1 \langle \varphi_1^*(t), B(v_{2,1}(t), v_{2,1}(t))\rangle \, dt = 0, \end{cases}$$

where $h_{11}(\tau) = h_{11,1}(\tau/T)/T$, we are able to obtain the two normal form coefficients as

$$\begin{aligned} a_1 = \frac{1}{6}\int_0^1 \langle v_{1,1}^*(t), C(t; v_{1,1}(t), v_{1,1}(t), v_{1,1}(t)) \\ + 3B(t; v_{1,1}(t), h_{20,1}(t)) - 6\alpha_1 A(t)v_{1,1}(t)\rangle \, dt, \end{aligned}$$

for $a_1 = Ta$, and

$$\begin{aligned} b = \frac{1}{2T}\int_0^1 \langle v_{1,1}^*(t), -2\alpha_1 A(t)v_{2,1}(t) + C(t; v_{1,1}(t), v_{1,1}(t), v_{2,1}(t)) \\ + B(t; h_{20,1}(t), v_{2,1}(t)) + 2B(t; h_{11,1}(t), v_{1,1}(t))\rangle dt \\ + \frac{1}{2T}\int_0^1 \langle v_{2,1}^*(t), C(t; v_{1,1}(t), v_{1,1}(t), v_{1,1}(t)) \\ + 3B(t; v_{1,1}(t), h_{20,1}(t)) - 6\alpha_1 A(t)v_{1,1}(t)\rangle dt. \end{aligned}$$

Concerning the implementation details we will just highlight the differences with respect to the previous cases. Formula (6.16) gives us the value of $v_{1,1}$ in the mesh points. However, since $v_{1,1}$ is used in the integral condition for $v_{2,1}$, we have to transfer this vector to the collocation points and multiply it with the Gauss-Legendre weights and the lenghts of the corresponding intervals, to obtain $v_{1,1W_1}$. The computation of $v_{2,1M}$ is then straightforward.

By making use of Proposition 6.6 on page 259, we can approximate the adjoint generalized eigenfunction $v_{2,1}^*$ by solving

$$\begin{bmatrix} (v_{2,1}^*)_W^{\mathrm{T}} & a \end{bmatrix} \begin{bmatrix} (D - TA(t))_{C\times M} & v_{2,1C} \\ \delta_0 + \delta_1 & 0_{n\times 1} \\ q_1^{\mathrm{T}} & 0 \end{bmatrix} = \begin{bmatrix} -T(v_{1,1}^*)_{W_1}^{\mathrm{T}} L_{C\times M} & 0 \end{bmatrix}.$$

Now, $h_{20,1M}$ is found by discretizing (6.22), i.e.

$$\begin{bmatrix} (D - TA(t))_{C\times M} & p \\ \delta_0 - \delta_1 & 0 \\ (\varphi_1^*)_{W_1}^{\mathrm{T}} L_{C\times M} & 0 \end{bmatrix} \begin{bmatrix} h_{20,1M} \\ a \end{bmatrix} = \begin{bmatrix} TB_{C\times M\times M} v_{1,1M} v_{1,1M} - 2\alpha_1 T g_C \\ 0_{n\times 1} \\ (\varphi_1^*)_{W_1}^{\mathrm{T}} B_{C\times M\times M} v_{1,1M} v_{2,1M} \end{bmatrix}.$$

Strong Resonance 1:3 bifurcation

The BVPs for the rescaled eigenfunction and its adjoint belonging to eigenvalue $e^{i\frac{2\pi}{3}}$ are determined by

$$\begin{cases} \dot{v}_1(t) - TA(t)v_1(t) = 0, \ t \in [0,1], \\ v_1(1) - e^{i\frac{2\pi}{3}} v_1(0) = 0, \\ \int_0^1 \langle v_1(t), v_1(t)\rangle dt - 1 = 0, \end{cases} \tag{6.23}$$

with $v(\tau) = v_1(\tau/T)/\sqrt{T}$, and

$$\begin{cases} \dot{v}_1^*(t) + TA^{\mathrm{T}}(t)v_1^*(t) = 0, \ t \in [0,1], \\ v_1^*(1) - e^{i\frac{2\pi}{3}} v_1^*(0) = 0, \\ \int_0^1 \langle v_1^*(t), v_1(t)\rangle dt - 1 = 0, \end{cases}$$

where $v^*(\tau) = v_1^*(\tau/T)/\sqrt{T}$. The adjoint eigenfunction φ_1^* corresponding to the trivial multiplier is given by (6.14).

The normal form coefficients α_1 and b can then be deduced from the expressions

$$\alpha_{1,1} = \int_0^1 \langle \varphi_1^*(t), B(v_1(t), \bar{v}_1(t))\rangle dt, \tag{6.24}$$

for $\alpha_{1,1} = T\alpha_1$, and

$$b_1 = \frac{1}{2}\int_0^1 \langle v_1^*(t), B(\bar{v}_1(t), \bar{v}_1(t))\rangle dt,$$

for $b_1 = \sqrt{T}b$.

The rescaled second order functions in the center manifold expansion are solutions of

$$\begin{cases} \dot{h}_{20,1}(t) - TA(t)h_{20,1}(t) - TB(v_1(t), v_1(t)) + 2\bar{b}_1 T\bar{v}_1(t) = 0, \ t \in [0,T], \\ h_{20,1}(1) - e^{i\frac{4\pi}{3}} h_{20,1}(0) = 0, \\ \int_0^1 \langle \bar{v}_1^*(t), h_{20,1}(t)\rangle dt = 0, \end{cases}$$

with $h_{20}(\tau) = h_{20,1}(\tau/T)/T$, and

$$\begin{cases} \dot{h}_{11,1}(t) - TA(t)h_{11,1} - TB(v_1(t), \bar{v}_1(t)) + \alpha_{1,1}TF(u_1(t)) = 0, \ t \in [0,1], \\ h_{11,1}(1) - h_{11,1}(0) = 0, \\ \int_0^1 \langle \varphi_1^*(t), h_{11,1}(t) \rangle dt = 0, \end{cases} \tag{6.25}$$

with $h_{11}(\tau) = h_{11,1}(\tau/T)/T$. This then all results in the following expression for the critical coefficient c

$$\begin{aligned} c = \frac{1}{2T} \int_0^1 \langle v_1^*(t), C(v_1(t), v_1(t), \bar{v}_1(t)) + 2B(v_1(t), h_{11,1}(t)) \\ + B(\bar{v}_1(t), h_{20,1}(t)) - 2\alpha_{1,1}Av_1(t) \rangle dt. \end{aligned}$$

We now discuss the implementation details in MatCont. We again highlight only the differences with the implementation details given in the previous cases. Eigenfunction v_1, determined by (6.23), is computed by solving

$$\begin{bmatrix} (D - TA(t))_{C\times M} & p_3 \\ \delta_0 - e^{-i\frac{2\pi}{3}}\delta_1 & \\ q_3^{\mathrm{H}} & 0 \end{bmatrix} \begin{bmatrix} v_{1M} \\ a \end{bmatrix} = \begin{bmatrix} 0_{M\times 1} \\ 1 \end{bmatrix},$$

where $a = 0$ as usual. We normalize v_{1M} by requiring $\sum_{i=0}^{N-1}\sum_{j=0}^{m}\sigma_j\langle (v_{1M})_{i,j}, (v_{1M})_{i,j}\rangle = 1$, where σ_j is the Lagrange quadrature coefficient. q_3 is the normalized right null-vector of $K = \begin{bmatrix} (D - TA(t))_{C\times M} \\ \delta_0 - e^{-i\frac{2\pi}{3}}\delta_1 \end{bmatrix}$ and p_3 the normalized right null-vector of K^{H}.

To compute the adjoint eigenfunction v_1^*, we apply Proposition 6.4 on page 257 with $\theta = \frac{2\pi}{3}$. Since $v_1^* \in Ker(\phi_2)$, this function can be obtained by solving

$$\begin{bmatrix} (v_1^*)_W^{\mathrm{H}} & a \end{bmatrix} \begin{bmatrix} (D - TA(t))_{C\times M} & p_3 \\ \delta_0 - e^{-i\frac{2\pi}{3}}\delta_1 & \\ q_3^{\mathrm{H}} & 0 \end{bmatrix} = \begin{bmatrix} 0_{1\times M} & 1 \end{bmatrix}. \tag{6.26}$$

v_{1W}^* is then rescaled such that $(v_1^*)_{W_1}^{\mathrm{H}} L_{C\times M} v_{1M} = 1$.

By computing first the complex conjugate of $h_{20,1}$ we can make use of the matrix

from (6.26), except for the last line that represents the integral condition, to get

$$\begin{bmatrix} (D - TA(t))_{C\times M} & p_3 \\ \delta_0 - e^{-i\frac{2\pi}{3}}\delta_1 & \\ (v_1^*)^{\mathrm{H}}_{W_1} L_{C\times M} & 0 \end{bmatrix} \begin{bmatrix} \bar{h}_{20,1M} \\ a \end{bmatrix} = \begin{bmatrix} TB_{C\times M\times M}\bar{v}_{1M}\bar{v}_{1M} - 2b_1 T v_{1C} \\ 0_{n\times 1} \\ 0 \end{bmatrix}.$$

Strong Resonance 1:4 bifurcation

The eigenfunction and the adjoint eigenfunction corresponding to multiplier $e^{i\frac{\pi}{2}}$ and defined on $[0,1]$ are the solutions of

$$\begin{cases} \dot{v}_1(t) - TA(t)v_1(t) = 0, \ t \in [0,1], \\ v_1(1) - e^{i\frac{\pi}{2}} v_1(0) = 0, \\ \int_0^1 \langle v_1(t), v_1(t)\rangle dt - 1 = 0, \end{cases}$$

with $v(\tau) = v_1(\tau/T)/\sqrt{T}$ and

$$\begin{cases} \dot{v}_1^*(t) + TA^{\mathrm{T}}(t)v_1^*(t) = 0, \ t \in [0,1], \\ v_1^*(1) - e^{i\frac{\pi}{2}} v_1^*(0) = 0, \\ \int_0^1 \langle v_1^*(t), v_1(t)\rangle dt - 1 = 0, \end{cases}$$

with $v^*(\tau) = v_1^*(\tau/T)/\sqrt{T}$, respectively. We also need the functions φ_1^* and $h_{11,1}$ defined by (6.14) and (6.25), and the value of $\alpha_{1,1}$ given by (6.24).

The other second order term is determined by

$$\begin{cases} \dot{h}_{20,1}(t) - TA(t)h_{20,1}(t) - TB(v_1(t), v_1(t)) = 0, \ t \in [0,1], \\ h_{20,1}(1) + h_{20,1}(0) = 0, \end{cases}$$

with $h_{20}(\tau) = h_{20,1}(\tau/T)/T$.

The critical coefficients are then given by

$$\begin{aligned} \bar{c} = \frac{1}{2T}\int_0^1 \langle \bar{v}_1^*(t), C(v_1(t), \bar{v}_1(t), \bar{v}_1(t)) + B(v_1(t), h_{02,1}(t)) \\ + 2B(\bar{v}_1(t), h_{11,1}(t)) - 2\alpha_{11}A(t)\bar{v}_1(t)\rangle dt \end{aligned}$$

and

$$d = \frac{1}{6T}\int_0^1 \langle v_1^*(t), C(\bar{v}_1(t),\bar{v}_1(t),\bar{v}_1(t)) + 3B(\bar{v}_1(t), h_{02,1}(t))\rangle dt.$$

The code is very similar to the one of the R3 case.

Fold-Flip bifurcation

The rescaled generalized eigenfunction $v_{1,1}$ associated to multiplier 1 is the solution of the BVP (6.4) and the rescaling of the eigenfunction $v_{2,1}$ associated to multiplier -1 is given by (6.13). The system (6.5) determines the adjoint eigenfunction φ_1^* and the generalized adjoint eigenfunction $v_{1,1}^*$ is the solution to (6.6). The last adjoint eigenfunction $v_{2,1}^*$ is determined by (6.15).

The coefficients in front of the ξ_1^2-terms in the normal form (4.12) are given by

$$a_{20} = \frac{1}{2}\int_0^1 \langle \varphi_1^*(t), B(v_{1,1}(t), v_{1,1}(t)) + 2A(t)v_{1,1}(t)\rangle\, dt$$

and $\alpha_{20} = 0$.

The second order functions of the center manifold expansion are defined by the BVPs

$$\begin{cases} \dot{h}_{20,1}(t) - TA(t)h_{20,1}(t) - TB(v_{1,1}(t), v_{1,1}(t)) + 2a_{20}Tv_{1,1}(t) \\ \qquad +2\alpha_{20}TF(u_1(t)) - 2TA(t)v_{1,1}(t) - 2TF(u_1(t)) = 0,\ t \in [0,1], \\ \qquad\qquad h_{20,1}(1) - h_{20,1}(0) = 0, \\ \qquad\qquad \int_0^1 \langle v_{1,1}^*(t), h_{20,1}(t)\rangle dt = 0, \end{cases}$$

with $h_{20}(\tau) = h_{20,1}(\tau/T)$,

$$\begin{cases} \dot{h}_{11,1}(t) - TA(t)h_{11,1}(t) - TB(v_{1,1}(t), v_{2,1}(t)) \\ \qquad +Tb_{11}v_{2,1}(t) - TA(t)v_{2,1}(t) = 0,\ t \in [0,1], \\ \qquad\qquad h_{11,1}(1) + h_{11,1}(0) = 0, \\ \qquad\qquad \int_0^1 \langle v_{2,1}^*(t), h_{11,1}(t)\rangle dt = 0, \end{cases}$$

with $h_{11}(\tau) = h_{11,1}(\tau/T)/\sqrt{T}$ and

$$\begin{cases} \dot{h}_{02,1}(t) - TA(t)h_{02,1}(t) - TB(v_{2,1}(t), v_{2,1}(t)) \\ \qquad +2a_{02,1}Tv_{1,1}(t) + 2\alpha_{02,1}TF(u_1(t)) = 0, \ t \in [0,1], \\ \qquad\qquad h_{02,1}(1) - h_{02,1}(0) = 0, \\ \qquad\qquad \int_0^1 \langle v_{1,1}^*(t), h_{02,1}(t)\rangle dt = 0, \end{cases}$$

with $h_{02}(\tau) = h_{02,1}(\tau/T)/T$, where

$$\begin{aligned} b_{11} &= \int_0^1 \langle v_{2,1}^*(t), B(v_{1,1}(t), v_{2,1}(t)) + A(t)v_{2,1}(t)\rangle \, dt, \\ a_{02,1} &= \frac{1}{2}\int_0^1 \langle \varphi_1^*(t), B(v_{2,1}(t), v_{2,1}(t))\rangle \, dt \end{aligned}$$

for $a_{02,1} = Ta_{02}$, and $\alpha_{02} = 0$.

The rescaling of the last four normal form coefficients of interest gives

$$\begin{aligned} a_{30} = \frac{1}{6}\int_0^1 &\langle \varphi_1^*(t), C(v_{1,1}(t), v_{1,1}(t), v_{1,1}(t)) + 3B(h_{20,1}, v_{1,1}(t)) - 6a_{20}h_{20,1}(t) \\ &+ 3(A(t)h_{20,1}(t) + B(v_{1,1}(t), v_{1,1}(t))) + 6(1-\alpha_{20})A(t)v_{1,1}(t)\rangle \, dt - a_{20}, \\ b_{21} = \frac{1}{2}\int_0^1 &\langle v_{2,1}^*(t), C(v_{1,1}(t), v_{1,1}(t), v_{2,1}(t)) + B(h_{20,1}(t), v_{2,1}(t)) \\ &+ 2B(h_{11,1}(t), v_{1,1}(t)) - 2a_{20}h_{11,1}(t) - 2b_{11}h_{11,1}(t) + 2(A(t)h_{11,1}(t) \\ &+ B(v_{1,1}(t), v_{2,1}(t))) + 2(1-\alpha_{20})A(t)v_{2,1}(t)\rangle \, dt - b_{11}, \\ a_{12} = \frac{1}{2T}\int_0^1 &\langle \varphi_1^*(t), C(v_{1,1}(t), v_{2,1}(t), v_{2,1}(t)) + B(h_{02,1}(t), v_{1,1}(t)) \\ &+ 2B(h_{11,1}(t), v_{2,1}(t)) - 2b_{11}h_{02,1}(t) - 2a_{02,1}h_{20,1}(t) + A(t)h_{02,1}(t) \\ &+ B(v_{2,1}(t), v_{2,1}(t)) - 2\alpha_{02,1}A(t)v_{1,1}(t)\rangle \, dt - \frac{a_{02,1}}{T} \end{aligned}$$

and

$$\begin{aligned} b_{03} = \frac{1}{6T}\int_0^1 &\langle v_{2,1}^*(t), C(v_{2,1}(t), v_{2,1}(t), v_{2,1}(t)) + 3B(h_{02,1}(t), v_{2,1}(t)) \\ &- 6a_{02,1}h_{11,1}(t) - 6\alpha_{02,1}A(t)v_{2,1}(t)\rangle \, dt. \end{aligned}$$

For the computation of the needed functions and coefficients, we refer to the previous sections.

6.2.4 Bifurcations with a 4D center manifold

We have extensively discussed the rescaling and the implementation of the (adjoint) eigenfunctions, the functions appearing in the expansion of the center manifold and the normal form coefficients for all bifurcations of limit cycles with a 2- or 3-dimensional center manifold in Section 6.2.2 and Section 6.2.3. What concerns the bifurcations with a 4- or 5-dimensional center manifold, we will just mention the relation between the functions and coefficients on $[0,T]$, as defined in Section 5.2.3 and Section 5.2.4, and the rescaled versions on $[0,1]$. The reader should then be able to write down their definitions and implement them by proceeding as in the previous sections.

Limit Point-Neimark-Sacker bifurcation

The relation between the generalized eigenfunction v_1 and the rescaled $v_{1,1}$ is given by $v_1(\tau) = v_{1,1}(\tau/T)$. For the eigenfunction corresponding with the complex multiplier it holds that $v_2(\tau) = v_{2,1}(\tau/T)/\sqrt{T}$. The relations for the adjoint eigenfunctions are given by $\varphi^*(\tau) = \varphi_1^*(\tau/T)/T, v_1^*(\tau) = v_{1,1}^*(\tau/T)$ and $v_2^*(\tau) = v_{2,1}^*(\tau/T)/\sqrt{T}$. The rescaling of the critical coefficient a_{200} is given by expression (5.90), but with φ^* replaced by φ_1^*, v_1 replaced by $v_{1,1}$ and the integral taken over $[0,1]$. We have that $h_{200}(\tau) = h_{200,1}(\tau/T), h_{020}(\tau) = h_{020,1}(\tau/T)/T$ and $h_{110}(\tau) = h_{110,1}(\tau/T)/\sqrt{T}$ where the rescaling of b_{110} is similar to expression (5.91). We then first define $a_{011,1}$ as the expression (5.92), but with φ^* replaced by φ_1^*, v_2 replaced by $v_{2,1}$ and the integral taken over $[0,1]$, such that $a_{011,1} = Ta_{011}$. Finally, $h_{011}(\tau) = h_{011,1}(\tau/T)/T$.

Period-Doubling-Neimark-Sacker bifurcation

The eigenfunctions corresponding to multiplier -1 and the complex multiplier are rescaled as follows: $v_1(\tau) = v_{1,1}(\tau/T)/\sqrt{T}, v_2(\tau) = v_{2,1}(\tau/T)/\sqrt{T}$. The relations for the adjoint eigenfunctions are given by $\varphi^*(\tau) = \varphi_1^*(\tau/T)/T, v_1^*(\tau) = v_{1,1}^*(\tau/T)/\sqrt{T}$ and $v_2^*(\tau) = v_{2,1}^*(\tau/T)/\sqrt{T}$. We define $\alpha_{200,1}$ as the expression (5.100) but with the replacement of the functions by their rescaled versions and the integral over $[0,1]$, such that $\alpha_{200,1} = T\alpha_{200}$. The second order function h_{200} leads to the relation $h_{200}(\tau) = h_{200,1}(\tau/T)/T$, solution of a BVP similar to (5.101) but where α_{200} is replaced by $\alpha_{200,1}$ in the differential equation. The other second order functions lead to the relations $h_{020}(\tau) = h_{020,1}(\tau/T)/T, h_{110}(\tau) = h_{110,1}(\tau/T)/T$ and $h_{011}(\tau) = h_{011,1}(\tau/T)/T$ where in the differential equation α_{011} is replaced

by $\alpha_{011,1}$, with $\alpha_{011,1} = T\alpha_{011}$ (as before). For all third order functions it holds that the rescaled functions are obtained by muliplying the unrescaled versions with $\sqrt{T}T$. We define a rescaled version of every critical third order coefficient such that the rescaled coefficient is T times the unrescaled one. These rescaled coefficients will appear in the differential equations of the third order functions.

6.2.5 Bifurcations with a 5D center manifold

Double Neimark-Sacker bifurcation

The rescaling of the eigenfunctions corresponding to the complex multipliers leads to the relations $v_1(\tau) = v_{1,1}(\tau/T)/\sqrt{T}$ and $v_2(\tau) = v_{2,1}(\tau/T)/\sqrt{T}$. For the adjoint eigenfunctions it holds that $\varphi^*(\tau) = \varphi_1^*(\tau/T)/T, v_1^*(\tau) = v_{1,1}^*(\tau/T)/\sqrt{T}$ and $v_2^*(\tau) = v_{2,1}^*(\tau/T)/\sqrt{T}$. All rescaled second order functions are obtained as T times the original ones and all rescaled third order functions as $\sqrt{T}T$ times the functions defined on $[0, T]$. The critical coefficients appearing in the differential equations are replaced by their rescaled versions, which are T times the original ones.

Note that in the LPNS, PDNS and NSNS case, we have not given the rescalings of the higher order terms from Section 5.A, but our discussion in this section should provide enough information to make the derivations. For efficiency reasons these higher order coefficients are not computed in MatCont, unless explicitly requested by the user. The implementation code for all cases is available in MatCont. Concerning the output in MatCont in the LPNS case, $E = NaN$ is reported when terms up to only the second order are computed. In the PDNS and NSNS cases, sign $l_1 = NaN$ is reported when terms up to only the third order are computed.

6.3 Examples

In this section we investigate what bifurcation curves exist around a codim 2 bifurcation of limit cycles and check whether this bifurcation scenario corresponds with the situation predicted by the values of the normal form coefficients.

6.3.1 Periodic predator-prey model

Our first model is a periodically forced predator-prey system, studied in [74] by using shooting techniques, and described by the following differential equations

$$\begin{cases} \dot{x} = r\left(1 - \dfrac{x}{K}\right)x - p(x,t)y, \\ \dot{y} = ep(x,t)y - dy, \end{cases} \tag{6.27}$$

where x and y are the numbers of individuals respectively of prey and predator populations or suitable measures of density or biomass. The parameters present in (6.27) are the intrinsic growth rate r, the carrying capacity K, the efficiency e and the death rate d of the predator. The function $p(x,t)$ is the predator functional response, for which the Holling type II is chosen, with constant attack rate a and half saturation $b(t)$ that varies periodically with period one (year), i.e.

$$p(x,t) = \frac{ax}{b(t)+x}, \qquad b(t) = b_0(1+\varepsilon\cos(2\pi t)).$$

Instead of system (6.27), we consider the extended autonomous system

$$\begin{cases} \dot{x} = r\left(1 - \dfrac{x}{K}\right)x - \dfrac{axy}{b_0(1+\varepsilon u)+x}, \\ \dot{y} = e\,\dfrac{axy}{b_0(1+\varepsilon u)+x} - dy, \\ \dot{u} = u - 2\pi v - (u^2+v^2)u, \\ \dot{v} = 2\pi u + v - (u^2+v^2)v, \end{cases} \tag{6.28}$$

where the last two equations have a stable limit cycle with $u(t) = \cos(2\pi t + \varphi)$ and a phase shift φ depending on the initial conditions.

With fixed $r = 2\pi$, $K = e = 1$, $a = 4\pi$ and $d = 2\pi$, we perform a bifurcation analysis w.r.t. the remaining parameters (ε, b_0), obtaining the bifurcation diagram reported in Figure 6.1. Since the system is periodically forced, no equilibria are present. The blue curves, with labels LPC2(1) and LPC2(2), are Limit Point of Cycles bifurcation curves of the second iterate, the purple curves are Neimark-Sacker bifurcations (of the first or of the second iterate, respectively labeled with NS1 and NS2); while the green curves are Period-Doubling bifurcations, dotted when subcritical and a solid line when supercritical (with notation PD1, PD2, PD4 and PD8).

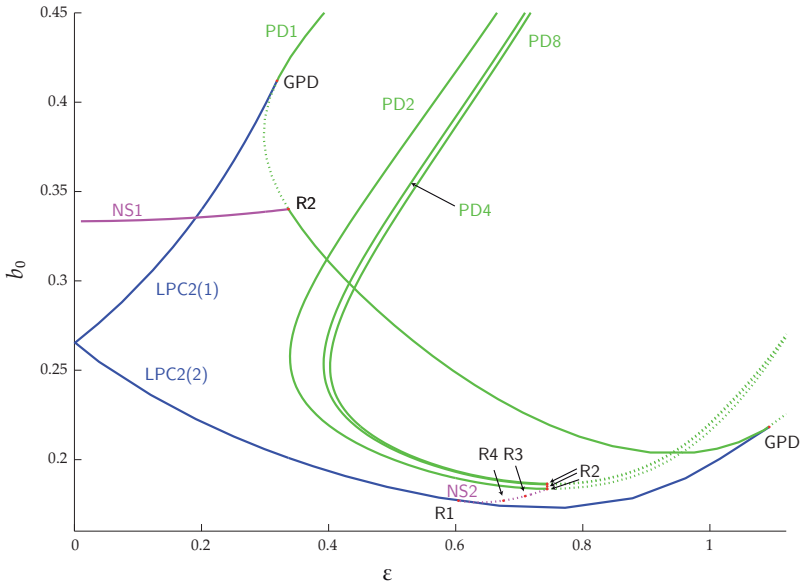

Figure 6.1: Bifurcation diagram of limit cycles in system (6.28). In blue are Limit Point of Cycles bifurcations, in green Period-Doubling bifurcations and in purple Neimark-Sacker bifurcations. Solid/dotted curves correspond to supercritical/subcritical bifurcations.

We have chosen this system as a first example since it allows us to check whether the computation of the normal form coefficients α_i is correct. Indeed, in a periodically forced system the return time is independent of the distance from the limit cycle, so the first equation in the periodic normal form should be $\frac{d\tau}{dt} = 1$. In the GPD, CH, PDNS and NSNS cases, as well as in the strong resonance cases R2, R3 and R4, this would imply that all α_i in the normal forms (4.5)-(4.15) must vanish. For the remaining CPC, R1, LPPD and LPNS (and even the codim 1 LPC) cases, the normal forms (4.5)-(4.15) derived for bifurcations of generic ODEs cannot be applied verbatim, because periodically forced systems are not generic due to a special Jordan structure of their monodromy matrix. We illustrate this phenomenon. Consider a continuation of a period doubled limit cycle in (6.28) and suppose that an LPC bifurcation is detected. For each point of the continuation, we compute

the singular values of the monodromy matrix minus the identity matrix. The two smallest singular values are shown in Figure 6.2. There is always one singular value equal to zero, but also the second one vanishes when approaching the LPC point. This means that instead of a Jordan block of length two (as is expected at the LPC-point in generic ODEs [59]), we have in fact two Jordan blocks of length one. Therefore, in a periodically forced system we can not apply the general theory derived for generic LPC points. A similar situation is encountered in the CPC, R1, LPPD and LPNS cases for periodically forced systems, which therefore should be treated separately. Normal forms for periodically forced ODEs were studied in [44].

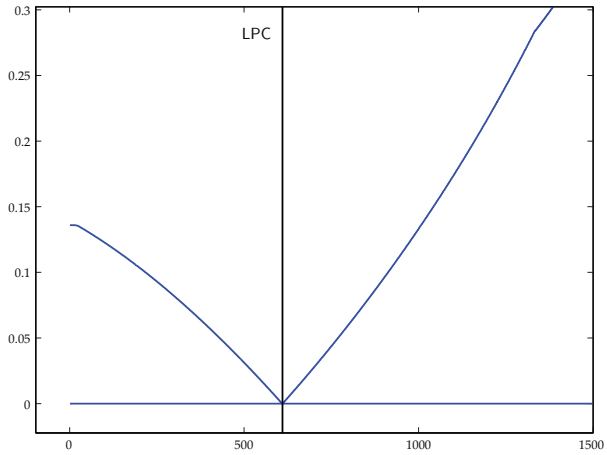

Figure 6.2: The two smallest singular values of $M(T) - I_n$.

As can be seen in Figure 6.1, an R1 point is detected in our periodically forced example. Due to the above remark, we will not attempt any normal form analysis for this point. We will analyze in detail all other detected codimension 2 points and report the normal form coefficients, computed as explained in Section 6.2.

The two Generalized Period-Doubling points

In Figure 6.1 the LPC2 curves are tangent to the PD1 curve in two different GPD points. In the first GPD point, with parameter values $(\varepsilon, b_0) = (0.319, 0.412)$, the Limit Point of Cycles curve is tangent to the subcritical Period-Doubling curve (type presented in Figure 4.2 (b)), while in the second one, for $(\varepsilon, b_0) = (1.093, 0.218)$,

the LPC2 curve is tangent to the supercritical part of the PD1 bifurcation curve (type presented in Figure 4.2 (a)).

Performing the computation of the GPD normal form coefficients at the first point, we obtain

- for the first equation of the GPD normal form (4.6) the two coefficients α_1 and α_2, up to a scaling term T and T^2 computed through formula (6.17) and (6.18) respectively, are zero, up to the accuracy of the computation.
- the normal form coefficient e of the second equation from (4.6), computed through formula (6.19), equals $e = -58.287$.

Notice that these results are in agreement with what we expected. Indeed, since we are in the case presented in Figure 4.2 (b), the normal form coefficient e is negative.

From the computation of the GPD normal form coefficients at the second critical point we obtain

- for the first equation of the GPD normal form (4.6) holds that the two coefficients α_1 and α_2 equal zero up to the accuracy of the computation.
- the value of the normal form coefficient in the second equation is $e = 41.544$.

Also in this case the obtained results are in agreement with the theory.

The Strong Resonance 1:2 points

We divide the Strong Resonance 1:2 points present in this model into two groups, namely the R2 point at $(\varepsilon, b_0) = (0.337, 0.340)$ and the cascade of resonance points in the right lower part of the graph.

The isolated R2 point forms the intersection of the NS1 curve, i.e. the supercritical Neimark-Sacker curve of a limit cycle with a period approximately equal to 1, and PD1. The situation is thus the one depicted in Figure 4.5 (a). Performing the normal form coefficient computation we obtain

- in the first equation of the R2 normal form (4.9) $\alpha = 0$.
- in the last equation of the R2 normal form we have $(a, b) = (3.401, -12.907)$.

Note that the obtained results are in accordance with the theory. Indeed, the absence of a secondary Neimark-Sacker curve implies that $a > 0$ and the supercriticality of the NS1 curve implies that $b < 0$.

In the lower right part of the bifurcation diagram a resonance cascade is present, which accumulates on the sequence of Period-Doubling curves. A zoom of this part is shown in Figure 6.3. Each resonance point of this cascade is a point of the type

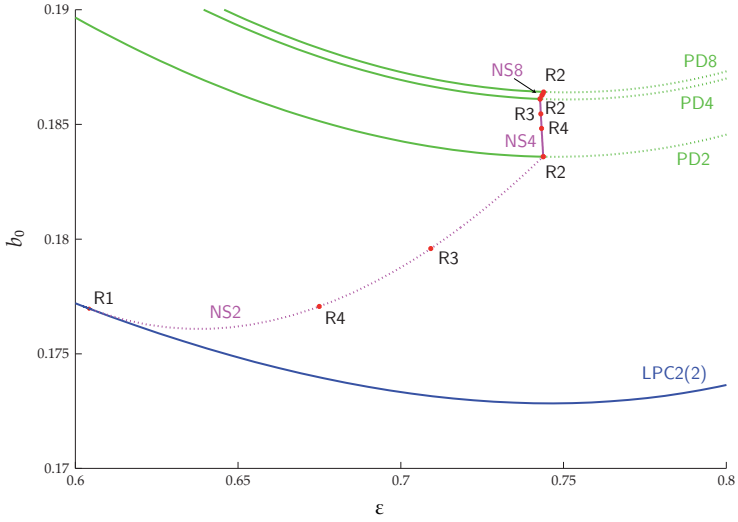

Figure 6.3: The resonance cascade in system (6.28). In blue are Limit Point of Cycles bifurcations, in green Period-Doubling bifurcations and in purple Neimark-Sacker bifurcations. Solid/dotted curves correspond to supercritical/subcritical bifurcations.

represented in Figure 4.5 (b) (so with $a < 0$ and the sign of b dependent on the criticality of the incoming Neimark-Sacker curve). Notice that the criticality of the NS curves changes at the R2 point (as depicted in Figure 4.5 (b)).

As first general result we observe that in the first equation of the R2 normal form (4.9) coefficient $\alpha = 0$ for all points (as expected since the system is periodically forced). We remark that for the calculation of the normal form coefficients in the ξ-equations, a computation to high accuracy is needed to get unambiguous results. The results are

(on PD2) In the R2 point $(\varepsilon, b_0) = (0.744, 0.184)$. To the left of the R2 point the PD2 curve is supercritical, to the right it is subcritical. The incoming NS2 curve is subcritical, while the outgoing NS4 curve is supercritical. We are thus in the

time reversed situation of Figure 4.5 (b). So we expect that $b > 0$ (subcritical incoming Neimarck-Sacker curve) and $a < 0$ (there is an outgoing secondary Neimarck-Sacker curve). The computed critical coefficients at the R2 point are $(a, b) = (-65.767, 16.267)$.

(on PD4) In the R2 point $(\varepsilon, b_0) = (0.743, 0.186)$. To the left of the R2 point the PD4 curve is supercritical, to the right it is subcritical. The incoming NS4 curve is supercritical, while the outgoing NS8 curve is subcritical. We are therefore in the situation depicted in Figure 4.5 (b). So we expect that $b < 0$ (supercritical incoming Neimarck-Sacker curve) and $a < 0$ (there is an outgoing secondary Neimarck-Sacker curve). The computed coefficients at the R2 point are $(a, b) = (-269.368, -18.151)$.

(on PD8) In the R2 point $(\varepsilon, b_0) = (0.744, 0.186)$. To the left of the R2 point the PD8 curve is supercritical, to the right it is subcritical. The incoming NS8 curve is subcritical, we are thus in the time reversed situation of Figure 4.5 (b). Thus, we expect that $b > 0$ (subcritical incoming Neimarck-Sacker curve) and $a < 0$ (there is an outgoing secondary Neimarck-Sacker curve, since the cascade continues). The computed critical coefficients at the R2 point are $(a, b) = (-921.701, 16.581)$.

All the obtained results are in agreement with the theory.

The Strong Resonance 1:3 points

There are two Strong Resonance 1:3 points, one on NS2, the other one on NS4, as can be seen in Figure 6.3. These two points behave in a different way. The Neimark-Sacker curve corresponding with the first R3 point at $(\varepsilon, b_0) = (0.709, 0.179)$ is subcritical, so we expect $\Re(c)$ to be positive (situation depicted in Figure 4.6 (b)). The Neimark-Sacker curve of the second point at $(\varepsilon, b_0) = (0.743, 0.185)$ is supercritical, so $\Re(c)$ should be negative (situation depicted in Figure 4.6 (a)). To check whether we are in a nondegenerate case, we also have to take the value of b into account, however, the sign of b is not relevant.

- for the first R3 point we have that $(b, \Re(c)) = (4.557 - 4.457i, 9.155)$.
- for the second R3 point we have that $(b, \Re(c)) = (0.405 + 12.143i, -8.820)$.

These results are in accordance with the theory.

The Strong Resonance 1:4 points

There are two Strong Resonance 1:4 points, one on NS2, the other one on NS4, as can be seen in Figure 6.3. These two points behave in the same way as the Strong Resonance 1:3 bifurcation points. The Neimark-Sacker curve corresponding with the first R4 point at $(\varepsilon, b_0) = (0.675, 0.177)$ is subcritical, so here we expect $\Re(A)$ to be positive. The Neimark-Sacker curve of the second R4 point at $(\varepsilon, b_0) = (0.743, 0.185)$ is supercritical, so $\Re(A)$ should be negative. Moreover, since those points are part of a resonance cascade, we should not have Limit Point bifurcations of nontrivial equilibria, so we are in region I of Figure 4.7. In order to assure that we are not in a degenerate case, we also need to check that $d \neq 0$.

- for the first R4 point it holds that $(c, d) = (11.624 - 84.897i, 65.072 + 92.254i)$, so $A = 0.103 - 0.752i$.
- for the second R4 point it holds that $(c, d) = (-8.580 - 414.721i, -416.641 - 489.172i)$, so $A = -0.01335 - 0.645i$.

The results are in accordance with the theory. For both bifurcation points the value of A belongs to region I of Figure 4.7.

6.3.2 The Steinmetz-Larter model

The following model of the peroxidase-oxidase reaction was studied by Steinmetz and Larter [91] and is used as test-example in [52, 68], i.e.

$$\begin{cases} \dot{A} = -k_1 ABX - k_3 ABY + k_7 - k_{-7} A, \\ \dot{B} = -k_1 ABX - k_3 ABY + k_8, \\ \dot{X} = k_1 ABX - 2k_2 X^2 + 2k_3 ABY - k_4 X + k_6, \\ \dot{Y} = -k_3 ABY + 2k_2 X^2 - k_5 Y, \end{cases} \tag{6.29}$$

where A, B, X, Y are state variables and k_1, k_2, k_3, k_4, k_5, k_6, k_7, k_8, and k_{-7} are parameters. We fix the parameters reported in the following table

Par.	Value	Par.	Value	Par.	Value	Par.	Value
k_1	0.1631021	k_2	1250	k_3	0.046875	k_4	20
k_5	1.104	k_6	0.001	k_{-7}	0.1175		

and we perform a bifurcation analysis in the remaining parameter space (k_7, k_8). A few curves are reported in Figure 6.4.

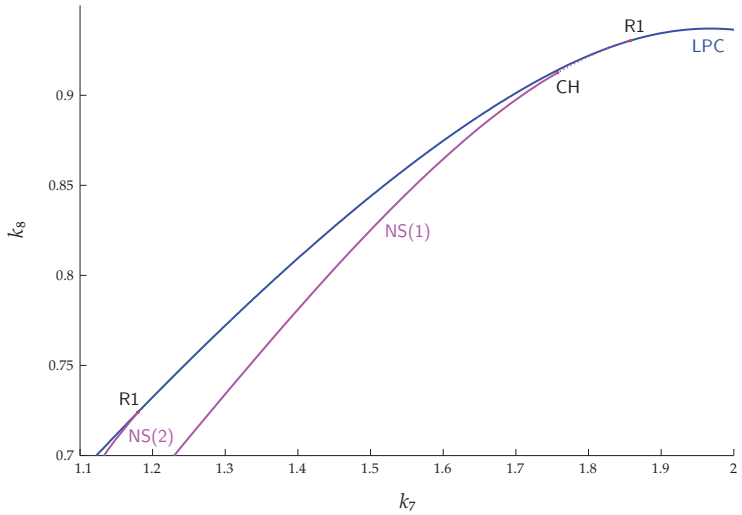

Figure 6.4: Bifurcation diagram of limit cycles in model (6.29). In blue are Limit Point of Cycles bifurcations and in purple Neimark-Sacker bifurcations. Solid/dotted curves correspond to supercritical/subcritical bifurcations.

The Strong Resonance 1:1 points

The two Strong Resonance 1:1 points behave differently, since in the left R1 point the Neimark-Sacker curve rooted at the bifurcation point is supercritical, while in the other one it is subcritical.

- for the R1 point in $(k_7, k_8) = (1.180, 0.724)$, the two coefficients of the last equation of the R1 normal form (4.8) are equal to $(a, b) = (-3.654 \cdot 10^{-3}, 0.735)$. Their product $ab = -2.686 \cdot 10^{-3}$ is negative, which corresponds with a supercritical NS curve rooted at the R1 point.

- for the R1 point in $(k_7, k_8) = (1.858, 0.930)$, the two coefficients of the last equation of the R1 normal form (4.8) are equal to $(a, b) = (-6.643 \cdot 10^{-2}, -2.157)$. Their product $ab = 0.143$ is positive, and indeed the NS curve rooted at the R1 point is subcritical.

So we can conclude that the results are in accordance with the theory.

The Chenciner points

In Figure 6.4 we see that a CH point is detected at $(k_7, k_8) = (1.757, 0.913)$. The critical coefficient at that bifurcation point equals $\Re(e) = 1.392$, hence positive. In order to verify if the normal form computation is correct, one might use tori continuation techniques [19, 36, 63, 76, 84, 85, 88]. However, these techniques are not stable near critical cases like the one we have. In order to validate our result we therefore rely on simulations.

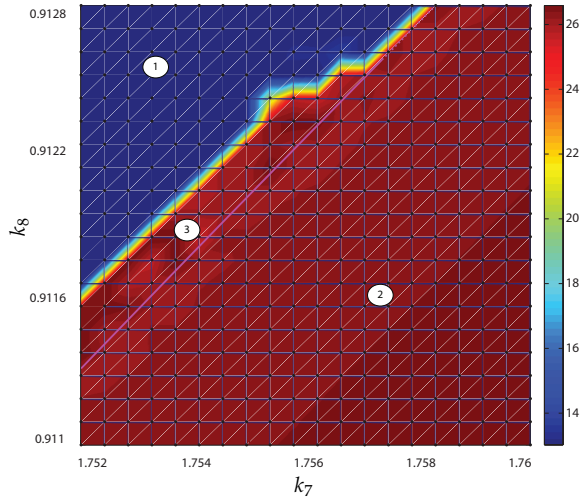

Figure 6.5: Simulations on a parameter grid (black points) of system (6.29). The purple solid/dotted line is the supercritical/subcritical Neimark-Sacker curve. The colour represents the value of the maximum of the first coordinate of the attractor reached through simulation from a point close to the limit cycle.

The obtained result is shown in Figure 6.5. The indicated regions correspond with the regions as denoted in Figure 4.3. The one point to which regions $1, 2$ and 3 are adjacent, corresponds with the CH point. The purple solid curve between regions 2 and 3 is the supercritical Neimark-Sacker curve, the purple dashed one between regions 1 and 2 is the subcritical Neimark-Sacker curve. For each point of the grid, we have started time integration from a point close to the orginal limit cycle (a 1 % perturbation) until an attractor was found. The maximum value of the

X-coordinate of an orbit with time length 1000 along the attractor is shown in the colormap. In region 2 this attractor is the original limit cycle, in region 3 it is the inner torus arisen through the supercritical Neimark-Sacker curve. In region 1 the original limit cycle is unstable, and so the trajectory that starts nearby converges to another attractor. Between regions 1 and 3 and regions 1 and 2 happens a catastrophic bifurcation, i.e. a drastic change of the attractor, identified from the change of color that varies from blue to red. Right above the Chenciner point, the catastrophic bifurcation is the subcritical NS curve, while left below it is the Limit Point of Tori (T_c) curve. Figure 6.5 gives evidence that the scenario that corresponds with a positive second Lyapunov coefficient is obtained.

6.3.3 The Lorenz-84 system

This model, taken from [78], is a meteorological model proposed by Lorenz in 1984 in order to describe the atmospheric circulation. The equations of the model are

$$\begin{cases} \dot{x} = -y^2 - z^2 - ax + aF, \\ \dot{y} = xy - bxz - y + G, \\ \dot{z} = bxy + xz - z, \end{cases} \tag{6.30}$$

where (a, b, F, G) are parameters. We fix $a = 0.25, b = 4$. This model, as found in [89,94], contains most of the analyzed codimension 2 bifurcations of limit cycles. We report in Figure 6.6 a bifurcation diagram recomputed and extended with MatCont in which the bifurcations of equilibria are thicker and the limit cycle bifurcations are thin. In particular, the blue curve is a Limit Point of Cycles bifurcation curve, the green ones are Period-Doubling bifurcation curves and the purple ones are Neimark-Sacker curves. The codimension 2 points are marked with a red dot, and from Figure 6.6 follows that almost all bifurcations where the dimension of the center manifold equals 2 or 3, except for the Chenciner bifurcation and the Fold-Flip bifurcation, are present in this model.

The Swallow-tail bifurcation

The first degeneracy we analyze is the vanishing of the coefficient c in the CPC normal form (4.5). This bifurcation, called the **Swallow-tail bifurcation**, is in our case characterized by the collision and disappearance of two Cusp Point of Cycles bifurcations. In order to capture this codimension 3 bifurcation we analyze part of the blue curve in Figure 6.6 for different parameter values of b. The result is

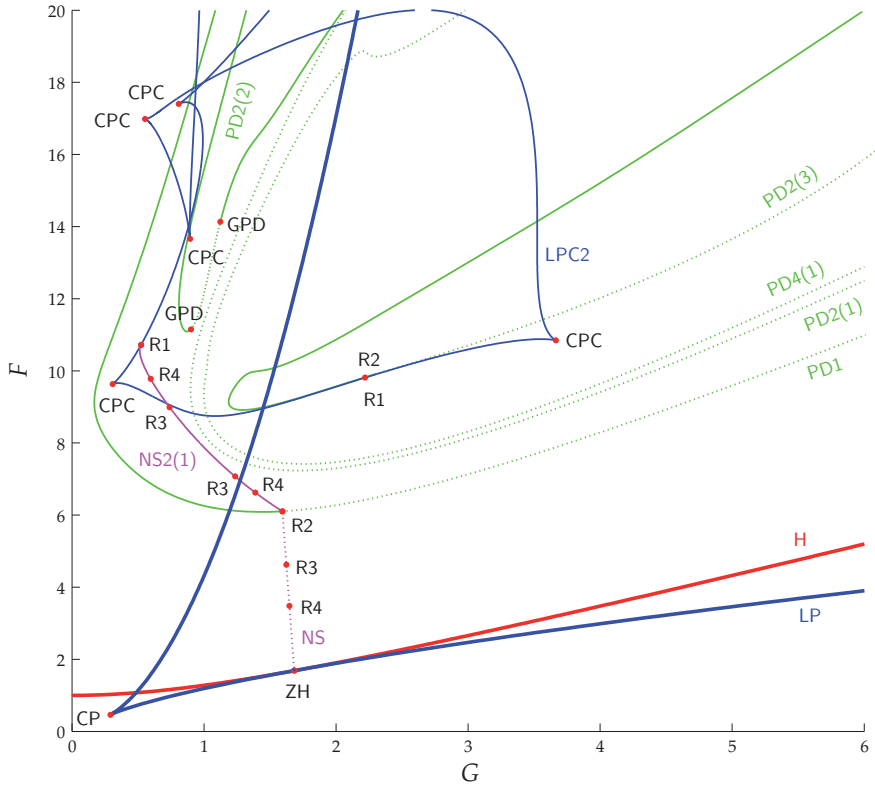

Figure 6.6: Bifurcation diagram of model (6.30). The thick curves are bifurcation curves of equilibria, the thin curves are bifurcation curves of limit cycles (in blue Limit Point of Cycles curves, in green Period-Doubling curves and in purple Neimark-Sacker curves). Solid/dotted curves correspond to supercritical/subcritical bifurcations.

shown in Figure 6.7. Part of the LPC-branch is plotted in the (G, F)-plane for several values of the parameter $b \in [2.91, 2.95]$ (from red to blue). In the table we can see the behaviour of the critical coefficient c (i.e. c_1 and c_2 for the two CPC points), where it exists (the colours from the table correspond with the ones from the bifurcation diagram). Note how the behaviour of this codim 3 bifurcation is captured by a smooth vanishing of the normal form coefficient.

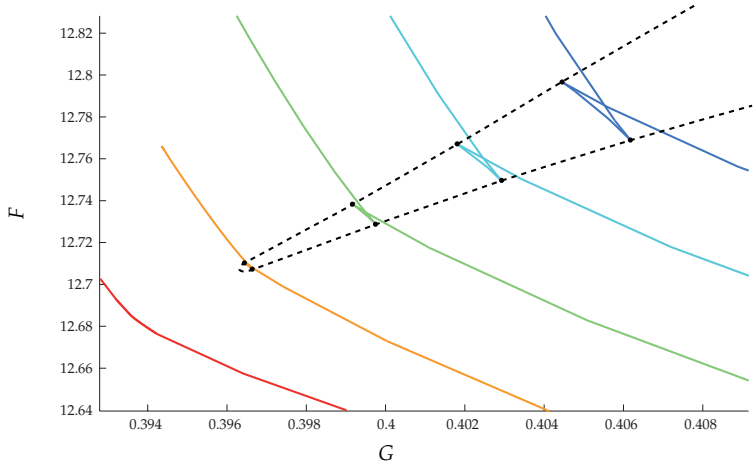

b	$(G,F)_1$	c_1	$(G,F)_2$	c_2
2.95	(0.406176,12.76893)	16.4570	(0.40445,12.79664)	-8.83567
2.94	(0.402934,12.74929)	13.3315	(0.40183,12.76712)	-7.77721
2.93	(0.399746,12.72891)	10.0534	(0.39917,12.73840)	-6.47271
2.92	(0.396624,12.70759)	6.30503	(0.39643,12.71071)	-4.67510
2.91				

Figure 6.7: Different Limit Point of Cycles bifurcation curves in the (G,F)-plane for different values of the parameter b. The parameter values are reported in the table.

The Generalized Period-Doubling points

On the green curve PD2(2) from Figure 6.6 there are two Generalized Period-Doubling points. Computing the normal form coefficient in the first GPD point, with parameter values $(G,F) = (0.900, 11.145)$, gives $e = -1.318 \cdot 10^{-3} < 0$. Therefore, there is a Limit Point of Cycles bifurcation curve that starts rightward tangent to the subcritical part of the Period-Doubling curve. In the second case, namely for $(G,F) = (1.124, 14.129)$, $e = 2.895 \cdot 10^{-3} > 0$, and so the LPC curve starts rightward tangent to the supercritical part of the PD curve. These conclusions following from the normal form analysis are clarified in Figure 6.8; in the upper panels the Poincaré maps of the limit cycles involved in the bifurcation are sketched. In region 0 there is a stable $2T$-periodic cycle. In region 1 the $2T$-periodic cycle becomes unstable and a stable $4T$-periodic curve appears. In region 2 we still

have this stable $4T$-curve, but a second (unstable) $4T$-periodic cycle appears and the $2T$-cycle becomes stable. We then cross the upper right PD2(2) curve such that another stable $4T$-periodic cycle appears. On the LPC4(2) curve the red limit cycle and the inner green limit cycle from region 3 collide and disappear, while on the LPC4(1) curve the two involved limit cycles from region 2 collide and disappear.

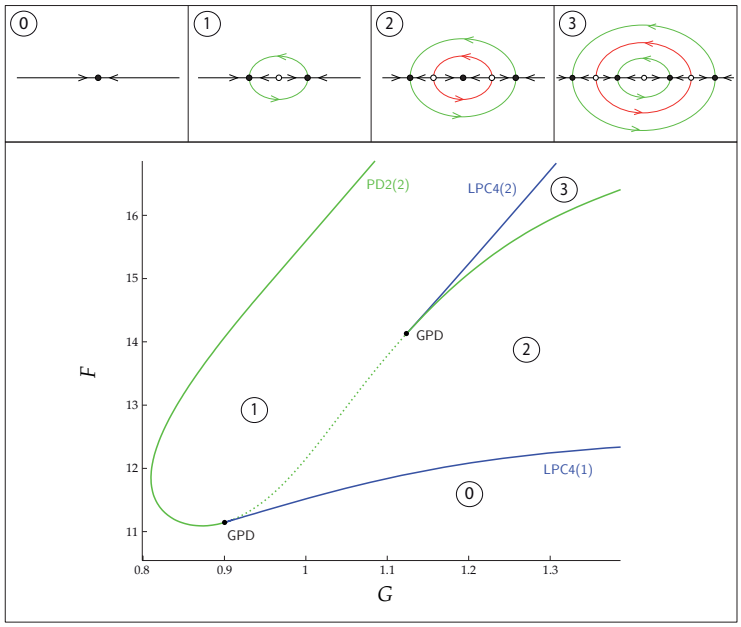

Figure 6.8: Two Generalized Period-Doubling points with different sign of normal form coefficients on the Period-Doubling bifurcation curve PD2(2) of Figure 6.6.

The Strong Resonance 1:1 points

Two R1 points are located on the LPC2 curve. These two points should have different products of normal form coefficients. In fact, for the first one, where $(G, F) = (0.522, 10.718)$, the Neimark-Sacker curve NS2(1) rooted at the bifurcation point is supercritical (i.e. the situation depicted in Figure 4.4 (a)), while for the second one, where $(G, F) = (2.220, 9.811)$, NS2(2) is subcritical (see the zoom in

Figure 6.9).

- For the first R1 point $(a, b) = (2.577, -1.266)$, so the product $ab = -3.262$ is negative.
- For the second R1 point $(a, b) = (-9.887, -2.005)$, so the product $ab = 19.819$ is positive.

These results are in accordance with the theory.

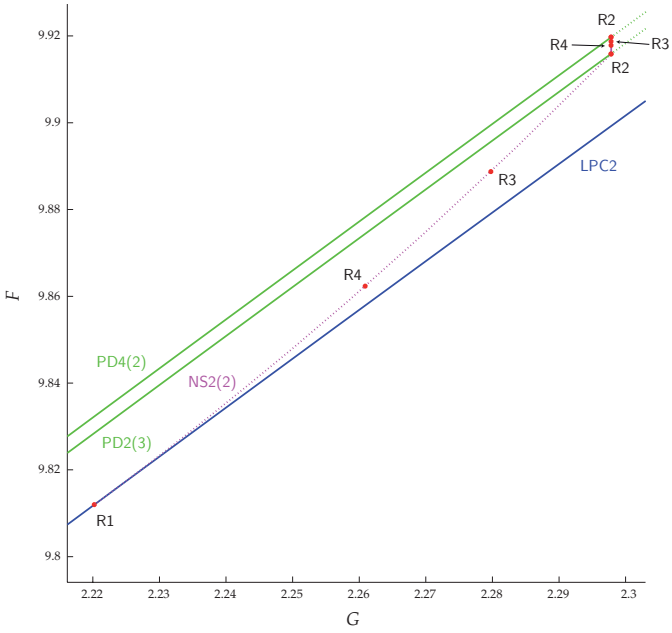

Figure 6.9: Zoom on the resonance cascade that starts at the right R1 point in Figure 6.6. In blue are the Limit Point of Cycles bifurcation curves, in green the Period-Doubling curves, in purple the Neimark-Sacker curves. Solid/dotted curves correspond to supercritical/subcritical curves.

The Strong Resonance 1:2 points

At the R2 point at $(G, F) = (1.593, 6.106)$ shown in Figure 6.6, the incoming Neimark-Sacker curve NS is subcritical (therefore we must have $b > 0$), while the

outgoing curve NS2(1) (that exists and thus $a < 0$) is supercritical, i.e. we are in the time reversed case of Figure 4.5 (b). The coefficients computed at the R2 point are $(a, b) = (-0.633, 0.179)$, in accordance with what we expected.

At the R1 point located at $(G, F) = (2.220, 9.811)$ starts a resonance cascade, as shown in Figure 6.9. On the cascade we find many resonance points, which we will analyze in what follows. In particular, since the R2 points belong to a cascade, they are of the type presented in Figure 4.5 (b) (so $a < 0$), with at successive R2 points a change of criticality of the incoming NS curve. The NS2(2) curve born at the R1 point is subcritical, so for the first R2 point we expect that $b > 0$, while for the second one $b < 0$.

- For the first R2 point at $(G, F) = (2.298, 9.916)$ we have that $(a, b) = (-1.316, 0.111)$.
- For the second R2 point at $(G, F) = (2.298, 9.920)$ we have that $(a, b) = (-2.623, -5.641 \cdot 10^{-2})$.

The results are in accordance with the theory.

The Strong Resonance 1:3 points

There are several Strong Resonance 1:3 points at which we can have a closer look. There is one R3 point located on the NS curve and two R3 points are detected on the NS2(1) curve. The R3 bifurcation point corresponding to the first iterate happens at $(G, F) = (1.624, 4.628)$, with a positive normal form coefficient of the Neimark-Sacker bifurcation; this corresponds with the situation from Figure 4.6 (b). The R3 points corresponding to the second iterate are at $(G, F) = (1.235, 7.072)$ and $(G, F) = (0.739, 8.989)$, where the Neimark-Sacker bifurcation is in both cases supercritical, so we are in the situation depicted in Figure 4.6 (a).

- For the R3 point at $(G, F) = (1.624, 4.628)$ we have that $(b, \Re(c)) = (0.191 - 0.546i, 6.186 \cdot 10^{-2})$.
- For the R3 point at $(G, F) = (1.235, 7.072)$ we have that $(b, \Re(c)) = (-0.446 - 0.190i, -3.612 \cdot 10^{-2})$.
- For the R3 point at $(G, F) = (0.7394, 8.989)$ we have that $(b, \Re(c)) = (-0.129 + 1.681 \cdot 10^{-2}i, -1.951 \cdot 10^{-2})$.

All these results are in accordance with the theory.

There are also R3 points on the cascade, shown in Figure 6.9. The first one corresponds with a subcritical NS2(2) curve, while the second one corresponds with a supercritical Neimark-Sacker curve.

- For the first R3 point at $(G, F) = (2.279, 9.889)$ we have that $(b, \Re(c)) = (-2.958 - 0.360i, 0.738)$.
- For the second R3 point at $(G, F) = (2.297, 9.919)$ we have that $(b, \Re(c)) = (2.745 + 3.539i, -0.385)$.

Also in this case all results are in accordance with the theory.

The Strong Resonance 1:4 points

There are five 1:4 resonance points at which we will have a closer look. One is located on the NS curve, two others on the NS2(1) curve and the last two lie on the resonance cascade (see Figure 6.9).

- For the R4 point at $(G, F) = (1.647, 3.376)$ we have that $(c, d) = (5.0045 \cdot 10^{-2} - 7.459 \cdot 10^{-2}i, 0.110 + 0.534i)$ and so $A = 9.179 \cdot 10^{-2} - 0.137i$ (subcritical NS curve, case I).
- For the R4 point at $(G, F) = (0.595, 9.777)$ we have that $(c, d) = (-1.513 \cdot 10^{-2} - 0.135i, -2.665 \cdot 10^{-2} - 4.112 \cdot 10^{-2}i)$ and so $A = -0.308 - 2.753i$ (supercritical NS curve, case VIII).
- For the R4 point at $(G, F) = (1.390, 6.620)$ we have that $(c, d) = (-4.172 \cdot 10^{-2} - 0.992i, -0.428 - 1.082i)$ and so $A = -3.584 \cdot 10^{-2} - 0.852i$ (supercritical NS curve, case I).

For the first and the last point no further bifurcation analysis is possible to confirm the correctness of the results since the curves rooted at the bifurcation point are global bifurcations of limit cycles. Instead, it is possible to continue all local bifurcations of limit cycles rooted at the second R4 point, obtaining the result shown in Figure 6.10. The meaning of the curve T^{in} is explained in Section 4.4.2 and shown in the bifurcation diagram of the R4 point, see Figure 4.9. Curve T corresponds with the Fold bifurcation of the $4T$-periodic cycle that happens on the 'big' cycle. For curve T^{in}, the fold bifurcation happens in the 'big' cycle. Curve NS (NS4)

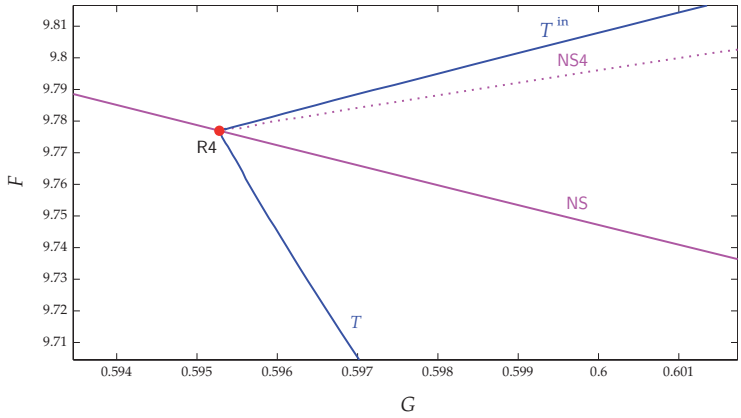

Figure 6.10: Bifurcation diagram at the R4 point at $(G, F) = (0.595, 9.777)$. In blue are the Limit Point of Cycles bifurcation curves, in purple the Neimark-Sacker curves. Solid/dotted curves correspond to supercritical/subcritical curves.

corresponds with curve N (N') from Figure 4.9. Note that we have not made the distinction between region VII and region VIII.

The first R4 point of the resonance cascade lies on a subcritical NS2(2) curve, while the second one lies on a supercritical Neimark-Sacker curve (see Figure 6.9). Moreover, since they are part of a cascade, we expect them to be of type I.

- For the first R4 point at $(G, F) = (2.298, 9.916)$ we have that $(c, d) = (5.185 \cdot 10^{-2} - 1.763i, -2.014 + 0.455i)$ and so $A = 2.510 \cdot 10^{-2} - 0.854i$.
- For the second R4 point at $(G, F) = (2.298, 9.919)$ we have that $(c, d) = (-2.821 \cdot 10^{-2} - 6.815i, -10.845 + 2.146i)$ and so $A = -2.550 \cdot 10^{-3} - 0.616i$.

Both points indeed belong to region I.

6.3.4 The extended Lorenz-84 system

As done in [73], it is possible to extend the Lorenz-84 system (6.30) by adding a fourth variable that takes the influence on the jet stream and the baroclinic waves of external parameters like the temperature of the sea surface into account. The

resulting system is

$$\begin{cases} \dot{x} = -y^2 - z^2 - ax + aF - \gamma u^2, \\ \dot{y} = xy - bxz - y + G, \\ \dot{z} = bxy + xz - z, \\ \dot{u} = -\delta u + \gamma ux + K. \end{cases} \tag{6.31}$$

We use the parameter values mentioned in [73], i.e.

$$a = 0.25,\ b = 1,\ G = 0.2,\ \delta = 1.04,\ \gamma = 0.987, F = 1.75,\ K = 0.0003.$$

Time integrating this system from the origin leads to the detection of a stable limit cycle. In a continuation with K as free system parameter the limit cycle undergoes a supercritical Period-Doubling bifurcation. Now, we can perform a two parameter continuation of PD bifurcations in (F, K) and obtain the bifurcation diagram reported in Figure 6.11 (cf. [73]).

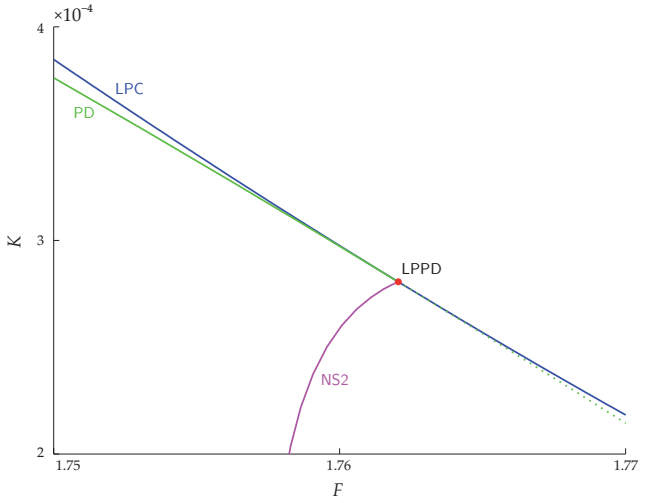

Figure 6.11: Bifurcation diagram of limit cycles in model (6.31). The blue curve is a Limit Point of Cycles curve, the green one is a Period-Doubling curve (solid/dotted parts correspond to supercritical/subcritical parts) and the purple curve is a supercritical Neimark-Sacker bifurcation curve of the period doubled limit cycle.

The Fold-Flip point

As can be seen in Figure 6.11, a Fold-Flip point is detected for $(F, K) = (1.762, 2.806 \cdot 10^{-4})$. Since there is a Neimark-Sacker curve of the period doubled limit cycle rooted at the bifurcation point and the NS2 curve (corresponding with curve NS from Figure 4.10) and the LPC curve (corresponding with curve F from Figure 4.10) lie on different sides of the PD curve (corresponding with curve P from Figure 4.10), we are in the situation represented in Figure 4.10 (a), i.e. we have $a_{20}b_{11} < 0$ and $a_{02}b_{11} < 0$. Moreover, since the NS2 curve is supercritical, C_{NS} should be negative. Numerically, we obtain that $b_{11} = 562.222$, $a_{20} = -0.576$, $a_{02} = -1.784 \cdot 10^{-5}$, $C_{NS} = -1.076 \cdot 10^{7}$. Hence, these results are in agreement with the theory. They also agree with [73], where the LPPD bifurcation was analyzed by computing the normal form coefficients for the critical Poincaré map, using the numerical integration of the variational equations to compute the multilinear forms in the Taylor expansion of this map.

6.3.5 Laser model

In [97] a single-mode inversionless laser with a three-level phaser was studied and shown to operate in various modes. These modes are 'off' (nonlasing), continuous waves, periodic, quasi-periodic and chaotic lasing. The model is a 9-dimensional system given by 3 real and 3 complex equations, namely

$$\begin{cases} \dot{\Omega}_l = -\frac{\gamma_{cav}}{2}\Omega_l - g\Im(\sigma_{ab}), \\ \dot{\rho}_{aa} = R_a - \frac{i}{2}(\Omega_l(\sigma_{ab} - \sigma_{ab}^*) + \Omega_p(\sigma_{ac} - \sigma_{ac}^*)), \\ \dot{\rho}_{bb} = R_b + \frac{i}{2}\Omega_l(\sigma_{ab} - \sigma_{ab}^*), \\ \dot{\sigma}_{ab} = -(\gamma_1 + i\Delta_l)\sigma_{ab} - \frac{i}{2}(\Omega_l(\rho_{aa} - \rho_{bb}) - \Omega_p\sigma_{cb}), \\ \dot{\sigma}_{ac} = -(\gamma_2 + i\Delta_p)\sigma_{ac} - \frac{i}{2}(\Omega_p(2\rho_{aa} + \rho_{bb} - 1) - \Omega_l\sigma_{cb}^*), \\ \dot{\sigma}_{cb} = -(\gamma_3 + i(\Delta_l - \Delta_p))\sigma_{cb} - \frac{i}{2}(\Omega_l\sigma_{ac}^* - \Omega_p\sigma_{ab}), \end{cases} \tag{6.32}$$

with $R_a = -0.505\rho_{aa} - 0.405\rho_{bb} + 0.45, R_b = 0.0495\rho_{aa} - 0.0505\rho_{bb} + 0.0055$ and $\Delta_l = \Delta_{cav} + g\Re(\sigma_{ab})\Omega_l$. The fixed parameters are $\gamma_1 = 0.275, \gamma_2 = 0.25525$, $\gamma_3 = 0.25025, \gamma_{cav} = 0.03, g = 100, \Delta_p = 0$. The parameters Ω_p and Δ_{cav} are varied. The bifurcation diagram of (6.32) is computed in [72] and is reproduced in Figure 6.12.

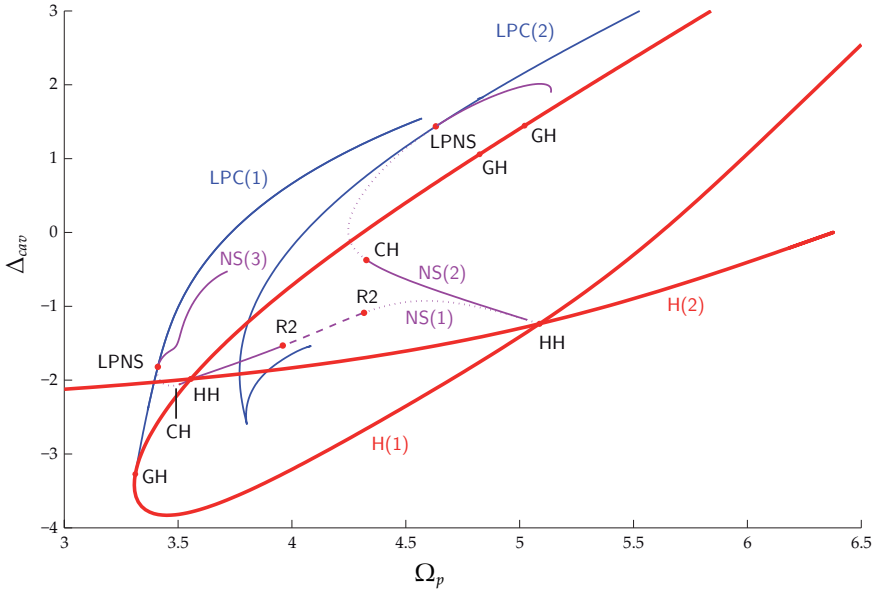

Figure 6.12: Bifurcation diagram of (6.32). The thick red curves are Hopf curves. In blue are Limit Point of Cycles bifurcations and in purple Neimark-Sacker bifurcations. Solid/dotted curves correspond to supercritical/subcritical bifurcations. The dashed curves are curves of neutral saddles.

The Limit Point-Neimark-Sacker points

Figure 6.12 shows three NS curves NS(1), NS(2) and NS(3) starting from two HH points. On NS(3) one of the richer situations possible at an LPNS point occurs. The normal form coefficients for the LPNS point at $(\Omega_p, \Delta_{cav}) = (3.411, -1.819)$ are $(s, \theta, E) = (1, -0.139, -911.248)$, so $s\theta < 0$. This means that there exists a 3-torus, which is stable since $\theta < 0$ and $E < 0$. Therefore, we are in the case represented in Figure 4.11 (c), but with a stable 3-torus. We will make use of Lyapunov exponents to check the validity of our calculations for the critical coefficients. For the computation of the Lyapunov exponents, we used a code written by V. N. Govorukhin (2004). We fix one parameter, in this case Ω_p, and vary the second one, in this case Δ_{cav}, where we stay in a close neighbourhood to the LPNS point, and compute the Lyapunov exponents for the considered range of parameter values. Figure 6.13 (a) shows the calculated Lyapunov exponents for Ω_p fixed at 3.45 and $\Delta_{cav} \in [-1.8; -1.6]$. More detail is shown in Figure 6.13 (b), where we get a clear view on the number of Lyapunov exponents equal to zero.

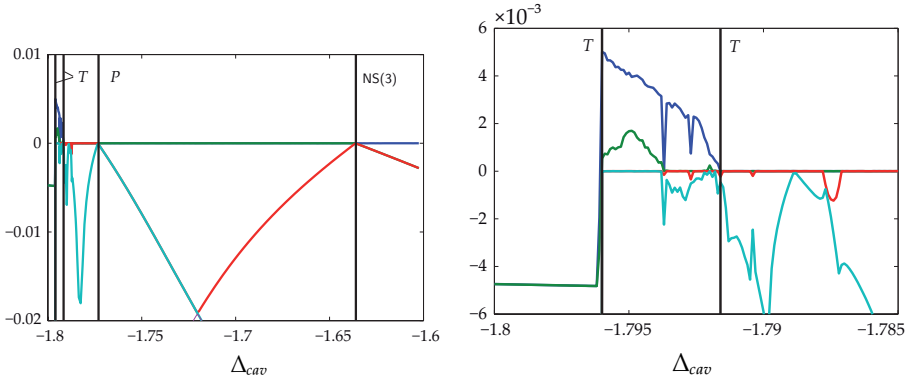

(a) (b)

Figure 6.13: Lyapunov exponents computed for $\Omega_p = 3.45$ close to the LPNS point at $(\Omega_p, \Delta_{cav}) = (3.411, -1.819)$: (a) For $\Delta_{cav} \in [-1.8; -1.6]$. (b) Zoomed in near the region with chaos due to heteroclinic tangles. The vertical black lines indicate the parameter values where a bifurcation occurs.

We now discuss Figure 6.13. For Δ_{cav} values to the right of -1.636, there is

one Lyapunov exponent equal to zero, which corresponds to the stable limit cycle from region 6 in Figure 4.11 (c). At $\Delta_{cav} = -1.636$, we cross NS(3) and arrive in region 5 from Figure 4.11 (c) where there is a stable 2-torus and therefore two Lyapunov exponents equal to zero. When crossing the P curve at $\Delta_{cav} = -1.773$, the stable 3-torus from region 4 arises, so we expect three Lyapunov exponents to be zero. However, remark that in some small intervals only two Lyapunov exponents are equal to zero (see Figure 6.13), but these correspond with resonances on the 3-torus. Then, in the interval $\Delta_{cav} \in [-1.796; -1.7916]$ positive Lyapunov exponents appear, which indicates that there is chaos. This zone corresponds with T. In fact, curve T from Figure 4.11 is a small zone. Finally, to the left of -1.796, we arrive in region 3, where all Lyapunov exponents are negative.

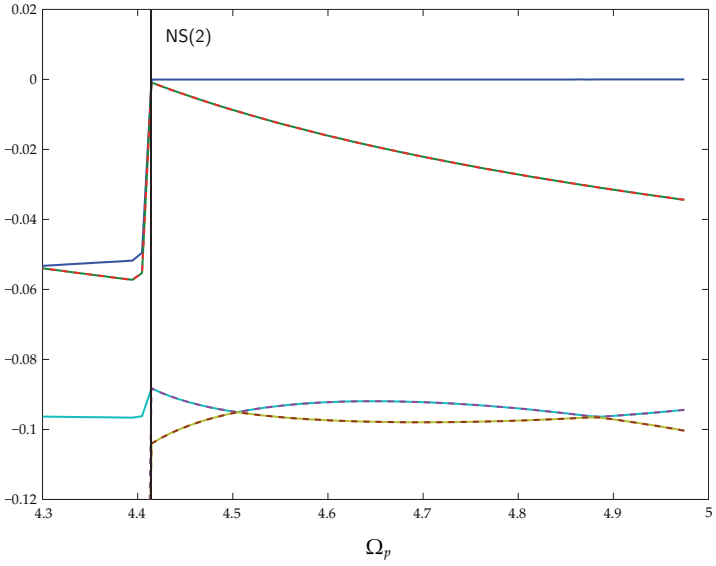

Figure 6.14: Lyapunov exponents computed close to the LPNS point at $(\Omega_p, \Delta_{cav}) = (4.632, 1.438)$. The two-coloured dashed lines reveal pairs of equally large Lyapunov exponents.

On the NS(2) curve there is an LPNS point for $(\Omega_p, \Delta_{cav}) = (4.632, 1.438)$. The normal form coefficients are $(s, \theta, E) = (1, 0.206, 808.009)$. The product $s\theta > 0$ is positive, so we are in a 'simple' case, where no 3-torus is present. Since $s = 1$, the

torus arisen through the Neimark-Sacker curve exists below the NS(2) curve (see Figure 4.11 (a)). We compute the Lyapunov exponents for a straight line where the beginning point $(\Omega_p, \Delta_{cav}) = (4.302, 0.673)$ and end point $(\Omega_p, \Delta_{cav}) = (4.984, 1.984)$ lie between the curves LPC(2) and NS(2), the first one to the left and the second one to the right of the LPNS point. In Figure 6.14, we plot the Lyapunov exponents for $\Omega_p \in [4.3, 4.98]$. The stable limit cycle is situated in the upper wedge between the LPC(2) and NS(2) curves, which corresponds to region 4 in Figure 4.11 (a), so there is one Lyapunov exponent equal to zero for Ω_p values larger than the subcritical NS(2) curve (i.e. for regions 3 and 4). At $\Omega_p \approx 4.41$, we cross the subcritical NS(2) curve, with to the left no zero Lyapunov exponents.

6.3.6 A two-patch periodic predator-prey model

We study a simple two-patch predator-prey system with periodic (seasonal) forcing. Simple predator-prey models lead to the 'paradox of enrichment', i.e. increasing the carrying capacity of the prey ultimately leads to extinction of the population [87]. Outside the laboratory, however, stable populations are observed and not an extinction. Here, spatial models have been put forward to explain this discrepancy. As the simplest spatial case, one may consider a two-patch predator-prey model [61] where predator and prey can migrate between the two patches by diffusion. This leads to a diffusive instability of large oscillations and stabilizes the total population size [62]. Here, we propose an extension where one of the patches experiences seasonal influences while the other can be seen as a wild-life refuge where human intervention minimizes seasonal influences. As a simplication we will only consider the case that the predators can move between the patches, i.e. they can cross the refuge barrier. On a proper time scale, the investigated system is defined by

$$\begin{cases} \dot{x}_1 = r_1 x_1(1-x_1) - \dfrac{c x_1 x_2}{x_1 + b_1(1+\varepsilon v_1)}, \\ \dot{x}_2 = -x_2 + \dfrac{c x_1 x_2}{x_1 + b_1(1+\varepsilon v_1)} + \gamma(y_2 - x_2), \\ \dot{y}_1 = r_2 y_1(1-y_1) - \dfrac{c y_1 y_2}{y_1 + b_2}, \\ \dot{y}_2 = -y_2 + \dfrac{c y_1 y_2}{y_1 + b_2} + \gamma(x_2 - y_2), \\ \dot{v}_1 = -v_2 + v_1(1 - v_1^2 - v_2^2), \\ \dot{v}_2 = v_1 + v_2(1 - v_1^2 - v_2^2). \end{cases} \tag{6.33}$$

The values of x_1 and x_2 denote the numbers of individuals (or densities) respectively of prey and predator populations living outside the refuge and y_1 and y_2 are the corresponding numbers or densities inside. The intrinsic growth rates r_i and the constant attack rate c are parameters of the model. For the predator outside the refuge, the Holling type II is chosen as functional response with a half saturation that varies periodically with period 2π. To this end, the last two equations are introduced; their solutions converge to a stable limit cycle $v_1(t) = \cos(t + \phi)$ with a phase shift ϕ depending on the initial conditions. The terms with parameter γ describe the coupling of the two patches. The fixed parameter values are $r_1 = 1$, $r_2 = 1, b_1 = 0.4, \gamma = 0.1, c = 2$. We will use the half saturation b_2 as a continuation parameter together with the amplitude of the seasonal forcing ε. We observe that a refuge can induce complex behaviour in a spatial population model with seasonal forcing.

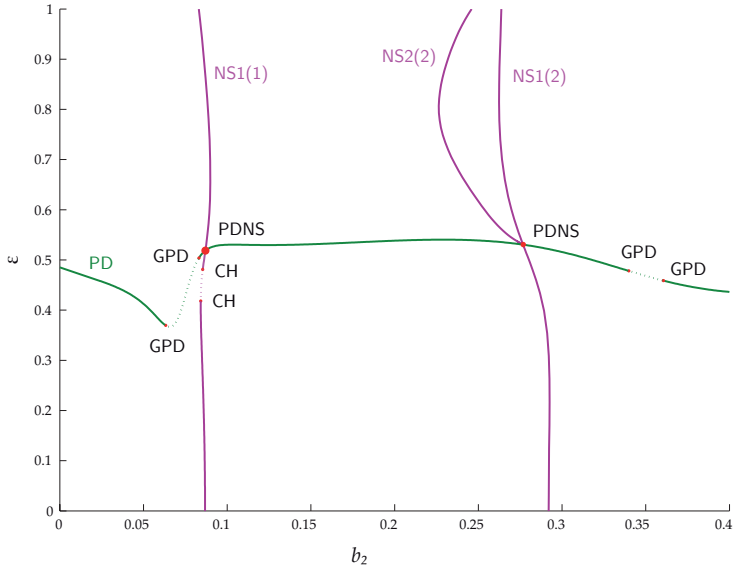

Figure 6.15: Bifurcation diagram of limit cycles in (6.33). In green are Period-Doubling curves and in purple Neimark-Sacker curves (of the first or of the second iterate, respectively labeled with NS1 and NS2).

The Period-Doubling-Neimark-Sacker points

Figure 6.15 represents a bifurcation diagram for system (6.33) where two PDNS points are detected. The right PDNS point has parameter values $(b_2, \varepsilon) = (0.277, 0.530)$. We are in the 'simple' case of a PDNS point because the product of the coefficients $p_{11} = -5.01 \cdot 10^{-2}$ and $p_{22} = -0.211$ is positive. Since $\theta = -0.320$ and $\delta = 1.087$, Figure 4.12 (a) indicates that the bifurcation diagram in a neighbourhood of the PDNS point is as in case III in Figure 4.13 (a), where $\mu_1 = 0$ corresponds with NS1(2) and $\mu_2 = 0$ with PD. Curve T_1 corresponds to the Neimark-Sacker curve of the period doubled cycle NS2(2) from Figure 6.15. Therefore, we expect the Period-Doubling curve T_2 of the torus to be situated to the left of NS1(2) and under the PD curve. The stable limit cycles are situated in the lower right quadrant of the PDNS point. The exact location of T_2 can be determined by computing Lyapunov exponents for fixed b_2 values smaller than the critical $b_2 = 0.277$ corresponding with the PDNS point. We have plotted a sketch of this T_2 curve in Figure 6.16, which represents a zoom of the neighbourhood of the PDNS point.

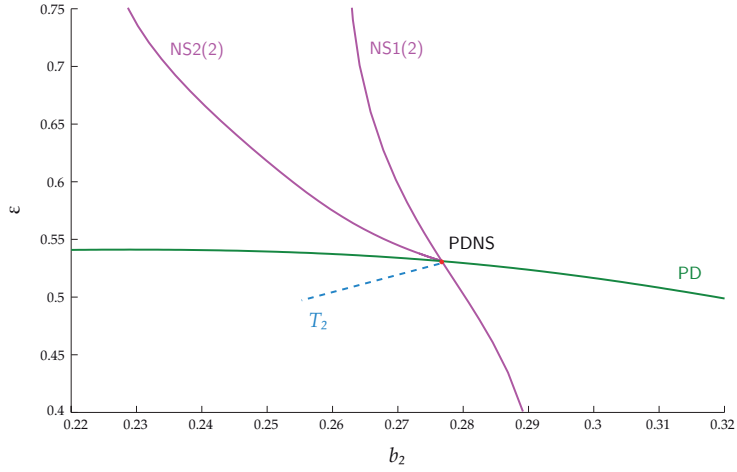

Figure 6.16: Zoom of the neighbourhood of the PDNS point at $(b_2, \varepsilon) = (0.277, 0.530)$ from Figure 6.15. In green are Period-Doubling curves, in purple Neimark-Sacker curves (of the first or of the second iterate, respectively labeled with NS1(2) and NS2(2)), in blue is the sketch of the T_2 'curve'.

We have computed the Lyapunov exponents for b_2 fixed at 0.261 and $\varepsilon \in [0.46; 0.62]$, see Figure 6.17. In this figure the black vertical lines indicate the position of the bifurcation curves. From the value of the Lyapunov exponents we derive that T_2 is crossed for $\varepsilon \approx 0.52$. To the left of the T_2 curve in Figure 6.17, we have a stable torus, arisen through the supercritical Neimark-Sacker curve NS1(2), corresponding with region 2 from Figure 4.13 (b). Between the curves T_2 and NS2(2), the 2-torus arisen through T_2 is attracting. These regions correspond with region 6 (between T_2 and PD) and region 5 (between PD and NS2(2)) from Figure 4.13 (b). When crossing the NS2(2) curve, the 2-torus disappears and the period doubled cycle becomes attracting. All this is in agreement with the fact that two Lyapunov exponents are equal to zero to the left of NS2(2), where afterwards only one zero Lyapunov exponent is left.

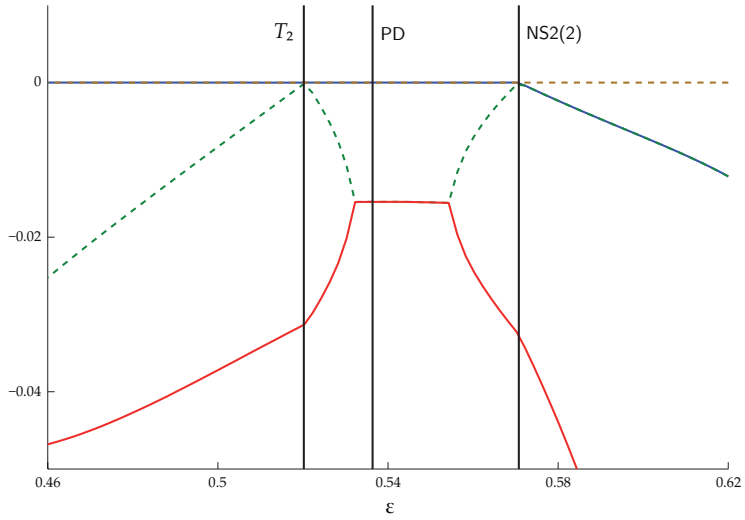

Figure 6.17: Lyapunov exponents computed for $b_2 = 0.261$, close to the PDNS point at $(b_2, \varepsilon) = (0.277, 0.530)$.

The left PDNS point at $(b_2, \varepsilon) = (8.699 \cdot 10^{-2}, 0.519)$ again belongs to one of the 'simple' situations that can happen at a PDNS point ($p_{11} = -0.447, p_{22} = -1.472$). The neighbourhood of the bifurcation point is as in case I in Figure 4.12 (a) since $(\theta, \delta) = (2.234, 1.304)$. Remark that the stable limit cycles are situated in the lower left quadrant of the PDNS point in Figure 6.18.

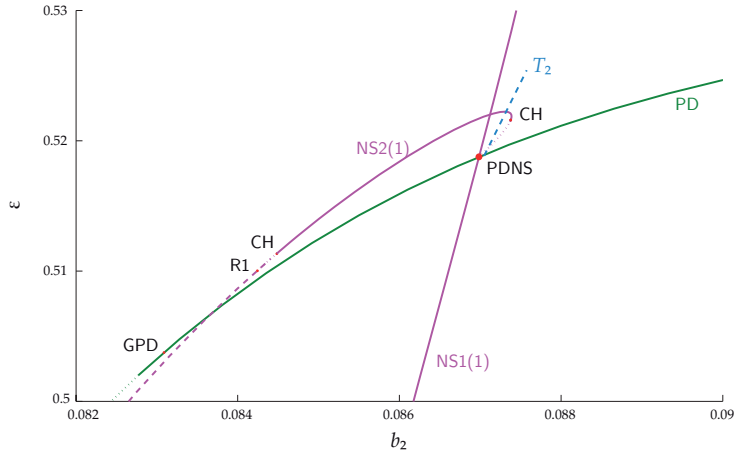

Figure 6.18: Zoom of the neighbourhood of the PDNS point at $(b_2, \varepsilon) = (8.699 \cdot 10^{-2}, 0.519)$ from Figure 6.15. In green are Period-Doubling curves, in purple Neimark-Sacker curves (of the first or of the second iterate, respectively labeled with NS1(1) and NS2(1)), in blue is the sketch of the T_2 'curve'.

The behaviour in a neighbourhood of this PDNS point can be derived from Figure 6.18, which includes a plot of the Neimark-Sacker curve NS2(1) of the period doubled cycle and also a sketch of the period doubled curve T_2 of the torus, made on the basis of the computation of the Lyapunov exponents. We have calculated the Lyapunov exponents for parameter values in the upper right quadrant, close to the PDNS point, for a fixed $b_2 = 0.08709$. The results are given in Figure 6.19.

Going from the left to the right, where we follow the solid lines, we start with two Lyapunov exponents equal to zero that correspond with the stable torus from the original cycle in the regions $2, 3$ and 4 from Figure 4.13. At the point where the second Lyapunov exponent becomes nonzero, the T_2 curve is located, namely at $\varepsilon \approx 0.5198$. We then arrive in region 12 from Figure 4.13 (b) where the 2-torus has lost his stability and the period doubled cycle is stable. Therefore, one zero Lyapunov exponent remains. We scan the Lyapunov exponents for a second time where we now go from the right to the left and follow the dashed lines. The second Lyapunov exponent now approaches zero not at the T_2 curve but at the NS2(1) curve. This is explained by the bistability happening in region 4, where one Lyapunov exponent equal to zero indicates the stable period doubled cycle and two

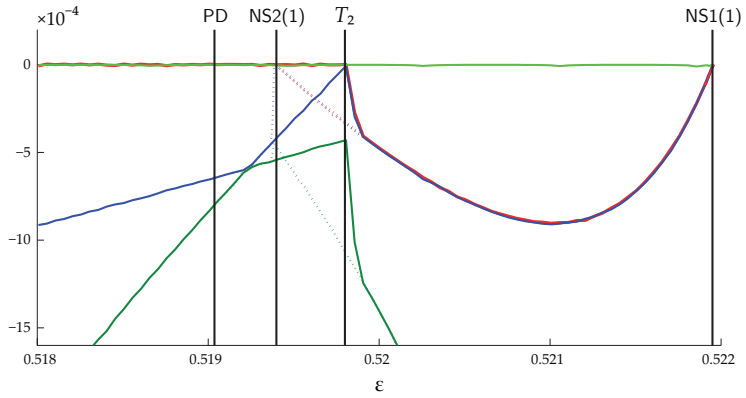

Figure 6.19: Lyapunov exponents computed for $b_2 = 0.08709$, close to the PDNS point at $(b_2, \varepsilon) = (8.699 \cdot 10^{-2}, 0.519)$. Exponents indicated with solid lines are computed by following the attractor with increasing ε, dotted lines with decreasing ε. This highlights the bistability between NS2(1) and T_2.

zero Lyapunov exponents indicate the stable torus. When we go further, we cross region 3 and 2, with the stable torus of the orginal cycle. Here too, the Lyapunov exponents corroborate the prediction based on the normal form coefficients.

Remark that since we deal with a periodically forced system the return time is independent of the distance from the limit cycle, so we could do this extra check. Indeed, for all PDNS points, the α_{ijk} in the first equation of the PDNS normal form (4.14) are zero up to the accuracy of the computation.

6.3.7 Control of vibrations

In [45] a two-mass system of which the main mass is excited by a flow-induced, self excited force is studied. A single mass that acts as a dynamic absorber is attached to the main mass and, by varying the stiffness between the main mass and the

absorber mass, represents a parametric excitation. The system is given by

$$\begin{cases} \dot{x}_1 = v_1, \\ \dot{x}_2 = v_2, \\ \dot{v}_1 = -k_1(v_1 - v_2) - Q^2(1 + \varepsilon y_1)(x_1 - x_2), \\ \dot{v}_2 = Mk_1(v_1 - v_2) + MQ^2(1 + \varepsilon y_1)(x_1 - x_2) - k_2 v_2 - x_2 + \beta V^2(1 - \gamma v_2^2)v_2, \\ \dot{y}_1 = -\eta y_2 + y_1(1 - y_1^2 - y_2^2), \\ \dot{y}_2 = \eta y_1 + y_2(1 - y_1^2 - y_2^2). \end{cases} \tag{6.34}$$

The following parameters are fixed: $\varepsilon = 0.1, k_2 = 0.1, \beta = 0.1, V = \sqrt{2.1}, \gamma = 4$, $Q = 0.95, M = 0.2$, k_1 and η will be the continuation parameters.

The Double Neimark-Sacker points

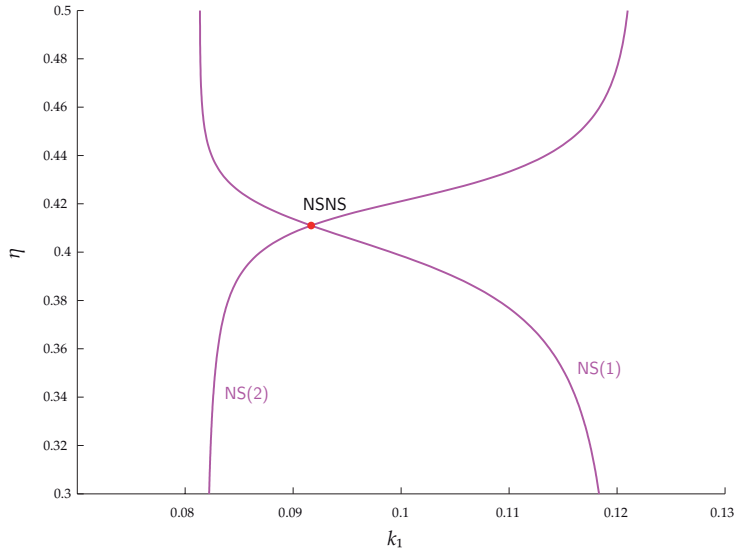

Figure 6.20: Partial bifurcation diagram of limit cycles in system (6.34). In purple are Neimark-Sacker curves.

An NSNS point is detected for $(k_1, \eta) = (9.167 \cdot 10^{-2}, 0.411)$, see Figure 6.20. The

normal form coefficients are

$$(p_{11}, p_{22}, \theta, \delta, \text{sign } l_1) = (-3.733 \cdot 10^{-3}, -6.494 \cdot 10^{-3}, 0.541, 1.203, 1).$$

The positive sign of the product $p_{11}p_{22}$ implies that we are in a 'simple' case that can happen at the NSNS point. Since $\delta > \theta$, the role of both coefficients has to be reversed. Therefore, the situation $\theta > 0, \delta < 0, \theta\delta < 1$ indicates that the NSNS bifurcation is located in region II in Figure 4.13 (a). As in the previous examples, we compute the Lyapunov exponents to check the obtained results of the normal form coefficients. We make the computations for k_1 fixed at 0.083 and $\eta \in [0.4; 0.42]$ (η values are between the NS curves). The results are shown in Figure 6.21.

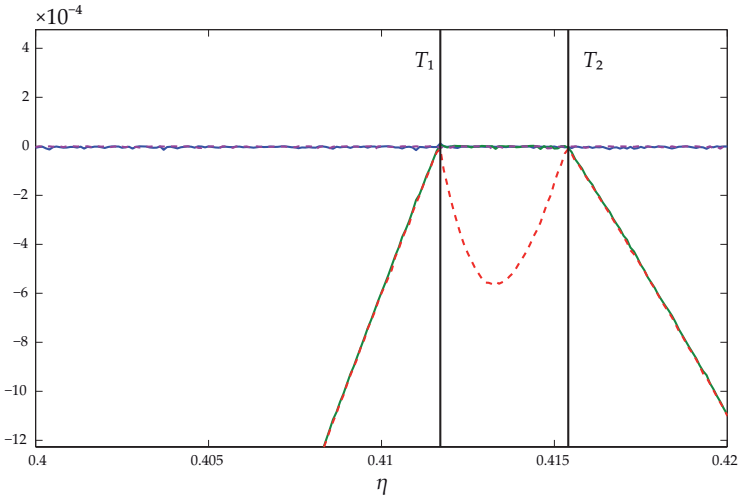

Figure 6.21: Lyapunov exponents computed for $k_1 = 0.083$ close to the NSNS point at $(k_1, \eta) = (9.167 \cdot 10^{-2}, 0.411)$.

For η values starting from 0.40, we are in region 3 (or 12 due to symmetry) in Figure 4.13 (b), where there is a stable 2-torus and thus two Lyapunov exponents equal to zero. A third Lyapunov exponent approaches zero and between $\eta \approx 0.4117$ and $\eta \approx 0.4154$ three Lyapunov exponents are equal to zero. This region denotes the appearance of a stable 3-torus and corresponds with region 5 from Figure 4.13 (b). The critical values of η correspond with the curves T_1 and T_2 in Figure 4.13 (a). For $\eta \geq 0.4154$, only a stable 2-torus remains and thus there are two zero Lyapunov

exponents. Therefore, the computed Lyapunov exponents are in agreement with the normal form coefficients.

6.4 Conclusion

In this chapter we discussed the implementation of the critical coefficients. The formulas for the normal form coefficients derived in Chapter 5 are directly suitable for numerical implementation using orthogonal collocation. They perfectly fit into a continuation context, where limit cycles and their bifurcations are computed using the BVP-approach, without numerical approximation of the Poincaré map or its derivatives. Being implemented into the Matlab toolbox MatCont [31, 32], the developed methods are freely available to assist an advanced two-parameter bifurcation analysis of dynamical systems generated by ODEs from various applications. The derivation of the normal form coefficients from Chapter 5 together with the extensive discussion of the implementation details in this chapter make an interested reader able to use the developed normal form theory and implement it in any (based on continuation) software.

We investigated numerous examples to check whether the bifurcation diagram, which we expect from the normal form analysis, corresponds with the bifurcation scenario obtained by a study around the bifurcation point in MatCont. Every codim 2 bifurcation of limit cycles was tested for and at each point the bifurcation study confirmed the results of the values of the normal form coefficients.

6.A Some results on differential-difference operators

In Section 6.2 we used the orthogonality with respect to the following inner product: if $\zeta_1, \zeta_2 \in \mathcal{C}^0([0,1], \mathbb{C}^n)$ and $\eta_1, \eta_2 \in \mathbb{C}^n$, then

$$\left\langle \begin{bmatrix} \zeta_1 \\ \eta_1 \end{bmatrix}, \begin{bmatrix} \zeta_2 \\ \eta_2 \end{bmatrix} \right\rangle = \int_0^1 \langle \zeta_1(t), \zeta_2(t) \rangle \, dt + \langle \eta_1, \eta_2 \rangle = \int_0^1 \zeta_1^{\mathrm{H}}(t)\zeta_2(t)dt + \bar{\eta}_1^{\mathrm{T}}\eta_2.$$

If this inner product vanishes, then we say that the corresponding vectors are orthogonal and write

$$\begin{bmatrix} \zeta_1 \\ \eta_1 \end{bmatrix} \perp \begin{bmatrix} \zeta_2 \\ \eta_2 \end{bmatrix}.$$

6.A. SOME RESULTS ON DIFFERENTIAL-DIFFERENCE OPERATORS

Below we list the propositions used in Section 6.2, with proofs of the statements.

Proposition 6.1. *Consider two differential-difference operators*

$$\phi_{1,2} : \mathcal{C}^1([0,1],\mathbb{R}^n) \to \mathcal{C}^0([0,1],\mathbb{R}^n) \times \mathbb{R}^n,$$

with

$$\phi_1(\zeta) = \begin{bmatrix} \dot{\zeta} - TA(t)\zeta \\ \zeta(0) - \zeta(1) \end{bmatrix}, \phi_2(\zeta) = \begin{bmatrix} \dot{\zeta} + TA^{\mathrm{T}}(t)\zeta \\ \zeta(0) - \zeta(1) \end{bmatrix}.$$

If $\zeta \in \mathcal{C}^1([0,1],\mathbb{R}^n)$, *then* $\zeta \in \mathrm{Ker}(\phi_1)$ *if and only if*

$$\begin{bmatrix} \zeta \\ \zeta(0) \end{bmatrix} \perp \phi_2(\mathcal{C}^1([0,1],\mathbb{R}^n)),$$

and $\zeta \in \mathrm{Ker}(\phi_2)$ *if and only if*

$$\begin{bmatrix} \zeta \\ \zeta(0) \end{bmatrix} \perp \phi_1(\mathcal{C}^1([0,1],\mathbb{R}^n)).$$

Proof. We will focus on the first assertion. If ζ lies in the kernel of ϕ_1, then $\dot{\zeta} - TA(t)\zeta = 0$ and $\zeta(0) - \zeta(1) = 0$. For all $g \in \mathcal{C}^1([0,1],\mathbb{R}^n)$ we have

$$\begin{aligned}
&\int_0^1 g^{\mathrm{T}}(t)\dot{\zeta}(t)dt - \int_0^1 Tg^{\mathrm{T}}(t)A(t)\zeta(t)dt = 0 \\
&\Rightarrow g^{\mathrm{T}}(t)\zeta(t)|_0^1 - \int_0^1 \dot{g}^{\mathrm{T}}(t)\zeta(t)dt - \int_0^1 Tg^{\mathrm{T}}(t)A(t)\zeta(t)dt = 0 \\
&\Rightarrow g^{\mathrm{T}}(1)\zeta(1) - g^{\mathrm{T}}(0)\zeta(0) - \int_0^1 (\dot{g}(t) + TA^{\mathrm{T}}(t)g(t))^{\mathrm{T}}\zeta(t)dt = 0 \\
&\Rightarrow -(g(0) - g(1))^{\mathrm{T}}\zeta(0) - \int_0^1 (\dot{g}(t) + TA^{\mathrm{T}}(t)g(t))^{\mathrm{T}}\zeta(t)dt = 0 \\
&\Rightarrow \left\langle \begin{bmatrix} \dot{g} + TA^{\mathrm{T}}(t)g \\ g(0) - g(1) \end{bmatrix}, \begin{bmatrix} \zeta \\ \zeta(0) \end{bmatrix} \right\rangle = 0.
\end{aligned}$$

Conversely, assume that $\left\langle \begin{bmatrix} \zeta \\ \zeta(0) \end{bmatrix}, \begin{bmatrix} \dot{g} + TA^{\mathrm{T}}(t)g \\ g(0) - g(1) \end{bmatrix} \right\rangle = 0$ for all $g \in \mathcal{C}^1([0,1],\mathbb{R}^n)$.

Then,

$$\begin{aligned}
&\int_0^1 \zeta^{\mathrm{T}}(t)(\dot{g}(t) + TA^{\mathrm{T}}(t)g(t))dt + \zeta^{\mathrm{T}}(0)(g(0) - g(1)) = 0 \\
&\Rightarrow \zeta^{\mathrm{T}}(1)g(1) - \zeta^{\mathrm{T}}(0)g(0) - \int_0^1 (\dot{\zeta}(t) - TA(t)\zeta(t))^{\mathrm{T}} g(t)dt \\
&\quad + \zeta^{\mathrm{T}}(0)(g(0) - g(1)) = 0 \\
&\Rightarrow -(\zeta(0) - \zeta(1))^{\mathrm{T}} g(1) - \int_0^1 (\dot{\zeta}(t) - TA(t)\zeta(t))^{\mathrm{T}} g(t)dt = 0.
\end{aligned}$$

If $\dot{\zeta}(t) - TA(t)\zeta(t) \neq 0$, then there exists a $g(t)$ with $g(1) = 0$ such that

$$\int_0^1 (\dot{\zeta}(t) - TA(t)\zeta(t))^{\mathrm{T}} g(t)dt \neq 0.$$

This is impossible, so $\dot{\zeta}(t) - TA(t)\zeta(t) = 0$. Hence $(\zeta(0) - \zeta(1))^{\mathrm{T}} g(1) = 0$ for all g; and thus there must hold that $\zeta(0) - \zeta(1) = 0$. From both observations it follows that $\zeta \in \mathrm{Ker}(\phi_1)$.

The proof of the second assertion is similar. □

Proposition 6.2. *Consider* $\phi_{1,2} : \mathcal{C}^1([0,1], \mathbb{R}^n) \to \mathcal{C}^0([0,1], \mathbb{R}^n) \times \mathbb{R}^n$, *where*

$$\phi_1(\zeta) = \begin{bmatrix} \dot{\zeta} - TA(t)\zeta \\ \zeta(0) + \zeta(1) \end{bmatrix}, \phi_2(\zeta) = \begin{bmatrix} \dot{\zeta} + TA^{\mathrm{T}}(t)\zeta \\ \zeta(0) + \zeta(1) \end{bmatrix}.$$

If $\zeta \in \mathcal{C}^1([0,1], \mathbb{R}^n)$, *then* $\zeta \in \mathrm{Ker}(\phi_1)$ *if and only if*

$$\begin{bmatrix} \zeta \\ \zeta(0) \end{bmatrix} \perp \phi_2(\mathcal{C}^1([0,1], \mathbb{R}^n)),$$

and $\zeta \in \mathrm{Ker}(\phi_2)$ *if and only if*

$$\begin{bmatrix} \zeta \\ \zeta(0) \end{bmatrix} \perp \phi_1(\mathcal{C}^1([0,1], \mathbb{R}^n)).$$

Proof. The proof is similar to the proof of Proposition 6.1. □

Proposition 6.3. *Consider* $\phi_{1,2} : \mathcal{C}^1([0,1],\mathbb{C}^n) \to \mathcal{C}^0([0,1],\mathbb{C}^n) \times \mathbb{C}^n$, *where*

$$\phi_1(\zeta) = \begin{bmatrix} \dot{\zeta} - TA(t)\zeta + i\theta\zeta \\ \zeta(0) - \zeta(1) \end{bmatrix}, \phi_2(\zeta) = \begin{bmatrix} \dot{\zeta} + TA^{\mathrm{T}}(t)\zeta + i\theta\zeta \\ \zeta(0) - \zeta(1) \end{bmatrix}.$$

If $\zeta \in \mathcal{C}^1([0,1],\mathbb{C}^n)$, *then* $\zeta \in \mathrm{Ker}(\phi_1)$ *if and only if*

$$\begin{bmatrix} \zeta \\ \zeta(0) \end{bmatrix} \perp \phi_2(\mathcal{C}^1([0,1],\mathbb{C}^n)),$$

and $\zeta \in \mathrm{Ker}(\phi_2)$ *if and only if*

$$\begin{bmatrix} \zeta \\ \zeta(0) \end{bmatrix} \perp \phi_1(\mathcal{C}^1([0,1],\mathbb{C}^n)).$$

Proof. If ζ is in the kernel of ϕ_1, then $\dot{\zeta} - TA(t)\zeta + i\theta\zeta = 0$ and $\zeta(0) - \zeta(1) = 0$. For all $g \in \mathcal{C}^1([0,1],\mathbb{C}^n)$ we have

$$\begin{aligned}
&\int_0^1 g^{\mathrm{H}}(t)\dot{\zeta}(t)dt - \int_0^1 Tg^{\mathrm{H}}(t)A(t)\zeta(t)dt + \int_0^1 i\theta g^{\mathrm{H}}(t)\zeta(t) = 0 \\
&\Rightarrow g^{\mathrm{H}}(t)\zeta(t)|_0^1 - \int_0^1 \dot{g}^{\mathrm{H}}(t)\zeta(t)dt - \int_0^1 Tg^{\mathrm{H}}(t)A(t)\zeta(t)dt + \int_0^1 i\theta g^{\mathrm{H}}(t)\zeta(t) = 0 \\
&\Rightarrow g^{\mathrm{H}}(1)\zeta(1) - g^{\mathrm{H}}(0)\zeta(0) - \int_0^1 (\dot{g}(t) + TA^{\mathrm{T}}(t)g(t) + i\theta g(t))^{\mathrm{H}}\zeta(t)dt = 0 \\
&\Rightarrow -(g(0) - g(1))^{\mathrm{H}}\zeta(0) - \int_0^1 (\dot{g}(t) + TA^{\mathrm{T}}(t)g(t) + i\theta g(t))^{\mathrm{H}}\zeta(t)dt = 0 \\
&\Rightarrow \left\langle \begin{bmatrix} \dot{g} + TA^{\mathrm{T}}(t)g + i\theta g \\ g(0) - g(1) \end{bmatrix}, \begin{bmatrix} \zeta \\ \zeta(0) \end{bmatrix} \right\rangle = 0.
\end{aligned}$$

The proofs of the reverse implication and the second assertion are similar. □

Proposition 6.4. *Consider* $\phi_{1,2} : \mathcal{C}^1([0,1],\mathbb{C}^n) \to \mathcal{C}^0([0,1],\mathbb{C}^n) \times \mathbb{C}^n$, *where*

$$\phi_1(\zeta) = \begin{bmatrix} \dot{\zeta} - TA(t)\zeta \\ \zeta(0) - e^{-i\theta}\zeta(1) \end{bmatrix}, \phi_2(\zeta) = \begin{bmatrix} \dot{\zeta} + TA^{\mathrm{T}}(t)\zeta \\ \zeta(0) - e^{-i\theta}\zeta(1) \end{bmatrix}.$$

If $\zeta \in \mathcal{C}^1([0,1],\mathbb{C}^n)$, *then* $\zeta \in \mathrm{Ker}(\phi_1)$ *if and only if*

$$\begin{bmatrix} \zeta \\ \zeta(0) \end{bmatrix} \perp \phi_2(\mathcal{C}^1([0,1],\mathbb{C}^n)),$$

and $\zeta \in \mathrm{Ker}(\phi_2)$ *if and only if*

$$\begin{bmatrix} \zeta \\ \zeta(0) \end{bmatrix} \perp \phi_1(\mathcal{C}^1([0,1],\mathbb{C}^n)).$$

Proof. If ζ is in the kernel of ϕ_1, then $\dot{\zeta} - TA(t)\zeta = 0$ and $\zeta(0) - e^{-i\theta}\zeta(1) = 0$. For all $g \in \mathcal{C}^1([0,1],\mathbb{C}^n)$ we have

$$\begin{aligned}
&\int_0^1 g^{\mathrm{H}}(t)\dot{\zeta}(t)dt - \int_0^1 Tg^{\mathrm{H}}(t)A(t)\zeta(t)dt = 0 \\
&\Rightarrow g^{\mathrm{H}}(t)\zeta(t)|_0^1 - \int_0^1 \dot{g}^{\mathrm{H}}(t)\zeta(t)dt - \int_0^1 Tg^{\mathrm{H}}(t)A(t)\zeta(t)dt = 0 \\
&\Rightarrow g^{\mathrm{H}}(1)\zeta(1) - g^{\mathrm{H}}(0)\zeta(0) - \int_0^1 (\dot{g}(t) + TA^{\mathrm{T}}(t)g(t))^{\mathrm{H}}\zeta(t)dt = 0 \\
&\Rightarrow -(g(0) - e^{-i\theta}g(1))^{\mathrm{H}}\zeta(0) - \int_0^1 (\dot{g}(t) + TA^{\mathrm{T}}(t)g(t))^{\mathrm{H}}\zeta(t)dt = 0 \\
&\Rightarrow \left\langle \begin{bmatrix} \dot{g} + TA^{\mathrm{T}}(t)g \\ g(0) - e^{-i\theta}g(1) \end{bmatrix}, \begin{bmatrix} \zeta \\ \zeta(0) \end{bmatrix} \right\rangle = 0.
\end{aligned}$$

The proofs of the reverse implication and the second assertion are similar. □

Proposition 6.5. *Consider two differential-difference operators* $\phi_{1,2} : \mathcal{C}^1([0,1],\mathbb{R}^n) \to \mathcal{C}^0([0,1],\mathbb{R}^n) \times \mathbb{R}^n$, *where*

$$\phi_1(\zeta) = \begin{bmatrix} \dot{\zeta} - TA(t)\zeta \\ \zeta(0) - \zeta(1) \end{bmatrix}, \quad \phi_2(\zeta) = \begin{bmatrix} \dot{\zeta} + TA^{\mathrm{T}}(t)\zeta \\ \zeta(0) - \zeta(1) \end{bmatrix}.$$

If $\zeta \in \mathcal{C}^1([0,1],\mathbb{R}^n)$, *then*

$$\phi_1(\zeta) = \begin{bmatrix} g \\ 0 \end{bmatrix}$$

if and only if

$$\left\langle \begin{bmatrix} \zeta \\ \zeta(0) \end{bmatrix}, \begin{bmatrix} \dot{h} + TA^{\mathrm{T}}(t)h \\ h(0) - h(1) \end{bmatrix} \right\rangle = -\left\langle \begin{bmatrix} g \\ 0 \end{bmatrix}, \begin{bmatrix} h \\ 0 \end{bmatrix} \right\rangle,$$

for all $h \in \mathcal{C}^1([0,1],\mathbb{R}^n)$. *Furthermore*

$$\phi_2(\zeta) = \begin{bmatrix} g \\ 0 \end{bmatrix}$$

if and only if

$$\left\langle \begin{bmatrix} \zeta \\ \zeta(0) \end{bmatrix}, \begin{bmatrix} \dot{h} - TA(t)h \\ h(0) - h(1) \end{bmatrix} \right\rangle = -\left\langle \begin{bmatrix} g \\ 0 \end{bmatrix}, \begin{bmatrix} h \\ 0 \end{bmatrix} \right\rangle,$$

for all $h \in \mathcal{C}^1([0,1],\mathbb{R}^n)$.

Proof. We focus on the first assertion. Suppose that $\dot{\zeta}(t) - TA(t)\zeta(t) = g(t)$ and $\zeta(0) - \zeta(1) = 0$. For all $h \in \mathcal{C}^1([0,1],\mathbb{R}^n)$ we have

$$\begin{aligned}
&\int_0^1 h^{\mathrm{T}}(t)\dot{\zeta}(t)dt - \int_0^1 Th^{\mathrm{T}}(t)A(t)\zeta(t)dt = \int_0^1 h^{\mathrm{T}}(t)g(t)dt \\
&\Rightarrow h^{\mathrm{T}}(t)\zeta(t)|_0^1 - \int_0^1 \dot{h}^{\mathrm{T}}(t)\zeta(t)dt - \int_0^1 Th^{\mathrm{T}}(t)A(t)\zeta(t)dt = \int_0^1 h^{\mathrm{T}}(t)g(t)dt \\
&\Rightarrow h^{\mathrm{T}}(1)\zeta(1) - h^{\mathrm{T}}(0)\zeta(0) - \int_0^1 (\dot{h}(t) + TA^{\mathrm{T}}(t)h(t))^{\mathrm{T}}\zeta(t)dt = \int_0^1 h^{\mathrm{T}}(t)g(t)dt \\
&\Rightarrow \int_0^1 \zeta^{\mathrm{T}}(t)(\dot{h}(t) + TA^{\mathrm{T}}(t)h(t))dt + \zeta^{\mathrm{T}}(0)(h(0) - h(1)) = -\int_0^1 g^{\mathrm{T}}(t)h(t)dt \\
&\Rightarrow \left\langle \begin{bmatrix} \zeta \\ \zeta(0) \end{bmatrix}, \begin{bmatrix} \dot{h} + TA^{\mathrm{T}}(t)h \\ h(0) - h(1) \end{bmatrix} \right\rangle = -\left\langle \begin{bmatrix} g \\ 0 \end{bmatrix}, \begin{bmatrix} h \\ 0 \end{bmatrix} \right\rangle.
\end{aligned}$$

The proofs of the reverse implication and the second assertion are similar. □

Proposition 6.6. *Consider two differential-difference operators* $\phi_{1,2} : \mathcal{C}^1([0,1],\mathbb{R}^n) \to \mathcal{C}^0([0,1],\mathbb{R}^n) \times \mathbb{R}^n$, *where*

$$\phi_1(\zeta) = \begin{bmatrix} \dot{\zeta} - TA(t)\zeta \\ \zeta(0) + \zeta(1) \end{bmatrix}, \quad \phi_2(\zeta) = \begin{bmatrix} \dot{\zeta} + TA^{\mathrm{T}}(t)\zeta \\ \zeta(0) + \zeta(1) \end{bmatrix}.$$

If $\zeta \in \mathcal{C}^1([0,1],\mathbb{R}^n)$, *then*

$$\phi_1(\zeta) = \begin{bmatrix} g \\ 0 \end{bmatrix}$$

if and only if

$$\left\langle \begin{bmatrix} \zeta \\ \zeta(0) \end{bmatrix}, \begin{bmatrix} \dot{h} + TA^{\mathrm{T}}(t)h \\ h(0)+h(1) \end{bmatrix} \right\rangle = -\left\langle \begin{bmatrix} g \\ 0 \end{bmatrix}, \begin{bmatrix} h \\ 0 \end{bmatrix} \right\rangle,$$

$\forall h \in \mathcal{C}^1([0,1],\mathbb{R}^n)$. *Furthermore*

$$\phi_2(\zeta) = \begin{bmatrix} g \\ 0 \end{bmatrix}$$

if and only if

$$\left\langle \begin{bmatrix} \zeta \\ \zeta(0) \end{bmatrix}, \begin{bmatrix} \dot{h} - TA(t)h \\ h(0)+h(1) \end{bmatrix} \right\rangle = -\left\langle \begin{bmatrix} g \\ 0 \end{bmatrix}, \begin{bmatrix} h \\ 0 \end{bmatrix} \right\rangle,$$

$\forall h \in \mathcal{C}^1([0,1],\mathbb{R}^n)$.

Proof. Suppose that $\dot{\zeta}(t) - TA(t)\zeta(t) = g(t)$ and $\zeta(0)+\zeta(1) = 0$. For all $h \in \mathcal{C}^1([0,1],\mathbb{R}^n)$ we have

$$\begin{aligned}
&\int_0^1 h^{\mathrm{T}}(t)\dot{\zeta}(t)dt - \int_0^1 Th^{\mathrm{T}}(t)A(t)\zeta(t)dt = \int_0^1 h^{\mathrm{T}}(t)g(t)dt \\
&\Rightarrow h^{\mathrm{T}}(t)\zeta(t)|_0^1 - \int_0^1 \dot{h}^{\mathrm{T}}(t)\zeta(t)dt - \int_0^1 Th^{\mathrm{T}}(t)A(t)\zeta(t)dt = \int_0^1 h^{\mathrm{T}}(t)g(t)dt \\
&\Rightarrow h^{\mathrm{T}}(1)\zeta(1) - h^{\mathrm{T}}(0)\zeta(0) - \int_0^1 (\dot{h}(t) + TA^{\mathrm{T}}(t)h(t))^{\mathrm{T}}\zeta(t)dt = \int_0^1 h^{\mathrm{T}}(t)g(t)dt \\
&\Rightarrow \int_0^1 \zeta^{\mathrm{T}}(t)(\dot{h}(t) + TA^{\mathrm{T}}(t)h(t))dt + \zeta^{\mathrm{T}}(0)(h(0)+h(1)) = -\int_0^1 g^{\mathrm{T}}(t)h(t)dt \\
&\Rightarrow \left\langle \begin{bmatrix} \zeta \\ \zeta(0) \end{bmatrix}, \begin{bmatrix} \dot{h} + TA^{\mathrm{T}}(t)h \\ h(0)+h(1) \end{bmatrix} \right\rangle = -\left\langle \begin{bmatrix} g \\ 0 \end{bmatrix}, \begin{bmatrix} h \\ 0 \end{bmatrix} \right\rangle.
\end{aligned}$$

The proofs of the reverse implication and the second assertion are similar. □

7
Future work

This chapter gives a brief summary of the topics that we discussed in this thesis and provides suggestions for future work.

In this thesis we discussed two main topics, namely the homotopy method for the initialization of homoclinic and heteroclinic orbits and the normal form theory for codimension 2 bifurcations of limit cycles. Both subjects offer possibilities for further research.

In Chapter 3 we first remarked that a homoclinic orbit can be initialized from a limit cycle with a large period. An alternative was offered by the homotopy method, which is a systematic procedure that searches for a better approximation of the homoclinic orbit in each step of the homotopy method. The consecutive steps lead to an orbit that can be used as start-up for the continuation of homoclinic orbits. The current version of MatCont now supports this method.

Homoclinic orbits are also known to bifurcate from certain codimension 2 bifurcations of equilibria, namely from a Bogdanov-Takens point, a Zero-Hopf point or a Double Hopf equilibrium (see [56,67] and references therein). For the start-up from a Bogdanov-Takens point, homoclinic predictors for the parameter and orbit are given in [11]. These formulas are implemented in MatCont. However, in practice,

the initialization often fails. This suggests that the method needs to be reconsidered. This, together with a rigorous study of the initialization from a Zero-Hopf and a Double Hopf point, is work currently under development.

Instead of starting up a homoclinic orbit from a limit cycle with a large period, the reverse could be done. Depending on the type of the equilibrium of the homoclinic orbit, either a unique limit cycle bifurcates from the homoclinic orbit or an infinite number of limit cycles is present in a neighbourhood of the homoclinic orbit. Either way, an initialization of a limit cycle from the homoclinic orbit could be envisaged. The tricky part would probably be to deal with the infinite time that the orbit spends near the equilibrium point.

The homotopy method that we considered in Chapter 3 concerned point-to-point connections, for homoclinic orbits as well as heteroclinic orbits. The method, however, could also be generalized to homoclinic cycle-to-cycle connections, heteroclinic point-to-cycle connections and heteroclinic cycle-to-cycle connections. These methods were studied in [42, 43] for 3-dimensional ODEs. They should be extended to the n-dimensional case, and the methods and their continuations incorporated in MatCont.

Chapter 4 listed the normal forms for all codimension 2 bifurcations of limit cycles and presented their unfoldings, which clarified what kind of bifurcation scenario occurs around the bifurcation point depending on the values of the normal form coefficients. In Chapter 5 we derived these normal form coefficients by making use of the homological equation approach. In Chapter 6 we considered the implementation in MatCont and verified our computations of the critical coefficients by numerous examples.

To fully support the two-parameter bifurcation analysis of ODEs, one further needs special methods to switch between various branches of codimension 1 bifurcations of limit cycles rooted at the codimension 2 points. Such methods have been developed and implemented in MatCont for codimension 2 equilibrium [72] and fixed point [51] bifurcations. Switching at codimension 2 points to the continuation of codimension 1 local bifurcations of limit cycles seems to be the next natural problem to attack, while that for codimension 1 bifurcations of homoclinic and heteroclinic orbits is more difficult and probably requires new ideas. Similar remarks can be made about quasi-periodic bifurcations of tori. Since there does not (yet) exist robust techniques for the continuation of invariant tori, we used Lyapunov exponents for the detection of the 2- and higher-dimensional tori.

Samenvatting

De analyse van dynamische systemen betreft het bestuderen van fenomenen die variëren doorheen de tijd. Een dynamisch systeem bevat een evolutieregel die specifieert hoe de toekomst en het verleden eruitzien op basis van het heden. De moderne theorie van dynamische systemen dateert van de 19^{de} eeuw, toen Poincaré baanbrekend werk leverde op het vlak van hemelmechanica en fundamentele problemen zoals de stabiliteit en de evolutie van het zonnestelsel bestudeerde. Zijn werk ligt aan de basis van de lokale en globale analyse van dynamische systemen.

Een eenvoudig voorbeeld van een dynamisch systeem wordt gegeven door een slinger. De slinger bestaat uit een staaf die vast hangt aan een welbepaald punt en heen en weer beweegt in een verticaal vlak. De toestand van de slinger wordt volledig bepaald door zijn positie en snelheid. De slinger is onderhevig aan de zwaartekracht, en de evolutieregel wordt gegeven door de wet van Newton $F = ma$, waarbij F de gravitatiekracht is, m de massa en a de versnelling.

Maar dit onderzoeksgebied kent toepassingen in vele vakgebieden, zoals in de fysica, biologie, chemie, economie en sociologie. Dit verklaart de populariteit van dynamische systemen in de laatste decennia. Om deze toepassingen te beschrijven, moet er een wiskundig model opgesteld worden. Gebruik makend van algoritmen en computationele methoden kunnen we dan de observaties verklaren aan de hand van dit model.

Een dynamisch systeem kan ofwel betrekking hebben op een continu systeem, ofwel op een discreet systeem. In het eerste geval wordt de evolutieregel gegeven door een stelsel gewone differentiaalvergelijkingen, in het tweede geval door een afbeelding. De meeste concepten en resultaten met betrekking tot een continu systeem hebben een analogon in het discrete geval. Dit doctoraat focust op de studie van gewone differentiaalvergelijkingen. We maken echter ook gebruik van bestaande resultaten voor afbeeldingen.

De geordende familie van punten die we bekomen door de evolutieregel toe te passen, wordt een baan genoemd. Beschouw een baan die vertrekt in een punt en

doorheen de tijd steeds in dat zelfde punt blijft. Zo een punt wordt een evenwichtspunt genoemd. Een evenwichtspunt is stabiel als banen in de buurt van het punt convergeren naar het evenwichtspunt.

Eén van de basisbegrippen in de theorie van dynamische systemen is dat van een bifurcatie. Onder de variatie van een parameter kan het dynamisch systeem op punten stoten waar het kwalitatief gedrag verandert. Dit is een bifurcatie. Het eenvoudigste voorbeeld van een bifurcatie is het verdwijnen van de stabiliteit van een evenwichtspunt.

Er bestaan twee soorten bifurcaties, namelijk lokale en globale bifurcaties. Een lokale bifurcatie kan gedetecteerd worden door een willekeurig kleine omgeving van een evenwichtspunt of periodieke baan te bekijken. Een voorbeeld van een lokale bifurcatie wordt gegeven door de Hopfbifurcatie, waarbij de stabiliteit van het evenwichtspunt verandert en een periodieke baan ontstaat. Er zijn echter ook bifurcaties die niet op deze manier kunnen gevonden worden. Dit zijn de globale bifurcaties. Een voorbeeld wordt gegeven door een heteroclinische baan, waarbij de baan naar een eerste evenwichtspunt convergeert voor positieve tijdswaarden en naar een tweede evenwichtspunt voor negatieve tijdswaarden.

Bij de detectie van een bifurcatie is het de bedoeling om de parameterruimte onder te verdelen in verschillende gebieden, zodat voor alle mogelijke parameterwaarden behorende tot eenzelfde gebied hetzelfde dynamisch gedrag wordt vertoond. Een bifurcatiediagram geeft zo een verdeling weer. Met elk gebied correspondeert er een faseportret, dat een voorstelling geeft van alle mogelijke banen in de faseruimte.

De analyse van een (niet-lineair) dynamisch systeem kan heel uitdagend zijn. Zelfs een eenvoudig systeem kan complex gedrag vertonen, waarbij geen expliciete formules kunnen gegeven worden voor de oplossingen. Numerieke methoden geven dan een antwoord. Numerieke simulatie vormt een eerste manier om een dynamisch systeem te bestuderen. Hiervan gebruik makend kunnen (stabiele) evenwichtspunten en periodieke banen gevonden worden. Op die manier verkrijgen we een ruwe schets van hoe het faseportret eruitziet. Continuatie toepassen is een tweede manier. Het idee is om een kromme te berekenen waarbij elk punt een oplossing is van een geschikt stelsel vergelijkingen dat het te onderzoeken dynamisch object definieert. Bijvoorbeeld, wanneer een (stabiel) evenwichtspunt wordt gedetecteerd, kunnen we gebruik maken van continuatietechnieken om een kromme van evenwichtspunten te berekenen onder de variatie van een parameter.

Een softwarepakket dat kan gebruikt worden voor de studie van continue dynamische systemen is MatCont. Dit pakket is ontwikkeld door onderzoeksgroepen uit België en Nederland, met de hulp van individuele wetenschappers uit andere landen.

Het is geschreven in Matlab en bijgevolg platform-onafhankelijk. Dankzij de grafische user interface is een interactieve studie van bifurcaties mogelijk. Het pakket is gebaseerd op numerieke continuatie, waarbij eerst een predictie wordt gemaakt, die vervolgens verbeterd wordt door de Moore-Penrose correctiemethode.

Tijdens de continuatie van evenwichtspunten kan een bifurcatie gedetecteerd worden, dit is ofwel een Limietpunt ofwel een Hopfbifurcatie. Dit zijn codimensie 1 bifurcaties, die gevonden worden onder de variatie van een enkele systeemparameter. Vervolgens kan een Limietpunt kromme of een Hopfkromme berekend worden door gebruik te maken van continuatie. Op deze krommen kunnen we opnieuw bifurcaties ontdekken. Dit zijn codimensie 2 bifurcaties, waarbij er twee systeemparameters vrij zijn. Een codimensie 2 bifurcatie wordt in feite bepaald door het opleggen van twee onafhankelijke voorwaarden. Codimensie 1 bifurcatiekrommen snijden transversaal of raken elkaar in codimensie 2 bifurcatiepunten. Er kunnen ook codimensie 1 bifurcatiekrommen ontspruiten uit een codimensie 2 punt. Bijvoorbeeld, in een Bogdanov-Takens punt ontstaat er een homoclinische bifurcatiekromme.

Theoretisch gezien kunnen er codimensie m bifurcaties voorkomen in een systeem dat m systeemparameters bevat. In de praktijk echter kan de analyse van een codimensie 2 punt al zeer complex zijn en in sommige gevallen is het volledige bifurcatieplaatje nog steeds onbekend. Daarom beperken we ons meestal tot de studie van codimensie 1 en 2 bifurcaties.

Er bestaan verschillende manieren om een periodieke baan te detecteren, bijvoorbeeld door tijdsintegratie of wanneer er zich een Hopfbifurcatie voordoet. De eerste manier is enkel van toepassing voor een stabiele periodieke baan en de initialisatie van een periodieke baan vertrekkende van een Hopfbifurcatie leidt niet altijd tot convergentie. Daarom is het belangrijk om over een aantal alternatieven te beschikken voor de initialisatie van bifurcatiekrommen.

Naast evenwichtspunten en periodieke banen spelen homoclinische banen een belangrijke rol in toepassingen. Een homoclinische baan is een periodieke baan waarvan de periode oneindig groot wordt. De continuatie van homoclinische banen kan opgestart worden vertrekkende van een continuatie van periodieke banen waarbij de periode alsmaar groter werd. De homotopiemethode vormt een alternatief. We focussen op deze methode in Hoofdstuk 3. Hiervan gebruik makend is het mogelijk om een homoclinische baan op te starten vertrekkende van een evenwichtspunt. Het is een systematische procedure waarbij in elke homotopiestap gezocht wordt naar een betere benadering van de exacte homoclinische baan. Aan het einde van de homotopiemethode verkrijgen we een baan, die (hopelijk) de exacte oplossing voldoende goed benadert zodat de Newton correcties tot convergentie leiden. Ook in

het geval van heteroclinische banen kan de homotopiemethode een voldoende goede benadering leveren voor de exacte heteroclinische baan. In Hoofdstuk 3 beschrijven we de homotopiemethodes voor beide types van banen en hun implementatie in een softwarepakket, in ons geval MatCont. De continuatie van heteroclinische banen is nu ook mogelijk in MatCont. We bespreken een aantal voorbeelden die de efficiëntie van de methode illustreren.

Om na te gaan wat er zoal gebeurt rond het bifurcatiepunt kunnen we de omgeving van het gedetecteerde punt scannen op zoek naar lokale en globale bifurcaties. Maar het zou veel handiger zijn indien we bij detectie onmiddellijk zouden weten welke bifurcatiekrommen aanwezig zijn en hoe deze zich verhouden ten opzichte van elkaar. Dit probleem kan aangepakt worden door te kijken naar de normaalvormen.

Bij de detectie van een bifurcatie wordt eerst een reductie van het dynamisch systeem tot een centrale variëteit gemaakt. De dimensie van deze centrale varieteit is klein. De definiërende vergelijkingen in de centrale variëteit worden dan vereenvoudigd. Deze vereenvoudigde vorm wordt de normaalvorm genoemd. Met welk type bifurcatie we te maken hebben, wordt afgeleid uit deze normaalvorm. De coefficiënten die voorkomen in de normaalvorm, de normaalvormcoëfficiënten, maken een onderscheid tussen de mogelijke bifurcatiescenario's voor het bifurcatiepunt. Bijvoorbeeld, een negatieve normaalvormcoëfficiënt horende bij een Hopfbifurcatie leidt tot het ontstaan van een stabiele periodieke baan, een positieve normaalvormcoëfficiënt tot een onstabiele periodieke baan. Indien parameters worden geïntroduceerd, kunnen we met elke bifurcatie een ontvouwing associëren. Deze geeft de verdeling van de parameterruimte in verschillende gebieden en de corresponderende faseportretten voor elk gebied. Het aantal ontvouwingsparameters dat voorkomt in de normaalvorm, is gelijk aan de codimensie van de bifurcatie.

In de hoofdstukken $4-6$ focussen we op codimensie 2 bifurcaties van periodieke banen, in totaal zijn dat er 11. De dimensie van de centrale variëteit voor deze bifurcaties varieert van 2 t.e.m. 5. De bifurcaties worden geordend volgens deze dimensie. Met elke periodieke baan kan een afbeelding geassocieerd worden, namelijk de Poincaré afbeelding. De periodieke baan is dan een vast punt van deze afbeelding. Deze associatie heeft tot voordeel dat resultaten die eerder ontwikkeld werden voor afbeeldingen, in zekere mate kunnen hergebruikt worden voor de op te bouwen theorie voor periodieke banen.

In Hoofdstuk 4 leiden we de normaalvormen voor alle 11 codimensie 2 bifurcaties van periodieke banen af en we maken duidelijk welke normaalvormcoëfficiënten aanleiding geven tot welk bifurcatiescenario. We bespreken hun ontvouwingen en verduidelijken de interpretatie van de banen die voorkomen in de faseportretten.

Merk op dat we de ontvouwing geven voor de getrunceerde normaalvorm. Het is logisch om ons dan af te vragen of de hogere ordetermen die voorkomen in de oorspronkelijke normaalvorm, de dynamica, die is afgeleid uit de studie van de getrunceerde normaalvorm, beïnvloeden. In sommige gevallen hebben de hogere orde perturbaties geen invloed op het bifurcatieplaatje dat overeenstemt met de getrunceerde normaalvorm. Jammer genoeg is dit niet altijd het geval. De aanwezigheid van globale bifurcaties kan de topologische equivalentie tussen de bifurcatiediagrammen die corresponderen met de getrunceerde en oorspronkelijke normaalvormen, in de weg staan. Een perturbatie door hogere ordetermen maakt de dynamica in de buurt van de globale bifurcaties complexer en wat er exact gebeurt, is in sommige gevallen nog steeds onbekend.

Het is vanzelfsprekend dat we formules voor de normaalvormcoëfficiënten nodig hebben. Deze worden bepaald aan de hand van de homologische vergelijking. In Hoofdstuk 5 bespreken we de methode en leiden we de uitdrukkingen voor alle noodzakelijke coëfficiënten af. Merk op dat deze uitdrukkingen zeer lang kunnen zijn. De aanpak is in alle gevallen dezelfde, maar elk geval heeft wel zijn eigen bijzonderheden.

De logische volgende stap is dan de implementatie van de normaalvormcoëfficienten. In Hoofdstuk 6 bespreken we hoe de uitdrukkingen op een efficiënte manier kunnen geïmplementeerd worden in MatCont. Voor de interpretatie van de normaalvormcoëfficiënten van de codimensie 2 bifurcaties van periodieke banen met een 4- of 5-dimensionale centrale variëteit wordt er een onderscheid gemaakt tussen de 'eenvoudige' en 'moeilijke' gevallen. In een 'moeilijk' geval is het bifurcatiescenario complexer en komt er een extra torus voor. Hogere ordetermen bepalen de stabiliteit van deze extra torus. Omdat deze torus niet altijd bestaat en omwille van complexiteitsargumenten, laten we de berekening van de hogere ordetermen in het algemeen achterwege. De uitdrukkingen zijn echter geïmplementeerd in MatCont zodat een geïnteresseerde gebruiker ze kan opvragen.

Om onze werkwijze te verifiëren bespreken we een aantal voorbeelden waarin alle 11 codimensie 2 bifurcaties voorkomen. Enerzijds berekenen we de normaalvormcoefficiënten. Op basis daarvan kunnen we de dynamica rond het gedetecteerde punt voorspellen aan de hand van de ontvouwing, besproken in Hoofdstuk 4. Anderzijds scannen we de omgeving van het gedetecteerde punt op zoek naar mogelijke bifurcatiekrommen. In alle voorbeelden leiden de twee werkwijzen tot hetzelfde bifurcatieplaatje. Dit overtuigt ons van de correctheid van de berekeningen voor de normaalvormcoëfficiënten.

Bibliography

[1] CAPD: Computer assisted proofs in dynamics. `http://capd.ii.uj.edu.pl`.

[2] TIDES: A taylor integrator for differential equations. `http://gme.unizar.es/software/tides`.

[3] V. I. Arnold. *Geometrical methods in the theory of ordinary differential equations*. Springer-Verlag, New York, 1983.

[4] V. I. Arnold, V. S. Afraimovich, Yu. S. Illyashenko, and L. P. Shilnikov. *Dynamical systems V*. Encyclopaedia of Mathematical Sciences. Springer-Verlag, Berlin, 1994.

[5] D. K. Arrowsmith and C. M. Place. *An introduction to dynamical systems*. Cambridge University Press, Cambridge, 1990.

[6] U. M. Ascher, R. M. M. Mattheij, and R. D. Russell. *Numerical solution of boundary value problems for ordinary differential equations*. SIAM, Philadelphia, PA, 1995.

[7] N. Aubry, P. Holmes, J. Lumley, and E. Stone. The dynamics of coherent structures in the wall region of a turbulent boundary layer. *J. Fluid Mech.*, 192:115–173, 1988.

[8] R. Barrio. Sensitivity analysis of ODEs/DAEs using the taylor series method. *SIAM J. Sci. Comput.*, 27(6):1929–1947, 2006.

[9] H. Berestycki and L. Nirenberg. Traveling fronts in cylinders. *Ann. Inst. H. Poincaré Anal. Non Linéaire*, 9(5):497–572, 1992.

[10] W. J. Beyn. The numerical computation of connecting orbits in dynamical systems. *IMA J. Numer. Anal.*, 10(3):379–405, 1990.

[11] W. J. Beyn, A. Champneys, E. Doedel, W. Govaerts, Yu. A. Kuznetsov, and B. Sandstede. Numerical continuation, and computation of normal forms. In B. Fiedler, editor, *Handbook of Dynamical Systems*, volume 2, pages 149–219, North-Holland, Amsterdam, 2002. Elsevier Science.

[12] D. Bindel, J. Demmel, and M. Friedman. Continuation of invariant subspaces in large bifurcation problems. *SIAM J. Sci. Comput.*, 30(2):637–656, 2008.

[13] V. V. Bykov. On the structure of the neighborhood of a separatrix contour with a saddle-focus. In *Methods of Qualitative Theory of Differential Equations*, pages 3–32, Gorkii State University, Gorkii, 1978. In Russian.

[14] V. V. Bykov. Bifurcations of dynamical systems close to systems with a separatrix contour containing a saddle-focus. In *Methods of Qualitative Theory of Differential Equations*, pages 44–72, Gorkii State University, Gorkii, 1980. In Russian.

[15] A. R. Champneys and Yu. A. Kuznetsov. Numerical detection and continuation of codimension-two homoclinic bifurcations. *Internat. J. Bifur. Chaos*, 4(4):785–822, 1994.

[16] A. R. Champneys, Yu. A. Kuznetsov, and B. Sandstede. A numerical toolbox for homoclinic bifurcation analysis. *Internat. J. Bifur. Chaos*, 6(5):867–887, 1996.

[17] S.-N. Chow. and D. Wang. Normal forms of bifurcating periodic orbits. *Contemp. Math.*, 56:9–18, 1986.

[18] L. Chua, C. Wu, A. Huang, and C. Zhong. A universal circuit for studying and generating chaos, part I: Routes to chaos. *IEEE Trans. on Circuits and Systems-I: Fundamental Theory and Applications*, 10(40):732–744, 1993.

[19] H. Dankowicz and G. Thakur. A Newton method for locating invariant tori of maps. *Internat. J. Bifur. Chaos*, 16(5):1491–1503, 2006.

[20] C. De Boor and B. Swartz. Collocation at Gaussian points. *SIAM J. Numer. Anal.*, 10(4):582–606, 1973.

[21] V. De Witte, F. Della Rossa, W. Govaerts, and Yu. A. Kuznetsov. Numerical periodic normalization for codim 2 bifurcations of limit cycles - computational formulas, numerical implementation, and examples. Accepted for publication in SIAM J. Appl. Dyn. Syst.

[22] V. De Witte and W. Govaerts. Convergence analysis of a numerical method to solve the adjoint linearized periodic orbit equations. *Appl. Numer. Math.*, 60(10):1007–1023, 2010.

[23] V. De Witte and W. Govaerts. Numerical computation of normal form coefficients of bifurcations of ODEs in Matlab. In *Proceedings of the 8th AIMS Conference: Dynamical Systems, Differential Equations and Applications, Volume I*, pages 362–372, Dresden, May 25 - 28 2011.

[24] V. De Witte, W. Govaerts, and Yu. A. Kuznetsov. Numerical implementation of a homotopy method for computing homoclinic and heteroclinic orbits. In *Proceedings of the 16th US National Congress of Theoretical and Applied Mechanics, USNCTAM2010*, State College, PA, June 27 - July 2 2010.

[25] V. De Witte, W. Govaerts, Yu. A. Kuznetsov, and M. Friedman. Interactive initialization and continuation of homoclinic and heteroclinic orbits in Matlab. *ACM Trans. Math. Software*, 38(3):18:1–18:34, 2012.

[26] V. De Witte, W. Govaerts, Yu. A. Kuznetsov, and H. G. E. Meijer. Numerical periodic normalization for codim 2 bifurcations of limit cycles with center manifold of dimension higher than 3. Submitted.

[27] V. De Witte, W. Govaerts, Yu. A. Kuznetsov, and H. G. E. Meijer. Numerical periodic normalization for codim 2 bifurcations of limit cycles with center manifold of dimension higher than 3. `http://arxiv.org/abs/1210.6205`.

[28] F. Della Rossa, V. De Witte, W. Govaerts, and Yu. A. Kuznetsov. Numerical periodic normalization for codim 2 bifurcations of limit cycles. `http://arxiv.org/abs/1111.4445`.

[29] J. W. Demmel, L. Dieci, and M. J. Friedman. Computing connecting orbits via an improved algorithm for continuing invariant subspaces. *SIAM J. Sci. Comput.*, 22(1):81–94, 2000.

[30] P. Deuflhard and A. Hohmann. *Numerische Mathematik I. Eine algorithmisch orientierte Einführung*. De Gruyter, Berlin, 1991.

[31] A. Dhooge, W. Govaerts, and Yu. A. Kuznetsov. MatCont: A Matlab package for numerical bifurcation analysis of ODEs. *ACM Trans. Math. Software*, 29(2):141–164, 2003. Available via http://sourceforge.net/projects/matcont/.

[32] A. Dhooge, W. Govaerts, Yu. A. Kuznetsov, H. G. E. Meijer, and B. Sautois. New features of the software MatCont for bifurcation analysis of dynamical systems. *Math. Comput. Model. Dyn. Syst.*, 14(2):147–175, 2008.

[33] A. Dhooge, W. Govaerts, Yu. A. Kuznetsov, W. Mestrom, and A. Riet. Cl_MatCont: A continuation toolbox in Matlab. In *Proceedings of the* 2003 *ACM Symposium on Applied Computing*, pages 161–166, Melbourne, FL, March 2003.

[34] L. Dieci and T. Eirola. On smooth decompositions of matrices. *SIAM J. Matrix Anal. Appl.*, 20(3):800–819, 1999.

[35] L. Dieci and M. J. Friedman. Continuation of invariant subspaces. *Numer. Linear Algebra Appl.*, 8(5):317–327, 2001.

[36] L. Dieci, J. Lorenz, and R. D. Russell. Numerical calculation of invariant tori. *SIAM J. Sci. Stat. Comput.*, 12(3):607–647, 1991.

[37] E. J. Doedel, A. R. Champneys, T. F. Fairgrieve, Yu. A. Kuznetsov, B. Sandstede, and X. Wang. Auto97: Continuation and bifurcation software for ordinary differential equations (with Homcont), 1997. http://indy.cs.concordia.ca/auto.

[38] E. J. Doedel and M. J. Friedman. Numerical computation of heteroclinic orbits. *J. Comput. Appl. Math.*, 26(1-2):155–170, 1989.

[39] E. J. Doedel, M. J. Friedman, and B. Kunin. Successive continuation for locating connecting orbits. *Numer. Algorithms*, 14(1-3):103–124, 1997.

[40] E. J. Doedel, M. J. Friedman, and A. C. Monteiro. On locating connecting orbits. *Appl. Math. Comput.*, 65(1-3):231–239, 1994.

[41] E. J. Doedel and J. P. Kernévez. Auto: Software for continuation problems in ordinary differential equations with applications. Technical report, Department of Applied Mathematics, California Institute of Technology, Pasadena, CA, 1986.

[42] E. J. Doedel, B. W. Kooi, Yu. A. Kuznetsov, and G. A. K. Van Voorn. Continuation of connecting orbits in 3D-ODEs: (II) cycle-to-cycle connections. *Internat. J. Bifur. Chaos*, 19(1):159–169, 2009.

[43] E. J. Doedel, B. W. Kooi, G. A. K. Van Voorn, and Yu. A. Kuznetsov. Continuation of connecting orbits in 3D-ODEs: (I) point-to-cycle connections. *Internat. J. Bifur. Chaos*, 18(7):1889–1903, 2008.

[44] C. Elphick, G. Iooss, and E. Tirapegui. Normal form reduction for time-periodically driven differential equations. *Phys. Lett. A*, 120(9):459–463, 1987.

[45] S. Fatimah and F. Verhulst. Suppressing flow-induced vibration by parametric excitation. *Nonlinear Dynam.*, 31:275–297, 2003.

[46] E. Freire, L. Franquelo, and J. Aracil. Periodicity and chaos in an autonomous electronic system. *IEEE Transactions on Circuits and Systems CAS*, 31(3):237–247, 1984.

[47] E. Freire, A. Rodriguez-Luis, E. Gamero, and E. Ponce. A case study for homoclinic chaos in an autonomous electronic circuit. *Physica D*, 62:230–243, 1993.

[48] P. Glendinning and C. Sparrow. T-points: A codimension two heteroclinic bifurcation. *J. Stat. Phys.*, 43(3-4):479–488, 1986.

[49] W. Govaerts. *Numerical methods for bifurcations of dynamical equilibria*. SIAM, Philadelphia, PA, 2000.

[50] W. Govaerts, V. De Witte, and L. Kheibarshekan. Using MatCont in a two-parameter bifurcation study of models for cell cycle controls. In *Proceedings of the ASME 2009 International Design Engineering Technical Conferences and Computers and Information in Engineering Conference*, San Diego, California, USA, August 30 - September 2 2009. IDETC/CIE.

[51] W. Govaerts, R. Khoshsiar Ghaziani, Yu. A. Kuznetsov, and H. G. E. Meijer. Numerical methods for two-parameter local bifurcation analysis of maps. *SIAM J. Sci. Comput.*, 29(6):2644–2667, 2007.

[52] W. Govaerts, Yu. Kuznetsov, and A. Dhooge. Numerical continuation of bifurcations of limit cycles in MATLAB. *SIAM J. Sci. Comput.*, 27(1):231–252, 2005.

[53] W. Govaerts and Yu. A. Kuznetsov. Interactive continuation tools. In B. Krauskopf, H. M. Osinga, and J. Galan-Vioque, editors, *Numerical Continuation Methods for Dynamical Systems*, pages 51–75. Springer, 2007.

[54] P. Gray and S. K. Scott. *Chemical oscillations and instabilities: Non-linear chemical kinetics*. Oxford University Press, Oxford, UK, 1990.

[55] A. Griewank, D. Juedes, and J. Utke. Algorithm 755: ADOL-C: A package for the automatic differentiation of algorithms written in C/C++. *ACM Trans. Math. Software*, 22(2):131–167, 1996.

[56] J. Guckenheimer and P. Holmes. *Nonlinear Oscillations, Dynamical Systems and Bifurcations of Vector Fields*. Springer-Verlag, New York, 1983.

[57] J. Guckenheimer and B. Meloon. Computing periodic orbits and their bifurcations with automatic differentiation. *SIAM J. Sci. Comput.*, 22(3):951–985, 2000.

[58] G. Iooss. *Bifurcations of Maps and Applications*. Lecture Notes, Mathematical Studies, North–Holland, Amsterdam, 1979.

[59] G. Iooss. Global characterization of the normal form for a vector field near a closed orbit. *J. Differential Equations*, 76(1):47–76, 1988.

[60] G. Iooss and M. Adelmeyer. *Topics in Bifurcation Theory and Applications*, volume 3. World Scientific, New York, 1992.

[61] V. Jansen. Regulation of predator-prey systems through spatial interactions: A possible solution to the paradox of enrichment. *Oikos*, 74(3):384–390, 1995.

[62] V. Jansen. The dynamics of two diffusively coupled predator-prey populations. *Theoretical Population Biology*, 59(2):119 – 131, 2001.

[63] I. G. Kevrekidis, R. Aris, L. D. Schmidt, and S. Pelikan. Numerical computation of invariant circles of maps. *Phys. D*, 16(2):243–251, 1985.

[64] R. Khoshsiar Ghaziani, W. Govaerts, Yu. A. Kuznetsov, and H. G. E. Meijer. Numerical continuation of connecting orbits of maps in Matlab. *J. Difference Equ. Appl.*, 15(8-9):849–875, 2009.

[65] B. Krauskopf. Bifurcation sequences at $1:4$ resonance: an inventory. *Nonlinearity*, 7(3):1073–1091, 1994.

[66] Yu. A. Kuznetsov. Numerical normalization techniques for all codim 2 bifurcations of equilibria in ODEs. *SIAM J. Numer. Anal.*, 36(4):1104–1124, 1999.

[67] Yu. A. Kuznetsov. *Elements of applied bifurcation theory*. Springer-Verlag, New York, third edition, 2004.

[68] Yu. A. Kuznetsov, W. Govaerts, E. J. Doedel, and A. Dhooge. Numerical periodic normalization for codim 1 bifurcations of limit cycles. *SIAM J. Numer. Anal.*, 43(4):1407–1435, 2005.

[69] Yu. A. Kuznetsov and V. V. Levitin. Content: A multiplatform environment for analyzing dynamical systems, 1997. http://ftp.cwi.nl/CONTENT.

[70] Yu. A. Kuznetsov and H. G. E. Meijer. Numerical normal forms for codim 2 bifurcations of fixed points with at most two critical eigenvalues. *SIAM J. Sci. Comput.*, 26(6):1932–1954, 2005.

[71] Yu. A. Kuznetsov and H. G. E. Meijer. Remarks on interacting Neimark-Sacker bifurcations. *J. Difference Equ. Appl.*, 12(10):1009–1035, 2006.

[72] Yu. A. Kuznetsov, H. G. E. Meijer, W. Govaerts, and B. Sautois. Switching to nonhyperbolic cycles from codim 2 bifurcations of equilibria in ODEs. *Phys. D*, 237(23):3061–3068, 2008.

[73] Yu. A. Kuznetsov, H. G. E. Meijer, and L. Van Veen. The fold-flip bifurcation. *Internat. J. Bifur. Chaos*, 14(7):2253–2282, 2004.

[74] Yu. A. Kuznetsov, S. Muratori, and S. Rinaldi. Bifurcations and chaos in a periodic predator-prey model. *Internat. J. Bifur. Chaos Appl. Sci. Engrg.*, 2(1):117–128, 1992.

[75] C. Laing and P. Glendinning. Bifocal homoclinic bifurcations. *Phys. D*, 102(1–2):1–14, 1997.

[76] Y. Lan, C. Chandre, and P. Cvitanovic. Newton's descent method for the determination of invariant tori. *Phys. Rev. E*, 74(4):46206:1–46206:10, 2006.

[77] E. N. Lorenz. Deterministic nonperiodic flow. *J. Atmospheric Sci.*, 20(2):130–141, 1963.

[78] E. N. Lorenz. Irregularity: A fundamental property of the atmosphere. *Tellus*, 36A(2):98–110, 1984.

[79] J. Los. Nonnormally hyperbolic invariant curves for maps in $\mathbb{R}^3$ and doubling bifurcation. *Nonlinearity*, 2(1):149, 1989.

[80] B. Malomed and R. Tasgal. Vibration modes of a gap soliton in a nonlinear-optical medium. *Phys. Rev. E*, 49(6):5787–5796, 1994.

[81] F. Moon. *Chaotic Vibrations: An Introduction for Applied Scientists and Engineers*. Wiley, New York, 1987.

[82] N. V. Petrovskaya and V. I. Judovich. Homoclinic loops of the Salzman-Lorenz system. In *Methods of Qualitative Theory of Differential Equations*, pages 73–83, Gorkii State University, Gorkii, 1980. In Russian.

[83] J. D. Pryce, R. Khoshsiar Ghaziani, V. De Witte, and W. Govaerts. Computation of normal form coefficients of cycle bifurcations of maps by algorithmic differentiation. *Math. Comput. Simulation*, 81(1):109–119, 2010.

[84] B. Rasmussen. *Numerical methods for the continuation of invariant tori*. PhD thesis, Georgia Institute of Technology, Atlanta, December 2003.

[85] B. Rasmussen and L. Dieci. A geometrical method for the approximation of invariant tori. *J. Comput. Appl. Math.*, 216(2):388–412, 2008.

[86] J. Rinzel and G. B. Ermentrout. Analysis of neural excitability and oscillations. In C. Koch and I. Segev, editors, *Methods in neuronal modeling: from synapses to networks*, pages 135–169, Cambridge, MA, 1989. MIT Press.

[87] M. Rosenzweig. Paradox of enrichment: Destabilization of exploitation ecosystems in ecological time. *Science*, 171(3969):385–387, 1971.

[88] F. Schilder, H. M. Osinga, and W. Vogt. Continuation of quasi-periodic invariant tori. *SIAM J. Appl. Dyn. Syst.*, 4(3):459–488, 2005.

[89] A. Shilnikov, G. Nicolis, and C. Nicolis. Bifurcation and predictability analysis of a low-order atmospheric circulation model. *Internat. J. Bifur. Chaos*, 5(6):1701–1711, 1995.

[90] C. Simó. Analytical and numerical computation of invariant manifolds. In C. Benest and C. Froeschlé, editors, *Modern Methods in Celestial Mechanics*, pages 285–330. Editions Frontiéres, 1990.

[91] C. G. Steinmetz and R. Larter. The quasi-periodic route to chaos in a model of the peroxidase-oxidase reaction. *J. Chem. Phys.*, 94(2):1388–1396, 1991.

[92] G. Torrini, R. Genesio, and A. Tesi. On the computation of characteristic multipliers for predicting limit cycle bifurcations. *Chaos Solitons Fractals*, 9(1-2):121–133, 1998.

[93] J. J. Tyson and B. Novak. Regulation of the eukaryotic cell cycle: Molecular antagonism, hysteresis, and irreversible transitions. *J. Theoret. Biol.*, 210(2):249–263, 2001.

[94] L. Van Veen. Baroclinic flow and the Lorenz-84 model. *Internat. J. Bifur. Chaos Appl. Sci. Engrg.*, 13(8):2117–2139, 2003.

[95] R. Vitolo, H. Broer, and C. Simó. Routes to chaos in the Hopf-saddle-node bifurcation for fixed points of 3D-diffeomorphisms. *Nonlinearity*, 23(8):1919–1948, 2010.

[96] R. Vitolo, H. Broer, and C. Simó. Quasi-periodic bifurcations of invariant circles in low-dimensional dissipative dynamical systems. *Regul. Chaotic Dyn.*, 16(1-2):154–184, 2011.

[97] S. Wieczorek and W. W. Chow. Self-induced chaos in a single-mode inversionless laser. *Phys. Rev. Lett.*, 97(11):Article 113903, 2006.

Index